UNIVERSITÀ DI PISA

FACOLTÀ DI INGEGNERIA

Dipartimento di Ingegneria meccanica, nucleare e della produzione

TESI DI LAUREA SPECIALISTICA IN INGEGNERIA NUCLEARE E DELLA SICUREZZA INDUSTRIALE

"Study of thermal-hydraulic phenomena in hot leg break LOCA of PWR systems"

Candidato:

Camilla Matteoli

Relatori:

Prof. Ing. Francesco D'Auria

Prof. Ing. Francesc Reventos

Dott. Ing. Alessandro Del Nevo

Anno accademico 2010/2011

(This page has been intentionally left blank)

Sommario

A partire dalla metà degli anni '70, nell'ambito della ricerca sulla sicurezza dei reattori nucleari di tipo pressurizzato, sono state eseguite campagne sperimentali in apparecchiature ad effetto integrale (cosiddette "Integral Test Facilities") atte ad investigare il comportamento, a livello di sistema, conseguente a postulati eventi incidentali. Tra questi, le medie e piccole rotture delle linee principali del sistema primario del reattore sono state particolare oggetto di studio, soprattutto, a seguito dell'incidente di TMI-2 (1979). Il principale obbiettivo era: il miglioramento della conoscenza del funzionamento del sistema in situazioni incidentali; lo studio dei fenomeni e dei processi termoidraulici coinvolti; l'ottimizzazione dei sistemi di emergenza utilizzati per moderare le conseguenze degli eventi postulati ed, infine, lo sviluppo e la validazione di avanzati strumenti di calcolo predittivi utilizzati per le analisi di sicurezza. Infatti, attraverso il confronto tra i dati sperimentali e i risultati ottenuti con codici termoidraulici di sistema, è possibile qualificare tali strumenti, ossia conoscere capacità e limiti nella simulazione dei fenomeni termoidraulici rilevanti per la sicurezza nucleare.

Tra i vari programmi sperimentali eseguiti, quelli che interessano il presente lavoro, riguardano l'apparecchiatura sperimentale LOBI, a due circuiti, costruita al JRC di Ispra (Italia), rappresentante un reattore KWU PWR da 1300MWe (Biblis in Germania), e l'apparecchiatura LSTF, di proprietà di JAERI, che rappresenta un PWR Westinghouse e si trova al centro di ricerca Tokai, in Giappone.

Gli esperimenti selezionati e riprodotti, tramite simulazioni col codice RELAP5/Mod3.3, sviluppato da US-NRC, sono stati i seguenti:

- *Test A1-84, rottura del 10% in "hot leg", eseguito su LOBI nel 1985. Questo transitorio ha come evento iniziatore la rottura nella prima parte della gamba calda, ed è caratterizzato da una veloce depressurizzazione, dalla transizione da circolazione forzata a circolazione naturale, dall'intervento, dopo circa 40s, dei sistemi di emergenza di alta pressione (disponibili 2 pompe su 4) e infine dall'attivazione dei sistemi accumulatori (i quali iniettano nelle "cold" e "hot legs" del "loop" intatto e nella "cold leg" del "loop" rotto).*
- *Test SB-HL-17, rottura dell'1% in "hot leg", eseguita su LSTF. Questo transitorio ha una fenomenologia abbastanza simile a quello precedente ma, essendo una piccola rottura (SB LOCA) evolve più lentamente ed ha pertanto una durata maggiore. Nel test SB-HL-17, i sistemi di sicurezza attuati sono quelli di alta pressione e gli accumulatori.*

Il contesto all'interno del quale I due lavori sono stati eseguiti è di grande importanza:

Il primo post-test, è stato messo a punto durante un periodo di tirocinio presso UPC-ETSEIB (Universitat Politecnica de Catalunya-Escola Tecnica Superior de Enginyeria Industrial de Barcelona), ed è inserito in un'attività più ampia, improntata allo studio di tre differenti esperimenti, tutti relativi all'apparecchiature sperimentale LOBI, con differenti condizioni al contorno, ma riprodotti sulla base di uno stesso stazionario, e di una stessa nodalizzazione,

In modo da validare il codice RELAP5/3.3, ed evidenziare la sua capacità di riprodurre I molti fenomeni termoidraulici che si verificano nella facility ed appartenenti a differenti esperimenti. I test utilizzati sono stati: A1-84, BL-44, BL-30.

La reciproca coerenze tra i tre calcoli è n punto molto rilevante, che conferisce maggiore valore ai risultati e conferma come valida, la procedura di implementare cambiamenti su una nodalizzazione di partenza che è comune ai tre tests.

I risultati del presente lavoro saranno d'aiuto nella qualificazione del modello rappresentativo di una ITF, e per le metodologie di valutazione delle incertezze.
Questo lavoro ha portato alla seguente pubblicazione:
"CONSISTENT POST-TEST CALCULATIONS FOR LOCA SCENARIOS IN LOBI INTEGRAL FACILITY".

La seconda attività è stata svolta nel contest dell' *OECD-PKL2 project, in particolar modo per l'OECD-PK2 meeting, svoltosi a Parigi, nel Novembre 2010.*

L'obiettivo del meeting era quello di contribuire alla scenta delle condizioni al contorno per un esperimento da eseguire sulle facilities ROSA V/LSTF e PKL2. Veniva richiesto di mettere a punto un calcolo di pre-test, per entrambe le apparecchiature, se possibile, con delle condizioni al bordo prefissate, che sarebbero state cambiate, da tutti i partecipanti, una volta visionati i primi risultati, per renderle adeguate per entrambe le facilities. Per LSTF è stata fornita una nodalizzazione, e per validarla è stato richiesto di eseguire il post-test di un esperimento simile a quello che sarebbe stato deciso in sede di meeting, utilizzato poi come counter part test. L'esperimento utilizzati per validare la nodalizzazione è proprio il test 1-2, trattato nel presente lavoro di tesi.

L'obiettivo di questo studio è quello di indagare e comprendere i fenomeni termoidraulici che avvengono durante un incidente di perdita di refrigerante, attribuibile ad una rottura considerata "piccola" o di "media grandezza". Le competenze acquisite durante l'esecuzione del primo post-test (esperimento A1-84) sono state applicate alla seconda attività, riguardante una diversa apparecchiatura sperimentale e un esperimento con differenti condizioni al contorno.

Dopo un primo capitolo introduttivo, il testo è suddiviso in tre parti:
*Nella **prima parte** (capitoli 2 e 3) si ha la descrizione delle due apparecchiature sperimentali e degli esperimenti scelti per l'attività di tesi. I test esaminati sono descritti in modo dettagliato, riportando le configurazioni delle apparecchiature sperimentali, i principali eventi dei transitori, e i fenomeni rilevanti, oggetto dell'attività di validazione del codice.*

*La **seconda parte** (capitolo 4) affronta la descrizione del codice di calcolo e descrive le nodalizzazioni utilizzate per le due apparecchiature, incluse le modifiche implementate per effettuare le simulazioni. E' da sottolineare, che nel caso dell'apparecchiatura LOBI, tutta la documentazione tecnica era a disposizione. Per quanto riguarda l'apparecchiatura LSTF, si è utilizzata una nodalizzazione fornita da JAERI (ente proprietario di LSTF), senza avere a supporto una documentazione esaustiva della descrizione geometrica modellata. Tale attività è stata svolta nell'ambito del progetto internazionale OECD/NEA/CSNI PKL-2.*

*La **terza parte** (capitoli 5 e 6) riguarda i risultati ottenuti dalla simulazione col codice RELAP5/Mod3.3, di entrambi gli esperimenti. I principali parametri che influenzano il*

transitorio incidentale vengono descritti, spiegati e commentati. L'attività di valutazione delle capacità del codice di predire i fenomeni termoidraulici rilevanti è stata effettuata seguendo la procedura utilizzata all'Università di Pisa che include analisi qualitative e quantitative. La valutazione quantitativa si basa sull'applicazione di uno strumento, detto FFTBM, basato sulla trasformata di Fourier discreta. Analisi di sensitività hanno riguardato il test A1-84 con l'obiettivo principale di indagare il modello di portata critica.

Abstract

Since the '70, several experimental programs have been carried out in Integral Test Facilities simulating the behavior of pressurized light water reactor systems at system level in off normal and accident conditions. Among the postulated events, the intermediate and the small break LOCAs became of particular importance after the severe accident at TMI Unit 2 nuclear power plant occurred in 1979. These research programs were aimed at improving the knowledge of the behavior of the system; at investigating and understanding the phenomena connected with the reactor safety; at optimizing the set up of the Emergency Core Cooling System, designed to mitigate the consequences of the initiating events and; last but not least, at developing, improving and validating advanced thermal hydraulic system codes used in the design, the safety analysis and the licensing processes. Indeed, the systematic comparison between the experimental data and the calculated results is a part of the process, which demonstrate the reliability of such codes in simulating the transient scenarios.

Among the experimental programs preformed, the present work addresses tests performed at LOBI, a two loops facility, simulating a PWR Siemens (Biblis NPP, Germany) and located at JRC, Ispra (Italy), and LSTF, a two loops ITF, property of JAERI and located at Tokai Research Establishment.

Two different experiments are analyzed, and two post-tests are set-up:

- *Test A1-84, a 10% hot leg break LOCA executed at LOBI facility in 1985. This transient, which initiating event is a rupture in the first section of the hot leg, shows a first phase of quick depressurization, after which the natural circulation phenomenon is established for several seconds. At around 40s in the transient there is the intervention of the high pressure injection system (2 pumps out of 4), which cannot compensate the break outflow. It will be decisive the accumulators injection, which defines the transient end.*
- *Test SB-HL-17, a 1% hot leg break LOCA performed at ROSA V/LSTF facility. This second transient selected, is similar to A1-84 experiment, at phenomenological level, but test 1-2, having a very small rupture (1%) respect on test A1-84, has a longer transient, and the NC phenomenon is more clear. The available safety injection systems in this test are the HPIS, the accumulators, and the LPIS, but the latter are not active for this experiment.*

The contexts in which these works have been developed are of great importance:

The first post-test, has been set up during a stage period at UPC-ETSEIB (Universitat Politecnica de Catalunya-Escola Tecnica Superior de Enginyeria Industrial de Barcelona), and it is inserted in a major activity devoted to the investigation of three different experiments executed at LOBI facility, with different boundary conditions, but set up with the same steady state calculation, in order to validate RELAP5/3.3 code and underline that the code is capable to reproduce several phenomena occurring in LOBI facility, belonging to different experiments. The test used for the study are A1-84, BL-44, BL-30.

The mutual consistency among the calculations is a relevant point that adds value to the results and confirms the procedure of implementing changes in a common nodalization valid for simulating tests occurred in a specific ITF.

The outcome of the analysis will be helpful to support the involved steps of integral plant model qualification procedures and uncertainty evaluation methodologies.

This work, united with the other tests investigations, brought to a publication:
"CONSISTENT POST-TEST CALCULATIONS FOR LOCA SCENARIOS IN LOBI INTEGRAL FACILITY".

The second activity was executed in the framework of the OECD-PKL2 project, particularly for the OECD-PKL2 meeting held in Paris in November 2010.

The aim of the meeting was to contribute to the choice of the boundary conditions for a new experiment to develop in LSTF and PKL facilities. The requirement was to set up a pre-test calculation, both for LSTF and PKL, with the suggested boundary conditions, and to change them in order to render those conditions suitable for the two facilities configurations and peculiarities. A nodalization (an input deck at steady state level) for LSTF facility, was furnished to the participants, and to validate the nodalization, it was required to execute a post-test analysis of an experiment similar to the one which would be executed, as a counterpart test, in the two facilities. That "similar" experiment is LSTF Test 1-2.

The aim of the work is to understand the phenomena occurring in a PWR S/IB-LOCA, and to apply the competences acquired during the execution of the first post-test analysis (test A1-84), to a different test performed in different ITF.

The text is subdivided into three main parts, besides the introduction and the conclusions (section 1 and 7, respectively):

*In **the first** one (sections 2 and 3), the two Integral Test Facilities, and the associated experiments analyzed, are described in depth. In particular, the scaling factors, and the facilities main components are emphasized, besides the facilities configurations, the imposed sequence of main events, the phenomenological windows of the transients and the relevant thermal-hydraulic phenomena.*

***The second part** (section 4) introduces the thermal hydraulic system code used for the analysis of the tests (i.e. RELAP5/Mod3.3), and the two nodalizations applied to reproduce the experiments, pointing out the modifications and improvements implemented. It has to be underlined that for LOBI facility the flow sheets, P&I and other technical documents were available. On the contrary, in the case of LSTF facility, it has been received an input deck by JAERI, but no exhaustive documentation was available regarding the system geometry. This activity has been performed in the framework of the OECD/NEA/CSNI PKL-2 international project.*

***The third part** (sections 5 and 6) reports the results obtained from the post-tests analysis. The parameters, which influence transient, are explained and commented. The code assessment addresses the code capability to predict the thermal-hydraulic phenomena relevant for the reactor safety on the basis of a standard procedure developed at University of Pisa. It involves qualitative and quantitative evaluations of the code results. The quantitative accuracy evaluation is performed by means of application of the Fast Fourier Transform Based Method. Sensitivity analyses are performed for the test A1-84 investigating the effect of the chocked flow model.*

LIST OF CONTENTS

Ringraziamenti

Voglio ringraziare la mia famiglia, babbo e mamma, due persone intelligenti, meritevoli di stima, informate, che mi sostengono nelle mie scelte, e mi spronano ad essere ambiziosa.

Bobi, il colpo di fulmine da cui non mi riprenderò mai.

Paolo, l'unico uomo che per ora sopporta il pesante fardello "Camilla" e i suoi frequenti deliri e monologhi "esteriori".

Le mie amiche, Marta, Francesca, Elena, Angela, Carlotta, Laura S, Irene, Federica, Sonia, Giulia, Laura B, Martina: amorose, sempre presenti, realmente interessate a ciò che mi succede, e che spesso cercano di comprendere i miei cambiamenti di carattere e di opinioni, senza giudicarmi.

Laura, la donna per cui spesso ho desiderato essere omosessuale.

I miei amici di università, Filippo, Matteo, Donato R, Simone, Donato L, Laura, Domenico, che mi hanno sempre aiutato e sostenuto, e mi hanno tirato su di morale quando certi scogli mi sembravano insormontabili.

Infine i miei professori, che hanno fatto diventare una facoltà, scelta senza realmente sapere cosa avrei studiato e cosa avrei affrontato, un vero amore, una grandissima passione e voglia di fare. Ho incontrato persone veramente interessate ai propri studenti, determinate a farli appassionare, e sempre disponibili. So per certo che non è così in tutte le facoltà, e non è così in molti corsi di ingegneria. Quindi mi ritengo fortunata e posso affermare che è stato un vero ONORE essere una studentessa di Ing. Nucleare e degli ottimi insegnanti che la rappresentano.

Un enorme grazie al professor D'Auria per le enormi possibilità di crescita personale e professionale che mi ha messo a disposizione, e per la fiducia che ha riposto in me.

Ringrazio il professor Reventos e Patricia per avermi seguito e aiutato durante il mio tirocinio a UPC, un'esperienza che non dimenticherò mai e che mi ha fatto capire molto di me stessa.

Ultimo, e veramente importante, il ringraziamento al mio "tutor", Alessandro Del Nevo, la persona più competente e disponibile che abbia mai conosciuto, un amico.
GRAZIE, per l'aiuto QUOTIDIANO conferitomi per qualsiasi aspetto del mio lavoro di tesi, dalla spiegazione di concetti e strumenti complessi, alle banalità, per cui mi sono quasi vergognata a chiedere aiuto; dai consigli sul mio futuro, a cos'è, e come si inserisce in un testo, un riferimento incrociato! Sarà una grossa perdita, e mi rattrista enormemente non lavorare più con te.

Camilla

List of Abbreviations

ACCU	Accumulator
ADS	Automatic Depressurization System
AIS	Accumulator Injection System
BAF	Bottom of Active Fuel
BE	Best Estimate
BDBA	Beyond Design Basis Accident
BIC	Boundary and Initial Conditions
BL	Broken Loop
BoT	Beginning of Transient
BRK	BReaK
CCFL	Counter Current Flow Limiting
CHF	Critical Heat Flux
CL	Cold Leg
CSNI	Committee on the Safety of Nuclear Installations
CT	Cooling Tower
DBA	Design Basis Accident
DC	DownComer
DIMNP	Dipartimento di Ingegneria Meccanica Nucleare e della Produzione
DNB	Departure from Nucleate Boling
DP	Pressure Drop
ECC	Emergency Core Cooling
ECCS	Emergency Core Cooling System
EoT	End of Transient
FFT	Fast Fourier Transform
FFTBM	Fast Fourier Transform Based Method
FW	Feed Water
HL	Hot Leg
HPIS	High Pressure Injection System
HT	Heat Transfer
HX	Heat Exchanger
ID	Identification
IL	Intact Loop
IPA	Integral Parameter
ITF	Integral Test Facility
KWU	Kraftwerk Union
LOBI	Lwr Off-normal Behavior Investigation
LOCA	Loss Of Coolant Accident
LP	Lower Plenum
LPIS	Low Pressure Injection System

LS	Loop Seal
LWR	Light Water Reactor
MCP	Main Coolant Pump
NA	Not available
NC	Natural Circulation
NDP	Non Dimensional Parameter
NEA	Nuclear Energy Agency
NPP	Nuclear Power Plant
NUREG	Nuclear REGulatory
OECD	Organization for Economic Cooperation and Development
PCT	Peak Cladding Temperature
PhW	Phenomenological Windows
PMI	Primary Mass Inventory
PRZ	Pressurizer
PS	Primary Side
PWR	Pressurized Water Reactor
R5	RELAP5
RCS	Reactor Coolant System
RHR	Residual Heat Removal
RPV	Reactor Pressure Vessel
RTA	Relevant Thermal-hydraulic Aspect
SG	Steam Generator
SGTR	Steam Generator Tube Rupture
SoT	Start of Transient
SS	Steady State
SVP	Single Valued Parameter
SYS	SYStem
TC	ThermoCouple
TH	Thermal-Hydraulic
TH-SYS	Thermal-Hydraulic SYStem (referred to code)
TSE	Time Sequence of Events
UH	Upper Head
UNIPI	Università di Pisa
UP	Upper Plenum
UPC	Universitat Politecnica de Catalunya
USNRC	United States Nuclear Regulatory Commission

List of Figures

List of Tables

1 Introduction

1.1 General overview on LOCAs

In the design of nuclear power plants, it is required that various operational occurrences are considered and that the consequences of such occurrences are analyzed so that suitable mitigating systems can be designed. Normal operation of the plant can be defined as operation within specified operational limits and conditions. Anticipated operational occurrences (AOOs) are operational processes deviating from normal operation, expected to occur at least once during the lifetime of a facility but which, in view of appropriate design provision, do not cause any significant damage to items important to safety or lead to accident conditions. The latter condition may be simply defined as deviations from normal operation more severe than anticipated operational occurrences. Accident conditions can be divided into design basis accidents (DBAs) and severe accidents. For the accident conditions there are acceptance criteria which must be fulfilled. For the design basis accidents the most fundamental acceptance criterion is typically that there should be no or at most very limited radiological consequences to the public. However, in order to fulfill this criterion there will be a number of other acceptance criteria related to the different safety systems of the reactor. How these criteria are formulated depend on the general design of the reactor and the various physical phenomena of importance to the occurrence of a particular design basis accident.

A Loss Of Coolant Accident (LOCA) is a postulated accident that would result from the loss of reactor coolant, at a rate in excess respect on the capability of the reactor coolant make up system [1]. The breaks in pipes of the reactor coolant pressure boundary are up to and including a break equivalent in size to the double-ended rupture of the largest pipe in the reactor coolant system.

The LOCAs are classified on the basis of their size, and this is connected to the accident occurrence probability. Many classifications are available, depending on the regulatory commission that has issued them. The USNRC classification[2] [3] based on leak rate is provided in Tab. 1. The NUREG/CR-5750 [4], issued by the USNRC in 1993, provides the data concerning LOCAs frequencies (
Tab. 2).

Tab. 1 – LOCAs classification.

Category	Leak Rate Threshold (gpm)	LOCA Size
1	> 100	SB
2	> 1500	MB
3	> 5000	LB
4	> 25,000	LB a
5	> 100,000	LB b
6	> 500,000	LB c

Tab. 2 – LOCAs frequencies per year.

Event	Functional Impact Event Category	Number of Functional Impact Occurrences[a]	Mean Frequency (per critical year)[b,c,k]
Loss-of-Coolant Accident (LOCA)	G		
Large Pipe Break LOCA: PWR	G7	0	5E-6[d]
Large Pipe Break LOCA: BWR	G7	0	3E-5[d]
Medium Pipe Break LOCA: PWR	G6	0	4E-5[d]
Medium Pipe Break LOCA: BWR	G6	0	4E-5[d]
Small Pipe Break LOCA	G3	0	5E-4[d]
Very Small LOCA/Leak	G1	4	6.2E-3

In a typical PWR system (see Fig. 1), the limiting design basis accident is a double-ended guillotine break in a cold leg between the reactor coolant pump and the reactor vessel. This means that is the most severe postulated scenario against which a nuclear power plant is designed on the basis of established design criteria. These criteria ensure the damage to the fuel and the release of radioactive material, thus requiring that the radiation dose to the population is "as low as reasonable achievable".

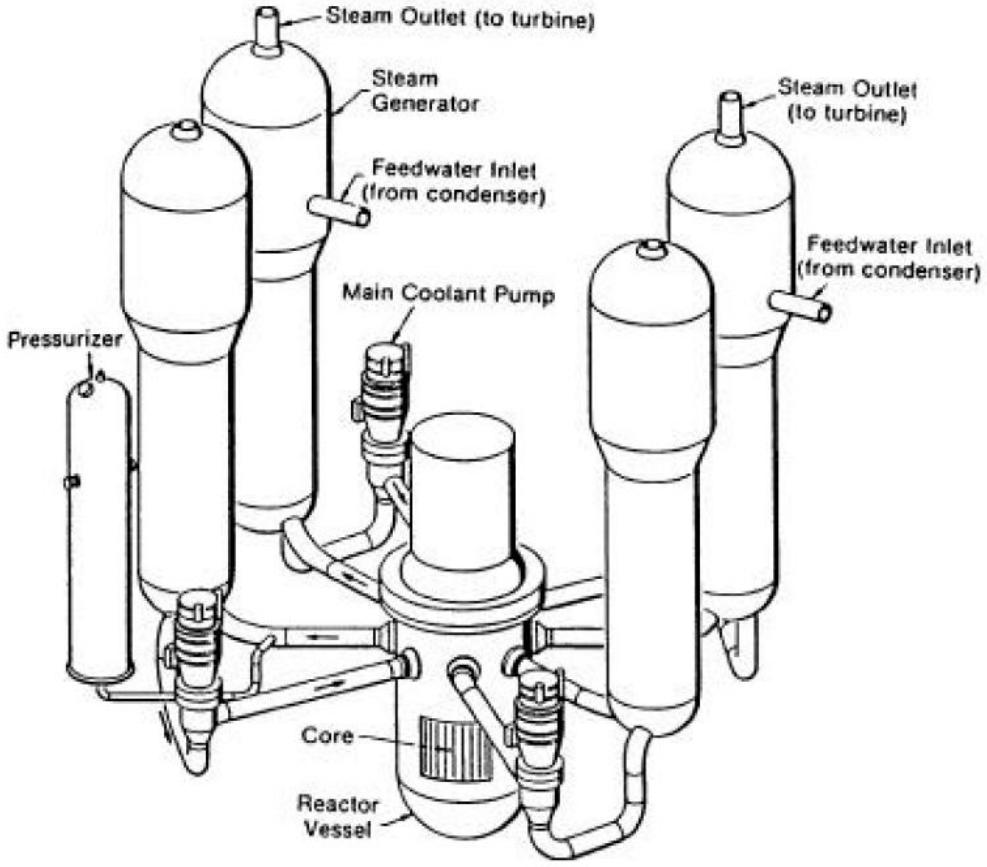

Fig. 1 – PWR primary system layout.

In general, the acceptance criteria for emergency core cooling systems are based on those specified in Appendix K of 10CFR50.46[1]. These criteria are:

- a peak clad temperature of <2200°F (1204°C),
- a maximum local clad oxidation of 17% of the clad thickness,
- a maximum hydrogen generation of no more than 1% of the total amount that could be generated by clad oxidation,
- the maintenance of a coolable geometry,
- the maintenance of long term cooling.

These criteria are applicable to both large and small break LOCAs. That is to say the limits on peak cladding temperature, cladding oxidation, and hydrogen generation must not be exceeded in a design basis accident.

The safety research programs during 70's were devoted mainly to support code development for large break LOCA. Following Three Mile Island Unit 2 (TMI-2) reactor accident, there was a reorientation of light water reactor safety research programs towards the small break LOCA and the connected phenomena. The experimental simulation of the natural circulation phenomena in the primary loops, including those in the two-phase stratified and counter-current flow regimes, is of primary importance to the thermal-hydraulic response of a nuclear power plant during such transients. The study of such phenomena required the availability of suitable facilities, thus modifying existing facilities constructed of LB LOCA issues investigations or the construction of new facilities.

It is to be noted that unlike the large break LOCA, the sequence of events following a small break LOCA can evolve in a variety of ways. Operator actions, reactor design, ECCS set points, break size, and location will have a bearing how the small break LOCA scenario unfolds. Therefore, in order to predict the integral system behavior during a small break LOCA, a best-estimate code must have sufficient modeling capabilities to take these factors into account. These codes are also needed to be assessed against integral system tests.

1.1.1 Large Break LOCA description

The blowdown period (0 – 30 s) occurs as a result of a break in the coolant system through which the primary coolant is rapidly expelled. Within a fraction of a second after the break, the core voids and goes through departure from nuclear boiling. The negative void reactivity rapidly shuts down the core. With the diminished cooling and the redistribution of stored energy in the fuel, the cladding heats up. Interactions between the pump and the break dynamics cause intermittent flow reversals. The primary system pressure rapidly decreases and the high-pressure safety injection begins, but most of this flow is lost out of the break.

With the continuous decreasing of the primary pressure, injection from the cold-leg accumulators begins, but much of the injected flow is swept around the downcomer, into the broken-loop cold leg and out the break (downcomer bypass phenomenon). As the blowdown progresses, an increasing amount of the accumulator injected coolant stays in the downcomer and some water begins to enter the lower plenum. The average peak cladding temperature (PCT) [7] during the blowdown phase of a large-break LOCA is approximately 800-1000 ˚C) and the PCT at 95% confidence level is even higher, assuming a loss-of-offsite power and the worst single failure assumption for the emergency core cooling system.

The refill period occurs between 30 and 40 s following the start of the LOCA. The primary pressure has decreased to a level at which the low pressure injection system activates and

begins to inject water into the system. The lower plenum begins to fill with accumulator water as coolant bypass diminishes. The refilling of the lower plenum is largely governed by how quickly the accumulator water can penetrate the downcomer annulus and reach the lower plenum. This is a complex three dimensional phenomenon. While refilling of the lower plenum is underway, however, the core heats up in a near adiabatic mode due to decay heat. Some fuel rods balloon and burst, causing blockage of some of the flow channels during refill. In the case of combined injection, typical of KWU SIEMENS designed PWR during the refill phase, water can penetrate the upper plenum and quench the top of the core.

The reflood period occurs between 40 and 200 s. It begins at the time when the lower plenum has filled and the core begins to refill. When the water injected by the accumulators fills the downcomer, it creates the driving head for refilling the core. A quench front is formed on the fuel rods and large amount of steam is generated by the energy released from the rods at high temperature. This steam produces a back pressure opposing the driving head of coolant in the annulus and thereby slowing or even reversing the water level rise in the core (steam binding phenomenon). Thus, the reflooding of the core proceeds with level oscillations (strong at the beginning, moderate later) occurring in both the core and downcomer.

The lower elevations of the core quench, generating a two-phase mixture that provides some cooling to the upper elevations of the core. However, the fuel rods continue to heat up until the quench front begins to move upward through the core. Some additional number of fuel rods may burst during the reflood period. Zirconium-water reactions can occur for high temperature regions of the core. As the quench front continues to advance, the fuel rod upper elevations are cooled by a dispersed non-equilibrium two-phase mixture of superheated steam and entrained droplets. Downstream the quench front, when the PCT is reached, there is sufficient cooling to cool the fuel rod cladding, thus decreasing its temperature. De-entrainment of liquid can occur on the upper tie plate and on the structures of the upper plenum; a liquid film on this structures is formed and droplets can be entrained to the hot leg by the steam flow or can fall downwards into the core. These droplets can lead to the formation of a water pool in the UP and/or a quench front which propagates downward into the core (top-down quenching)[5]. The average reflood PCT during this period is approximately above 900 ˚C) and the PCT at 95% confidence is about 1100 ˚C [5][7]. The maximum amount of cladding oxidized at a given location during this phase of the LOCA is about 10% for beginning-of-life (BOL) UO_2 fuel and the total oxidation is less than 1% [8].

1.1.2 Small Break LOCA description

Breaks with flow areas typically less than 1-ft^2 and greater than 3/8 in. in diameter, span the category of small breaks. A small break [6] is sufficiently large that the primary system depressurizes to the high-pressure safety injection set point and a safety injection or “S” signal is generated, automatically starting the High-Pressure Safety Injection (HPSI) system. Breaks smaller [5]than 3/8-inch in diameter do not depressurize the reactor coolant system because the reactor charging flow can replace the lost inventory.

The control rods [8] shut down the reactor such that only decay heat is generated in the core. The limiting small-break LOCA is determined by the inter-play between core power level, the axial power shape, break size, the high-head safety injection performance, and the pressure at which the accumulator begins to inject. The limiting break is one that is large enough that the high-pressure safety injection system cannot make-up the mass loss from the reactor system but small enough that the reactor system does not quickly depressurize to the accumulator set

point, and this is the major difference between a large break LOCA and a small break, which is characterized by an extended period, after the break, during which the primary system remains at a relatively high pressure.

For Westinghouse plants [8], the limiting breaks are typically in the 2-4 inch range. A spectrum of break sizes has been calculated for a Westinghouse three-loop plant. Calculations were performed assuming both fresh fuel and fuel with burnup between 30 and 54 GWd/t. These calculations are thought to accurately display the effect of burnup on fuel performance. As an example, with fresh fuel, a three-inch break was found to produce the highest PCTs for breaks in the range of 2 to 6 inches. The PCT of about 1000 ˚C occurred at approximately 1480 s. The core average cladding oxidation was 0.5%. No bursting of the fuel is predicted for fresh fuel, but if burnup increases, some of the fuel will burst and experience double-sided cladding reactions. However, the burnup reduces the linear heat rate such that the calculated PCTs are below those for fresh fuel and are, therefore, less limiting. At 54 GWd/t, the hot rod PCT is predicted to be approximately 800 ˚C).

A few seconds after the rupture, and after the "S" signal, as soon as the pumps are tripped, either automatically or manually, gravity-controlled phase separation occurs: gravitational forces dominate the flow and distribution of coolant inside the primary system (for a large break it is dominated by inertial forces), single-phase and then two-phase natural circulation develop in the primary loops and voids form in the upper regions of the steam generators; When NC at the top of the U-tubes cannot be sustained further, complete phase separation occurs. The core experiences pool boiling and counter current flow is set up in the hot legs with reflux condensation in the ascending parts of the U-tubes. During this period the cladding temperature remain close to the saturation temperature of the coolant in the vessel, the decay heat is transferred to the steam generators by the boiling and reflux condensation process.

The subsequent sequence of events, whether or not the core uncovers and is recovered or reflooded, depends not only on the location, shape, and size of the break, but also on the overall behavior of the primary and secondary systems. This behavior is strongly influenced by both automatic and operator initiated mitigation measures. This combination of circumstances could lead to a core uncover [5].

During a PWR small break LOCA, there is the potential for three distinct core heat ups [5]. The first heat up is caused by loop seal formation and the manometric core liquid level depression. Loop seal clearing and break uncover mitigate this heat up. It has to be noticed that loop seal has no influence on small hot leg breaks, because the vapor is directly discharged from the break; as soon as the vapor, or from the descending U-tubes, or from the uncovered cold legs, can escape round the bottom of the loop seal, it relieves the pressure difference between the loops and water from the downcomer fully refloods the core. The second heat up occurs following the core quench caused by loop seal clearing and is caused by a simple core boiloff. During this period the primary pressure is decreasing to the accumulator set point and the steam produced by the core boil-off leaves the system through the break. Any heat up that occur during this period is mitigated by the reflood from the accumulator water. The third possible heat up can occur following depletion of the accumulator tanks and before LPIS injection begins.

Various factors affect the magnitudes of the three potential core heat ups. Some examples are break size, break direction and location, availability of HPIS, and the degree of upper head to

downcomer bypass flow. Although the magnitudes of the core heat ups may vary, ECCS performance must be such that the criteria, for example, 10 CFR 50.46[1] is not exceeded.

After the possible heat ups, the core is generally reflooded by the accumulator and the LPIS injecting simultaneously. The complex phenomena involved with reflooding of core during a small break LOCA, such as bottom-up quenching, entrainment and de-entrainment of coolant, top-down quenching are similar to those observable for large break LOCA. The main difference is that reflooding takes place at somewhat higher pressure and may progress more slowly.

It is to be noted that there is no unique path of development of events following a small break LOCA in PWRs. The scenarios may change drastically by many factors such as the reactor design (e.g., U-tube or once-through steam generators, such as TMI-2), the break size, the core bypass size (allowing some fraction of the inlet cold leg flow directly into the core upper structure without passing through the core), and most importantly, by different operator interactions. As an example, the primary circulation pumps may be shut down early in a small break LOCA transient or they may be allowed to run and circulate the coolant through the core for a long time. These alternative actions can make a large difference in the nature of discharge flow, early heat removal from the core, and the liquid inventory in the system after one hour or so in the transient. Another important possibility of different interactions is through the steam generators. The secondary side of steam generators can be isolated (no feed water flow) or they can be used for a controlled heat removal. It is also possible to cool the reactor through the so-called “feed and bleed” process (on the primary side).

It has to be underlined that an adequate set of modeling capabilities for any of the plausible scenarios will be equally adequate for all other relevant scenarios. This is because the phenomena and processes are the same but their interactions and timing of various developments change in different operations. Therefore, in order to predict the integral system behavior during a small break LOCA, a best-estimate code must have sufficient modeling capabilities to take these factors into account.

1.2 Objective of the activity

The main objectives of the activity, in relation to intermediate and small hot leg break in PWR system are:

- to acquire competences in performing safety analysis studies and in using thermal-hydraulic system codes;
- to understand important phenomena /processes observed in the transients;
- to assess the predictive capabilities of RELAP 5 code in the domains of interest;
- to indentify limitation of the existing best estimate codes;
- to draw conclusions on the possible use of the codes for safety analysis.

Additional items to be considered are:

- importance of different scaling ratios of ITFs, when comparing calculation results or thermal-hydraulic phenomena;
- the possibility to work in an international framework (stage at UPC) as well as the participation in the OECD/NEA CSNI PKL-2 Project.

1.3 Structure of the thesis

The present work addresses the post test analysis of two experimental tests: the first is a 10% hot leg break, in LOBI ITF and, the second a 1% hot leg break in LSTF/ROSA V facility. The thesis is divided into seven sections.

After an introduction (the current section 1), which provides an overview of the LOCA transients and the objectives of the activity, the following sections 2 and 3 provides the description of the test facilities and the tests analyzed.

LOBI facility and test A1-84 are described in section 2. At first, a general description of the facility is furnished, then the facility configuration of test A1-84 is exposed. The test is divided into phenomenological windows, identifying for each of them the thermal hydraulic phenomena relevant for the safety. Section 3 provide analogous description of the LSTF ROSA V test SB-HL-17.

Section 4 reports the description of the nodalization adopted. The nodalization of LOBI facility by RELAP5/Mod3.3 is provided into details identifying the correspondence between the hydraulic model and the facility zones. An overview of the LSFT facility is reported as well.

The results of the post test analysis of LOBI test A1-84 are provided in section 5. It includes the achievement of the steady state conditions and the transient results. The thermal hydraulic phenomena reproduced by the code are underlined, and the differences between experiment and calculation are justified from qualitative and quantitative point of view. The overall picture of the parameters compared in the analysis is provided in Appendix A. Sensitivity analysis is also discussed.

The post test analysis of the 1% HL break in LSTF/ROSA facility is also provided in section 6, following the logics already addressed in section 5.

Then, conclusions of the activity are discussed in the last section 7.

2 Description of LOBI facility and the experiment

2.1 LOBI-MOD2 facility

The LOBI-MOD2 facility (Fig. 2) [9] is an high pressure integral system test facility (ITF) which simulates the geometrical and operating configuration of a four loops pressurized water reactor, with an electrical power of 1300 MW (scaling factor 1:712). In particular, this facility reproduces the KWU PWR nuclear power plant of Biblis (Germany) [33]. The LOBI facility was designed and operated at the Joint research Centre (JRC) of Ispra (Italy).

It has two primary loops [10]: the intact, representing three loops, and having three times the capacity in water volume and mass flow of the other, and the broken loop, representing one loop (see Fig. 3). Each primary loop (active loop) includes a MCP and is connected with a steam generator (Fig. 5). The simulated core consists of a 64 directly electrically heated rod bundle arranged in a 8x8 square matrix. Nominal heating power is 5.3 MW. There are seven different thickness for the hollow cylinder simulating the rods, and this allows to obtain a cosine shaped axial power profile.

Lower plenum, upper plenum, an annular downcomer and an externally mounted upper head are additional major components of the reactor model assembly. The system pressurizer is connected to the intact loop hot leg. The primary cooling system operates at normal PWR conditions: about 158 bar for the pressure and 294-326 °C for the temperatures.

In the MOD2 configuration (Fig. 5) emergency core cooling water (ECC) can be supplied by the High Pressure Injection System (HPIS) and by the Accumulator injection system (AIS). At the time of test A1-84 execution the Low Pressure Injection System (LPIS) was not represented.

The secondary cooling circuit contains the main feedwater pump and the auxiliary feed water system (Fig. 5). The nominal condition of the secondary circuit are approximately 210°C for the feed water temperature and 64.5 bar for the pressure. However, the secondary circuit is designed to operate until a temperature of 310°C and a pressure of 100 bar.

The facility [11] and individual components are scaled to preserve, as good as possible, a similarity of thermo-hydraulic behavior respect on the reference plant, during normal, off-normal and accident conditions. The scaling rationales, which required a capacity ratio between the intact and the broken loop steam generator of 3:1, with reference to major thermal hydraulic parameters, lead to an heat exchange power of 1.83 MW for the broken loop (8 U-Tubes + 1 installed spare SG), and to a heat exchange power of 3.96 MW for the intact loop (24 U-Tubes + 1 installed spare SG).

The steam generators (see Fig. 4) are composed by a cylindrical pressure vessel with an annular downcomer separated from the riser region by a skirt tube. This tube is supported above the tube plate, and carries the coarse separator. A fine separator is arranged in the uppermost part of the steam dome. The U-tubes are positioned in a circle within the riser region, around an axially mounted filler tube, with the U-bends crossing over one another above it. This configuration permits cross flow between co-current and counter current legs of the U-tubes over their entire length, and mass and heat transfer between riser and downcomer to account for the recirculation characteristics of the prototypical system. An adjustable

throttle device is installed at the lower end of the downcomer to allow the recirculation rates in the two steam generators to be set-up. A proper connection between the secondary side at the tube plate elevation and the inlet or outlet plenum on the primary side, can be established for the simulation of steam generator tube rupture (SGTR) accident.

Scaling ratios

The power input, the primary circuit coolant mass flow and the volume are scaled down from the reactor values by a factor of 712, leading to 5.3 MW heating power in the 8x8 heater rod bundle of the reactor pressure vessel model, and to 28 kg/s core mass flow [9]. For the 12mm annular downcomer configuration, the total primary coolant volume contains about 0.6 m3. All the other most relevant quantities, such as operating temperature, pressure, lengths and pressure drops along heat transfer surface have been scaled 1:1. Also the absolute heights and relative elevations of the individual system components have been kept at reactor values, thus preserving the gravitational heads.

LOBI-MOD2 measurement system

The measurement system [9] consists of a total of about 470 measurement channels. It allows the measurement of all relevant thermo-hydraulic quantities at the boundaries (inlet and outlet) of each individual loop component and within the reactor pressure vessel model and steam generator. Each heater rod in the bundle is supplied with three cromel-alumel thermocouples brazed into grooves of 0.8 mm depth and 10 mm length, machined into the outer surface of the heater rod tubes and then led through the wall to the inside of the tubes; they leave the rods through the open upper end (see Fig. 6a). The position of the thermocouples in the riser side of the vessel are reported in Fig. 7.

The LOBI-MOD2 steam generators are instrumented to provide a maximum of information on both the magnitude, and location of the heat transfer process taking place between primary and secondary circuit. In particular, the instrumentation is concentrated in the region of the lowest U-Tubes bend, and immediately above the tube plate, in order to detect changes in heat transfer regime.

A process control system allows the simulation of both the reactor pump hydraulic behavior by appropriate speed control of the main coolant circulation pumps, and the fuel decay heat and stored heat by controlling the power input to the heater rod bundle.

Upper head connection and by-pass flow paths

The externally mounted upper head is connected to the upper plenum and to the upper downcomer through a connection line having a 8mm diameter orifice. The layout is reported in Fig. 6b. An additional connection exists between the downcomer and the top of the upper head (shut-off valve), and this is used for conditioning the fluid in the upper head to about the temperature of the downcomer. This line is normally isolated sufficient time before transient initiation.

The by-pass flow between upper downcomer and upper plenum includes three main flow paths:

- Upper head connection lines (about 1% nominal flow in A1-84 test, see Tab. 3);
- Two holes of ϕ=5mm in the core barrel tube, each connecting downcomer and upper plenum at the uppermost elevation;

- Possible hot leg to core barrel clearance fit (1mm gap between hot legs and their housing to take in account possible thermal expansion).

The sum of the last two by-pass flows mentioned (5 mm diameter holes and 1 mm gap) has been estimated from 2.4 to 3.7 % of nominal core flow.

Break assembly
The break assembly [12] consists of a T-shaped spool piece inserted within the hot leg pipework (test A1-84) and provides a communicative break configuration. It includes a side oriented break orifice, a quick opening on/off valve for initiation of the rupture and a measurement insert for density, velocity as well as pressure and temperature of the outflow (see Fig. 8). Information on the break system configuration for test A1-84 is also reported in Tab. 3.

Main coolant pump seal water drainage
The operation of the LOBI main coolant pumps [12] requires proper pump seal cooling. Before the initiation of the accident, the fraction of cooling water which enters the primary system is normally drained from the upper plenum using the pressurizer water level control system. After rupture the draining system is isolated and the injected seal water is added to the inventory of the primarily system. The LOBI-MOD2 test facility has also a closed loop pump seal water compensation system which is generally activated in small break loss of coolant experiments and in intact loop circuit faults simulations.

Simulation of pump locked rotor resistance
The locked-rotor hydraulic resistance of the LOBI main coolant pumps [12] is used to obtain the same resistance as in the reference reactor. Since the two pumps are identical, it exists the potential for asymmetry of flow distribution in the two loops during period of natural circulation following pump coast-down. To ensure a more symmetrical mass flow behavior in such conditions, the pump locked rotors simulators are installed at the pump discharge, each consisting in a valve that can be properly orificed to provide the required additional resistance. In the intact loop the locked rotor resistance is negligible (because of the intact loop mass flow, respect on the broken one) but, in the broken loop it is significant and a perforated plate type orifice is installed. In test A1-84, the orifice provides an area reduction of about 18% of the normal flow area, and it is normally inserted 4 s after starting of pump coast-down.

2.2 LOBI Test A1-84

2.2.1 Objectives of Test A1-84

The main objectives of the Test A1-84 are (see Refs. [12] and [13]):

- to obtain experimental data for validation of thermal-hydraulic codes applied to hot leg break scenario (the main phenomena/processes are reported in Tab. 6);
- to investigate the thermo-hydraulics behavior of a simulated PWR primary and secondary cooling system;
- to use the experimental results for the development and improvement of analytical models;

2.2.2 Configuration of the facility, boundary and initial conditions of the experiment

Test A1-84 [12], [13] simulates a 10% hot leg break (break orifice ϕ=9.5 mm, side oriented) in the main coolant pipe of a pressurized water reactor (PWR). Cooldown is applied to the secondary side at a rate of 100 K/h. Emergency core cooling water is injected into the primary loops by the accumulators and the High Pressure Injection System (HPIS). The accumulators [14] are connected to both the legs of the intact loop and to the cold leg of the broken loop. The high pressure injection system is connected to the hot leg of the intact loop. The injection rate is representative of two (out of four) injection pumps. The remaining two pumps (existing in the reference plant), are assumed to be in maintenance and connected to the broken loop, respectively.

The imposed sequence of main events (see Tab. 5) is based on the instrumentation and control system of the reference plant after leak detection. The LOBI electric heater bundle simulates the decay heating curve of nuclear fuel after the SCARM occurrence. The main coolant pumps are controlled, by the speed curves, to stop in order to preserve the characteristic differential pressure over the pump, expected in the reference plant.

The boundary conditions for the test are hereafter summarized.

- The instant of break opening defines the blowdown time "zero". The valve is fully open within 1.5 s.
- Core power remains constant for the first 1.7 s after the rupture. The core power trip is set to start power decay at an upper plenum pressure of 13.2 MPa, with a delay of 0.5 s.
- After transient start, both pumps remain at constant speed for the first 7.0 s (because the main coolant pumps coastdown starts at 11MPa plus a delay of 1s, and the time at which this occurs is 7s after rupture). To simulate this event, a trip governed by time is entered in the input (if time is greater than 7s, start the pumps coastdown). The intact and broken loop pumps are controlled to come to rest after 100.1 s and 102.4 s after transient start, respectively.
- The locked rotor resistance simulator for the broken loop pump is introduced 106 s after the break.
- HPIS injection starts effectively at 40.6 s after transient start.
- The secondary feed lines and the steam line start to close 1.7 s after tube rupture (valve closure time 1.5 s). the steam generators remain connected via steam line, during the transient. In the RELAP5 simulation the feedwater isolation trip is given by time because the feedwater valve is modeled as a time dependent junction and this component doesn't allow to give a closure time, like the motor valve, used downstream the steam line. The feedwater junction stops to inject when the scram signal is effectively active
- The steam relief valves of the secondary side have a set point of 8.3 MPa.
- The secondary side cooldown (100 K/h) stats at 1 s after the break.
- Accumulator injection starts at 347 s for the intact loop (hot and cold legs), and at 350s for the broken loop cold leg. At this time the pressure is about 2.8 MPa. The accumulators injection in stops at the reaching of a pressure of 11MPa, plus 500s: in the simulation this signal is given by accumulator water volume; when the water volume of the tank reaches a certain value, the injection stops; the volume indicated in the simulation corresponds to that reached in the experiment 500s after the reaching of the 11MPa set-point.

- The secondary side cooldown actuation in the experiment is connected with the scram signal, in fact, the cooldown is effectively active 0.3s after the scram, because of the opening time of the valve. In the simulation, the cooldown process starts 13s after the rupture, and is given by time in the input. It was decided to make this choice, in order to make the secondary pressure (of the simulation) reaching a peak, without imposing a pressure trend, to see if the peak pressure was correctly reproduced by the code.

The facility conditions at the beginning of the transient are reported in Tab. 4.

2.2.3 Description of LOBI Test A1-84

The resulting sequence of main events [12], [13], which characterize the course of the transient is shown in Tab. 6.

Blowdown Phase.
Within 1 s after rupture, the primary system depressurizes to 132 bar, and this enable the core heating power and the secondary system cooldown signals (Fig. 9). The isolation procedure (closure of feedwater valves and main steam valve at condenser inlet) together with the automatic cooldown (100 K/h) of the secondary system, are actually initiated at 1.3 s after the rupture, and this causes a delay in the primary and secondary pressures responses (Fig. 10).

Saturation pressure in hot leg is reached at about 2 s. The attainment of this pressure brings to a moderate change in primary system depressurization, which continues at a reduced rate as the fluid, in the upper vessel internals, started to flash.

At 5 s from SoT, the HPIS pressure set point (117 bar) is reached, but the system start to inject with a delay of 35 s, at about 40.6 s, because of the loss of onsite power assumption with SCRAM occurrence. Notwithstanding the HPIS injection, the primary system mass (Fig. 11) continues to decrease throughout the initial part of the transient. The depletion of the primary mass stops after the accumulators injection.

The coastdown of the main coolant pump starts at 7 s, on the basis of the low primary system pressure signal (110bar) occurring at 6 s. After the main coolant pumps coast-down is completed, the fluid flow in the primary system is governed by the pressure differentials originated by the rupture and by the balance between the buoyancy and the resistance forces in the primary system (natural circulation).

When the forced circulation (driven by the MCPs) stops, the onset of two phase natural circulation and of the reflux condenser heat transfer modes, is essentially shattered by the early voiding of the upper parts of the primary system and by the loss of the heat sink (steam generators), as the secondary pressure overtakes the primary one.

The pressurizer surge line connection uncovers at about 17.5 s. The saturation front reaches the cold leg elevation at 23 s from SoT, and 19 s later the primary pressure drops to the saturation pressure of the fluid in the lower plenum (overall primary system is in saturation conditions).

The primary system behavior is practically decoupled from the secondary cooldown except for the early phase of depressurization. After 84 s from SoT, the primary system pressure drops below the secondary side, thus reverse heat transfer is established. Anyway, the heat

transfer from the secondary to the primary side is negligible due to the voiding of the U-Tubes.

After the uncovering of the break, at about 150 s, the primary cooling system depressurizes faster, and about 200 s later, it reaches the set-point for the accumulators actuation (2.8 MPa).

Core uncover driven by inventory loss phase.
The fluid flow through the core is generally in the upward direction, being enhanced by the position of the rupture, in hot leg. A temperature excursion occurs in the upper part of the rod bundle at 335 s, so dryout conditions are reached, but immediately interrupted by the accumulator injection at 347 s.

Reflood phase.
After the accumulator actuation the primary side mass inventory stops to decrease, and it settles around an almost constant value. After 850 s the primary system pressure is 1 MPa, which is the set-point for test termination.

Tab. 3 – LOBI-Mod2, Test A1-84: facility configuration.

#	SYSTEM	CHARACTERISTICS	STATUS	REMARKS
1	PRZ connection status	Connected to IL HL	--	--
2	Upper head connection lines	Connected to upper plenum and upper downcomer by 3 flow paths:	--	
	First flow path	Upper head connection line	Connected	1% RPV mass flow
	Second flow path	2 holes of Φ=5mm in core barrel	Connecting downcomer to upper plenum	--
	Third flow path	HL to core barrel clearance fit	--	1mm gap between HL and its housing
3	Break component	Connected with HL BL. Orifice: Φ=9.5mm which corresponds to 0.1A	--	Communicative, side oriented
4	ECCS Accumulators	3 trains available; 2 trains connected to both CL, 1 train connected to IL HL	Operated	--
5	ECCS HPIS	1 train connected to IL HL	Operated	--
6	ECCS LPIS	--	Not operated	--
7	MCP	2 MCP in operation	Active	Start of coastdown 110 bar
8	Cool-down system	--	Active	100 K/h
9	Locked rotor resistance simulator	--	Operated	--
10	FW	--	Not operated	--
11	AFW /EFW	--	Not operated	--

Tab. 4 – LOBI-Mod2, Test A1-84: relevant initial and boundary conditions.

#	QUANTITY	ID	Unit	Y_{EXP}
1	Core thermal power	WhPower	kW	5200
2	PRZ heaters thermal power	--	kW	--
3	PRZ pressure	PA40	MPa	15.8
4	SG-1 IL (top of the SG) pressure	PA87S	MPa	6.54
5	SG-2 BL (top of the SG) pressure	PA97S	MPa	6.52
6	HL IL coolant temperature	TF11H180	°C	327
7	HL BL coolant temperature	TF21H180	°C	328
8	CL IL coolant temperature	TF16H180	°C	294
9	CL BL coolant temperature	TF26H180	°C	291
10	PRZ coolant temperature	TF40V000	°C	346
11	FW IL & BL coolant temperature	--	°C	209
12	Steam line IL & BL coolant temperature	--	°C	281
13	CL IL mass flow rate	--	kg/s	20.2
14	CL BL mass flow rate	--	kg/s	6.2
15	FW IL mass flow rate	--	kg/s	2.07
16	FW BL mass flow rate	--	kg/s	0.61
17	Pump seal water injection IL	QS71	kg/s	0.014
18	Pump seal water injection BL	QS72	kg/s	0.011
19	PRZ level (collapsed)	CL4340	m	5.346
20	SG-1 IL level (collapsed)	CL93BT	m	8.81
21	SG-1 IL level (collapsed)	CL83BT	m	8.21
22	Recirculation ratio IL	--	--	6.2
23	Recirculation ratio BL	--	--	4.4

Tab. 5 – LOBI-Mod2, Test A1-84: imposed sequence of main events.

#	IMPOSED EVENT DESCRIPTION	SYSTEM	SIGNAL (TIME OR SET POINT)	SIGNAL IN THE INPUT	REMARKS
1	0.1A BRK opening in HL	Break component	0s	--	--
2	Scram	Core	13.2 MPa + 0.5 s (1s)	Pressure Upper Plenum <13.2MPa+0.5s delay	Pressure measured in UP
3	Secondary side cooldown 100K/h actuation	SG	13.2 MPa+ 1.5s valve closure time (1.3s)	Time>1013.2s	Condition imposed by time in the calculation
4	MCP's start coastdown	MCP	11MPa+1.0s (7s)	Time>1007.0s	--
5	HPIS Actuation	HPIS	11.7MPa+35s delay (40s)	Pressure Upper Plenum <11.7MPa+35s delay	--
6	MCPs stop	MCP	102s		--
7	Accumulator actuation IL/BL	Accumulator	347.0/349.9s (2.8MPa)	Pressure Prz<2.8MPa	Disabled at 11MPa+500s in CL
8	Accumulator injection stops IL	Accumulator	509.0s	Accu vol<0.2007m3 = Accu lev<3.35m	--
9	Accumulator injection stops BL	Accumulator	520.0s	Accu vol<0.0652m3 = Accu lev<3.1m	--
10	End of test	--	850.0s	Time>1900s	It ends at 0.1MPa

Tab. 6 – LOBI-Mod2, Test A1-84: phenomenological windows and resulting sequence of main events.

Ph.W.	DESCRIPTION & PHENOMENA/PROCESSES	TIME SPAN [S]	EVENT	EXP [s]	Note
I	Blowdown: – **PRZ thermo-hydraulics (depressurization, evaporation, condensation)** – **Void formation** – **Phase separation** – **natural circulation (single phase and two phase)** – **reflux condenser mode** – **break (critical) flow** – **heat transfer in core covered** – **reverse heat transfer from SS to PS**	**0 – 335**	*SoT (break opening) in BL HL*	**0**	Imposed
			Scram	**1**	Imposed
			Secondary side cooldown actuation	**1.3**	Imposed
			Saturation in Hot Legs	**2**	--
			Pressure in primary side 11.7 Mpa	**5**	--
			MCPs start coastdown	**7**	Imposed
			PRZ surgeline uncovers	**17.5**	--
			PRZ empties	**21.1**	--
			HPIS actuation	**40**	Imposed
			Saturation in lower plenum	**42**	--
			PS pressure falls below SS pressure IL	**90.8**	--
			PS pressure falls below SS pressure BL	**97.8**	--
			MCPs Stop	**102**	--
			Break uncovers	**150**	--
II	Core uncover, driven by inventory loss: – **stratification (horizontal) during ECCS injection** – **heat transfer in core covered** – **heat transfer in core uncovered**	**335-350**	*Temperature excursion*	**335**	--
			Occurrence of minimum primary side mass	**347**	--
			Accumulator Actuation IL CL and HL	**347**	Imposed
			Accumulator actuation BL CL	**349.9**	Imposed
III	Reflood: – **heat transfer in covered core** – **possible steam binding** – **bottom up quenching** – **entrainment and de-antraniment of coolant**	**350-850**	*Rewet at the uppermost elevation of the rod bundle*	**351**	--
			Accumulator injection stops IL CL	**509**	Imposed
			Accumulator injection stops BL CL	**520**	Imposed
			Accumulator injection stops IL HL	**849**	--
			Pressure reaches 0.1 MPa	**850**	--
			End of test	**850**	Imposed

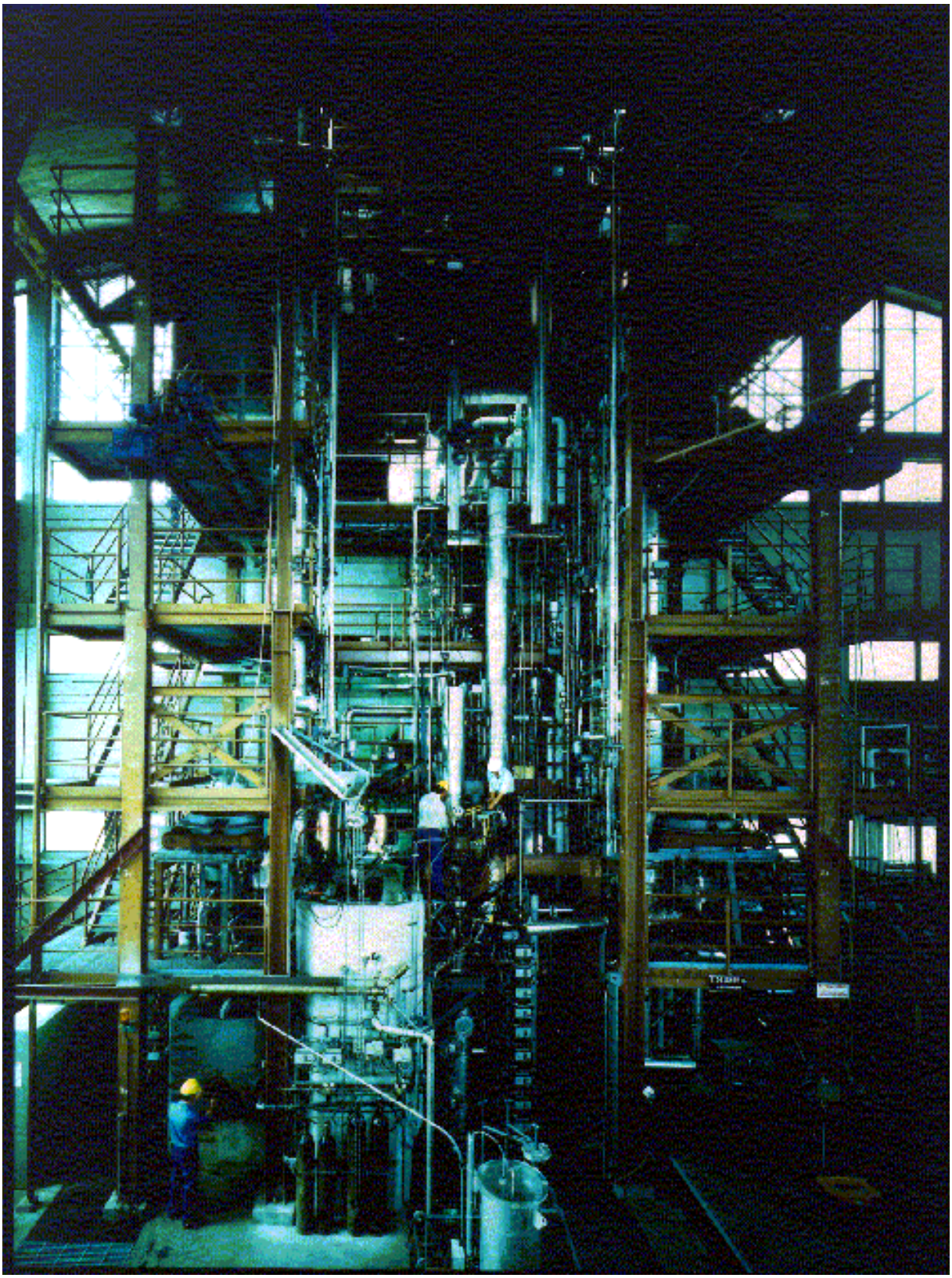

Fig. 2 – LOBI-Mod2 facility.

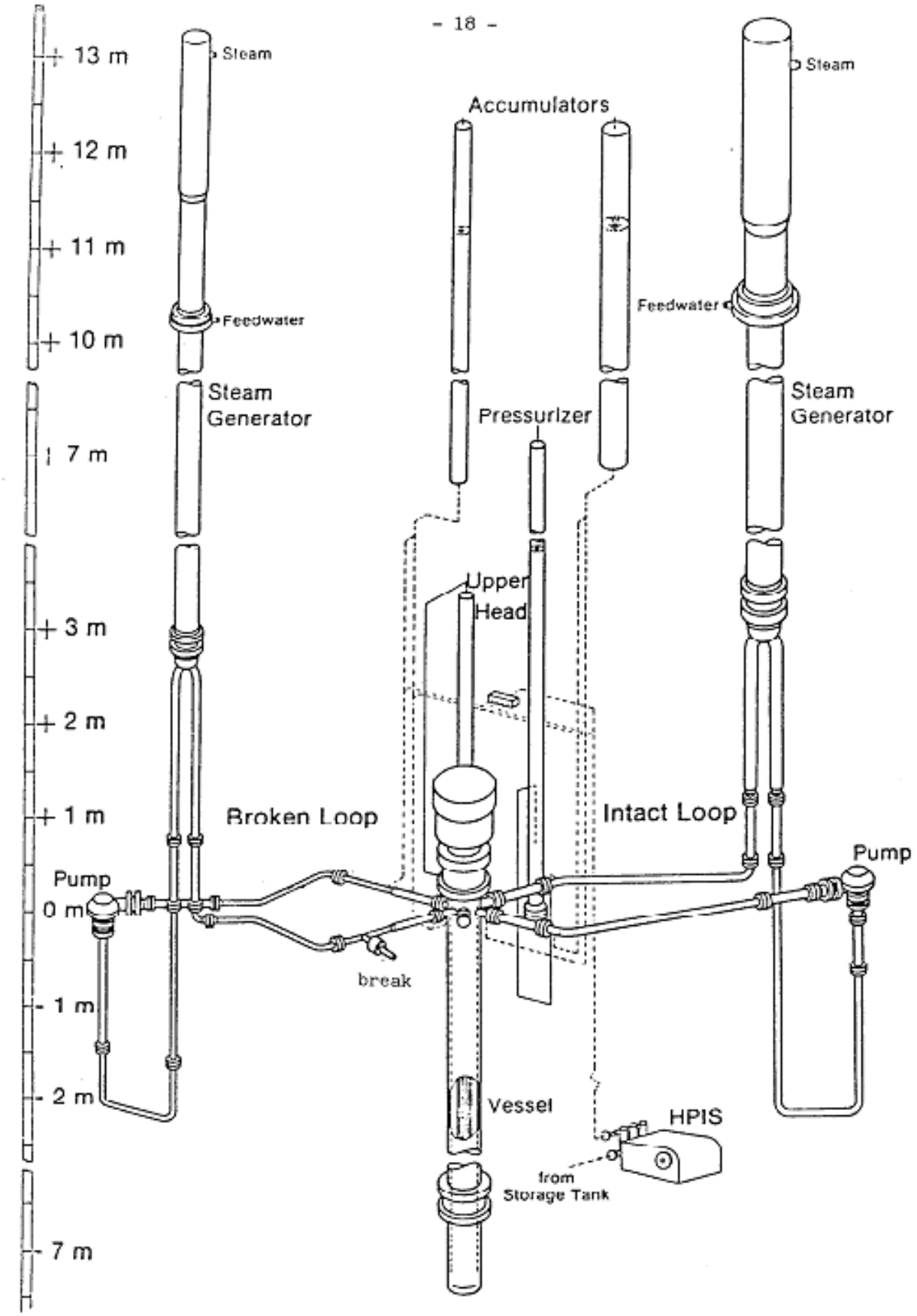

Fig. 3 – LOBI-Mod2 facility: overall view of the facility layout.

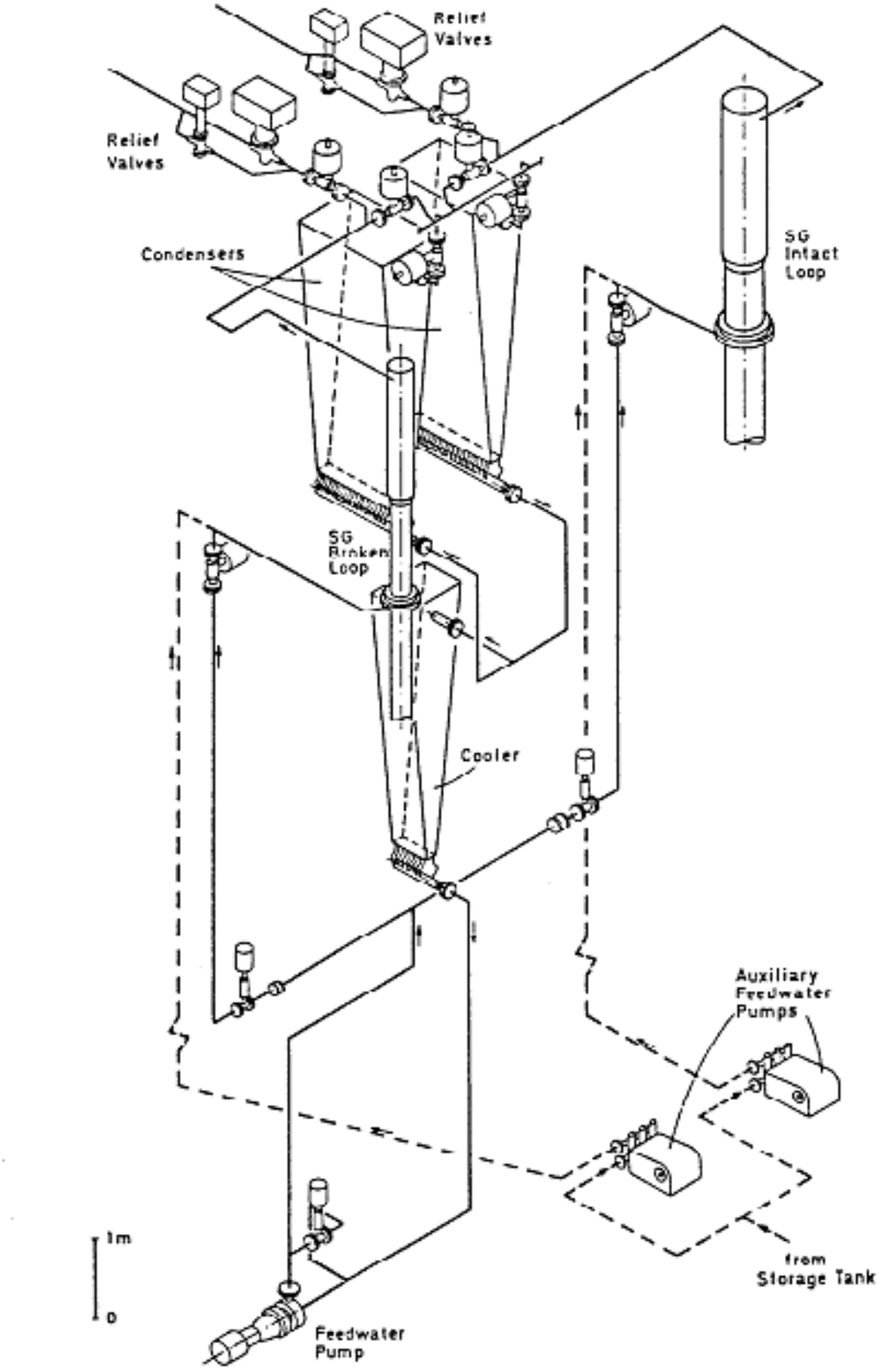

Fig. 4 – LOBI-Mod2 facility: secondary side flow paths.

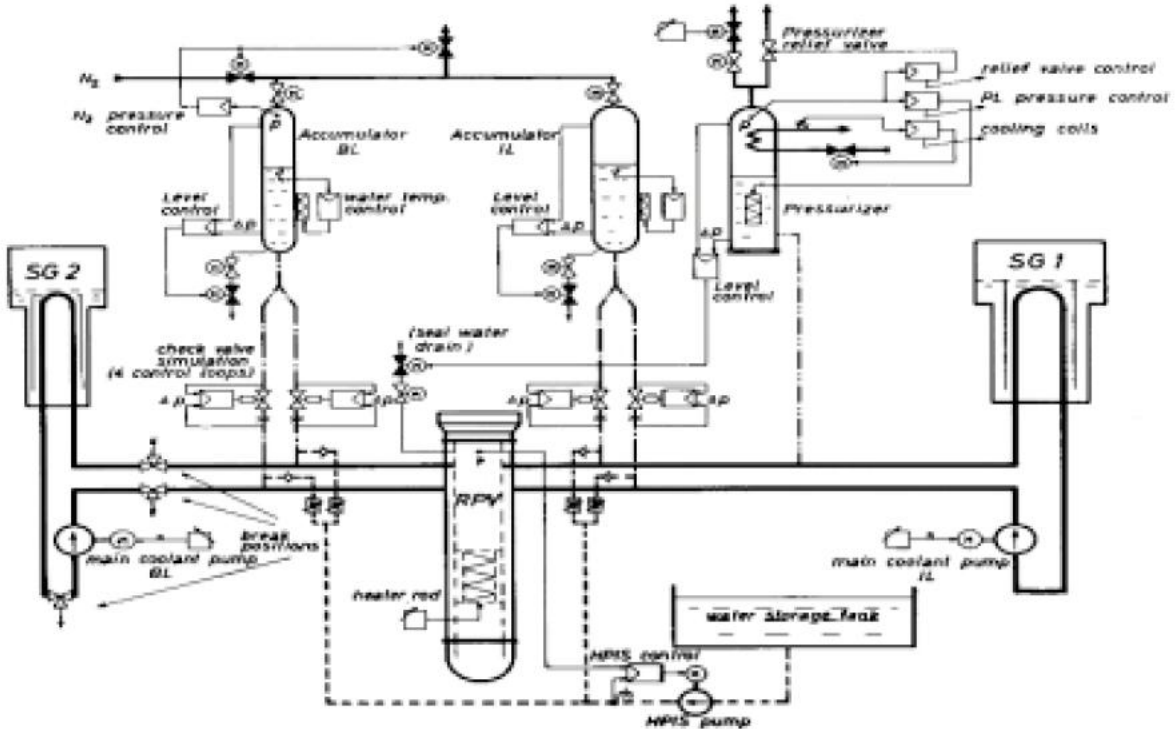

Fig. 5 – LOBI-Mod2 facility: flow diagram.

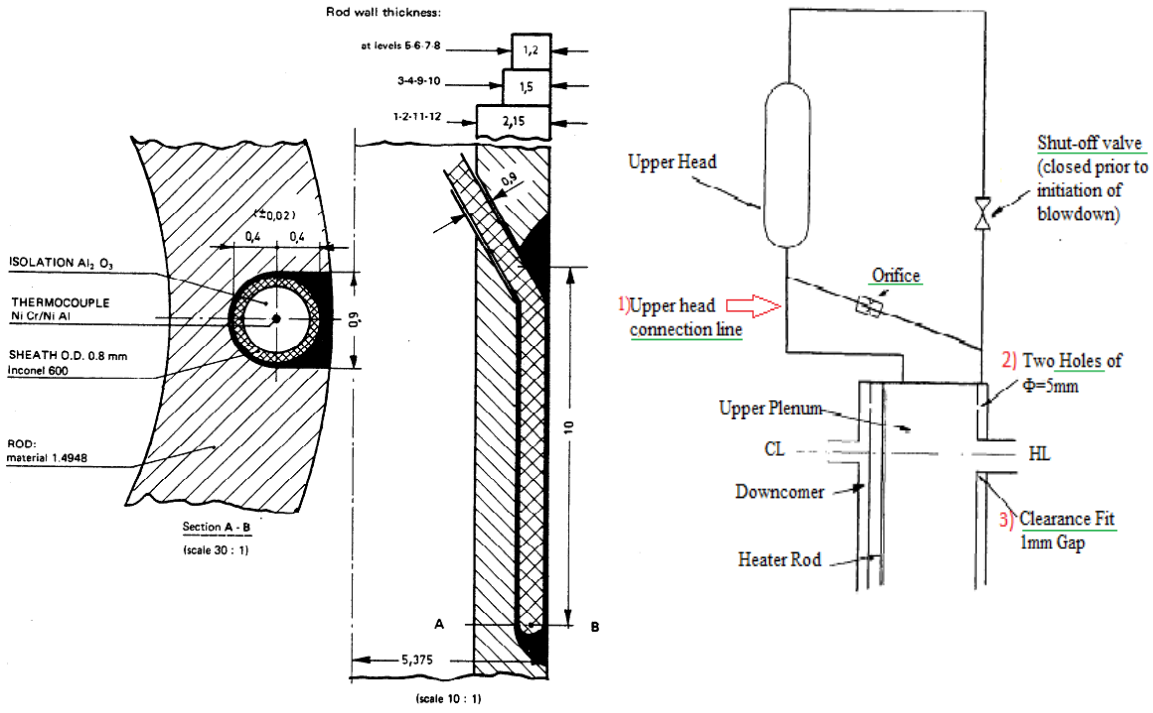

(a) *(b)*

Fig. 6 – LOBI-Mod2 facility: thermocouples position (a) and upper head layout (b)

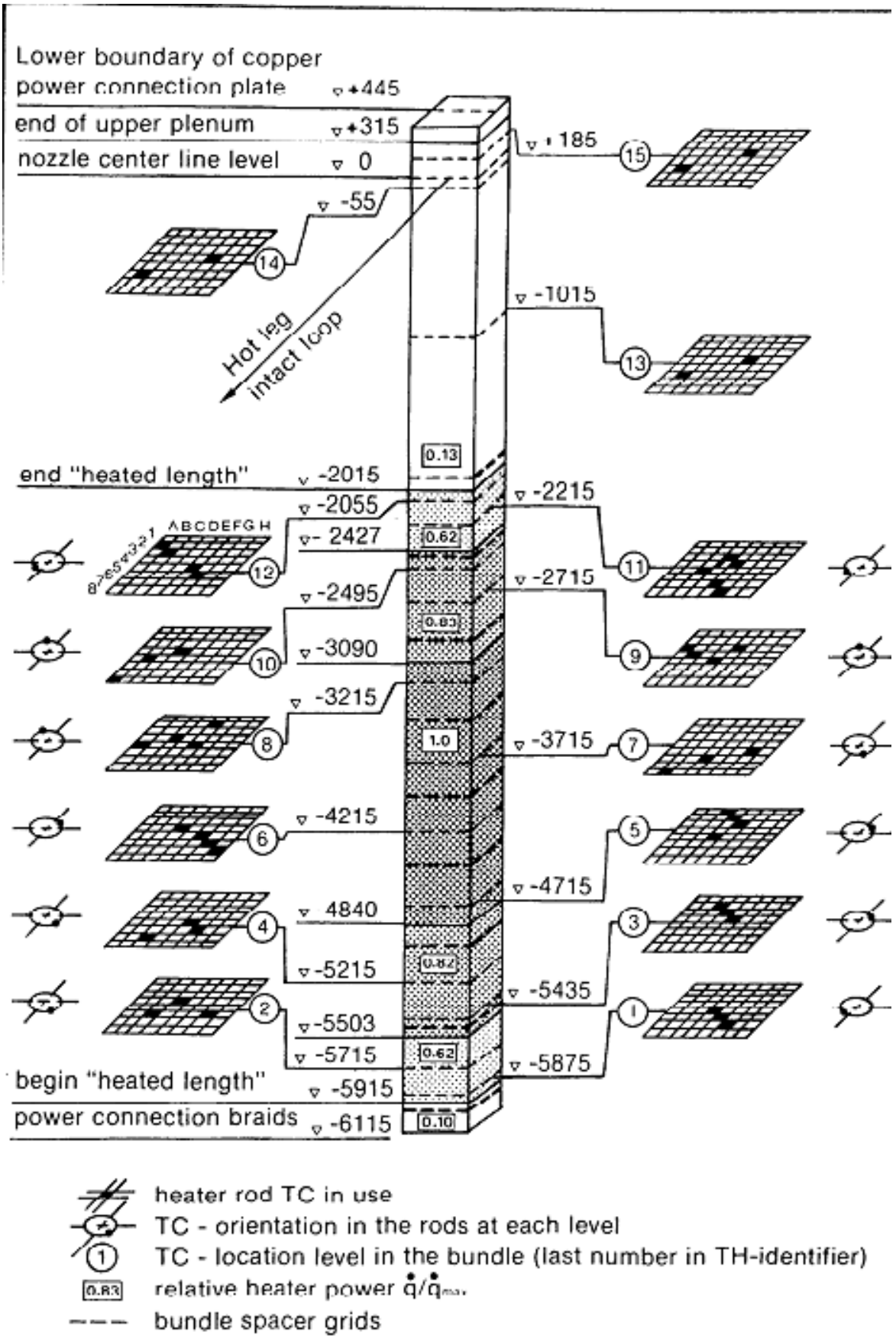

Fig. 7 – LOBI-Mod2 facility: thermocouples position.

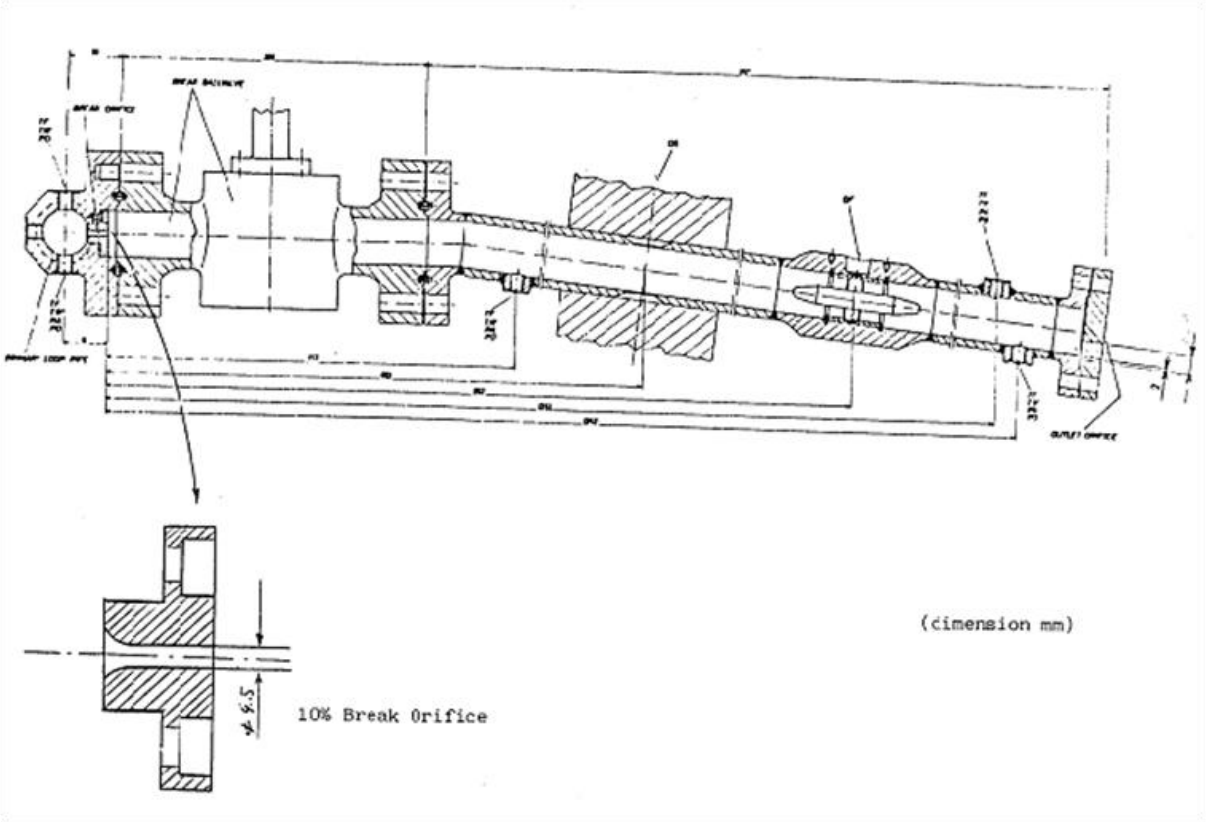

Fig. 8 – LOBI-Mod2 facility: break system

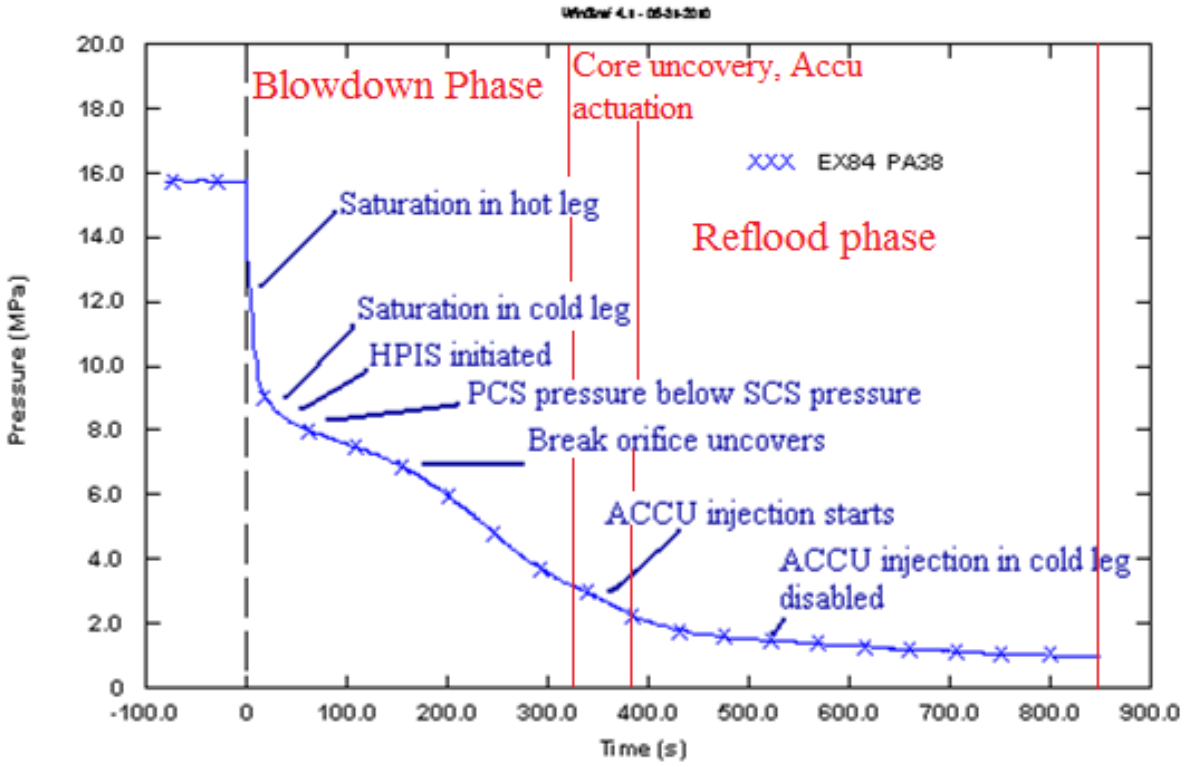

Fig. 9 – LOBI A1-84 test: primary pressure and main thermal hydraulic events

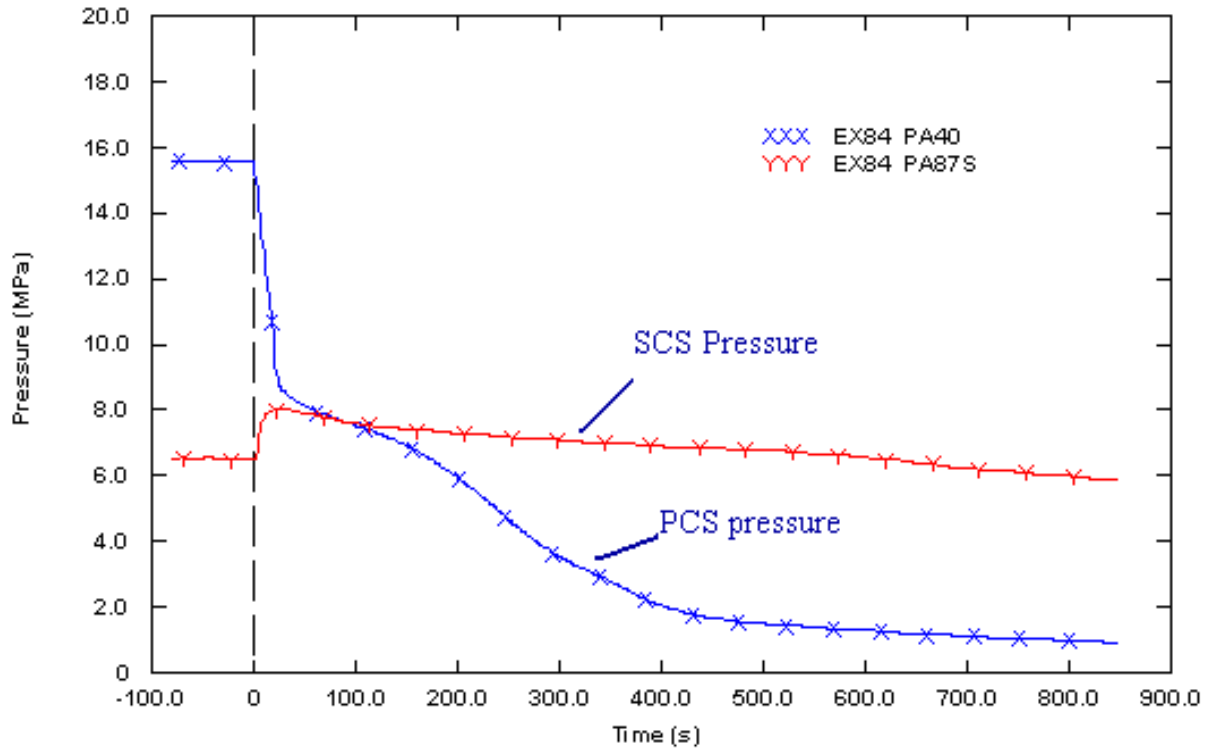

Fig. 10 – LOBI A1-84 test: primary and SG IL pressure

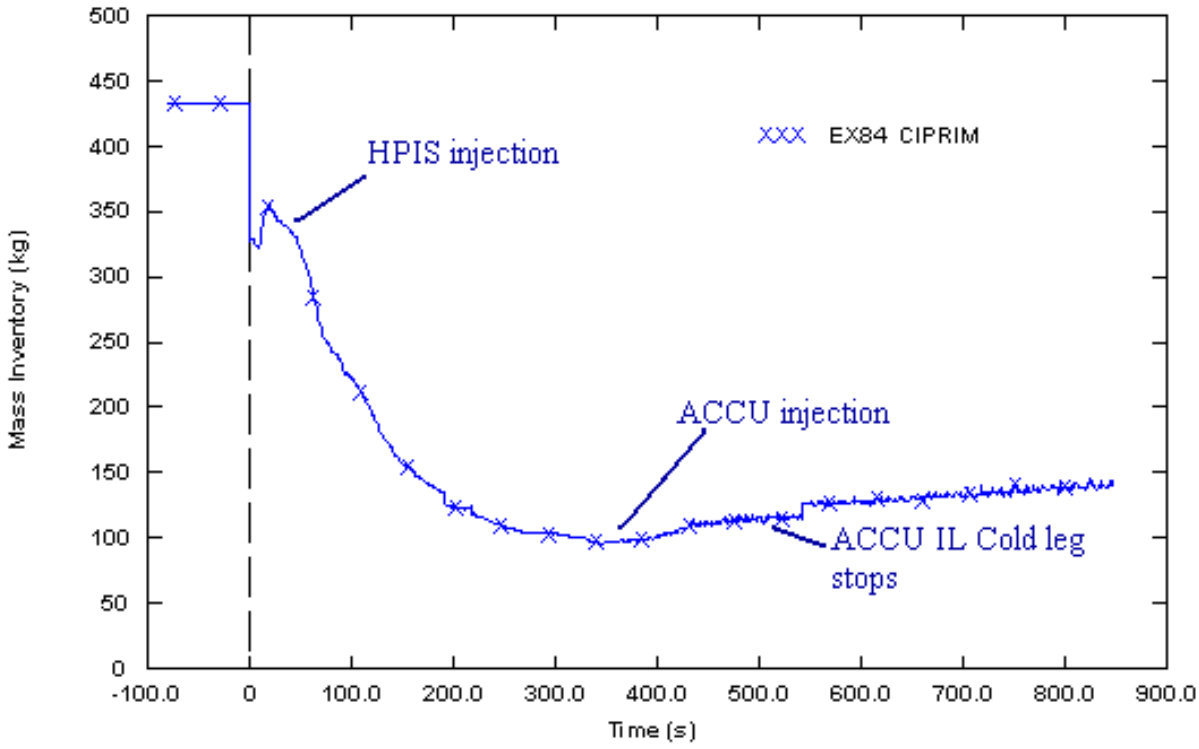

Fig. 11 – LOBI A1-84 test: primary mass inventory

3 Description of Rosa V/LSTF facility and the experiment

3.1 Rosa V/LSTF facility

The LSTF facility is located at the Tokai Research Establishment of the Japan Atomic Energy Research Institute (JAERI) [15].

The ROSA/LSTF is an experimental facility designed to model a full height primary system of a reference PWR. The four primary loops of the reference PWR are represented by two equal-volume loops. The overall facility scaling factor is l/48. The overall scaling factor was used as follows:

- **Elevations**: preserved, i.e., one to one correspondence with the reference PWR. Because the LSTF hot and cold leg inner diameters (IDS) are smaller than those of the reference PWR, only the top of the primary hot and cold legs (IDS) were set equal to those of the reference PWR.
- **Volumes**: scaled by the facility scaling factor l/48.
- **Flow area**: scaled by l/48 in the pressure vessel and l/24 in the steam generators. However, the hot and cold legs were scaled to conserve the ratio of the length to the square root of pipe diameter, i.e., $L/\sqrt{D}$ for the reference PWR. Such an approach was taken to better simulate the flow regime transitions in the primary loops.
- **Core power**: scaled by l/48 at core powers equal to or less than 14% of the scaled reference PWR rated power. The LSTF rated and steady-state power is 10 MWt, i.e., 14% of the rated reference PWR core power scaled by l/48.
- **Fuel assembly**: dimensions, i.e., fuel rod diameter, pitch and length, guide thimble diameter pitch and length, and ratio of number of fuel rods to number of guide thimbles, designed to be the same as the 17 x17 fuel assembly of the reference PWR to preserve the heat transfer characteristics of the core. The total number of rods was scaled by 1148 and is 1064 for heated and 104 for unheated rods.
- **Design pressures**: roughly the same as the reference PWR.
- **Fluid flow differential pressures**: designed to be equal to the reference PWR for scaled flow rates.
- **Flow capacities**: scaled by the overall scaling factor where practicable.

Primary Coolant System
The primary coolant system is composed by the pressure vessel containing an electrically heated core, primary loop piping, coolant pumps and pressurizer. Each component is described in detail below (see Fig. 12 and Fig. 13).

Pressure Vessel and Internal Structures
Pressure Vessel Assembly. The pressure vessel houses a full-length core with 1064 electrically heated rods and 104 unheated rods. The vessel is fabricated out of stainless steel (SUS316L) clad carbon steel (SB49) and rated at a pressure of 17.95 MPa and temperature of 630.2 K. It is 11.0 m tall with an inside diameter of 0.64 m and wall thickness of 61 mm including the clad. The LSTF pressure vessel and the reactor vessel of the reference PWR are compared graphically in Fig. 14 and Fig. 16. The vessel's internal space can be divided into the core, annular downcomer, lower plenum and the upper plenum. The lengths of the core and downcomer, as well as the elevations of various internal components relative to the

bottom of the heated zone, are conserved with respect to those of the reference PWR (when practicably possible). Relative elevations of the pressure vessel components in LSTF and PWR are compared in Tab. 7. The nozzles for the hot and cold leg piping are located at the same elevation above the top of the core. Two primary coolant loops are attached to the pressure vessel at these locations.

Pressure Vessel Internals. The upper plenum structure and internals are shown in Fig. 16. Most of the components are made of stainless steel. Support plate and upper core plate are located at respectively the same elevation as in the reference PWR. The upper core support plate is attached to the support barrel which is fixed to the pressure vessel shell head. The upper core plate is also attached to the bottom of the top section of the core barrel and hung from the upper core support plate by means of core support columns. Some control rod simulators are attached to both the core support plate and upper core plate. The core barrel consists of three separate barrels stacked up in series.

Core and Lower Plenum. In comparison with the reference PWR, the length of the heated zone, fuel rod diameter and pitch, power peaking factor and number of spacers are conserved. The core volume and the number of fuel rods are scaled at a ratio of l/48. The bottom section of the core barrel has openings which effectively form the flow channel between the downcomer and the lower plenum. The top of the openings corresponds to the bottom of the downcomer and the elevation relative to the bottom of the heated zone is the same as in a PWR. The core contains 16 square 17 x17 bundles and 8 semi-crescent shaped bundles. The core power profile is chopped cosine in shape with a peaking factor of 1.495 Fig.. Eight bundles contain high power-density heater rods (1.4 kW), and the remaining bundles contain low power-density heater rods (0.97 kW). Each bundle contains heated fuel rods, with non-instrumented and instrumented types. The core instrumentation consists of heater rod cladding and fluid thermocouples and conduction probes attached to heater and non-heating instrument rods (see Tab. 8).

Pressurizer

The pressurizer's function is to control the primary loop pressure and to accommodate any changes in the coolant volume during normal and abnormal plant conditions. The LSTF's pressurizer consists of a 4.19 m tall cylindrical vessel, immersion-type electrical heaters and nozzles used to connect the surge line, pressure vessel vent line, and safety and pressure relief valve lines (see Fig. 18). The LSTF's pressurizer is scaled to have l/48 of the volume and the same height-to-diameter ratio as the pressurizer of a PWR. The normal coolant volume is also scaled at l/48, while the coolant level above the bottom of the core is the same as that of a PWR. The pressurizer is normally connected through the surge line to the primary loop at the A loop hot leg. The power operated relief valve and safety valve are designed to simulate those in a PWR. The spray line is connected to the cold leg of loop A to provide relatively cooler primary coolant for pressure control. The pressurizer control logic built into the LSTF, is the same as that of the reference PWR. The system pressure is controlled by either heating the coolant in the pressurizer or by spraying relatively cooler primary coolant taken from the cold leg. The pressurizer heater consists of 21 heater rods with sheath made of SUS 316L.

Primary Coolant Loops

The LSTF's primary coolant loop consists of two identical loops each representing two loops of the reference four-loop PWR. Major characteristics of the primary loop are summarized and also compared with those of a PWR in Tab. 7. The details of the loop are shown in Fig. 17.

Reactor Coolant Pumps
The reactor coolant pumps (PCs) installed in both primary loops drive the primary coolant into the core to remove the heat generated in the core. In order to simulate the pump characteristics of the reference PWR, the PC of LSTF was designed as follows:

- The type of PC is a canned-type centrifugal pump with configuration of the impeller, casing, inlet and outlet regions similar to those of the PWR reactor coolant pump.
- Pump speed can be controlled electrically to simulate the transient flow characteristics of the PWR reactor coolant pump.
- The capacity of PC is larger than 14% of the 2/48 scaled cold leg flow rate of the reference PWR. The two PCs (PC-A and PC-B) have the same pump characteristics.
- The reverse rotation of PC is not permitted as in the PWR.

Secondary coolant system
The secondary coolant system of LSTF is designed to simulate the steady state and transient responses of the steam and feedwater flows and primary-to-secondary side heat transfer. The main components, such as steam generators and main and auxiliary feedwater pumps of the reference PWR are simulated in LSTF as closely as possible, including the control and trip logics. However, the LSTF has a steam condensing system instead of the turbine generator system in PWR.

There are two steam generators (SG-A and SG-B) each with maximum heat removal capacity of 35 MW, which is l/24 scaled capacity of a PWR SG. Each SG has 141 U-tubes made of stainless steel, arranged in a square array in each SG. The inner diameter and wall thickness of the U-tubes are 19.6 mm and 2.9 mm, respectively (see Fig. 19). The secondary coolant system consists of four subsystems:

- steam generation system i.e., the SG secondary-side,
- steam condensation system including a jet condenser (JC) and cooling towers,
- feedwater system including main and auxiliary feedwater pumps
- pipings and related components including valves, orifices and flow meters. main piping in the secondary system coolant loop, consist of three groups; main steam line, main feedwater line and auxiliary feedwater line.

Blowdown System
The LSTF blowdown system consists of a break unit, blowdown piping and a break flow storage tank (ST). Nineteen break locations are provided in LSTF including the cold and hot legs, the crossover leg, the lower plenum and upper head of the pressure vessel, the pressurizer, the steam generator tube, the steam generator feedwater line and the main steam line. In the cold and hot legs of the primary coolant loop B, the top, middle or bottom break of the pipe can be simulated. The break unit consists of a venturi flow meter, a spool piece to measure two-phase break flow rate and density, a break area simulation orifice and a break simulation valve (see Fig. 20). The effluence from the break is collected in the ST. The liquid level change in the ST is used to measure the break flow rate.

Emergency core cooling system
The LSTF emergency core cooling systems (ECCSs) consist of a high pressure injection system (HPIS), a low pressure injection system (LPIS), an accumulator (ACCU) injection

system, and a residual heat removal (RHR) system. There are several ECC injection locations as a test parameter.

High Pressure Injection System
The HPIS is designed to be able to change the injection location during a test. The system has two pumps. One is a high pressure injection pump (PH) and the other is a charging pump (PJ). The injection flow rates are automatically controlled by the controller with the programmed head-flow curves.

Low Pressure Injection System
The low pressure injection pump for LPIS is a centrifugal type Pump. The flow rate is controlled by a flow control valve.

Accumulator Injection System
LSTF has two accumulator tanks. One Is the ACC-Cold simulating an actual PWR Accumulator tank, and the other is the ACC-Hot, designed to inject hot water into the primary system to investigate the effect of ECC subcooling. The Accumulators flow rates are controlled by the orifices in the surge lines. The volume of each Accumulator tank is 4.8 m^3, which is 1.5 times larger than the volume scaled at l/48 of four Accumulator tank volumes of the reference PWR. Electric heaters (140 kW and 280 kW) are installed in the ACC-Cold and -Hot tanks, respectively. The pressure and temperature of the Accumulator coolant water are controlled by the heater output and N2 gas pressure.

Residual Heat Removal System (RHR)
The RHR system consists of a low pressure injection pump (PL) and a RHR heat exchanger (HX). The fluid in the hot leg is cooled through the RHR-HX and re-injected into the cold leg by the PL, which functions as the RHR Pump when the RHR system is operated. The coolant temperature and flow rate are controlled by the flow control valve and the heat exchanging rate.

3.2 Rosa V/LSTF Test SB-HL-17

3.2.1 Objectives of Test SB-HL-17

Experimental programs in scaled integral test facilities are set up to solve open issues of actual nuclear power plant design, in order to demonstrate the technical feasibility of innovative designs, and to obtain reference databases, required to support codes development and assessment. Experimental data are fundamental for demonstrating the reliability of computer codes in simulating the behavior of a NPP during a certain accident scenario. The OECD/NEA CSNI PKL-2, intends to study some selected accident scenarios at system level, understanding the thermal hydraulic phenomena which occurs in a pressurized water reactor, and so validating and improving thermal-hydraulic system codes used in safety analysis. In this framework, this particular activity is devoted to support the design of the PKL-LSTF counterpart test, an experiment which will be carried out in PKL-2 facility (by AREVA NP in Erlangen, Germany), and in ROSA/LSTF facility (JAERI).

This two ITF have different layout, different scaling concepts and different scaling ratios. The aim of the project is to compare the behavior of the two facilities simulating the same accident, a SB-LOCA, in order to understand the phenomena that they reproduce differently, improve the setting up of future tests and improve the knowledge about SB-LOCA.

The difficulties, when setting up the same test for two different facilities, are many and difficult to overcome. The main design differences between the two facilities are as follows:

- PKL is a 4 loop facility, ROSA/LSTF is a 2 loop facility
- Differences in scaling ratios
- Differences in the ECCS design

Besides, there is another fundamental difference: PKL works at low pressures (maximum pressure: 45 bar), ROSA/LSTF works at full pressure (150bar).

In this work, in order to propose initial conditions suitable for the two facilities' tests, the problem that has been addressed was to obtain a sequence of events, during the transient of ROSA/LSTF facility, feasible even for PKL-2 facility, which starts its transient at 40 bars.

Logical steps of the work
LSTF/ROSA investigations by RELAP5/Mod3.3:

- achieving a reliable nodalization of LSTF ITF by means of a posttest analysis of a similar scenario, test 1.2 (SB-HL-17);
- investigating (pretest) LSTF ITF performances in order to define a suitable scenario fulfilling the objectives of the project, (defined in the next paragraphs), possibly, including low pressure pre-tests for mastering the pressure scaling approach;

In this chapter the attention will be focused on the setting up of the post-test of ROSA/LSTF experiment 1.2 (with RELAP5/Mod3.3 code), used to validate the code. This has been the basis to built the blind test, and make a proposal in deciding the initial conditions of the counterpart-test, that will soon executed in the ITFs already mentioned.
PKL-2 calculations were executed with Cathare code at GRSPG.

3.2.2 Description of SB-HL-17

LSTF test 1.2 is a 1.0% hot leg break LOCA simulation. This test has been used to validate the code to reproduce an SB-LOCA, and the nodalization has been used to set-up the pretest. The break location was in the hot-leg B so as not to disturb the cold-leg flows. A downward oriented flash-type break orifice with the inner diameter of 10.1 mm was used. The flow area of the break orifice corresponds to 1.0 % of the volumetrically-scaled cross-sectional area of the reference PWR cold leg.

The high-pressure injection system (HPIS) and the accumulator injection system were actuated automatically. Specified operational set points and conditions are shown in
Tab. 10. A single failure was assumed for HPIS of the reference PWR, and the flow rate used in Test 1-2 was a half of the scaled flow rate. In LSTF, HPIS is simulated with the charging pump (PJ) and the high-pressure injection pump (PH). However, PH cannot be operated at the pressure higher than 10.5 MPa because of its pump head. Thus, PJ is used alone to inject into A and B loops at higher pressures, and PJ and PH are, respectively, used to inject into A and B loops at lower pressures in LOCA experiments. The injection ratio of these ECCS water to A and B loops was 1:1.

Each cold leg has the accumulator, and the flow rates of the accumulator water is almost the same for A and B loops. The initial core power was 10 MW with the profile in Fig. 15.

One of the existing video probes installed in hot legs was used to see the flow condition in hot-leg B. The video probe in hot-leg B was directed to the pressure vessel in this experiment, though the video probes in hot legs are usually directed to SGs in other experiments. [16]

The hot-leg break experiment was started by opening the break valve after the steady-state was established. The chronology of major events observed in this experiment is shown in Tab. 11.

In this test the break flow changes from single-phase liquid to two-phase mixture at about 100 s, and then from two-phase mixture with low void fraction to two-phase mixture with high void fraction at about 900 s. The HPIS is actuated at 92 s. The accumulator injection flow rates are calculated from the accumulator tank levels.

The pump rotation speed is increased to the maximum of about 26 rps immediately after break to improve the similarity of LSTF to the reference PWR. The secondary pressures increase after the main steam line valve is closed at 52 s, and the SG relief valves open several times. The flow rates in the primary side loops are increased by the increase in pump rotation speed immediately after break, and decreased due to pump coast down. The primary loop flows almost stop at about 450 s.

The liquid level in the core decreases first after the primary pressure reaches the saturation pressure. The hot-leg liquid levels decrease with a delay if compared with the core level, and the liquid levels in the upper plenum and in the upper head are then decreased due to an accumulation of steam. The downcomer liquid level then decreases to the cold-leg level, and the cold-leg liquid level finally starts to decrease. The downcomer liquid level decreases to the cold-leg level at about 250 s, and does not change much thereafter. The two-phase flows appear in the cold legs after 250 s. The primary loop flows stop at about 450 s, and the injected ECCS water flows into the core through the stratified flow region in the cold legs. Since the loop flow stops, the flow condition in the cold legs is complicated: the cold ECCS water flows at the bottom toward the downcomer, mixing occurs with the upper hot water, there may be flows in the upper hot water, condensation occurs at the two-phase interface, and there may be some steam flows above the liquid surface. The upper plenum and cold-leg liquid levels slightly increase after 1000 s, and the core and hot-leg liquid levels increase after about 2000 s, since the ECCS flow rates are higher than the break flow rate. The core is shown to become full of liquid at about 3400 s, and the liquid levels in both cold and hot legs reach the top of the legs at about 4100 s.

The break flow is single-phase liquid before the hot-leg liquid levels start to decrease, and two-phase mixture when the liquid level is kept relatively higher until 900 s. Thanks to the video probes installed in the loops (see Fig. 21), is it possible to better understand the changing in the flow regimes during the transient. It’s possible to see that the hot legs do not become empty after 900 s, and the break flow with a small flow rate is thus not pure single-phase vapor but two-phase mixture with high void fraction.

Liquid levels are formed in cold legs from about 250 to 4100s. The injected ECCS water jet is also observed. The flow regime is a horizontal stratified flow. The natural circulation is stopped at about 450 s. The temperature distribution in the cold legs is greatly affected by the ECCS injection (see Tab. 11and Tab. 12).

Tab. 7 – Major design characteristics of LSTF and PWR.

#	CHARACTERISTIC	LSTF	PWR	PWR/LSTF
1	Pressure (MPa)	16	16	1
2	Temperature (K)	598	598	1
3	Number of fuel rods	1064	50952	48
4	Core height (m)	3.66	3.66	1
5	Fluid Volume V (m^3)	7.23	347	48
6	Core Power P (MW)	10	3423(th)	342
7	P/V (MW/m^3)	1.4	9.9	7.1
8	Core inlet flow (ton/s)	0.0488	16.7	342
9	Downcomer gap (m)	0.053	0.26	4.91
10	Hot Leg diameter (m)	0.207	0.737	3.56
11	L (m)	3.69	6.99	1.89
12	$L/\sqrt{D}$ ($m^{\frac{1}{2}}$)	8.15	8.15	1
13	Number of loops	2	4	2
14	Number of tubes in steam generator	141	3382	24
15	Length of steam generator tube (average) (m)	20.2	20.2	1

Tab. 8 – LSFT facility: major core characteristics.

#	ITEM	LSTF	PWR	RATIO
1	Number of rod bundles	24	193	--
2	Bundle size	7x7 (square)	17x17	--
3	Total number of fuel rods	1168	55777	1/47.75
4	Number of heater rods	1064	50952	1/47.89
5	Nr of non-heating rods	104	4825	1/46.39
6	Diameter of heater rods (mm)	9.5	9.5	1
7	Diameter of non-heating rods (mm)	12.24	12.24	1
8	Rod pitch (mm)	12.6	12.6	1
9	Heated length (m)	3.66	3.66	1
10	Cladding thickness (mm)	1	0.57	1.754
11	Cladding material	Inconel	Zr-4	--
12	Number of spaces	9	9	--
13	Core volume (m^3)	0.4078	17.5	1/42.91
14	Core flow area at spacer (m^2)	0.06774	3.7	1/54.62
15	Core flow area below the spacer (m^2)	0.1134	4.75	1/41.89
16	Core flow area at lower nozzle (m^2)	0.06653	2.988	1/44.91

Tab. 9 – LSFT facility: design characteristics for steam generators.

#	ITEM	LSTF	PWR	RATIO
1	Number of SGs	2	4	1/2
2	Maximum heat removal rate (MW)	35	856	1/24
3	Number of U tubes	144	3382	1/24
4	Feedwater flow rate (m/s)	2.76	469	1/170
5	Steam flow rate (m/s)	2.76	468	1/170
6	Pressure in SG steam dome (MPa)	7.34	6.13	1.2
7	Temperature in SG steam dome (K)	562.2	550.2	1.02
8	Primary coolant flow rate (kg/s)	24.5	8352	1/341
9	Pressure in primary loop (MPa)	15.61	15.61	1
10	Inner diameter of U-tubes (mm)	19.6	19.6	1
11	Outer diameter of U-tubes (mm)	25.4	22.13	1.14
12	Average length of U-tubes (m)	19.7	20.2	1
13	Pitch of U-tubes (mm)	32.5	32.5	1
14	Total inner surface area of U-tubes (m^2)	171	4214	1/25
15	Total outer surface area of U-tubes (m^2)	222	4780	1/22

Tab. 10 – LSTF test SB-HL-17: facility configuration.

#	SYSTEM	SYMBOL	CHARACTERISTICS	STATUS	REMARKS
1	PRZ connection status	--	Loop #A	--	--
2	PRZ safety valve	--	Nozzle: Φ= 14.4mm	Active	Not operated during the transient
3	UH – DC bypass	--	Orifice: Φ=9.619mm;	--	--
4	Break component	--	Connected with hot leg B. Orifice: Φ= 10.1mm (1%)	--	Flash type, downward
5	ECCS Accumulators	--	2 systems available connected with both cold legs. Initial P = 4.51 MPa	Active	System isolated if the mass inventory discharged by each ACCU is equal 1050kg
6	ECCS HPIS	--	2 trains connected with both CL	2 trains active	Flow rate of a HPIS pump regulated
7	ECCS LPIS	--	2 trains connected with both CL	Not operated	--
8	MCP	--	2 MCP in operation	Active	MCP operated at 13.9 rpm corresponding to 25.3 kg/s per loop
9	SG safety valve	--	Orifice: Φ =26.6mm	Active	Not operated during the transient
10	SG relief valve		Orifice: Φ =16.2mm	Active	--
11	Residual Heat Removal System	--	--	Not operated	--
12	FW	--	--	Active	Flow rate regulated to maintain the level
13	AFW /EFW	--	--	Not operated	--

Tab. 11 – LSTF test SB-HL-17: imposed sequence of main events.

#	IMPOSED EVENT DESCRIPTION	SYSTEM	SIGNAL (TIME OR SET POINT)	REMARKS
1	1.0% BRK opening in Hot leg B	Break component	0 s	--
2	Reactor scram	--	P=12.97 MPa	The power start to decrease after 18 s from the low pressure signal to preserve the energy in the fuel rod
3	Trip of the MCP and coast-down	MCP	Event #2	Connected with reactor SCRAM
4	PRZ heaters turned off	PRZ heaters	Event #2	Connected with reactor SCRAM
5	Main steam line valve close	--	Event #2 + 3.0 s	Connected with reactor SCRAM
6	MSIV close	--	Event #2 + 3.0 s	Connected with reactor SCRAM
7	FW stops	--	Event #2 + 6.0 s	Connected with reactor SCRAM
8	SG relief valve on /off		8.03 / 7.82 MPa	--
9	SG safety valve on /off		8.68 / 7.69 MPa	--
10	Safety injection signal		P=12.27MPa	--
11	HPIS injection	2 PH trains	Event #10 +12s delay	Flow rate of a HPIS pump regulated
12	ACCU on		P = 4.51MPa	--

Tab. 12 – LSTF test SB-HL-17: phenomenological windows and resulting sequence of main events.

Ph.W.	DESCRIPTION & PHENOMENA/PROCESSES	TIME SPAN [S]	EVENT	EXP [s]	Note
I	**Blowdown:** – **PRZ thermo-hydraulics (depressurization, evaporation, condensation)** – **Void formation** – **Phase separation** – **natural circulation (single phase and two phase)** – **reflux condenser mode** – **break (critical) flow** – **heat transfer in core covered** – **reverse heat transfer from SS to PS**	**0 – 900**	*SoT (break opening) in BL HL*	**0**	Imposed
			Scram	**49**	Imposed
			PRZ proportional heaters switched off	**49**	With scram
			Stop of FW pumps	**49**	With scram
			MCPs start coastdown	**49**	With scram
			Main steam line turbine valve closes	**49**	With scram (3s)
			FW stops	**55**	--
			Main steam isolation valve closes A/B	**72/74**	Imposed
			Safety injection signal	**77**	Imposed
			HPIS start	**89**	Imposed
			Downcomer liquid level decreases to CL level	**250**	--
			Two phase flow in CL	**250**	--
			MCPs Stop	**303**	--
			Primary loop flow stops	**450**	--
			NC stops	**450**	
			Hot leg empty	**900**	
II	**Minimum core level occurrence, due to two phase discharge at high void fraction:** – **stratification (horizontal) during ECCS injection** – **heat transfer in core covered** – **heat transfer in core uncovered**	**900-2537**	*Occurrence of minimum RPV level*	**989**	--
			CLs level starts to increase	**1000**	
			HLs and core level start to increase	**2000**	
			Accumulator Actuation IL CL	**2537**	Imposed
			Accumulator actuation BL CL	**2537**	Imposed
III	Reflood: – **heat transfer in covered core** – **possible steam binding** – **bottom up quenching** – **entrainment and de-entrainment of coolant**	**3400-4697**	*Rewet at the uppermost elevation of the rod bundle*	**3400**	--
			Liquid level in CLs and HLs reach the top of the legs	**4100**	--
			Accumulator injection stops IL CL	**4697**	--
			Accumulator injection stops BL CL	**4697**	--
			End of test	**4697**	Imposed

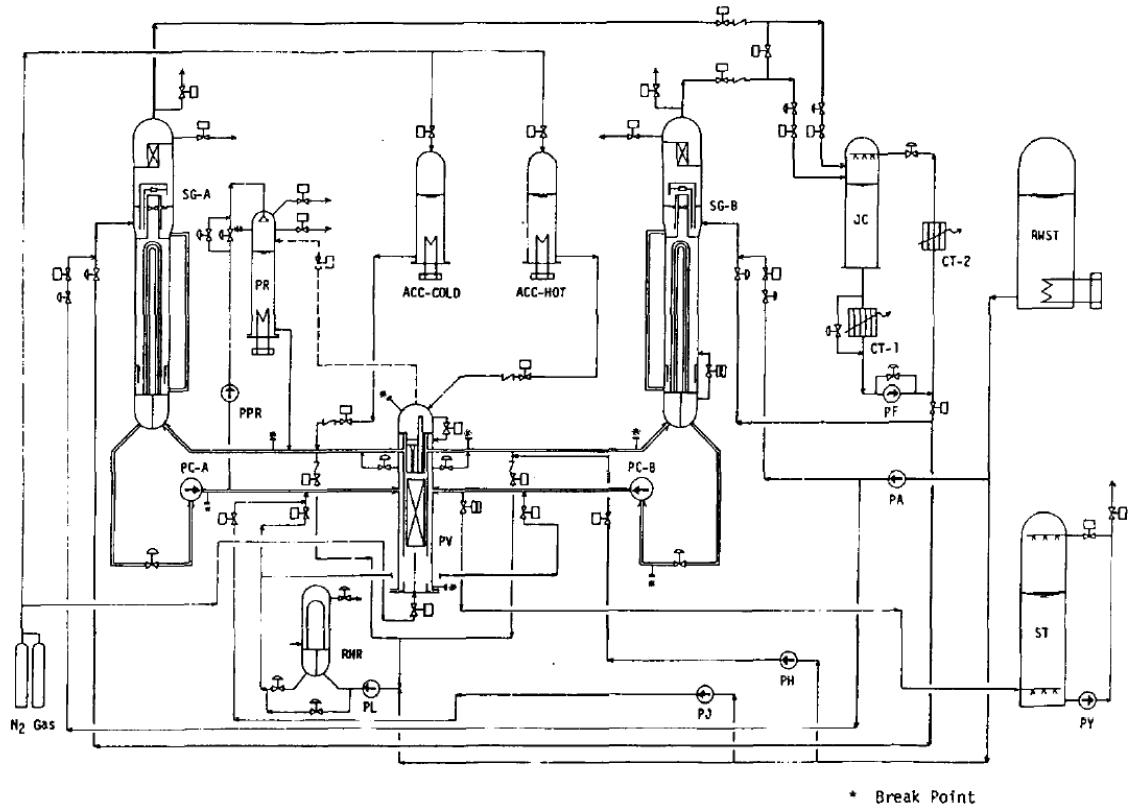

Fig. 12 – LSTF facility: flow diagram

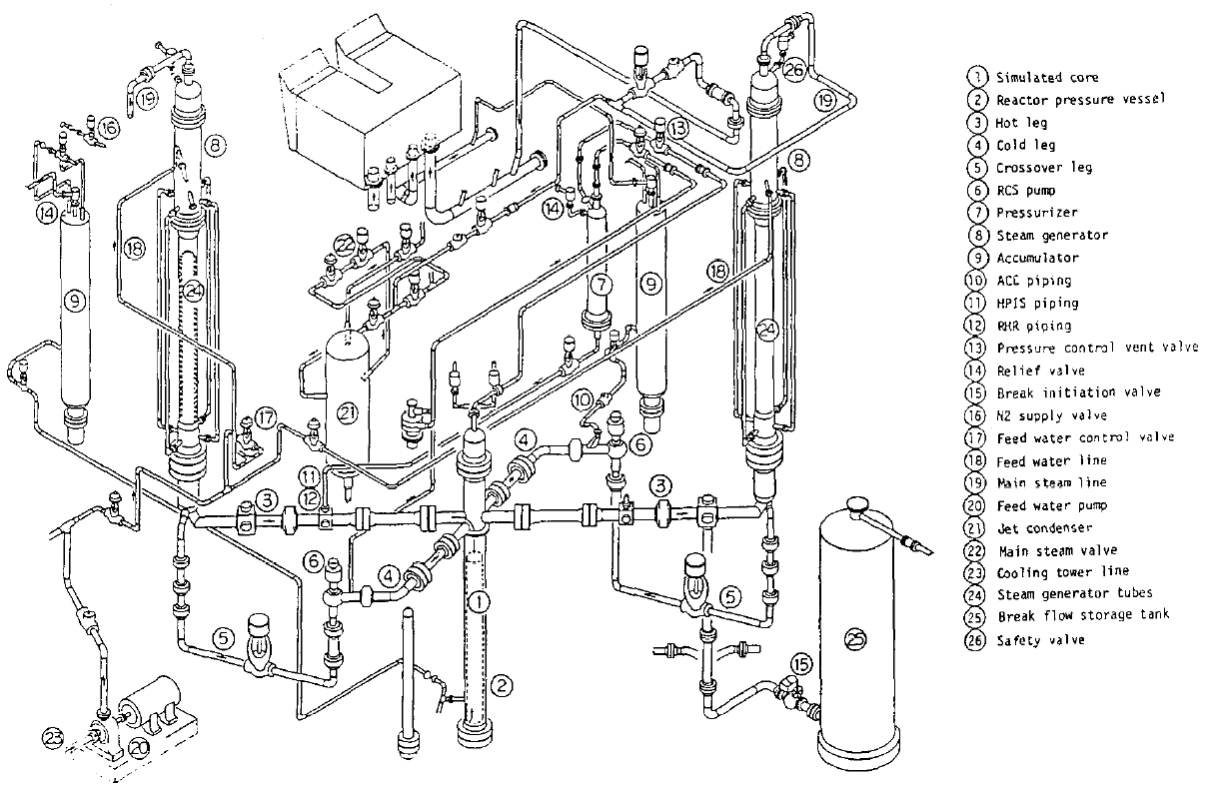

Fig. 13 – LSTF facility: general view.

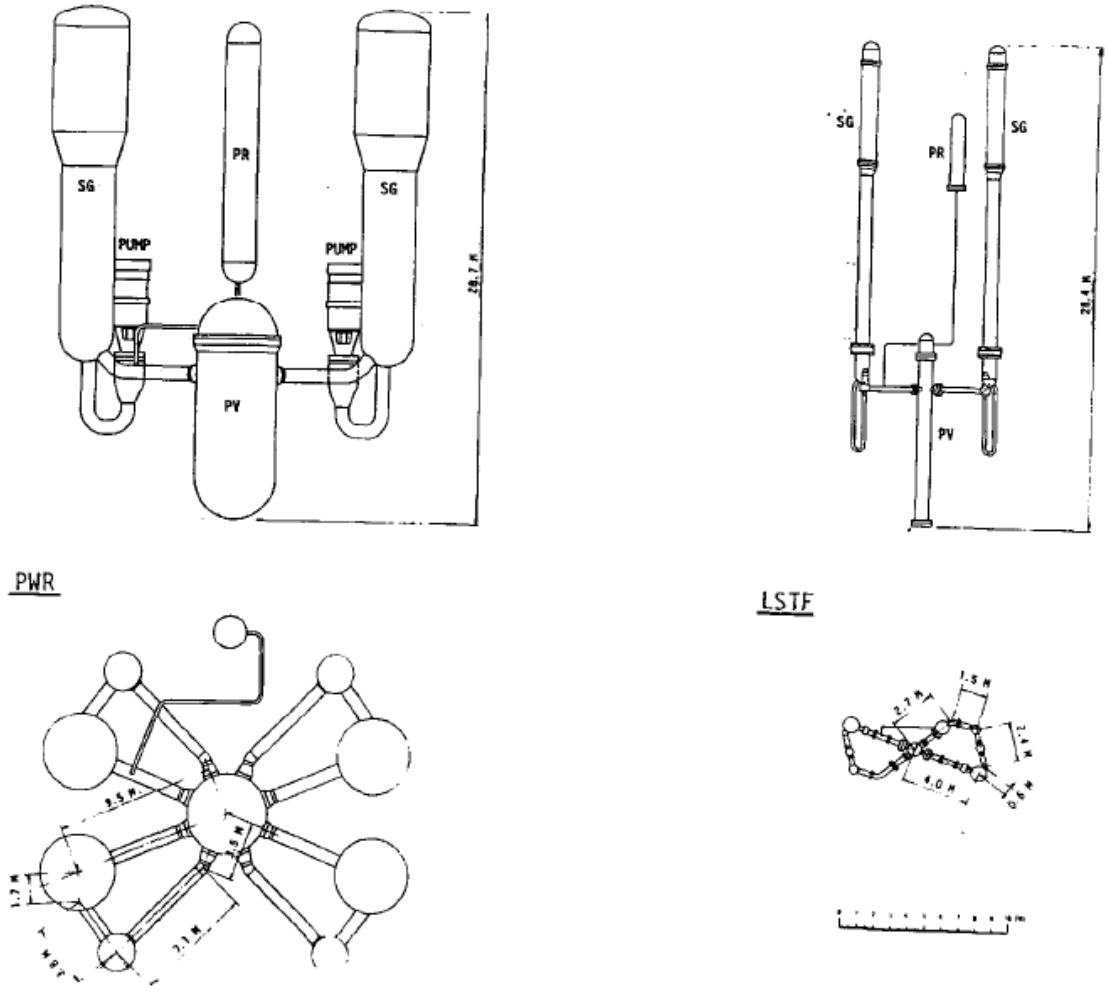

Fig. 14 – Comparison between PWR and LSTF facility.

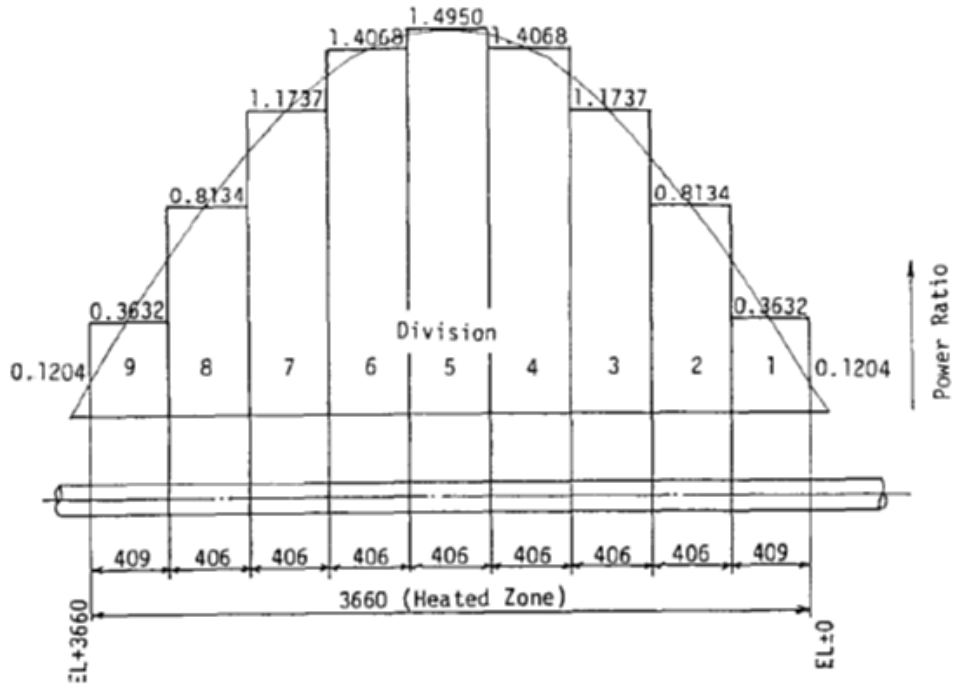

Fig. 15 – LSTF facility: axial core power profile

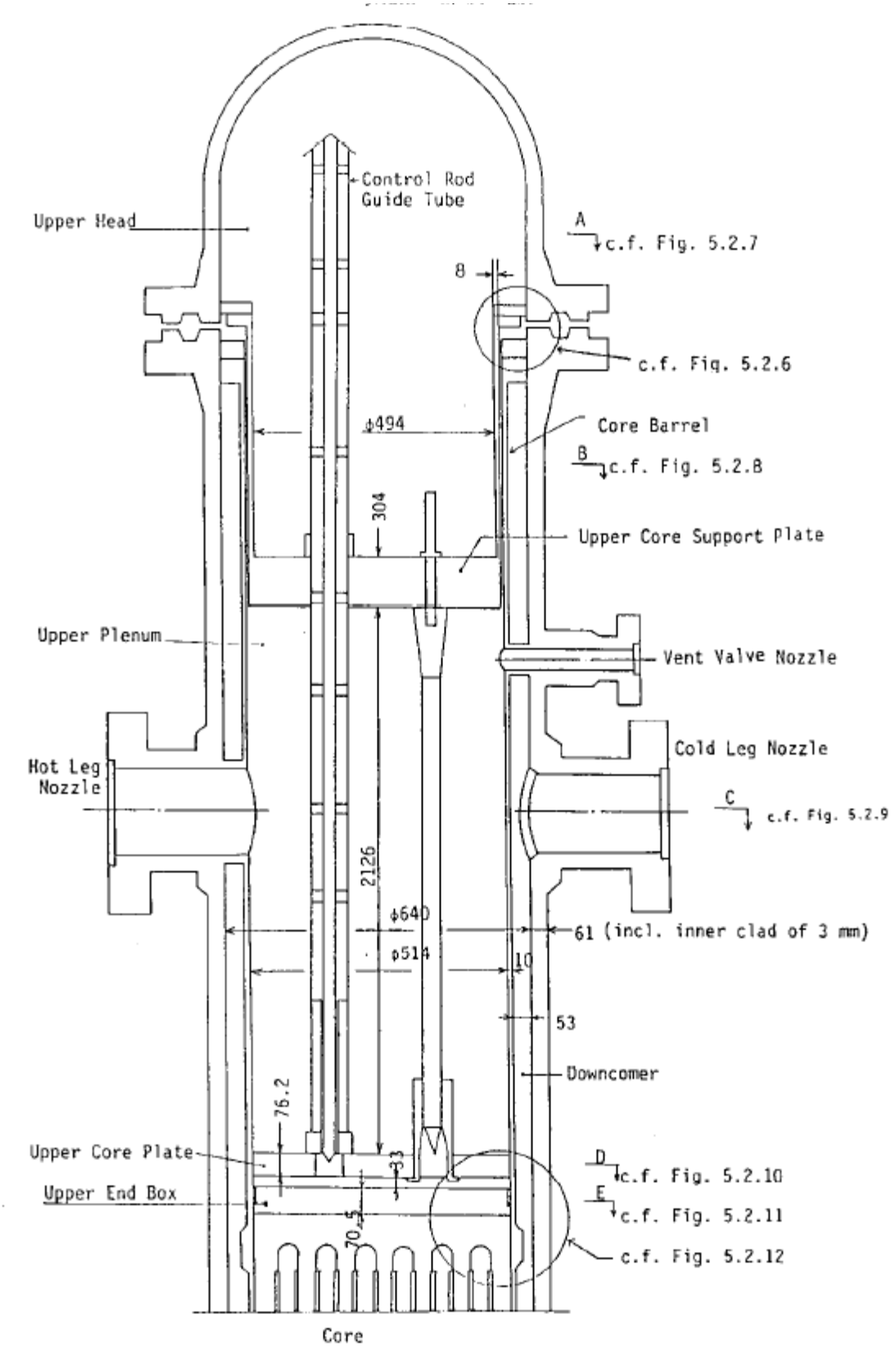

Fig. 16 – LSTF facility: pressure vessel internals

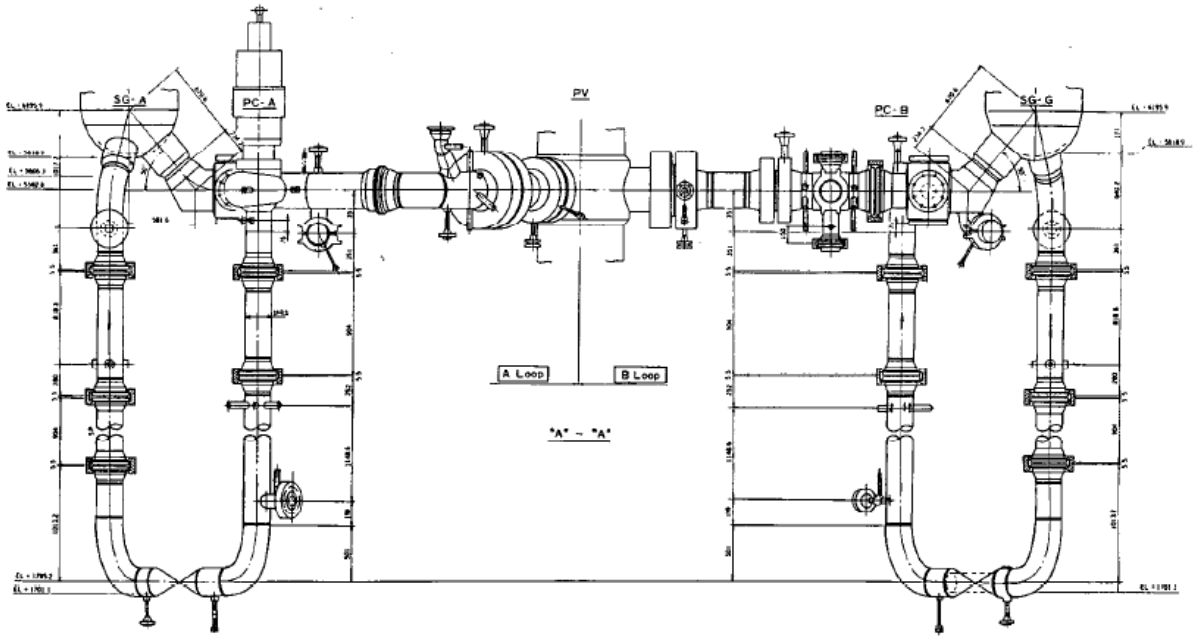

Fig. 17 – LSTF facility: primary coolant loops

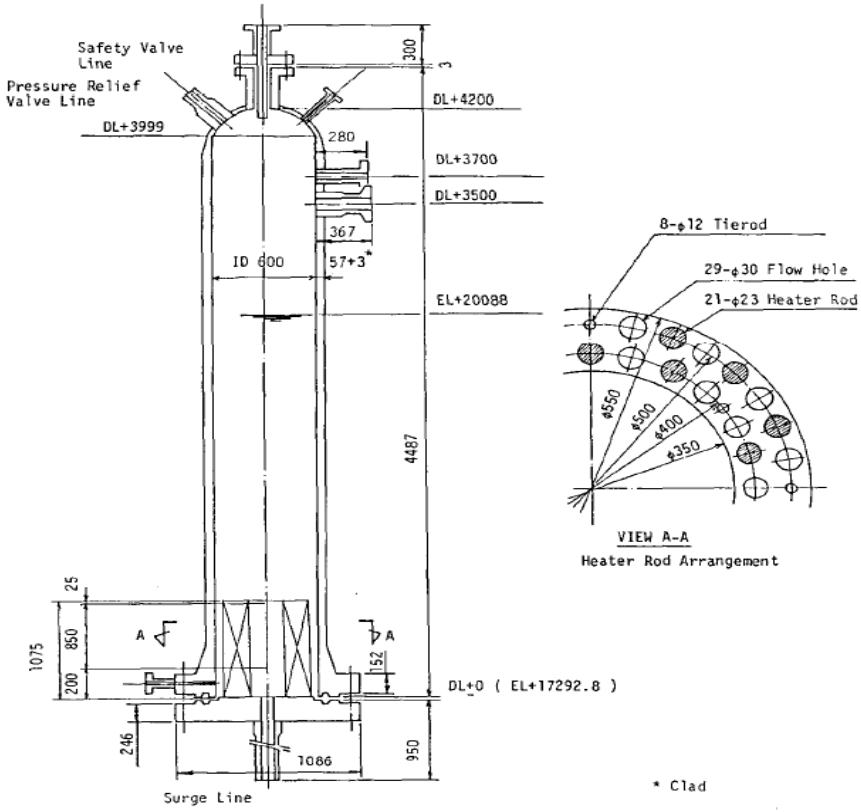

Fig. 18 – LSTF facility: pressurizer

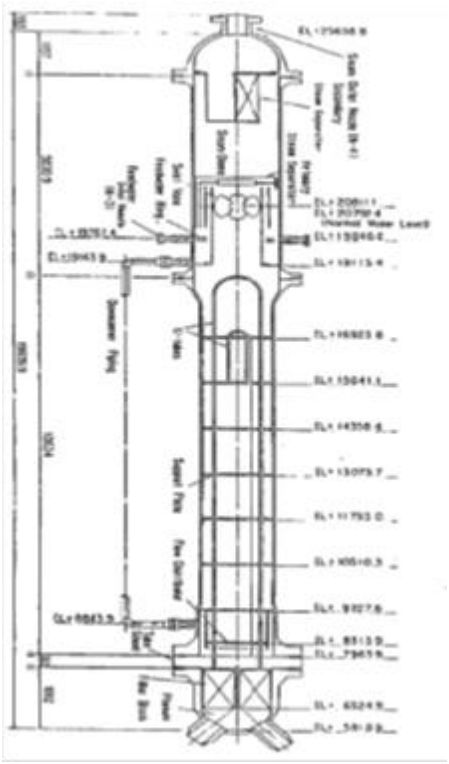

Fig. 19 – LSTF facility: steam generator

Location	Description	Material
1	Venturi Flow Meter	SUSF316L
2	Spool Piece	SUS316L
3	R.O. Piece 1/2	SUS316L
4	R.O. Piece 1/2	SUS316L
5	Break Valve	SCS13

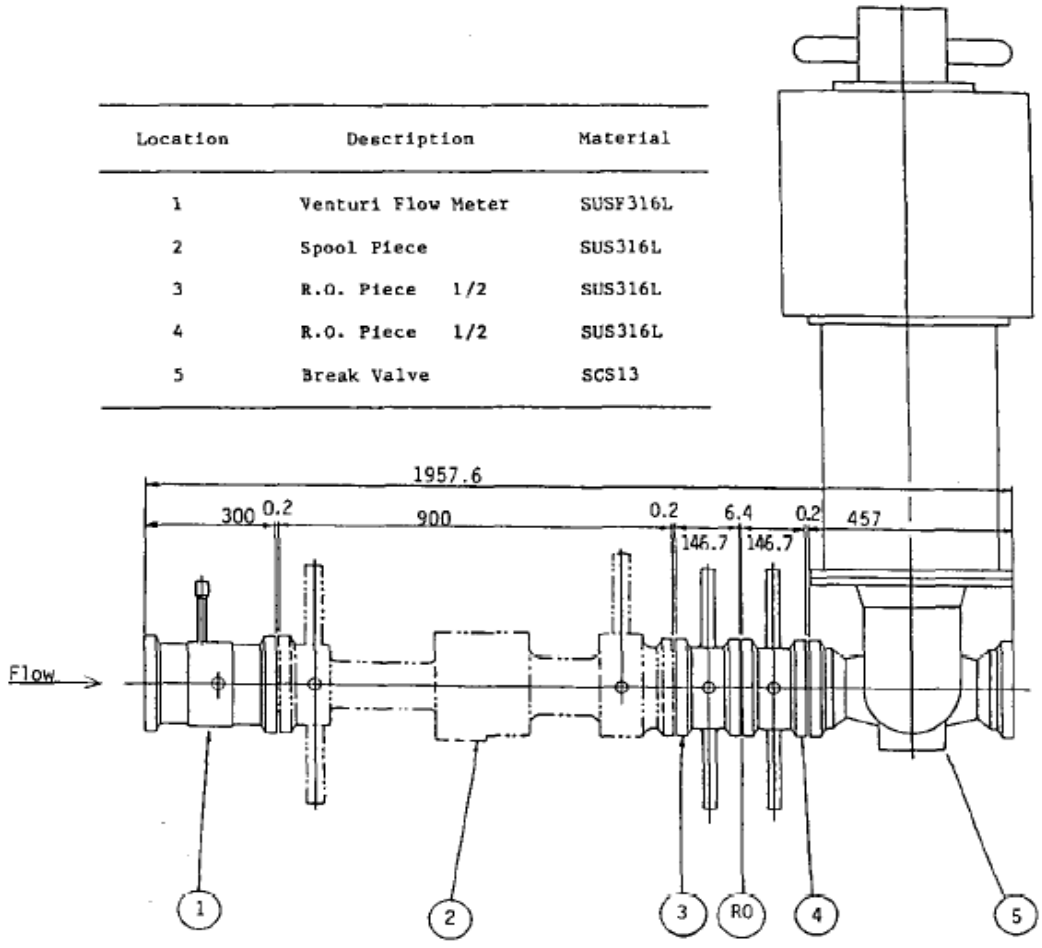

Fig. 20 – LSTF facility: break assembly

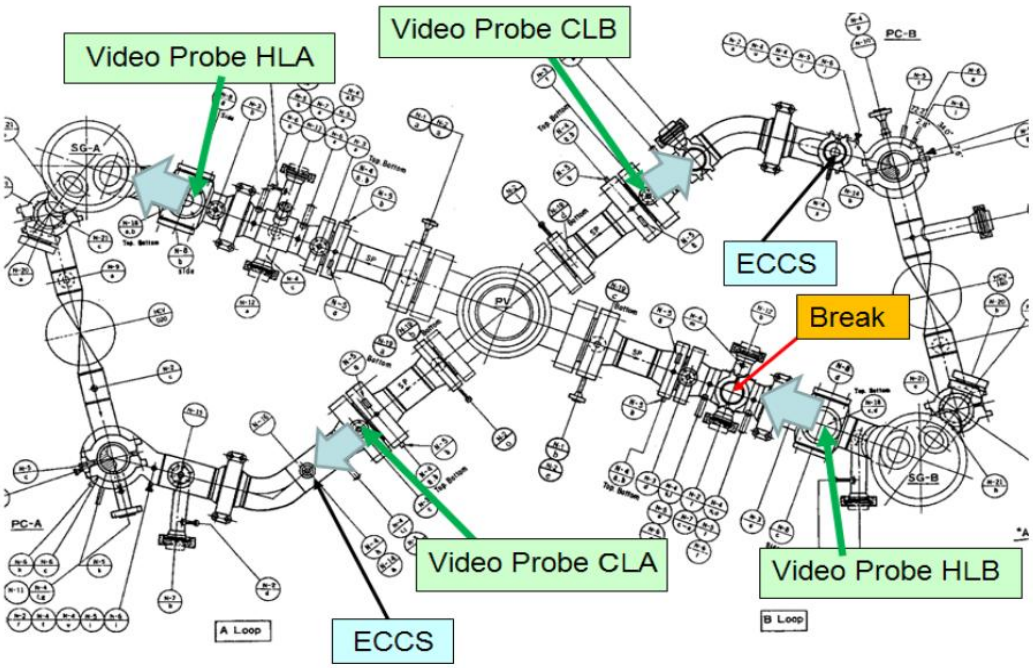

Fig. 21 – LSTF facility: location of break, ECCS and video probes

4 Adopted code and nodalizations

4.1 RELAP5/Mod3.3 code

The light water reactor transient analysis code, RELAP5[17], was developed at Idaho National Engineering Laboratory (INEL) for the U.S. Nuclear Regulatory Commission (NRC). The RELAP5 code has been developed for the best estimate simulation of light water reactor coolant system transients during postulated accidents. The code models, the coupled behavior of the reactor coolant system and the core for simulating accidents in LWR such as loss of coolant, Anticipated Transients Without Scram (ATWS) and operational transients, such as loss of feed-water, loss of offsite power and turbine trip. A generic modeling approach is used that permits simulating a variety of thermal hydraulic systems such as turbines, condensers and secondary feed-water system. The component models include also pumps, valves, pipes, heat releasing or absorbing structures, reactor point kinetics, electric heaters, jet pumps, etc.

The RELAP5/Mod3.3 version has been developed by NRC and by the members of the International Code Assessment Program (ICAP) and its successor organization, Code Application and Maintenance Program (CAMP). Acknowledge also needs to be given to various Department of Energy sponsors, including INEL.

This code [18], [19], [20] is highly generic and can be used for simulation of a wide variety of hydraulic and thermal transients in both nuclear and non-nuclear system involving mixtures of steam, water, non-condensable and solute. The developers of the RELAP5/Mod3.3 wanted create a code version suitable for the analysis of all transient and postulated accidents in LWR system, including small and large break Loss Of Coolant Accidents (LOCA).

Based on one-dimensional, transient, and non-homogeneous and non-equilibrium hydrodynamic model for the steam and liquid phases, RELAP5/Mod3.3 code uses a set of six partial derivative balance equations and can treat a non-condensable component in the steam phase and a non-volatile component (boron) in the liquid phase.

A partially implicit numeric scheme is used to solve the equations inside control volumes connected by junctions. The direction associated to the control volume is positive from the inlet to the outlet. The fluid scalar proprieties (pressure, energy, density and void fraction) are the average fluid condition in the volume and are viewed located at the control volume center. The fluid vector properties, i.e. velocities, are located at the junctions and are associated with mass and energy flows between control volumes that are connected in series, using junctions to represents flow paths.

Heat flow paths are also modeled in an one-dimensional sense, using a staggered mesh to calculate temperatures and heat flux vectors. Heat structures and hydrodynamic control volumes are connected through heat flux, calculated using a boiling heat transfer formulation. These structures are used to simulate pipe walls, heater elements, nuclear fuel pins and heat exchanger surfaces.

Several new models, improvements to previously existing models, have been added, as for instance:

- the Bankoff counter-current flow limiting correlation,

- the ECCMIX component for modeling of the mixing of sub-cooled emergency core cooling system (ECCS) liquid and the resulting interfacial condensation,
- a zirconium-water reaction model to model the exothermic energy production on the surface of zirconium cladding material at high temperature,
- a surface-to-surface radiation heat transfer model with multiple thermal radiation enclosures defined through user input,
- a thermal stratification model.

4.2 LOBI/MOD2 nodalization

The RELAP5 input deck adopted for simulating the LOBI/MOD2 facility is a nodalization carried out with a "sliced" approach. This nodalization scheme is suitable for a better code response, especially in natural circulation and/or during low flow rate regimes. It is based on the input deck applied for previous post test analyses, e.g. BL-44 [21], [22], BL-30 [23]. The noding scheme can be seen in Fig. 23. Information about the code resources is given in Tab. 13. The correspondence between the zones of the facility and the nodes of the code model are exposed in Tab. 15.

The table reports the general zones according to the flow paths of the facility. Each one is divided in regions or components, which are associated with the corresponding RELAP5 hydraulic components numbers and types.

A description of the nodalization is summarized below distinguishing between the primary and the secondary systems.

4.2.1 Primary system model

The RPV flow paths, including the bypasses have been modeled separately, as they are in the facility. The vessel model consists of 29 hydraulic components, connected by 48 junctions. The RPV heat structures are composed by 47 heat slabs, divided in:

- 13 active structures for the electrical heaters;
- 30 heat slabs for the vessel wall (passive structures);
- 4 internal non active structures.

The by-pass flow paths are modeled, as reported hereafter.

- Core by-pass from downcomer to upper plenum (through two holes of ϕ=5mm) is represented by junction 430-02. The k-loss of the junction are adjusted in order to have a mass flow rate in the range 2-2.5% of total core mass flow.
- Hot legs - upper plenum by-passes are modeled with the junctions 500-03 and 700-03. They represents the gap existing in the connections between the hot legs and the barrel. Indeed, the hot legs are not welded, and lay on the barrel wall. The dimension of the gap is strictly dependent on the thermal expansion of the leg itself. The by-pass mass flow rate is approximately 1% of total core mass flow rate.
- Downcomer-Upper head by-pass is simulated by node 440-01. It is set-up in order to have a mass flow rate equivalent to 1% of total core flow rate.

The two loops (broken and intact) of the reactor coolant system are modeled separately. Each loop includes a hot leg, a steam generator, a pump, a loop seal and a cold leg. They represent

the geometry of LOBI/MOD2 facility in detail. The broken loop is modeled with a larger number of nodes than the intact loop to improve the simulation of the most important thermal-hydraulic phenomena expected in the loop during the transient.

The hydraulic resistance of the main coolant pump are modeled accurately in the facility and in the nodalization. Indeed, the LOBI/MOD2 facility includes a device, which activates a partial obstruction downstream the pump outlet for simulating the pressure drop of the real NPP when the main coolant pump is at rest. This device is modeled with the RELAP5 component MOTOR VALVE placed in the same position as in the facility.

The pressurizer is connected to the intact loop via the surge line. On its top the relief valve (PORV) is reproduced and at the bottom PRZ heaters are simulated. The PRZ housing is modeled with a PIPE and BRANCH components (from 539 to 541). Two regulations systems are added in the nodalization:

- a pressure control system modeled with a TIME DEPENDENT VOLUME and a VALVE;
- a PRZ level control system (injecting saturated water) represented with a TIME DEPENDENT JUNCTION and a TIME DEPENDENT VOLUME.

These systems are operated during the steady state phase.

The HPIS is modeled with a tank, a MOTOR VALVE and an injection pipe, which is connected to the hot leg of the intact loop. The low pressure injection system (LPIS) is not used in the transient analyzed. It should be added that when the test A2-84 was executed, the facility was not equipped with low pressure injection tank, which was installed successively.

The two accumulators systems are modeled in each loop with proper RELAP5 ACCUMULATOR components. They are connected to both hot and cold legs of the intact loop, and to the cold leg of the broken loop.

The heat losses of the facility are simulated using a general table (HTC vs. Temperature) and assigning the environmental temperature.

4.2.2 Secondary system

The nodalization of the secondary side is similar for both steam generators. Four zones can be identified, as follows:

- the downcomer, modeled as a single stack of nodes, simulating a multi-tubular structure;
- the riser, which contains the U-Tubes, and where the heat transfer primary to secondary occurs;
- the upper part of the SG, including the separator, the dryer and the steam dome region;
- the steam lines, which are simulated by 2 pipes, a MOTORVALVE at the end of each pipe and a time dependent volume downstream the valve.

The steam generators are connected to three time dependent volumes, which accomplish the following functions:

- feed water injection system (one each loop), modeled with a time dependent volume and a time dependent junction;
- auxiliary feed water injection system (one each loop), simulated with a time dependent volume and a time dependent junction (not used in test A1-84); and
- safety tanks (one per loop), modeled with a time dependent volume and a trip valve.

4.2.3 Set up of the nodalization

The simulation of the A1-84 is carried out with the nodalization derived for the post test analysis of the test BL-44 test (6% cold leg break) [22]. The nodalization has been updated and set up, adding or modifying the systems relevant for simulating the test A1-84. The accumulator lines and the ECCS system (Fig. 22) is renewed. In particular, the realistic accumulator injection is simulated modeling both lines injecting in hot a cold leg of the intact loop. The model includes the ball valves located at the height as in the facility. These ball valves are opened when the set point of the accumulator injection is reached. The model of the HPIS is modified, changing the position where the system inject in the intact hot leg. The injection now is at the beginning of the hot leg, close to the upper plenum, as specified in Ref. [12].

The RELAP5 components and junctions are initialized at the right pressures, temperatures and mass flows. The control system is implemented in the input deck according with the specifications of the test A1-84.

The Ransom-Trapp chocked flow model is selected for simulating the break flow rate of the transient. This choice is based on the break system layout[12] (i.e. L/D, size, orientation, position, etc.) used in the test A1-84. An accurate modeling of the rupture outflow (see also section 5.3) is achieved modifying the discharge coefficients of the model (see Refs. [17] and [24]). The following three coefficients are selected:

- subcooled discharge coefficient → 1.0 (default value)
- two-Phase discharge coefficient → 0.9
- superheated discharge coefficient → 0.7

The first two values are the same used in the post test analysis of the BL-44 experiment[22]. The superheated discharge coefficient is decreased in order to account for the different position and orientation of the break[24] [25].

Tab. 14 summarized the main modifications implemented in the nodalization.

Tab. 13 – LOBI-Mod2 nodalization by RELAP5 code: adopted code resources.

Number of nodes	233
Number of junctions	242
Number of heat structures	252
Number of mesh points	669
Number of core active structures	105

Tab. 14 – LOBI-Mod2 nodalization by RELAP5 code: modifications and set-up.

#	MODIFICATIONS	REMARKS
1	Ransom-Trap chocked model coefficient for the break valve changed	1.0, 0.9, 0.7
2	Introduced Accumulator for the broken loop	Only one line to Cold leg
3	Introduced HPIS tank	Only one line to Hot leg BL
4	Two Accumulator lines modeled for IL, as described in the facility flow sheets	Ball valves positioned at the right height
5	Roughness in the U-tubes changed	From 4*e-5 to 0.22*e-6
6	Steam line time dependent junction removed	Replaced with a motor valve
7	Control volume of secondary side pressure removed	--
8	Control of the secondary side level introduced	Operating on the FW injection junction
9	Steam lines introduced	Steam line motor valve inserted downstream, like in the facility configuration
10	Implementation of secondary side cooldown	100 K/h
11	Energy loss coefficients of the two loops changed with reference to the LOBI facility report	--
12	U-tubes Hydraulic diameter changed with reference to LOBI facility report	--

Tab. 15 – LOBI-Mod2 nodalization by RELAP5 code: correspondence between hydraulic nodes and facility zones.

STRUCTURE	NAME	NUMBER	TYPE
		200	annulus
	DOWNCOMER REGION	202	branch
		210	branch
	LOWER PLENUM	102	branch
		106	branch
		400	pipe
	CORE REGION	410	branch
		420	branch
PRESSURE VESSEL		430	branch
	UP BLEED TANK	431	valve
		432	tmdpvol
		440	branch
		450	branch
		455	branch
	UPPER HEAD	460	pipe
		465	sngljun
		466	branch
		470	snglvol
	VESSEL NOZZLE	500	branch
		507	branch
		510	branch
	HOT LEG	511	branch
		512	branch
		550	snglvol
		555	sngljun
		560	pipe

STRUCTURE	NAME	NUMBER	TYPE
	SG INLET PLENUM	565	branch
INTACT LOOP	U-TUBES	570	pipe
	SG OUTLET PLENUM	575	branch
		580	pipe
		582	sngljun
		585	snglvol
	LOOP SEAL	587	sngljun
		590	pipe
		595	branch
	PUMP	600	pump
		605	branch
	COLD LEG	610	pipe
		612	branch
	VESSEL NOZZLE	700	branch
		702	branch
	HOT LEG	705	pipe
		710	branch
		712	pipe
	SG INLET PLENUM	718	branch
	U-TUBES	720	pipe
	SG OUTLET PLENUM	722	branch
BROKEN LOOP		725	pipe
	LOOP SEAL	727	sngljun
		730	pipe
	PUMP	740	pump
		745	branch
		747	valve
		750	pipe
	COLD LEG	770	branch
		772	branch
		774	branch
		776	branch
		520	pipe
	SURGE LINE	532	sngljun
		530	branch
		535	pipe
	PRESSURIZER	537	sngljun
	VESSEL	539	branch
PRESSURIZER		540	snglvol
	PORV VALVE	543	valve
	PORV TANK	544	tmdpvol
	SRV VALVE	545	valve
	SRV TANK	546	tmdpvol
	SRV+PORV VALVE	547	valve
	SRV+PORV TANK	548	tmdpvol
	FEEDWATER TANK	834	tmdpvol
	FEEDWATER JUN.	835	tmdpjun
	AUX FW TANK	836	tmdpvol
	AUX FW JUN.	837	tmdpjun
		830	branch
	DOWNCOMER	840	branch
SECONDARY SIDE		845	sngljun
INTACT LOOP		850	annulus
		800	pipe

STRUCTURE	NAME	NUMBER	TYPE
	RISER	805	sngljun
		810	pipe
	SEPATATOR	815	separatr
	STEAM DOME	820	branch
	STEAM LINE JUN.	828	valve
	STEAM LINE	831	pipe
	STEAM LINE TANK	829	tmdpvol
	COOLDOWN VALVE	821	valve
	COOLDOWN VOLUME	822	tmdpvl
	SAFETY VALVE	838	valve
	SAFETY TANK	839	tmdpvol
	FEEDWATER TANK	934	tmdpvol
	FEEDWATER JUN.	935	tmdpjun
	AUX FW TANK*	936	tmdpvol
	AUX FW JUN.*	937	tmdpjun
		930	branch
	DOWNCOMER	940	branch
SECONDARY SIDE		945	sngljun
BROKEN LOOP		950	annulus
		900	pipe
	RISER	905	sngljun
		910	pipe
	SEPATATOR	915	separatr
	STEAM DOME	920	branch
	STEAM LINE JUN.	928	valve
	STEAM LINE	931	pipe
	STEAM LINE TANK	929	tmdpvol
	COOLDOWN VALVE	921	valve
	COOLDOWN VOLUME	922	tmdpvl
	SAFETY VALVE	938	valve
	SAFETY TANK	939	tmdpvol
	INTACT LOOP ACC.	615	accum
	ACC. SURGE LINE	616	branch
	BALL VALVE IL CL	675	valve
	INTACT LOOP ACC. INJECTION LINE CL	670	branch
ACCUMULATORS	INTACT LOOP ACC. INJECTION LINE HL	671	branch
	BALL VALVE IL HL	676	valve
	BROKEN LOOP ACC.	780	accum
	ACC. BL SURGE LINE	783	branch
	BALL VALVE BL CL	782	valve
	BROKEN LOOP ACC. INJECTION LINE CL	781	branch
	PRZ CONTROL	541	tmdpvol
CONTROL	PRESSURE	542	valve
COMPONENTS	PRZ CONTROL	531	tmdpjun
	LEVEL	534	tmdpvol
	BREAK VALVE	760	valve
BREAK	BREAK VOLUME	761	tmdpvol
	HPIS JUNCTION	625	tmdpjun
HPIS	HPIS TANK	630	tmdpvol
	EXIT SEAL WATER	602	tmdpvol
		604	tmdpjun

STRUCTURE	NAME	NUMBER	TYPE
PUMP SEAL WATER	IL PUMP SEAL	603	tmdpvol
	WATER	601	tmdpjun
	BL PUMP SEAL	742	tmdpvol
	WATER	744	tmdpjun
IL-BL SG CONNECTION		870	valve

* auxiliary feed water is not used in test A1-84

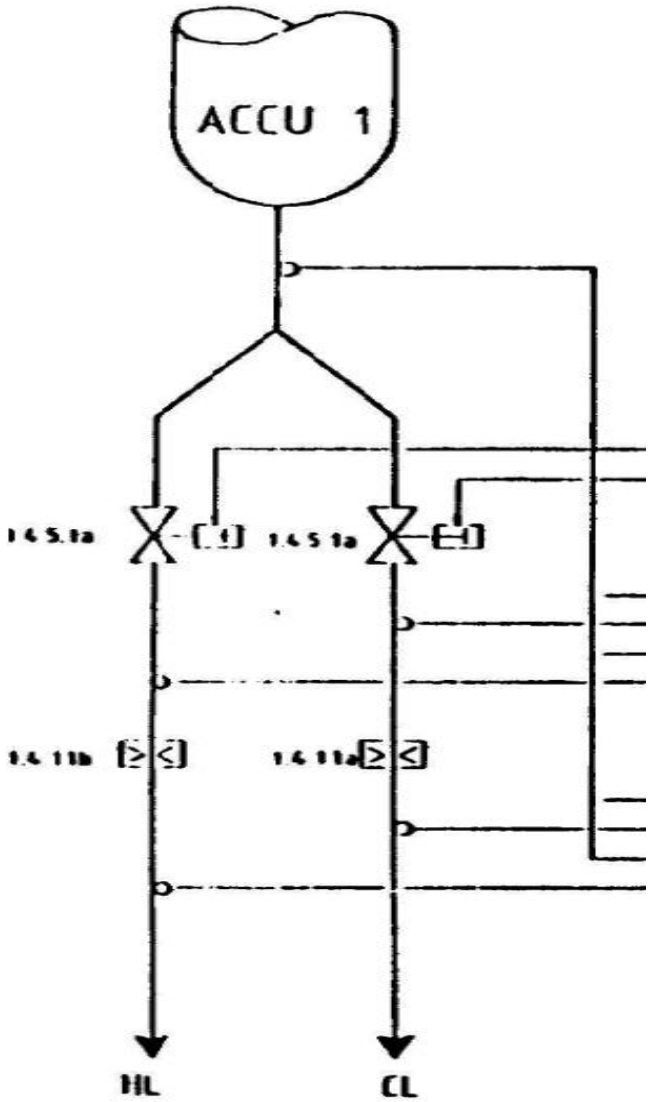

Fig. 22 – Accumulator injection line.

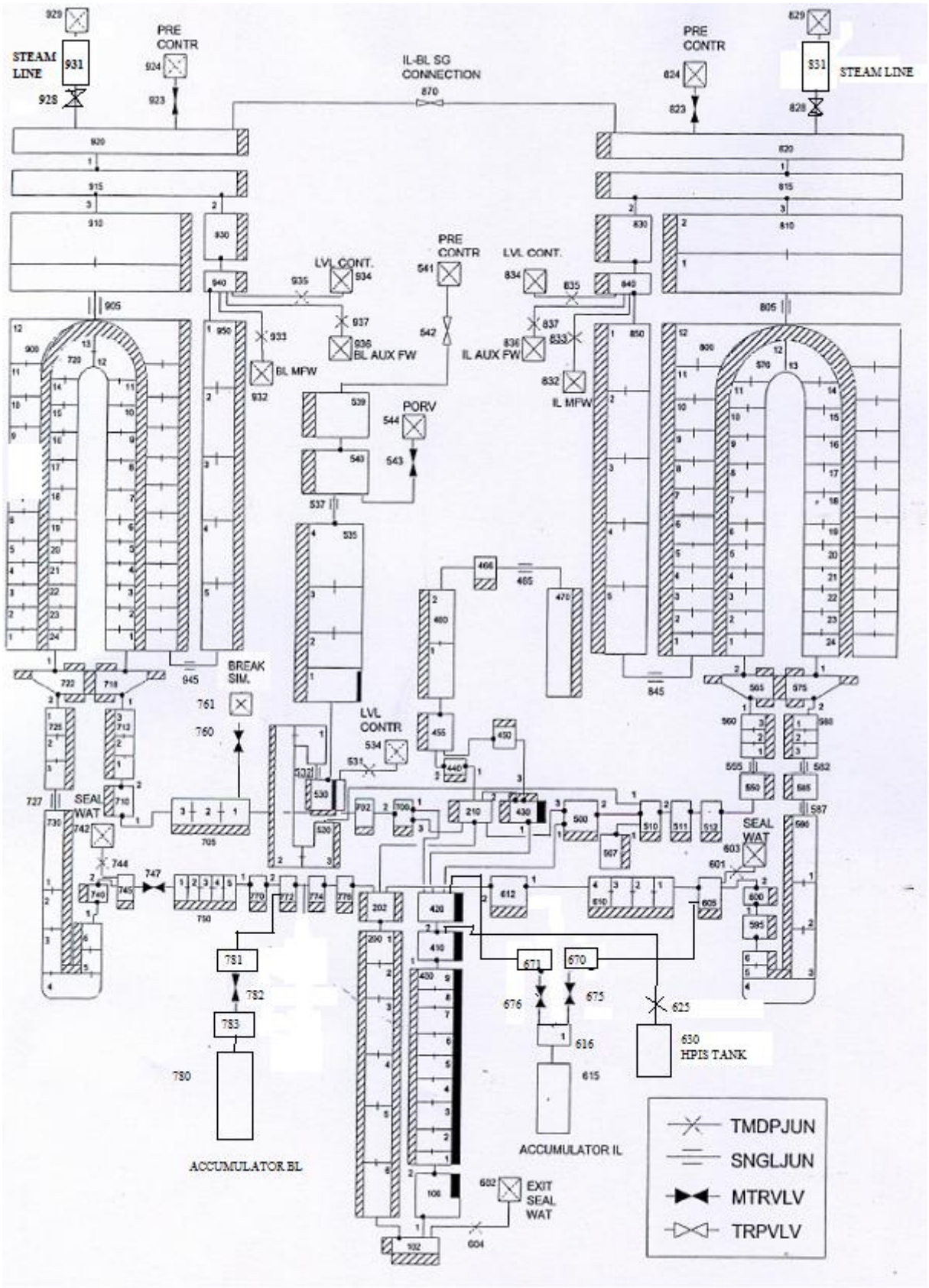

Fig. 23 – LOBI nodalization by RELAP5 code: overall sketch.

4.3 ROSA V/LSTF nodalization

The overall nodalization [26] is showed in Fig. 24 and hereafter outlined. The RPV (Fig. 25) has been divided into two main regions: the downcomer, simulated as an ANNULUS component, the core, modeled as a PIPE and the upper core region, composed mainly by the upper plenum and the upper head, simulated with several branches and pipes, in order to render the simulation very accurate. The active core is represented by a heat structure subdivided in three parts.

The two loops are modeled separately; each loop includes a hot leg, a steam generator, a pump, a loop seal and a cold leg. The pressurizer, simulated as a pipe, is connected to the hot leg of the intact loop, via the surge line; on its top the relief valve (PORV) is reproduced and connected to a time dependent volume, which simulates the environment. At the bottom of the PRZ, heaters are simulated.

The SG primary side is schematized with a U-tube, subdivided into 9 volumes, which reproduces the same flow area of the 141 U-tubes of the facility (these data are referred to a single SG). The SG secondary side has four different zones:

- the down-comer, that is simulated as an annulus, composed by 5 volumes,
- the outer part of the Steam generator, the blanket which covers the U-tubes, reproduced as a pipe
- the separator and the steam dome (a single volume component)
- the steam line, composed by two branches and two single volumes, among whom the main steam isolation valve (a motor valve component was chosen) is inserted.

The feed water in the facility has one injection point: a time dependent volume and a time dependent junction represent it; the time dependent junction ensures the prescribed mass flow rate. An additional time dependent junction plus time dependent volume system is connected to the steam generator with the function of level control system, which injects water if the level is too low.

The secondary relief and safety valves are of great importance in the facility, for the transient analyzed, because in the first part of the experiment, the secondary pressure cope with many oscillation, and the relief valves are opening and closing continuously for several seconds. For this reason, particular attention on the modeling of these valves was given. The relief valves have been modeled as trip valves, and the safety valves as servo valves.

The Emergency Core Cooling System active in the simulated experiment are two accumulators, connected to both the cold legs and two HPIS tanks, connected to the cold legs. The LPIS is not active. The Accumulator are both simulated as an ACCUMULATOR component, connected to a single volume and to a valve, which directly discharges in the cold leg. The HPIS is reproduced by a time dependent volume, that simulates the tank, and a time dependent junction which drives the water injection.

Tab. 16 summarizes the adopted code resources.

Tab. 16 – ROSA V/LSTF nodalization by RELAP5 code: adopted code resources.

Number of nodes	223
Number of junctions	233
Number of heat structures	215
Number of mesh points	233
Number of core active structures	81

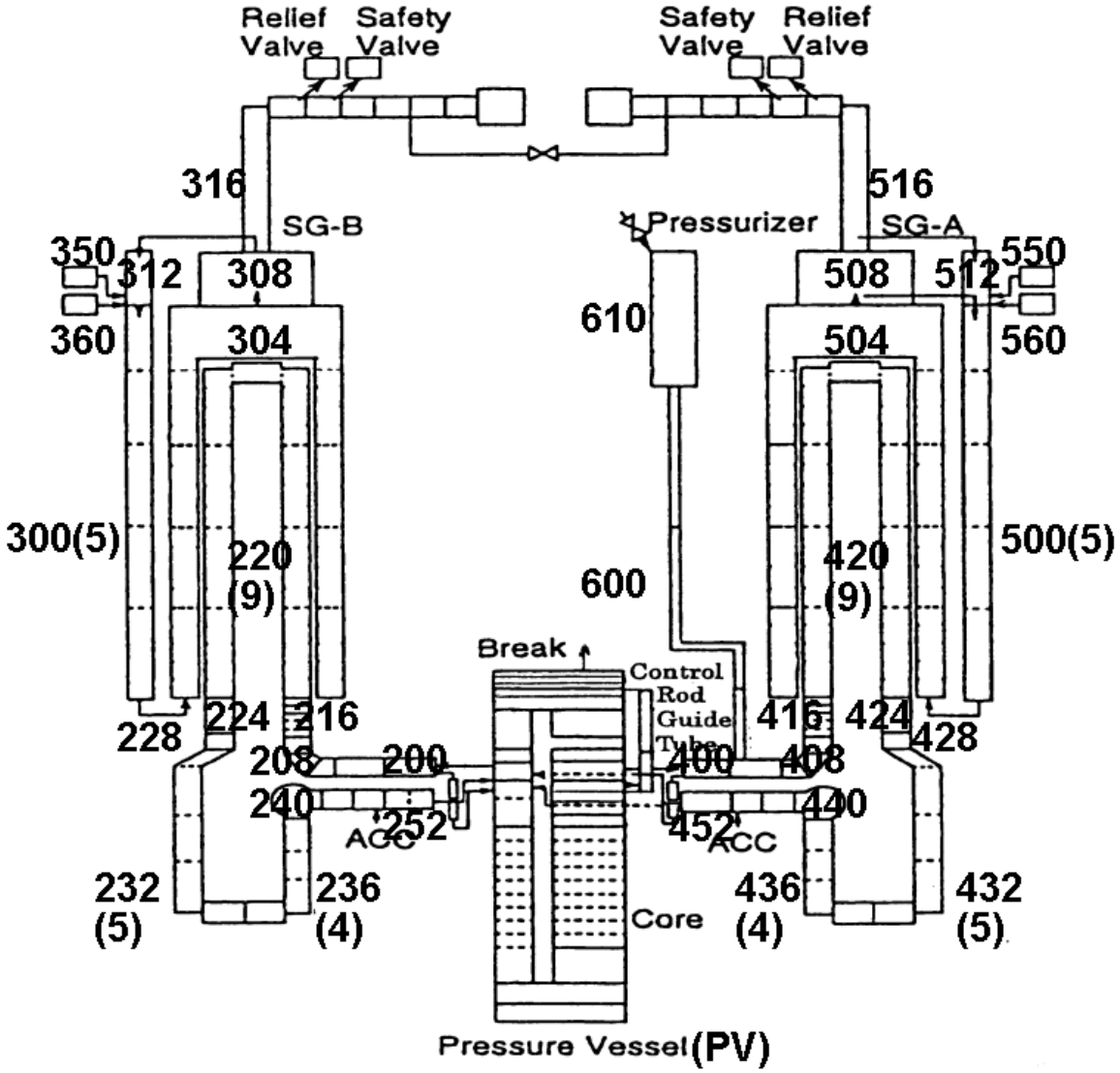

Fig. 24 – ROSA V/LSTF nodalization by RELAP5 code: overall sketch.

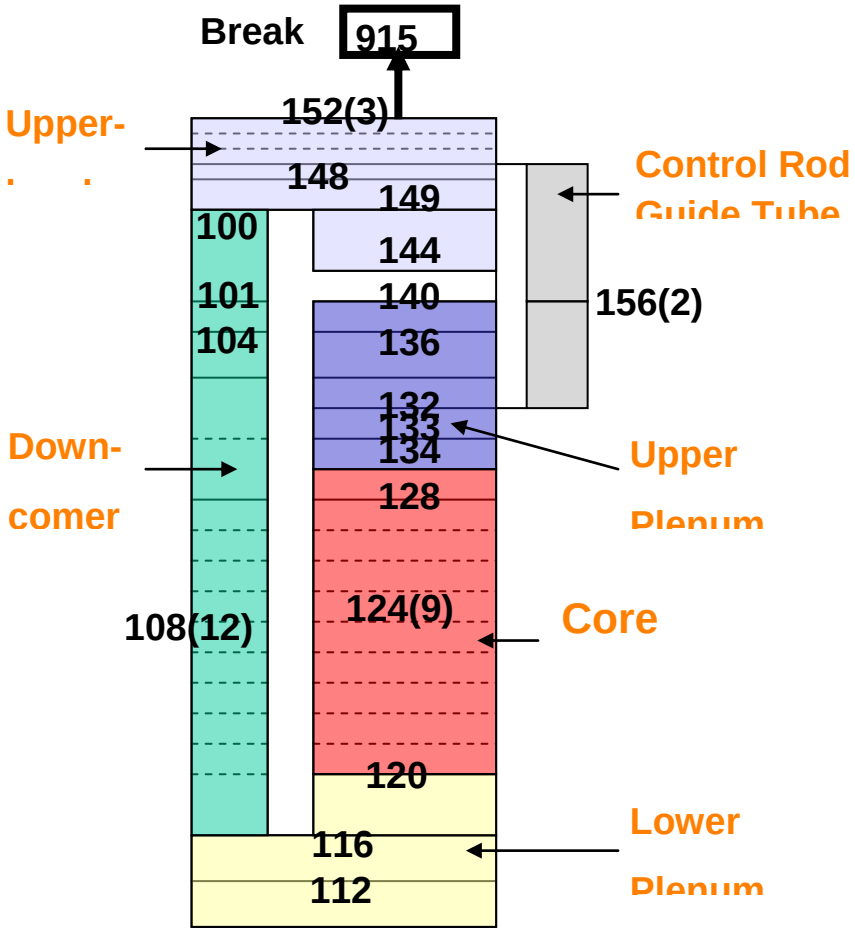

Fig. 25 – ROSA V/LSTF nodalization by RELAP5 code: RPV.

5 Post-test analysis of LOBI test A1-84

The post-test analysis of LOBI test A1-84 has been pursued on the basis of the procedure for code assessment developed at University of Pisa (see Refs. [27], [28] and [29]). The assessment of a thermal-hydraulic system code involves the availability of a code, of a qualified nodalization, of qualified experimental data from a qualified experimental facility. It also requires standard procedures and the fulfillment of specific criteria. In this context, references have been provided by University of Pisa to define the meaning of "qualified nodalization"; to develop the procedure and the criteria necessary for preparing a "qualified nodalization"; to perform the assessment activities and, finally, to execute qualified computer code calculations.

The procedure for code assessment consists of three main steps:

1. The steady state results (i.e. "*steady state qualification*"), which may include the nodalization development phase (e.g. volume, heat transfer area, elevations, pressure drops distribution, etc.). This step is concluded with the simulation of the nominal steady state conditions against specific acceptability thresholds (see section 5.1).
2. The reference calculation results (i.e. "*on transient qualification*") that shall satisfy qualitative and quantitative accuracy related criteria (see section 5.2). According with this procedure, the reference calculation is not "the best" calculation achievable by the code.
3. The results from sensitivity study (see section 5.3), which is also part of the "*on transient qualification*", is carried out to demonstrate the robustness of the code calculations, to characterize the reasons for possible discrepancies between measured and calculated trends, to optimize code results and user options choices, and to improve the knowledge of the code by the user.

5.1 Steady state results

The steady state check deals with the comparisons between the experimental measurements and the calculated results at the SoT. The selection of the key parameters for the steady state verification was done taking into account the checks requested by the procedure above and the availability of the experimental data.

The stationary conditions are achieved after 1000s of "null transient" (steady state) calculation in order to stabilize the system. The code results at the end of the stationary phase are compared with the correspondent experimental values in Tab. 17. This table includes the specification of the quantity considered, the measurement unit, the errors in the measures, the codes results and finally the threshold limits associated to each specific parameter, according with Ref. [28]. No error is considered if the calculated value is inside the bands of the measurement accuracy. If it is outside, then it is calculated as the difference between the calculated value and upper or lower limit of the measured value.

The verification of the pressure drop along the piping length, for the intact and the broken loop respectively is reported in Fig. 26 and Fig. 27. The general trend of the pressure drop versus length in the two loops is in good accordance with the calculations. Errors are observed between the pumps outlet and the cold legs outlet: the experimental value is underestimated in the code simulation. This difference remains, notwithstanding the energy loss coefficients

implemented in the nodalization have been checked on the basis of the final LOBI geometrical data report [30]. On the contrary, the difference observed at the entrance of the vessel is only a propagation of error: the pressure drop between the cold leg outlet and the vessel inlet is correctly simulated.

The analysis of the results brings to the following conclusions:

- the calculated results are stable (see Appendix A);
- the relative error in the primary pressure is acceptable if the upper plenum pressure is considered while it is slightly above the limit if the PRZ pressure is considered;
- the relevant initial conditions of the test are acceptable, thus the discrepancies of some calculated parameters respect on the experimental values are all within the acceptability criteria.

5.2 Reference calculation results

A comparison between measured and calculated data was performed with the objective to verify the capabilities of the code to reproduce the relevant thermal-hydraulic phenomena observed in the experiment. The analysis allows also verifying the correctness of the imposed boundary conditions and of the systems actuated in the transient.

The reference calculation is labeled "A1-84-11.0". The related time trends and the resulting sequence of the events are reported, together with experimental data from Fig. 28 to Fig. 50, in Tab. 18 and in Appendix A. It may be noted that, given the objectives above, the reference calculation is not the "best" simulation. The reference input deck shall have the boundary and initial conditions within their uncertainty range, and user choices (i.e. nodalization noding, models selection, etc.) consistent with other analyses addressing the same phenomena and processes. Investigations related, the effect of the boundary and initial conditions and of the user choices are part of the sensitivity analysis discussed in section 5.3.

The post test analysis is performed by means of a comprehensive comparison between measured and calculated trends or values, including the following steps:

a) comparison between experimental and calculated data on the basis of the most relevant quantities (discussed in the present section);
b) comparison between values of the parameters, which characterize the sequence of resulting events (see Tab. 18);
c) qualitative evaluation of calculation accuracy on the basis of the Relevant Thermal-hydraulic Aspects (RTA), see section 5.2.1;
d) quantitative evaluation of calculation accuracy utilizing the FFT based method (FFTBM), see section 5.2.2.

Comments related to items a) and b) are given below, distinguishing groups of homogeneous variables, while the discussion about items c) and d) is given in sections 4.2.1 and 4.2.2.

Absolute pressures
The primary system pressure is well predicted by the code (see Fig. 28 and Appendix A). The phenomenological windows, according with the description of the LOBI test in section 2.2.3, are clearly distinguished also in the code simulation. The single phase blowdown is initiated

by the break opening. Depressurization occurs and continues until saturation conditions are reached (about 100s) in the hottest region of the primary side. During the depressurization, the pressurizer empties and the scram signal is actuated (in perfect accordance with the experiment), the ECC system signal is started, the containment isolated and the turbine is tripped. When saturation is reached, boiling occurs in the upper core regions and voids are formed in the upper plenum, upper head and hot leg: the depressurization rate is reduced drastically. During the initial depressurization, while the MCP are coasting down, the primary coolant flow is driven by the MCP's inertia. When the pumps are stopped the coolant is driven by gravitational effects, in particular by natural circulation, guaranteed by the SGs, which are cooled down and represent a heat sink, until the ECCS injection is not effective. The decrease in reactor coolant inventory is insufficient to uncover the core, because the HPIS injection (perfectly predicted) compensate the break outflow. The time of accumulator injection, both in intact and in broken loop is well predicted, and the accumulators stop is reasonably well predicted. A small delay in time is observed because the accumulator level follows the primary pressure that, in the last part of the transient is under-predicted by the code.

The secondary pressure is in a perfect accordance with the experimental, thanks to the correct implementation of the secondary cooldown of 100 °C/h (see Fig. 29 and Fig. 30).

Fluid temperatures
The coolant temperatures in the primary system are well predicted (see from Fig. 31 to Fig. 35 and in Appendix A).

The PRZ temperature is well predicted by the code. The timing when the level drops below the thermocouple high is clearly visible both in the experiment and in the code calculation. Then, the thermocouple measures the temperature of the gas phase. Form this time on, the gas temperature calculated by the code over-predicts systematically the experimental results. This might be attributed to the influence of the wall temperature[12] as well as on the influence on the steam condensation.

The code simulation shows a good accuracy in predicting the core inlet (Fig. 32) and core outlet (Fig. A - 20) coolant temperatures. The experimental trend of the core outlet evidences when the swelled level drops the elevation of the thermocouple.

The upper head coolant temperature (Fig. 33) is correctly simulated by the code. A difference is observed when the level drops the axial elevation of the thermocouple. The reasons are already explained above, discussing the PRZ coolant temperature. Nevertheless, from this time on, the measured temperature is always bounded by the temperatures calculated by the code for the liquid and gas phases.

The analysis of the coolant temperatures in the loop shows a qualitative agreement with the experimental measurements. In particular, the comparison is affected by the temperature measures in stratified condition of horizontal flow.

Mass flow rates and residual mass
The calculated mass flow rate at the core inlet and in the loops are reported in Fig. A - 39, Fig. A - 40 and Fig. A - 41. The experimental data of these parameters are not available for the comparison.

The measurement system provides the trend of the mass flow rate injected in the primary system by the HPIS. This is the only mass flow rate measured in the test. Fig. A - 66 demonstrates that the HPIS injection is correctly implemented in the input deck.

The primary mass inventory (Fig. 36) is well predicted by the code. In particular, excellent results are observed from 50s until the EoT, with a slight underprediction of the experimental trend after 150s. The mass inventory is a calculated parameter: it is the sum of the inventories calculated in individual components evaluated on the basis of pressure drop, absolute pressure and density data. On this basis the integral break flow rate is derived, see Fig. A - 43. The calculated results of the break flow rate is reported in Fig. A - 42 for sake of completeness.
When the break opens, the experimental data highlight a sharp decrease of the mass inventory, which appears unrealistic until 50s on the basis of the break dimension. The primary mass decrease is less steep as soon as the HPIS are on. At about 350s, it reaches a minimum, which corresponds with the accumulator injection and therefore the primary system recovery. The dryout occurrence at the top of the core is not observed because it is prevented by the accumulator injection.

The secondary side mass inventory is quite well predicted (Fig. 37 and Fig. 38). The calculated results show a stabilization at different values with respect the experimental data; This difference is larger in the broken loop. Nevertheless, the experimental trend appears not fully reliable at the beginning of the transient on the basis of the available information about the FW isolation occurrence and the steam line closure.

Pressure Drops
The pressure drop trend are well predicted by the code (see Fig. 48, Fig. 49, Fig. 50 and Appendix A). Comparing the pressure drops across the U-Tubes and the hot leg of the intact loop, three phases are distinguished. During the first phase (from 0s to 40s), the pressure drop in the hot leg increases before the MCP coastdown starts (see Fig. 50) as consequence of the break opening. This effect is slightly underestimated in the code simulation, nevertheless it is very well matched in the broken loop (see Fig. A - 51). As soon as the MCP are stabilized, the pressure drops in the loops experienced a plateau (phase 2, from 40 to 120s). Finally, when the natural circulation is interrupted and reflux condenser mode occurs, the code simulation highlights the presence of liquid phase in the U-tubes in the descending part.

The code results of the pressure drop in the core demonstrate the amount of liquid phase in the core is simulated with good accuracy.

Levels
The pressurizer level is well reproduced in the calculation (Fig. A - 44), demonstrating the correct set up of the surge line hydraulic behavior and the simulation of the break flow rate. The collapsed level of the pressure vessel is qualitatively predicted in the code simulation. Nevertheless, differences are observed after the first 50s from SoT. The code simulation underpredicts the level (see Fig. 39). In order to explain the difference, the following considerations have to be taken into account:

- primary mass inventory of the code simulation is in good agreement with the experimental data (Fig. 11);
- the core pressure drop calculated by the code have a very good trend respect on the experimental one (Fig. 48);

- the prediction of the RPV pressure drop is consistent with the available experimental data (Fig. A - 48);
- similar difference is already observed in the simulation of other LOBI tests (i.e. BL-44 post test calculation, see Ref. [31]).
- it might be possible the temporary pool formation in the upper plenum above the connection with the hot legs.

The SG's levels are slightly overestimated (Fig. 40 and Fig. 41), especially considering the broken loop. This is consistent with difference in the secondary mass inventories already discussed above. It should be noted that the large variation of the level observed at the beginning of the transient is not expected to occur.

Rod surface temperatures
Representative experimental data at three levels of the core (bottom, middle and top region), in the axial direction, have been chosen and compared with the calculated data (see Fig. 44, Fig. 45 and Fig. 46). The trend is well simulated. The experimental data show a temperature excursion due to dry-out condition occurrence, in the top region of the core (lev. 12 in Fig. 6). The CHF conditions are achieved few seconds before the set point of the accumulator injection is reached. Therefore, the temperature excursion in the core is local and of few degrees. This local dryout condition is negligible and not predictable by the code, which model the average condition in the channel.

Moreover, according with Ref. [32] simulating LOFT ITF tests, it was observed, that RELAP5 Mod3.3 underpredicts the cladding temperatures at the higher elevations in the core. These results are different from those achieved running the previous version Mod3.2. This difference was explained with the way the code handles choked flow and interphase drag.

The heat structure of the upper plenum experiences a temperature higher than the saturation for a lasting period of about 200s (from 200s to 400s from SoT). Therefore this is observed before and during the operation of the accumulator. The code predicts with a good accuracy such trend, and more in general the overall behavior (Fig. 47).

5.2.1 Qualitative Accuracy

The qualitative accuracy evaluation is based upon a systematic procedure consisting in the identification of phenomena (CSNI list) and of RTA. It essentially derives from a visual observation of the experimental and predicted trends discussed section 5.2, and consist in comparing relevant quantities, which characterize each RTA. In this context, the evaluation of the RTA is based on an engineering judgments. Five levels of judgment are introduced: E, R, M, U. Their meanings are listed below:

a) "E" mark: the code predicts qualitatively and quantitatively the parameter (Excellent – the calculation result is within experimental data uncertainty band);
b) "R" mark: the code predicts qualitatively, but not quantitatively the parameter (Reasonable – the calculation result shows only correct behavior and trends);
c) "M" mark: the code does not predict the parameter, but the reason is understood and predictable (Minimal – the calculation result lies within experimental data uncertainty band and sometimes does not have correct trends);
d) "U" mark: the code does not predict the parameter and the reason is not understood (Unqualified - calculation result does not show correct trend and behavior, reasons are unknown and unpredictable).

The related results are reported in Tab. 19, where are also given the information related to RELAP5/3.3 results. A positive overall qualitative judgment is reached if "U mark" is not present in the table. Furthermore, the parameters characterizing the RTA (i.e., SVP= Single Valued Parameter, TSE= parameter belonging to the Time Sequence of Events, IPA= Integral Parameter, NDP= Non Dimensional Parameter) give an idea of the amount of the discrepancy; they are used to evaluate the accuracy of the code simulation, from a qualitative point of view. In this investigation the following conclusions are achieved:

- U mark is not present;
- All RTAs of the experiment are present in the calculation;
- The accuracy evaluation adopted (RTA plus Key phenomena) brings to the conclusion that the calculation is qualitatively correct.

5.2.2 Quantitative Accuracy

To evaluate the quantitative accuracy a methodology, based on the fast Fourier Transform, is applied [29]. The results of the application of the method are given in Tab. 20, where are also furnished the information about RELAP5/3.3 calculation.

The so called Fast Fourier Transform Based Method developed at University of Pisa, is used for the quantification of the accuracy of the code results. It is well known that the Fourier transform is essentially a powerful problem solving technique. Its importance is based on the fundamental property that one can analyze any relationship from a completely different viewpoint, with no lack of information with respect to the original one. The Fourier transform can translate a given time function g(t), in a corresponding complex function defined, in the frequency domain, by the relationship:

$$\tilde{g}(f) = \int_{-\infty}^{+\infty} g(t) * e^{-j2\pi f t}\, dt$$

Afterwards, it is assumed that the experimental and calculated trends, to which the Fourier transform is applied, verify the analytical conditions required by its application theory.

The FFTBM tool gives an accuracy coefficient (AA) and a weighted frequency (WF) for each variable and for the overall transient. Roughly, the value assumed by AA represents the error in the calculation of the considered variable. The WF factor provides information whether the calculated discrepancies, between the measured and calculated trends, are more important at low frequencies (small value of WF) or high frequencies (large value of WF). In this last case, it can be stated that the discrepancies come from various kinds of noise and so it is less important.

24 parameters are selected for the application of the method to the LOBI test A1-84. They are selected as the reasonable number, necessary to describe the transient, considering both the peculiarities of the transient and the availability of the experimental data as well. These parameters are then combined to give an overall picture of the accuracy of a given calculation. The total average amplitude of the transient is the result of the sum of all the average amplitudes with their "weights".

The "weight" of each contribution is dependent by the experimental accuracy, the relevance of the addressed parameter, and a component of normalization with reference to the average amplitude evaluated for the primary side pressure. The figure of merit of the method is

usually consists of three values: the average amplitudes of the 1) primary pressure and of the 2) global (or total) response, consistently with the typical application of the method, plus the 3) coolant temperature at the affected SG outlet, due to the peculiarity of the test. The procedure for code assessment, considers, in case of LOCA transients, two acceptability limits: $AAp \leq 0.1$ for the average amplitude of the primary pressure and $AAtot \leq 0.4$ for the total average amplitude.

The method is applied at all the transient, from 0s to 850s. The achieved results bring to the considerations hereafter summarized (see Tab. 20).

- The average accuracy for the primary pressure, considering the overall transient, is excellent: AA=0.04 if the pressurized pressure is considered and AA=0.11 in the case of the other pressure.
- The accuracy is excellent also for the secondary side pressure, for which the average accuracy is 0.06.
- The coolant temperature, in several section of the ITF shows a good accuracy, AA is lower than 0.26. It is excellent in the case of the lower plenum temperature: AA=0.04.
- The prediction of the mass inventories has a reasonable accuracy: AA below 0.4.
- The pressure drops show bigger discrepancies between the experimental and the calculated data. Nevertheless, good accuracy is achieved in the case of the RPV pressure drop and in particular for the pressure drop across the core.
- The average accuracy of the calculated heated rods temperatures are excellent: below 0.05. The temperatures taken in account are measured at different heights of the heated length.
- The secondary side levels are not well simulated (AA<0.6). This is a confirmation of what is observed in Fig. 40 and Fig. 41 and stated in section 5.2.
- The total average accuracy is AA=0.180, which means that the overall transient is simulated with a very good accuracy.

5.3 Sensitivity calculations

Considering the reference calculation (Run 0), a series of sensitivity analyses (Tab. 21) have been carried out, in order to investigate the robustness of the code results and to evaluate the relevance of some selected parameters and/or user choices on the results.

The sensitivities are focused on the models that most influence the transient, and on the initial conditions of the transient. This last calculations are useful to understand how a certain modification of the initial conditions can affect the evolution of the transient.

Six sensitivity calculations have been performed starting from the Run 0 and hereafter discussed.

- RUN 1 (input ID “A1-84_10.9”). Several sensitivities have been made changing the Ransom-Trapp coefficients, changing only one coefficient per run and leaving fixed the other two coefficients. The objective of this sensitivity was to find the coefficients which showed the best results achievable using Ransom-Trap model. The best set of discharge coefficients is achieved with this sensitivity, which shows a prediction of the results improved with respect the reference results. The primary experimental pressure is perfectly matched, and the temperatures trends are improved. The intact

loop accumulator injects exactly at the same time as in the experiment. Nevertheless, no study has been found in literature using superheated discharge coefficient as low as 0.6. The main results are reported in Fig. 51 and Fig. 52.

- RUN 2 (input ID "A1-84_bl44break"). The sensitivity is related to the chocked flow model. It is performed using the same discharge coefficients used in BL-44 test simulation [22], in order to render more complete the comparison between the two simulations. The critical flow model used is Ransom-Trapp and the coefficients that are used in the simulation are 1.0, 0.9, 1.0. The code results are poor: the trend of the primary pressure is qualitatively predicted in the early blowdown period, and the temperatures poorly simulated. The heater rods suffer a dry-out between 200 and 500s, with a peak temperature, at level 6, of 489°C. Summary of the results are available in Fig. 53.
- RUN 3 and 4 (input ID "A1-84_8.1" and "A1-84_10.0"). The sensitivities are related to the chocked flow model. In these sensitivities the chocked flow model was changed, in order to understand if the 10% hot leg break analyzed was physically well reproduced by Henry-Fauske model. Henry-Fauske chocked flow model utilizes two different coefficients, implemented by the user. These are the discharge coefficient and the non-equilibrium constant. In these sensitivities they were set up as follows:
  Run A1-84_8.1:
  - Discharge coefficient: 0.6
  - Thermal non-equilibrium constant:0.35

  Run A1-84_10.0:
  - Discharge coefficient: 0.63
  - Thermal non-equilibrium constant:0.14 (default value)

  In literature, it is possible to find simulations with discharge coefficients lower than the default value, 1.0. This is the outcome achieved by the validation activity performed on separate effect test facility, see Ref. [32]. Anyway the use of such low value remains questionable. The results reported in Fig. 54 , Fig. 55 and Fig. 56 shows the best results achieved with Henry-Fauske model.
- RUN 5 and 6 (input ID "A1-84.11klevel" and "A1-84.11k.l"). These sensitivities were performed in order to improve the simulation of the secondary side level or at least to understand the reason of the discrepancies. The hypothesis is that the steady state level is not the real one, and the only level to take in account for a comparison is the level after the scram. Therefore, this last value was set as the reference value during the steady state. Run 5 consist in a simple reduction of the initial level according with the consideration above. On the contrary Run 6 involves also a modification of the energy loss coefficient between downcomer and riser (decreased). The results demonstrates in case of Run6 an improvement of the recirculation ratio in the SG. The code results are available in Fig. 57, Fig. 58, Fig. 59 and Fig. 60.

Tab. 17 – LOBI test A1-84: comparison between measured and calculated relevant initial conditions.

#	QUANTITY (*)	Unit	Exp Y_{exp}	Err. $\pm\varepsilon_{exp}$	R5 Y_{calc}	Err. ε_{calc}	Acc. ε (°) (°°)
1	**PRIMARY CIRCUIT POWER BALANCE**						**2%**
1-1	*Core thermal power*	MWth	5.15	--	5.15	0.00%	
2	**SECONDARY CIRCUIT POWER BALANCE**						**2%**
2-1	*SG-IL power exchanged*	MWth	3.79	--	3.85	1.50%	
2-2	*SG-BL power exchanged*	MWth	1.22	--	1.26	3.53%	
3	**ABSOLUTE PRESSURE**						**0.10%**
3-1	*PRZ pressure (top of the PRZ)*	MPa	15.80	±0.20%	15.78	0.00%	
3-2	*Upper plenum pressure*	MPa	15.76	±0.20%	15.83	0.24%	
3-3	*Hot leg pressure IL*	MPa	15.80	±0.04	15.8	0.00%	
3-4	*Hot leg pressure BL*	MPa	15.80	±0.04	15.80	0.00%	
3-5	*Cold leg pressure IL*	MPa	15.87	±0.04	15.96	0.31%	
3-6	*Cold leg pressure BL*	MPa	15.92	±0.04	15.95	0.00%	
3-7	*Steam dome pressure IL*	MPa	6.55	--	6.55	0.00%	
3.8	*Steam dome pressure BL*	MPa	6.52	--	6.52	0.00%	
4	**FLUID TEMPERATURE**						**0.5 % (**)**
4-1	*PRZ fluid temperature (middle)*	°C	346.6	±2.0	346.2	0.00%	
4-2	*Core inlet temperature (LP top)*	°C	295.2	±2.0	295.3	0.00%	
4-3	*Core outlet temperature (UP)*	°C	326.8	±2.0	326.9	0.00%	
4-4	*Upper head temperature*	°C	293.6	±2.0	293.8	0.00%	
4-5	*SG-IL DC pipe bottom temperature*	°C	273.9	±2.0	272.7	0.00%	
4-6	*SG-BL DC pipe bottom temperature*	°C	277.7	±2.0	275.0	0.26%	
4-7	*Hot leg- IL*	°C	328.9	±2.0	326.9	0.04%	
4-8	*Hot leg-BL*	°C	329.4	±2.0	326.9	0.19%	
4-9	*Cold leg-IL*	°C	294.2	±2.0	293.9	0.00%	
4-10	*Cold leg-BL*	°C	292.3	±2.0	292.2	0.00%	
5	**ROD SURFACE TEMPERATURE**						**10 °C**
5-1	*Heater rod temperature (bottom level-4EXP-03CALC)* (***)	°C	327.4	--	319.3	8.1	
5-2	*Heater rod temperature (middle level-6EXP-05CALC)* (***)	°C	340.3	--	333.1	7.2	
5-3	*Heater rod temperature (high level-9EXP-07CALC)* (***)	°C	343.1	--	339.2	3.9	
5-4	*Heater rod temperature (high level-12EXP-09CALC)* (***)	°C	336.4	--	328.7	7.7	
5-5	*Heater rod temperature (above TAF-13EXP-410CALC)* (***)	°C	335.9	--	334.6	1.3	
5-6	*Heater rod temperature (above TAF -15EXP-430CALC)* (***)	°C	338.5	--	338.4	0.1	
6	**PUMP VELOCITY**						**1 %**
6-1	*IL velocity*	rpm	4833	±78	4927	0.34%	
6-2	*BL velocity*	rpm	3912	±78	3912	0.00%	
7	**HEAT LOSSES (#)**						**10 %**
7-1	*RPV vessel*	kW	26	--	27	3.80	
7-2	*Primary side*	kW	56	--	53	-5.30	
7-3	*SG secondary side IL*	kW	6.7	--	6.4	-4.40	

#	QUANTITY (*)	Unit	Exp Y_{exp}	Err. $\pm\varepsilon_{exp}$	R5 Y_{calc}	Err. ε_{calc}	Acc. ε (°) (°°)
7-4	*SG secondary side BL*	kW	4.9	--	4.9	0.00	
8	**MASS INVENTORY IN PRIMARY CIRCUIT**						**2%**
8-1	*Primary mass inventory*	kg	432.86	--	440.33	1.73%	
9	**MASS INVENTORY IN SECONDARY CIRCUIT**						**5%**
9-1	*SG IL mass inventory*	kg	327.06	--	311.9	4.64%	
9-2	*SG BL mass inventory*	kg	81.22	--	81.46	0.3%	
10	**FLOW RATES**						**2%**
10-1	*Core inlet mass flow rate*	Kg/s	25.51	--	25.538	0.11%	
10-2	*Core outlet mass flow rate*	Kg/s	25.51	--	25.538	0.11%	
10-3	*HL IL mass flow rate*	Kg/s	20.2	--	20.02	0.89%	
10-4	*HL BL mass flow rate*	Kg/s	6.2	--	6.175	0.4%	
10-5	*SG IL feedwater mass flow*	Kg/s	2.07	--	2.038	1.55%	
10-6	*SG BL feedwater mass flow*	Kg/s	0.61	--	0.643	5.41%	
11	**BY-PASS MASS FLOW RATES**						**10%**
11-1	*Core by-pass*	Kg/s	--	--	0. 384	--	
11-2	*DC HL IL*	Kg/s	--	--	0.179	--	
11-3	*DC HL BL*	Kg/s	--	--	0.06	--	
11-4	*UH DC by-pass*	Kg/s	--	--	0.2643	--	
12	**PRZ LEVEL**						**0.05m**
12-1	*PRZ collapsed level*	m	5.346	--	5.346	0	
13	**VESSEL LEVEL**						**--**
13-1	*Vessel riser level*	m	8.09	--	8.12	0	
14	**SECONDARY SIDE LEVEL**						**0.1m**
14-1	*SG-IL*	m	8.81	--	8.819	0.009	
14-2	*SG BL*	m	8.21		8.13	0.08	
15	**PRESSURE DROPS**						**10%**
15-1	*RPV pressure drop*	kPa	99.3	3.1kPa	101.5	2.22%	
15-2	*Core pressure drop*	kPa	112.6	1kPa	118.4	5.15%	
15-3	*PS IL pressure drop*	kPa	179.5	1.3kPa	167.75	6.54%	
15.4	*PS BL pressure drop*	kPa	146.9	1.3kPa	153.9	4.77%	
15-5	*SG IL pressure drop*	kPa	58.44	1.2kPa	53.08	9.17%	
15.6	*SG BL pressure drop*	kPa	50.4	1.2kPa	48.1	4.56%	

(°) The % error is defined as the ratio |*reference or measured value– calculated value*|/*reference or measured value*. The "dimensional error" is the numerator of the above expression
(°°) The "acceptable errors" are defined as part of the UNIPI method for nodalization qualification (UMAE)
(*) With reference to each of the quantities below, following a one hundred s "transient-steady-state" calculation, the solution must be stable with an inherent drift < 1% / 100 s.
(**) And consistent with power error. The errors are calculated in K.
(***) According with LOBI measurement description in and nodalization description in section 4.2.
(#) at nominal steady state.

Tab. 18 – LOBI test A1-84: resulting sequence of main events.

#	EVENT DESCRIPTION	EXP (sec)	Relap5/3.3 (sec)
1	Start of transient (break opening) in BL HL	0	0
2	Scram signal (13.2MPa+0.5s delay)	1.0	1.0
3	Secondary side cooldown 100K/h actuation (at 13.2 MPa + 1.5s valve closure time)	1.3	13 (imposed by time)
4	Pressure in PS 11.7 MPa	5	4.76
5	MCPs start coastdown (at 11.0 MPa + delay 1.0s)	7	7
6	Upper plenum in saturation conditions	15.8	19.3
7	HPIS actuation (at 11.7 MPa + delay 35s)	40.0	39.8
8	PS pressure falls below SS pressure IL/BL	90.8/97.8	101.3/101.83
9	Occurrence of minimum primary side mass	347.4	350.0
10	Accumulator actuation IL/BL (at 2.8 MPa, disabled at 11Mpa + delay 500s in cold leg, not disabled in hot leg)	347.0/349.9	335.1/335.0
11	Accumulator injection stops Cold leg IL/BL)	509.0/520.0	487.4/558.7
12	Accumulator injection stops Hot leg IL	849.0	849.0
13	End of the test (0.1Mpa)	850.0	850.0

Tab. 19 – LOBI test A1-84: judgment of the code calculation on the basis of RTA.

#		UNIT	EXP	CALC	JUDGMENT
	RTA: PRESSURIZZER EMPTYING				
TSE	*Emptying time*	s	21.1	25.58	E/R
IPA	*Integrated flow from surge line*	kg	-	22.39	-
	RTA: SECONDARY SIDE STEAM GENERATORS BEHAVIOUR				
TSE	*Feed water valve closure*	s	1.565	1.7	E
TSE	*Steam line valve closure*	s	1.565	3.88	R
TSE	*Cooldown actuation*	s	1.565	13	E*
SVP	*SG IL level*	--	--	--	--
	When HPIS starts(40.06calc 39.5exp)	m	7.76	7.76	E
	When subcooled blowdown ends (42s)	m	7.75	7.76	E
	When PS pressure equals SS pressure	m	7.72	7.86	E/R
	When ACCU starts	m	7.76	7.84	E/R
SVP	*SG BL Level*	--	--	--	--
	When HPIS starts (40.06calc 39.5exp)	m	6.194	6.85	R
	When subcooled blowdown ends (42s)	m	6.173	6.86	R
	When PS pressure equals SS pressure	m	6.35	6.94	R
	When ACCU starts	m	6.45	6.89	R
SVP	*SG IL Pressure*	--	--	--	--
	When HPIS starts (40.06calc 39.5exp)	MPa	7.99	7.99	E
	When subcooled blowdown ends (42s)	MPa	7.98	7.98	E

#		UNIT	EXP	CALC	JUDGMENT
	When PS pressure equals SS pressure	MPa	7.68	7.64	E
	When ACCU starts	MPa	7.04	7.06	E
SVP	*SG BL Pressure*	--	--	--	--
	When HPIS starts (40.06calc 39.5exp)	MPa	7.96	7.99	E/R
	When subcooled blowdown ends (42s)	MPa	7.95	7.98	E/R
	When PS pressure equals SS pressure	MPa	7.61	7.62	E
	When ACCU starts	MPa	6.99	7.04	E/R
	RTA: MASS DISTRIBUTION PRIMARY SIDE				
TSE	*Time of minimum mass inventory occurrence*	s	347.4	350.1	E
SVP	*Minimum primary side mass*	kg	95.56	70.03	R
	Minimum mass/Primary Volume	kg/m3	--	--	--
	RTA: HPIS INTERVENTION				
TSE	*HPIS starts*	s	39.5	40.06	E
IPA	*Integrated flow*	kg	68.16	72.4	E
NDP	*Mass inventory at HPIS start/Total mass inventory*	--	77.5%	77.61%	E
	RTA: SUBCOOLED BLOWDOWN				
TSE	*Upper plenum in saturation conditions*	s	15.8	19.3	E/R
IPA	*break flow up to 30s*	kg	-	66.28	-
	RTA: SATURATED BLOWDOWN				
TSE	*PS pressure equal to SS pressure IL-BL*	s	90.8-97.78	101.3-101.83	E/R
SVP	*Break flow at 89s*	kg/s	--	1.702	--
	Break flow at 849s	kg/s	--	0.242	--
IPA	*Integrated flow between 89 and 849s*	kg	--	303.85	--
	RTA:ACCUMULATOR IL BEHAVIOUR				
TSE	*Injection starts*	s	347	335.1	E
	Injection stops	--	--	--	--
	Hot leg	s	849	849	E
	Cold leg	s	509	487.2	E
IPA	*Total mass delivered*	kg	-	105.75	-
NDP	*Minimum of mass Inventory Primary side/Total mass inventory*	-	22.07%	15.90%	E/R
	Mass inventory at ACCU IL start/ Total mass inventory	-	22.08%	16.64%	E/R
	RTA: ACCUMULATOR BL BEHAVIOUR				
TSE	*Injection starts*	s	349.4	335	E
	Injection stops	s	520	558.7	E
IPA	*Total mass delivered*	kg	-	14.56	--
NDP	*Mass inventory at ACCU BL start/ Total mass inventory*	-	22.41%	16.64%	E/R
*cooldown starts after secondary side peak pressure.					

Tab. 20 – LOBI test A1-84: summary of results obtained by the application of FFTBM.

#	PARAMETER		AA (0-850S)	WF (0-850S)
	Description	ID (Exp)		
1	***Prz pressure [MPa]***	*PA40*	**0.04**	**0.136**
2	***IL HL pressure [MPa]***	*PA11*	**0.11**	**0.202**
3	***BL HL pressure [MPa]***	*PA21*	**0.11**	**0.203**
4	***IL CL pressure [MPa]***	*PA16*	**0.11**	**0.203**
5	***BL CL pressure [MPa]***	*PA26*	**0.11**	**0.204**
6	***SG BL Pressure [MPa]***	*PA87S*	**0.06**	**0.123**
7	***SG IL Pressure [MPa]***	*PA97S*	**0.06**	**0.123**
8	***PRZ temparature [K]***	*TF40V000*	**0.22**	**0.122**
9	***Lower plenum temperature [K]***	*TF35V135*	**0.04**	**0.119**
10	***UH temperature [K]***	*TF39*	**0.26**	**0.154**
11	***Primary side mass [kg]***	*CIPRIM*	**0.40**	**0.174**
12	***IL mass [kg]***	*CISGIL*	**0.28**	**0.100**
13	***BL mass [kg]***	*CISGBL*	**0.37**	**0.126**
14	***RPV pressure drop [Pa]***	*PD3D3RBA*	**0.21**	**0.103**
15	***Core pressure drop [Pa]***	*PD3RUG11*	**0.16**	**0.090**
16	***IL pressure drop [Pa]***	*PD161133*	**1.93**	**0.174**
17	***BL pressure drop [Pa]***	*PD262133*	**1.89**	**0.172**
18	***Rod surface temperature bottom level [K]***	*TH35E404*	**0.03**	**0.069**
19	***Rod surface temperature middle level [K]***	*TH36G106*	**0.03**	**0.059**
20	***Rod surface temperature top level [K]***	*TH38A210*	**0.04**	**0.069**
21	***Rod surface temperature top level [K]***	*TH32A312*	**0.05**	**0.062**
22	***Heat structure temperature UP [K]***	*TH36B214*	**0.10**	**0.087**
23	***IL SG level [m]***	*CL93BT*	**0.24**	**0.142**
24	***BL SG level [m]***	*CL83BT*	**0.60**	**0.164**
TOTAL AVG. ACCURCAY			**0.180**	**0.1299**

Tab. 21 – LOBI test A1-84: sensitivity calculation matrix.

Run #	ID	DESCRIPTION	OBJECTIVE	NOTES & RESULTS
0	A1-84_11.0	Reference calculation, Ransom-Trapp chocked flow model used: Subcooled Discharge coefficient:1.0 Two phase discharge coefficient: 0.9 Superheated discharge coefficient:0.7	--	All the trends are very well reproduced
1	A1-84_10.9	As Run 0 Ransom-Trapp superheated discharge coefficient changed: 0.6	Improve the calculation result, using a coefficient not present in literature. Understand if the coefficients which give the best result, are realistic	All the trends are well reproduced, with a slight improvement in the results.
2	A1-84_bl44break	As Run0 BL-44 discharge coefficients used: subcooled discharge coefficient: 1.0, two phase discharge coefficient: 0.9; superheated discharge coefficient: 1.0	Understand if the coefficient used for the BL44 transient are suitable even for A1-84 test.	Occurrence of dry-out, trends of main of main parameters not acceptable
3	A1-84_10.0	As RUN 0. Choked flow model changed: Henry-Fauske used; Discharge coefficient: 0.63, Non-equilibrium coefficient: 0.14 (default)	Understand if Henry-Fauske critical flow model, can reproduce the transient as well as Ransom-Trapp model.	All the parameters are well reproduced, but no improvement is introduced.
4	A1-84_8.1	As Run 0 Choked flow model changed: Henry-Fauske used; Discharge coefficient: 0.6, Non-equilibrium coefficient: 0.35	Understand if Henry-Fauske critical flow model, can reproduce the transient as well as Ransom-Trapp model.	All the parameters are well reproduced, but no improvement is introduced. Run3 preferred because of the more realistic factors implemented.
5	A1-84.11klevel	As Run 0 Steady state imposed level in the level control system, lowered 20cm for IL and 50cm for BL	Match the level trend in the transient simulation	BL level acceptable, IL level too low. Recirculation ratio not perfect. No improvements reached.
6	A1-84.11k.l	As Run 0 Steady state imposed level in the level control system, lowered 15cm for IL and 35cm for BL. End of downcomer loss coefficients lowered to 14.9 for IL, and to for BL	Match the level trend in the transient simulation	BL level perfectly matched, IL level acceptable. Recirculation ratio perfectly matched.

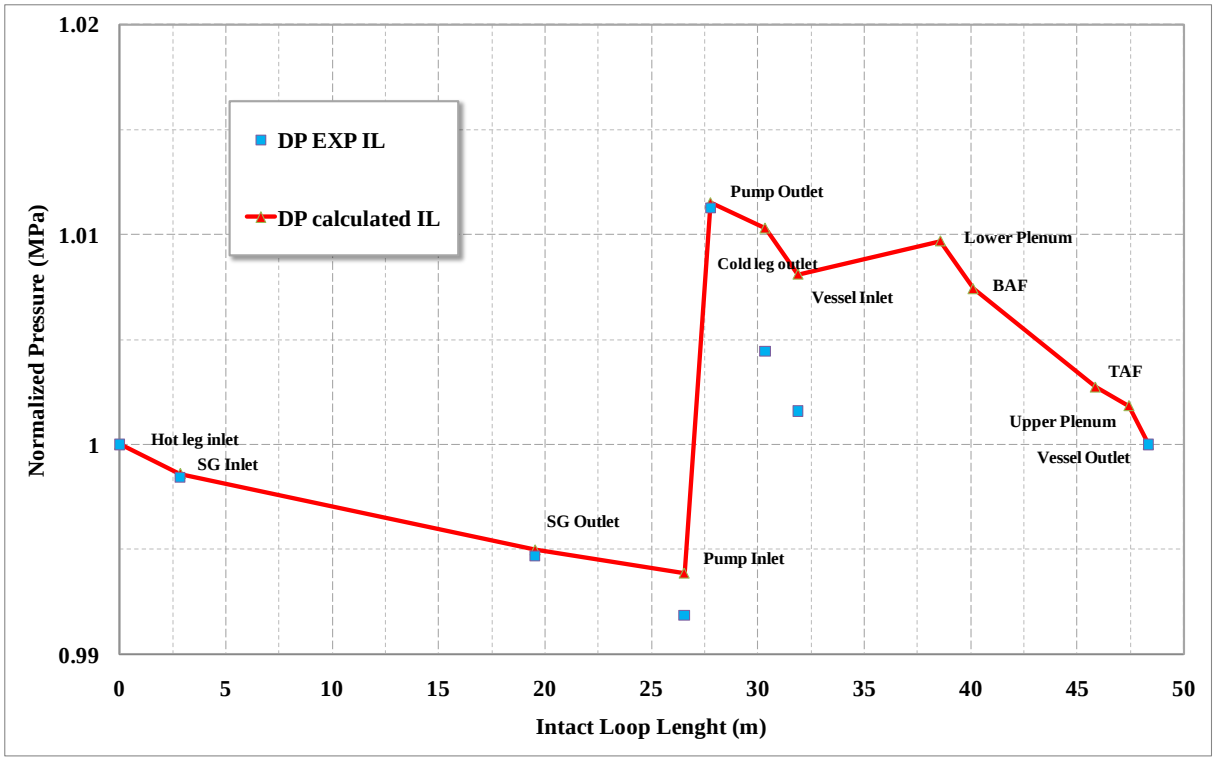

Fig. 26 – LOBI test A1-84: pressure drop vs IL length.

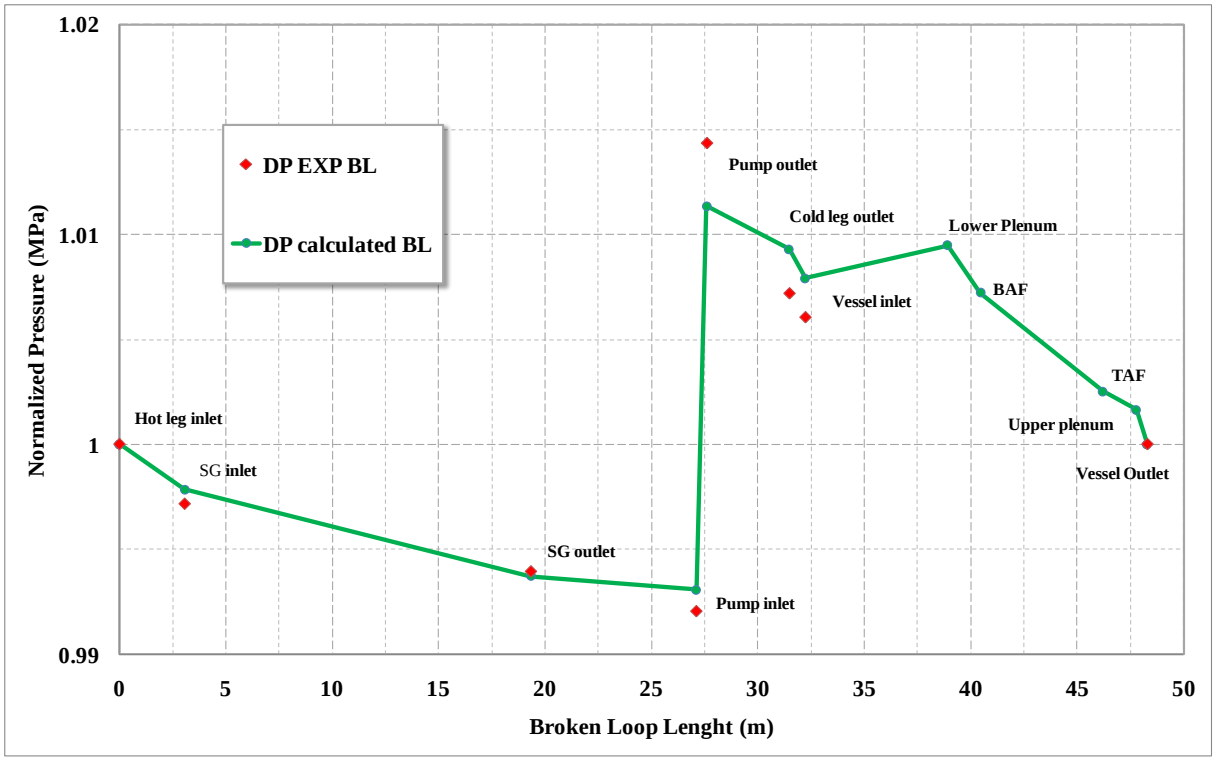

Fig. 27 – LOBI test A1-84: pressure drop vs BL length.

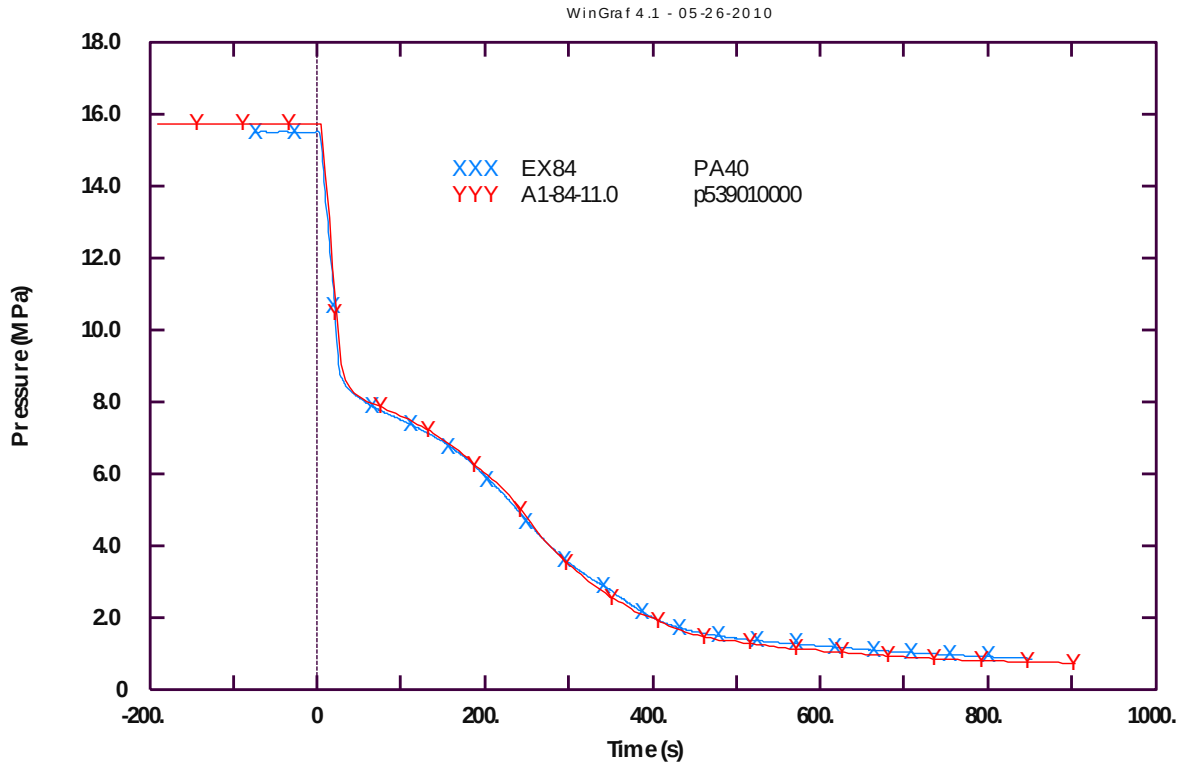

Fig. 28 – LOBI test A1-84: PRZ pressure.

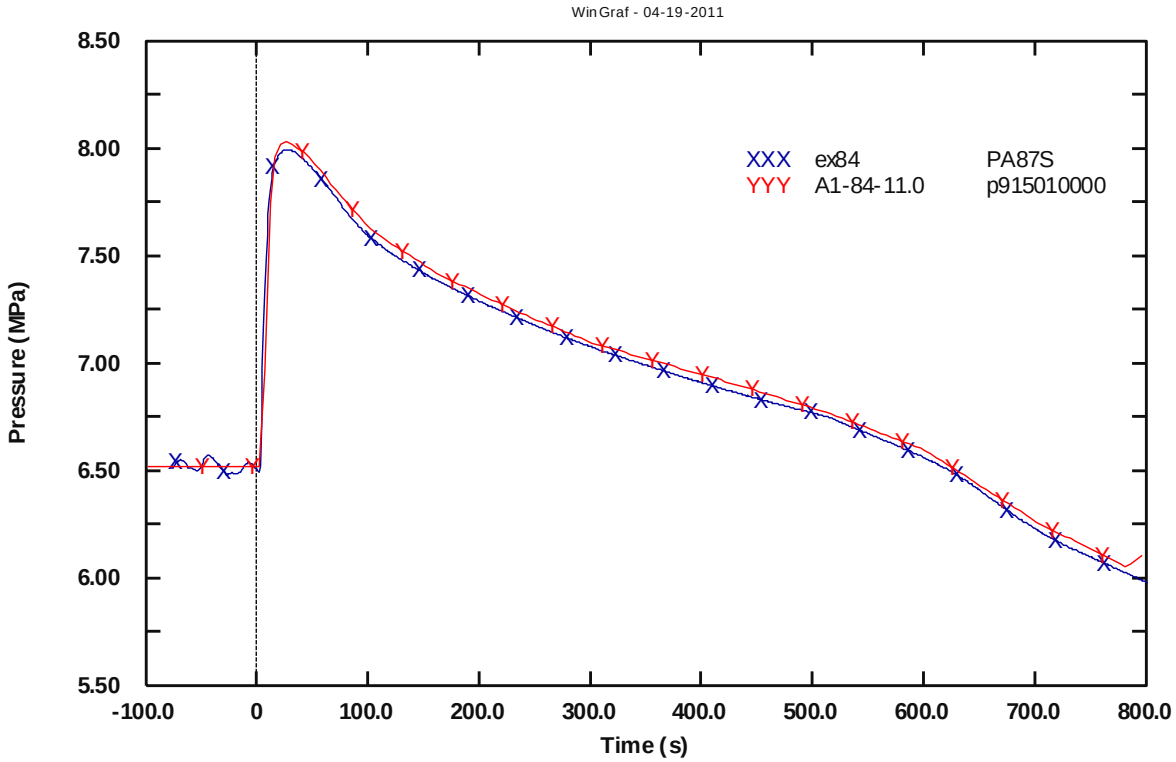

Fig. 29 – LOBI test A1-84: SG IL pressure.

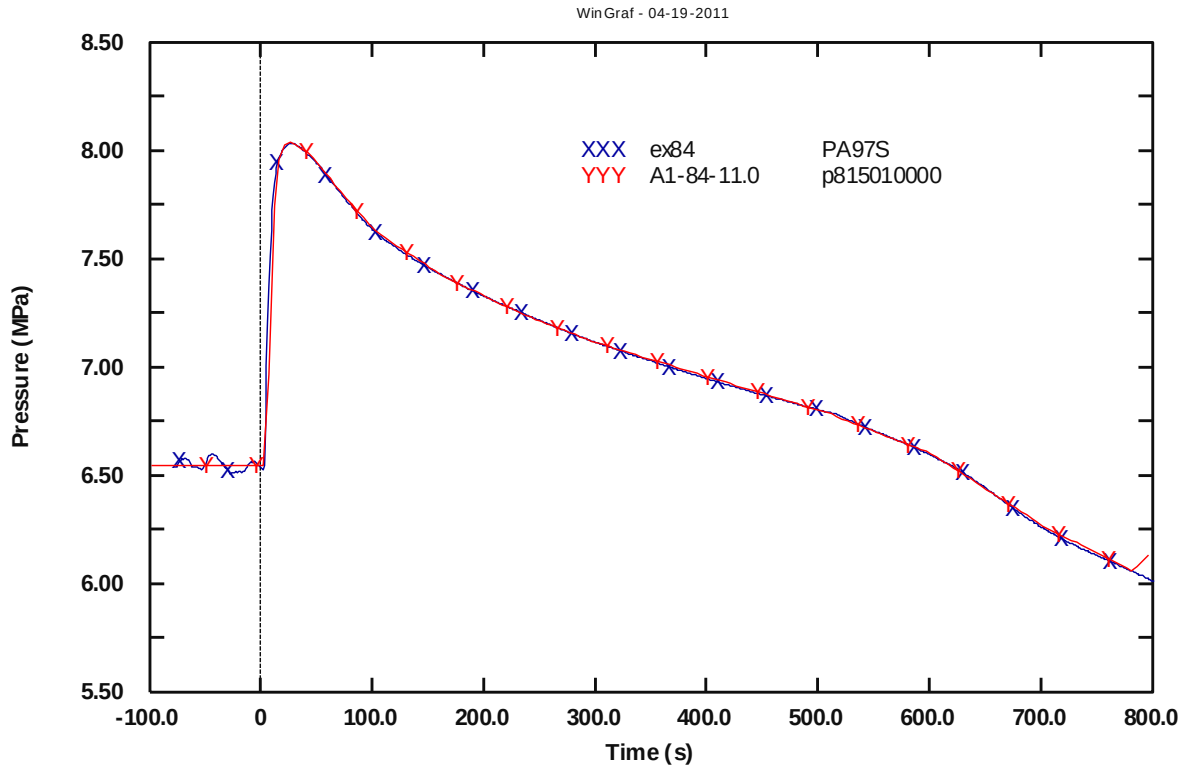

Fig. 30 – LOBI test A1-84: SG BL pressure.

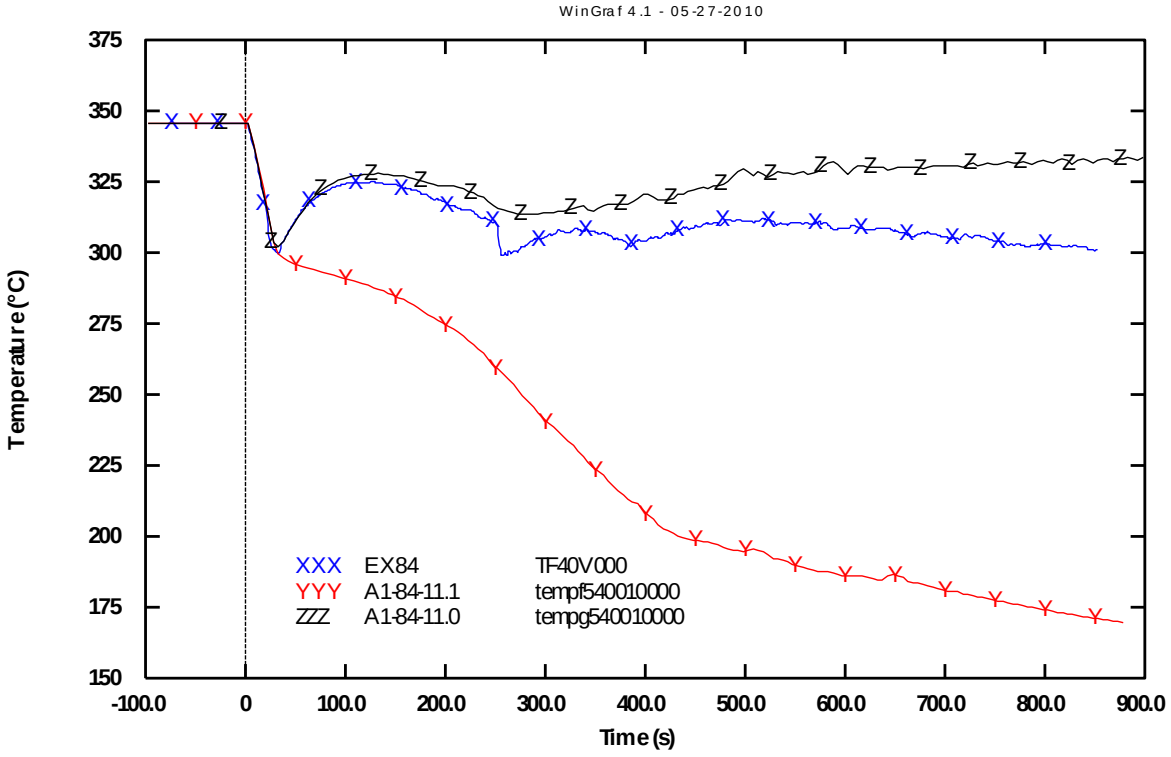

Fig. 31 – LOBI test A1-84: PRZ coolant temperature.

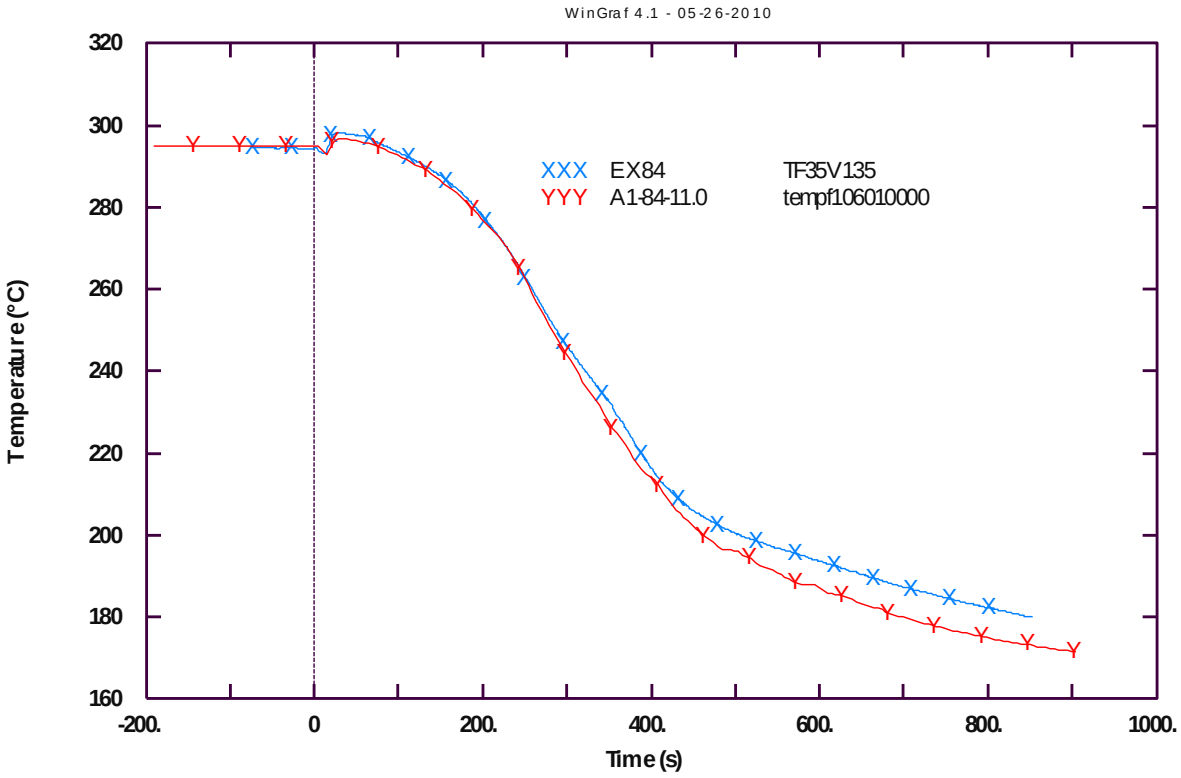

Fig. 32 – LOBI test A1-84: core inlet coolant temperature.

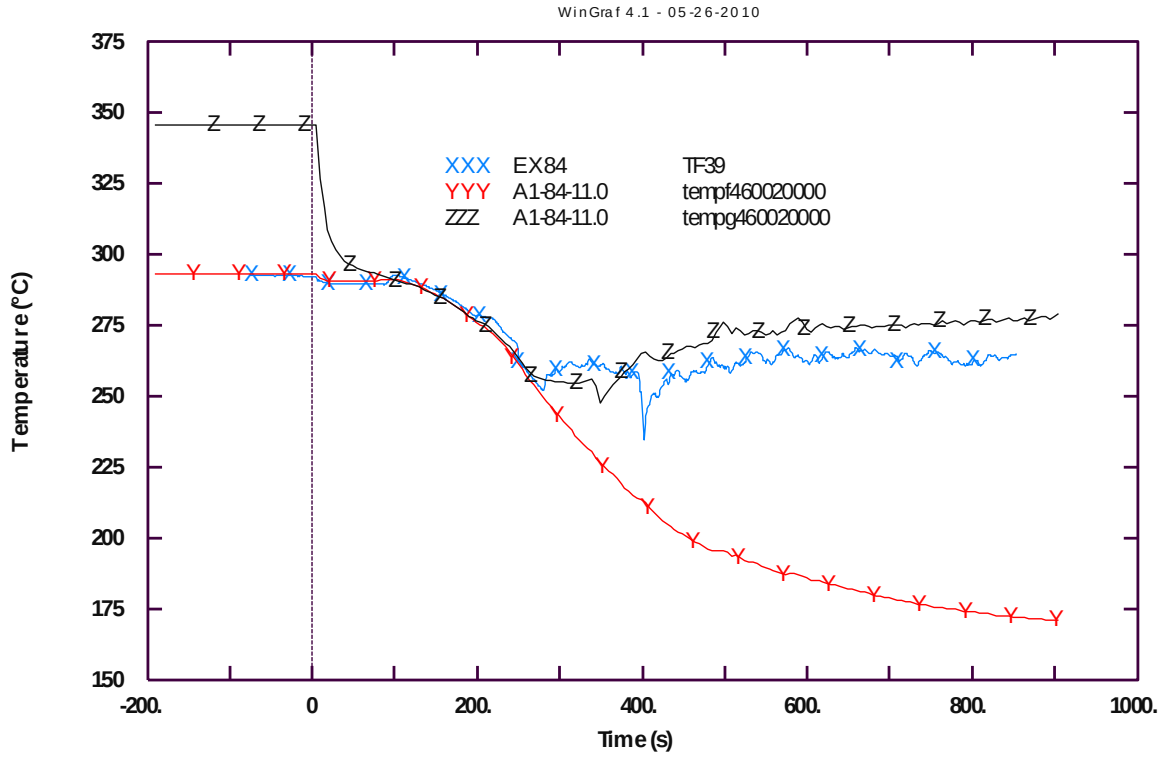

Fig. 33 – LOBI test A1-84: UH coolant temperature.

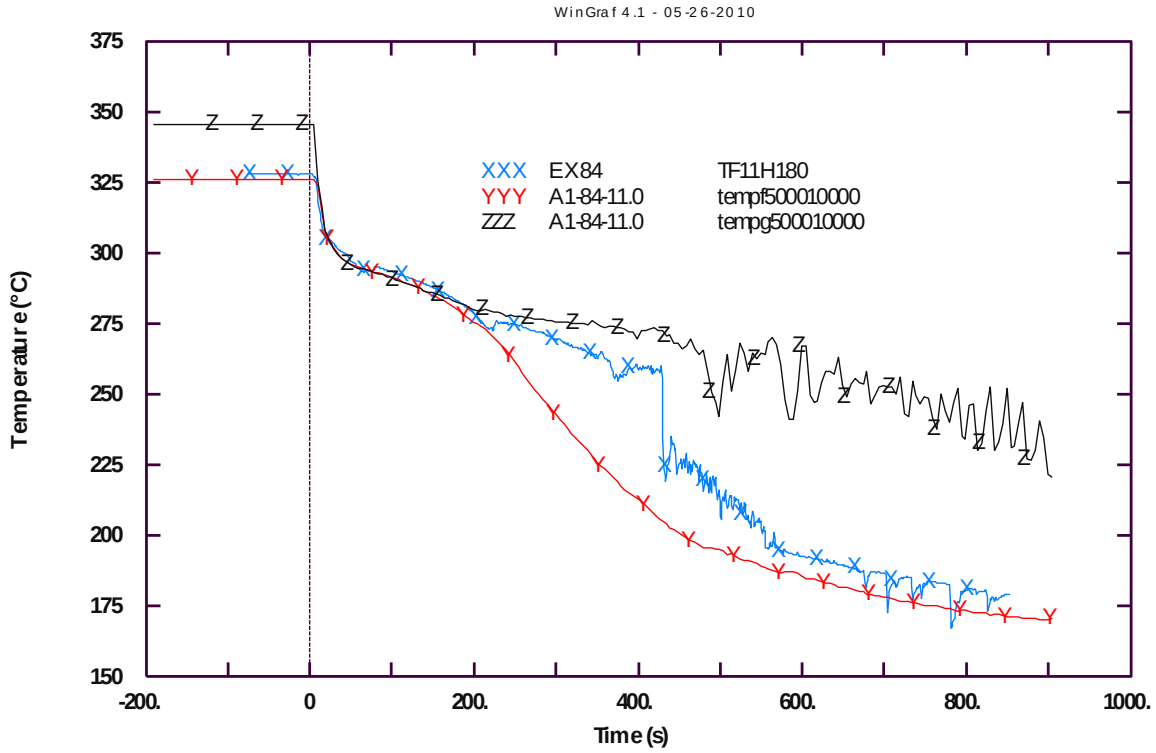

Fig. 34 – LOBI test A1-84: IL HL coolant temperature.

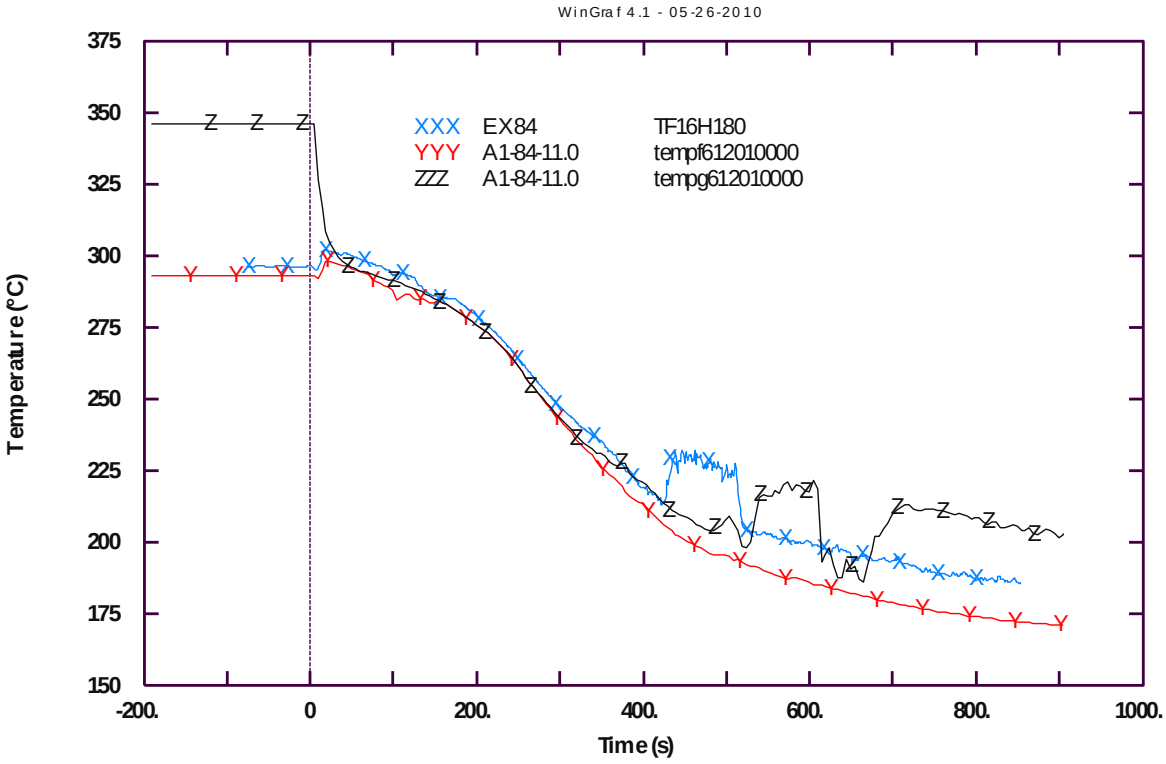

Fig. 35 – LOBI test A1-84: IL CL coolant temperature.

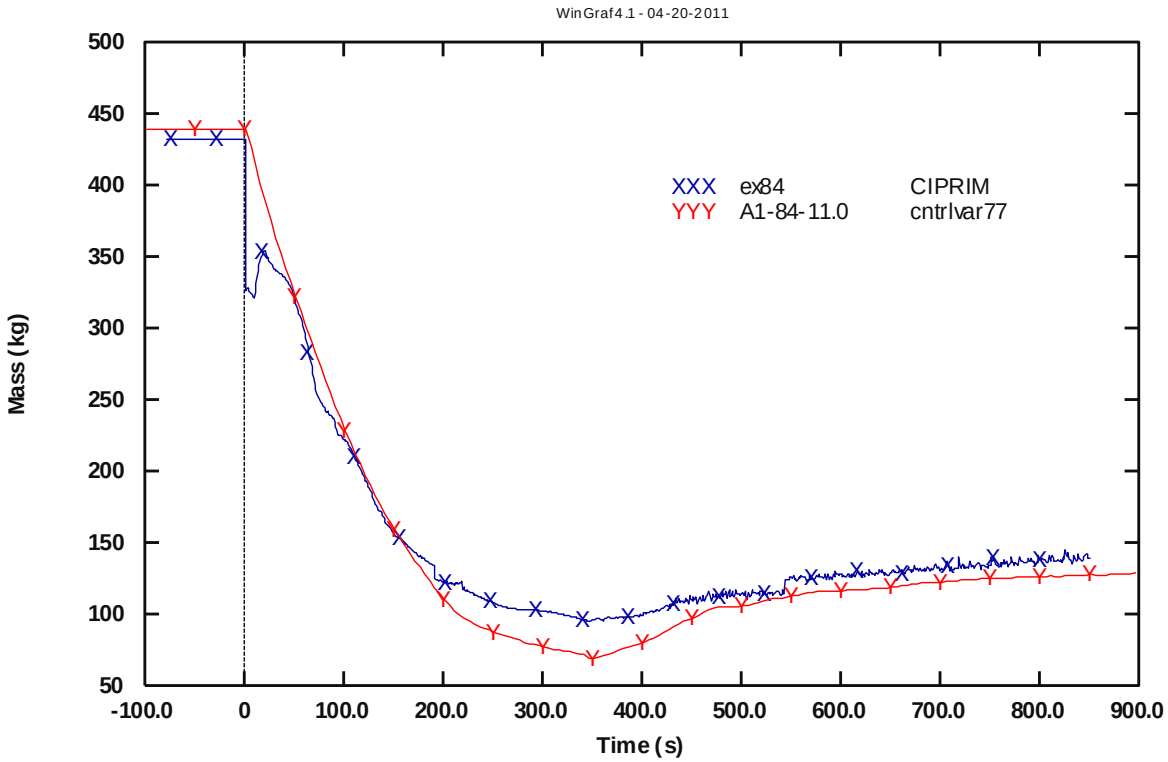

Fig. 36 – LOBI test A1-84: primary mass inventory.

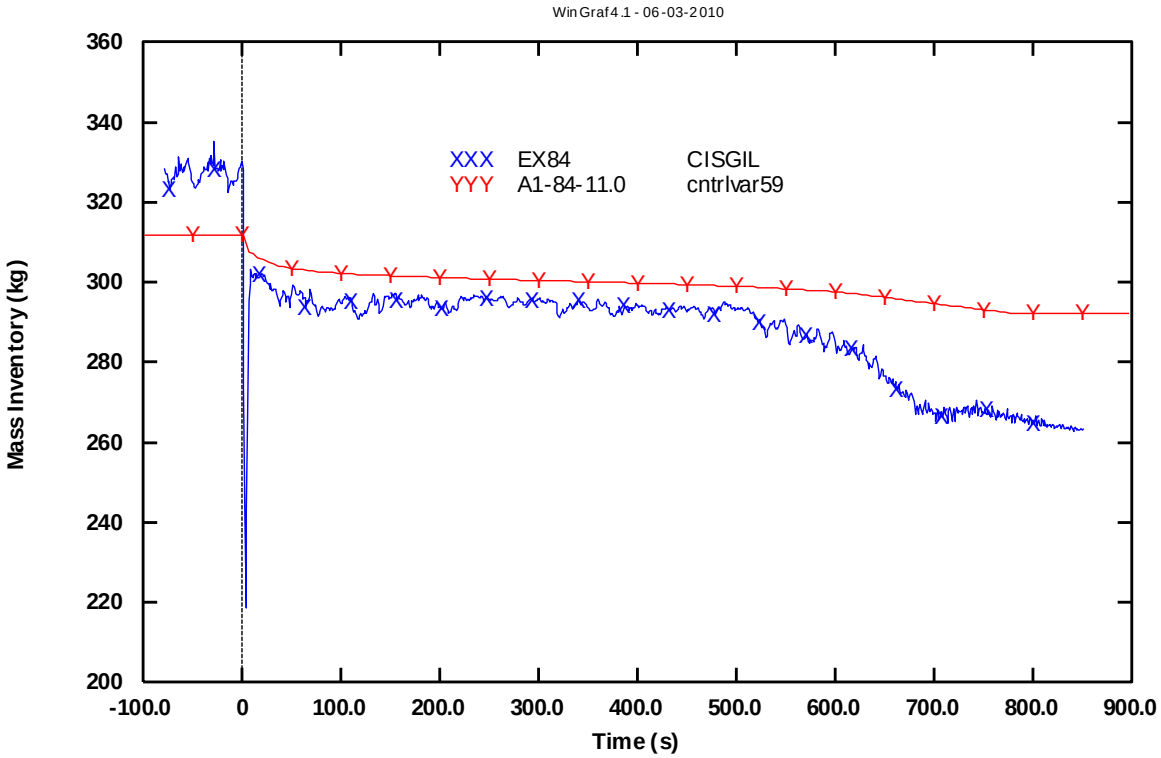

Fig. 37 – LOBI test A1-84: SG IL mass inventory.

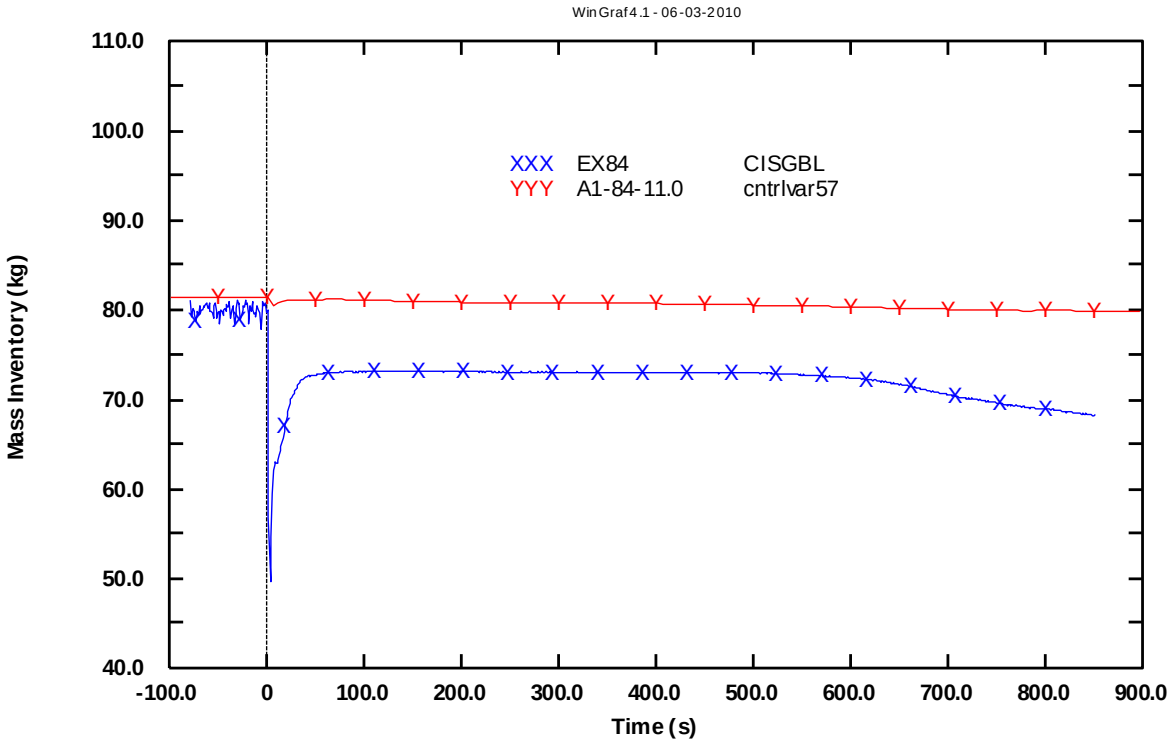

Fig. 38 – LOBI test A1-84: SG BL mass inventory.

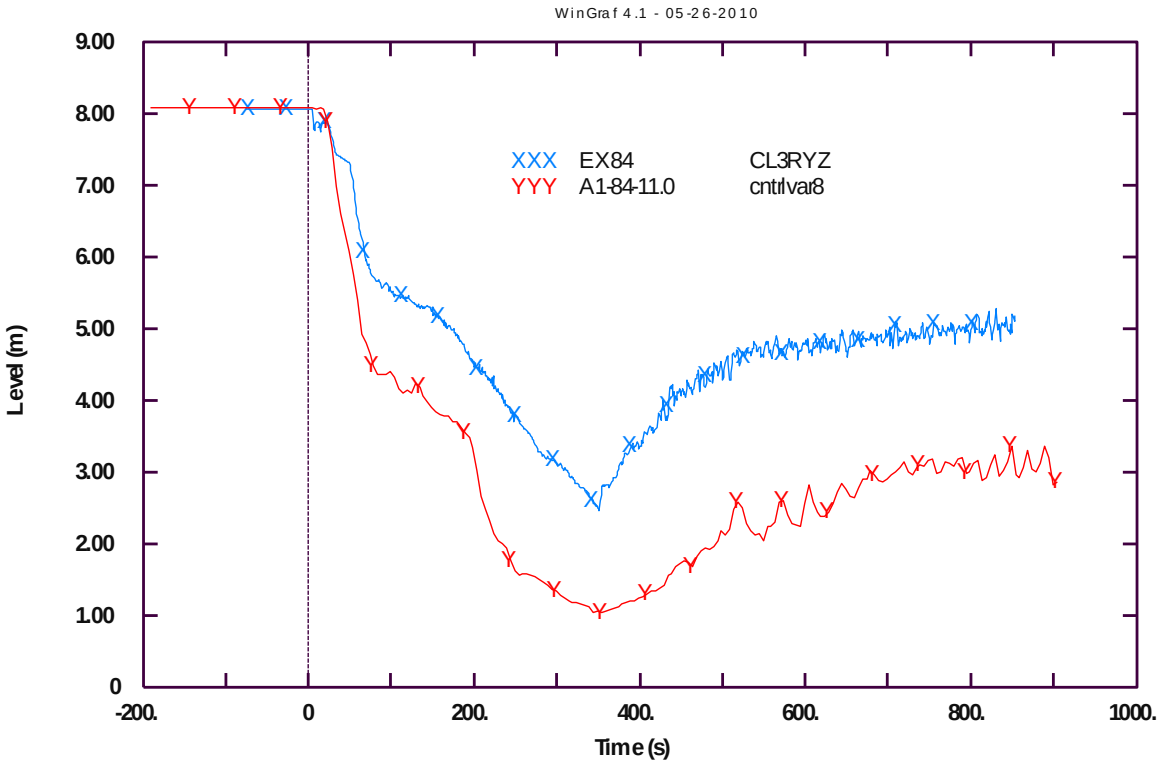

Fig. 39 – LOBI test A1-84: RPV collapsed level.

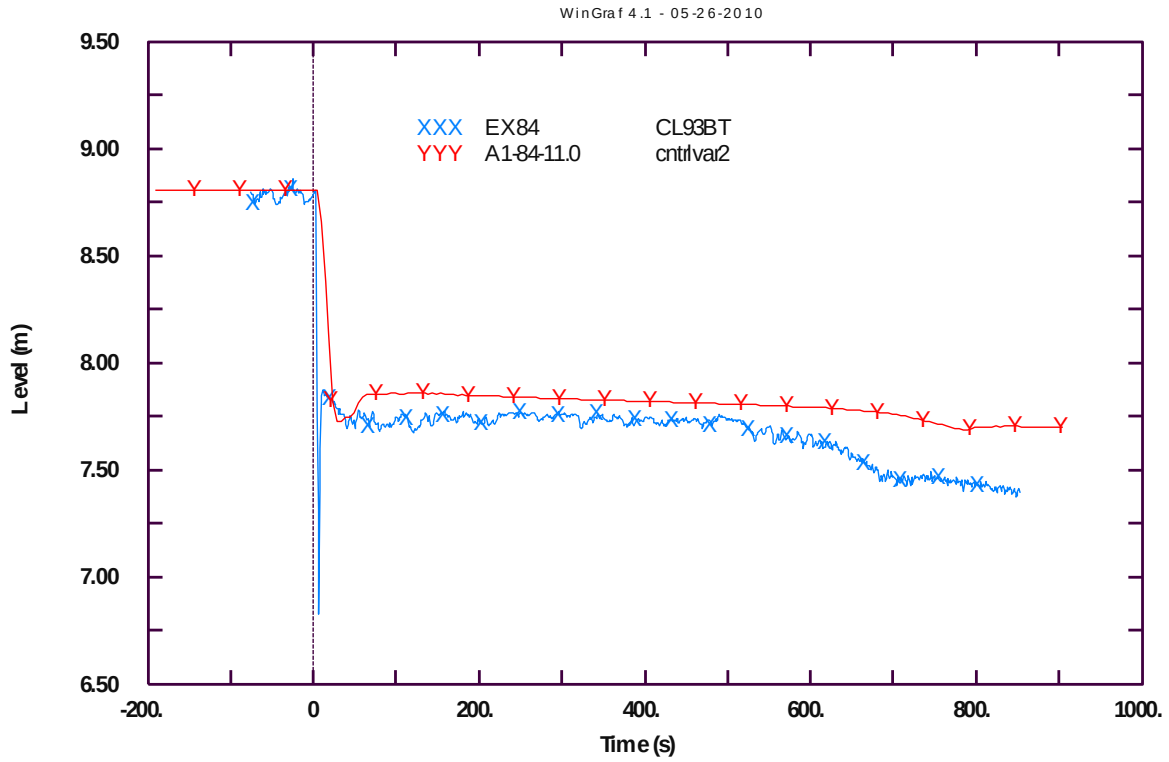

Fig. 40 – LOBI test A1-84: SG IL level.

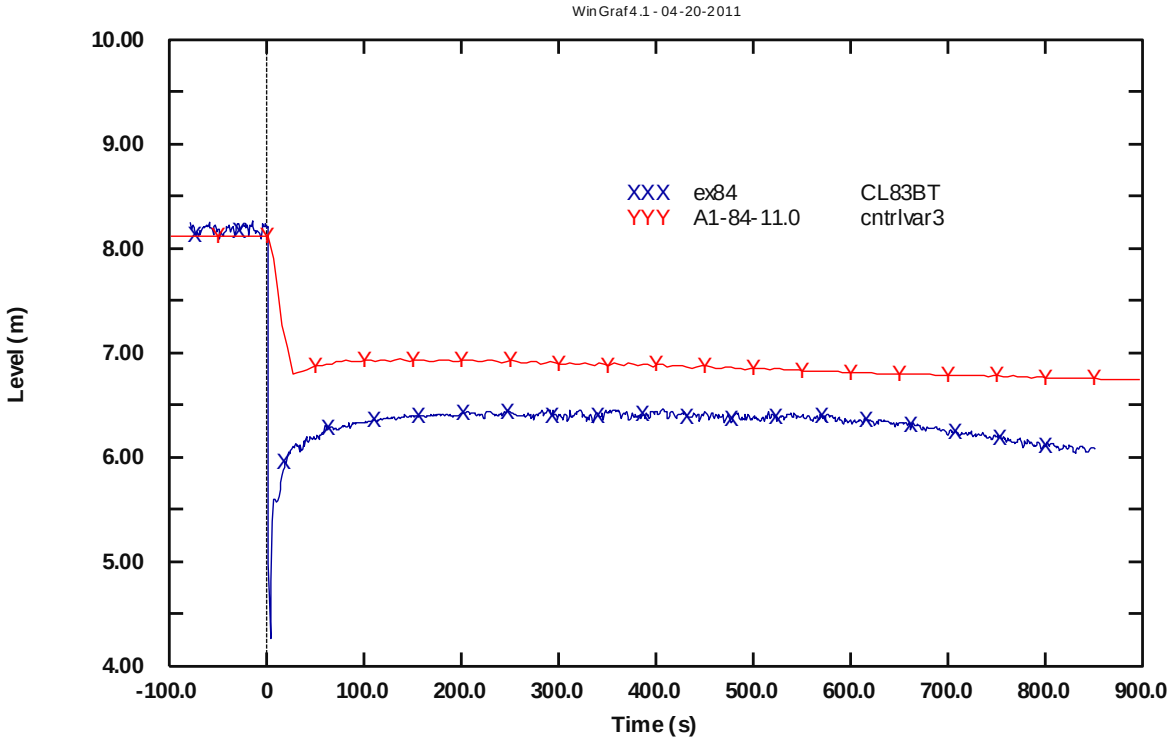

Fig. 41 – LOBI test A1-84: SG BL level.

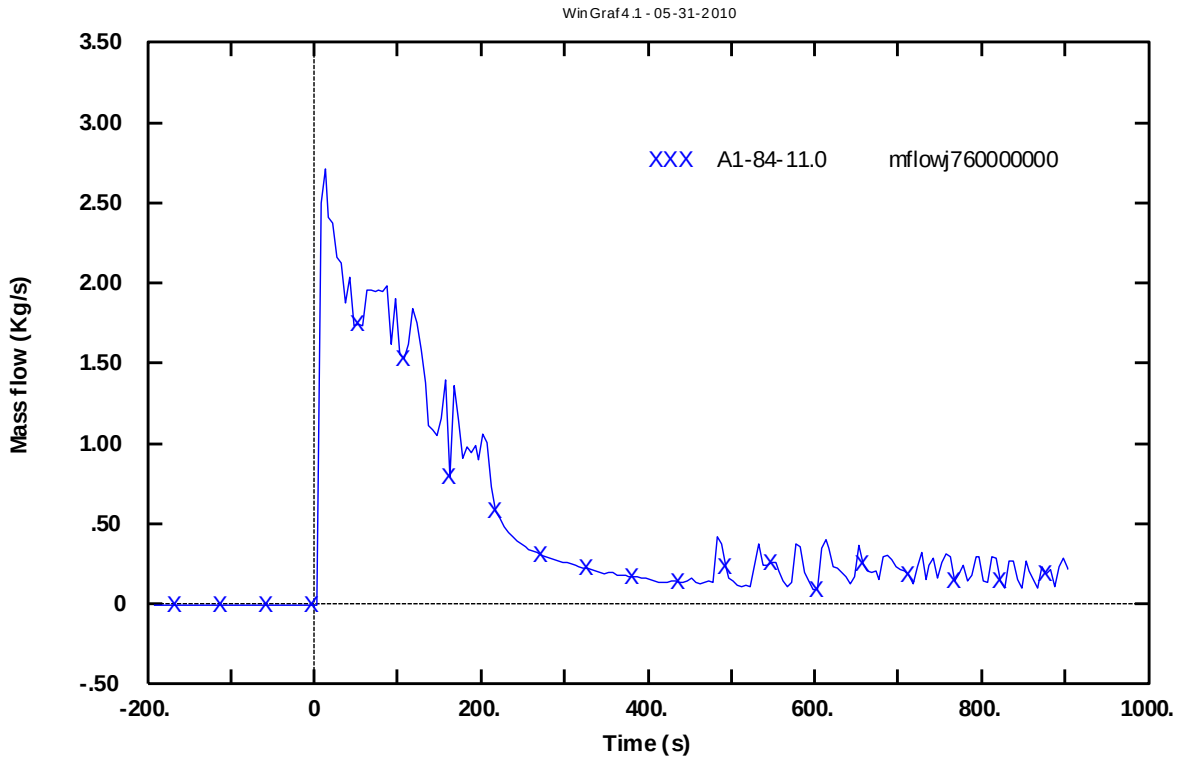

Fig. 42 – LOBI test A1-84: break mass flow rate.

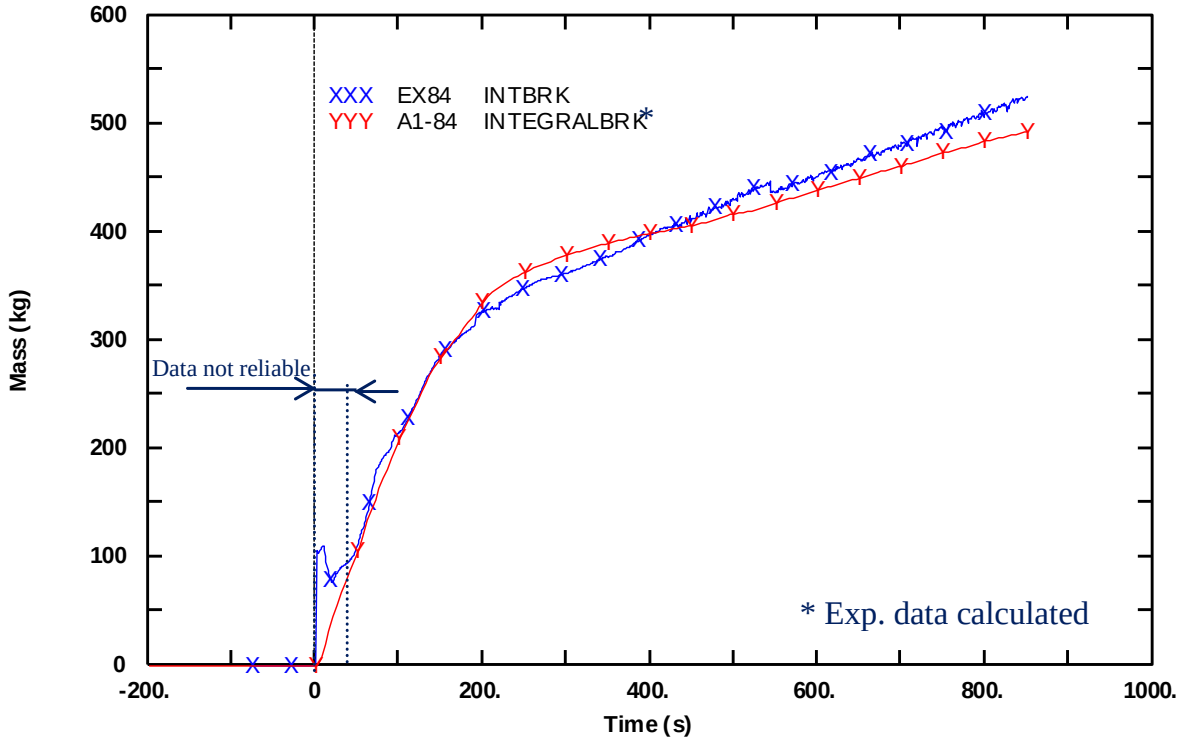

Fig. 43 – LOBI test A1-84: integral break flow rate.

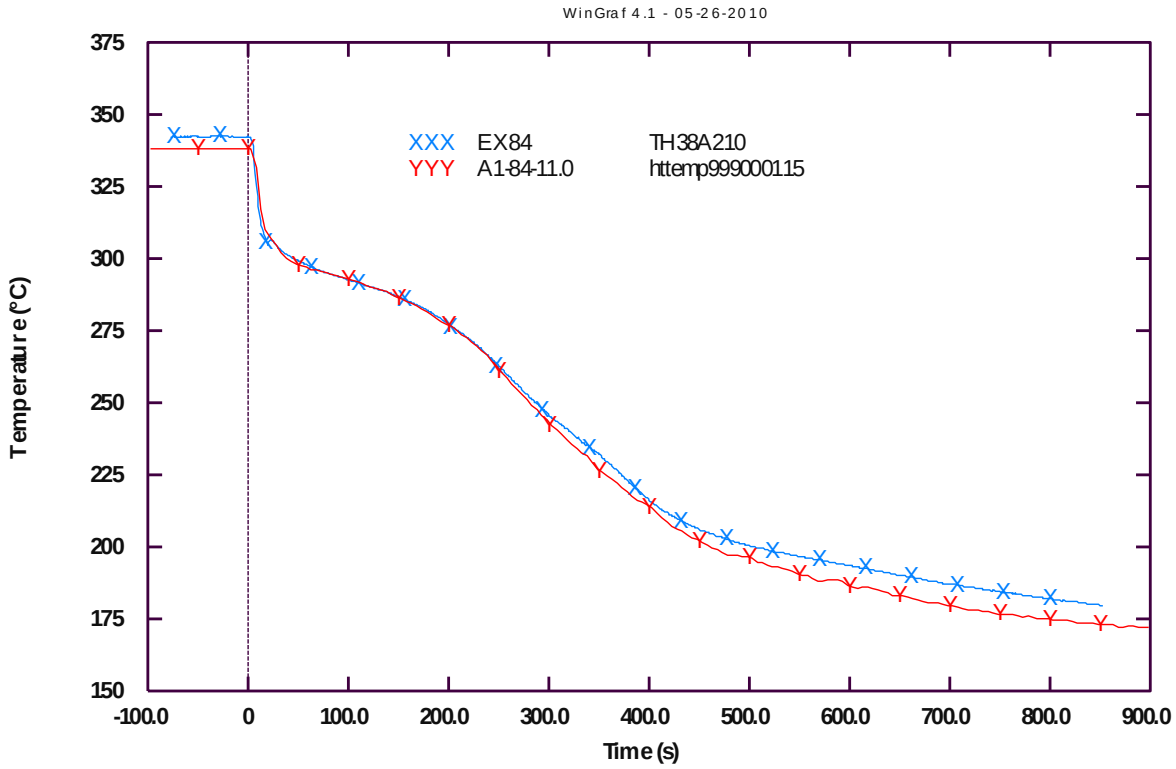

Fig. 44 – LOBI test A1-84: heater rod temperature, bottom level.

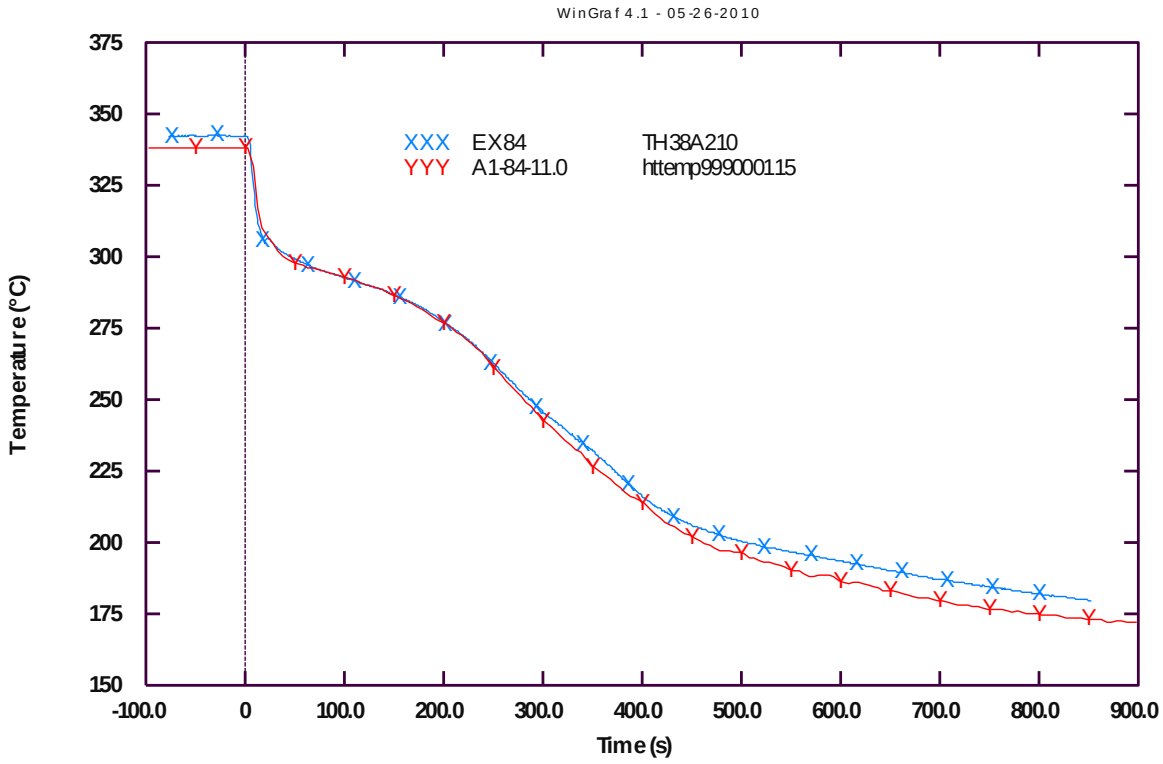

Fig. 45 – LOBI test A1-84: heater rod temperature middle level.

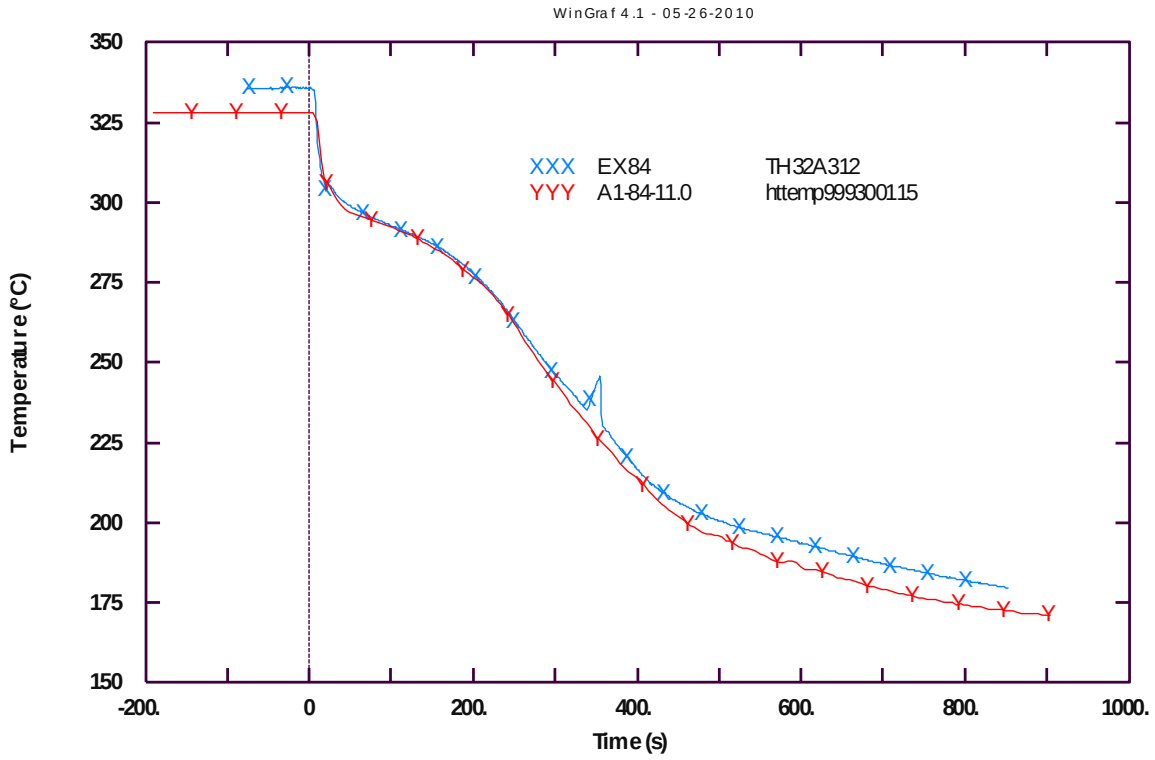

Fig. 46 – LOBI test A1-84: heater rod temperature top level (level 12).

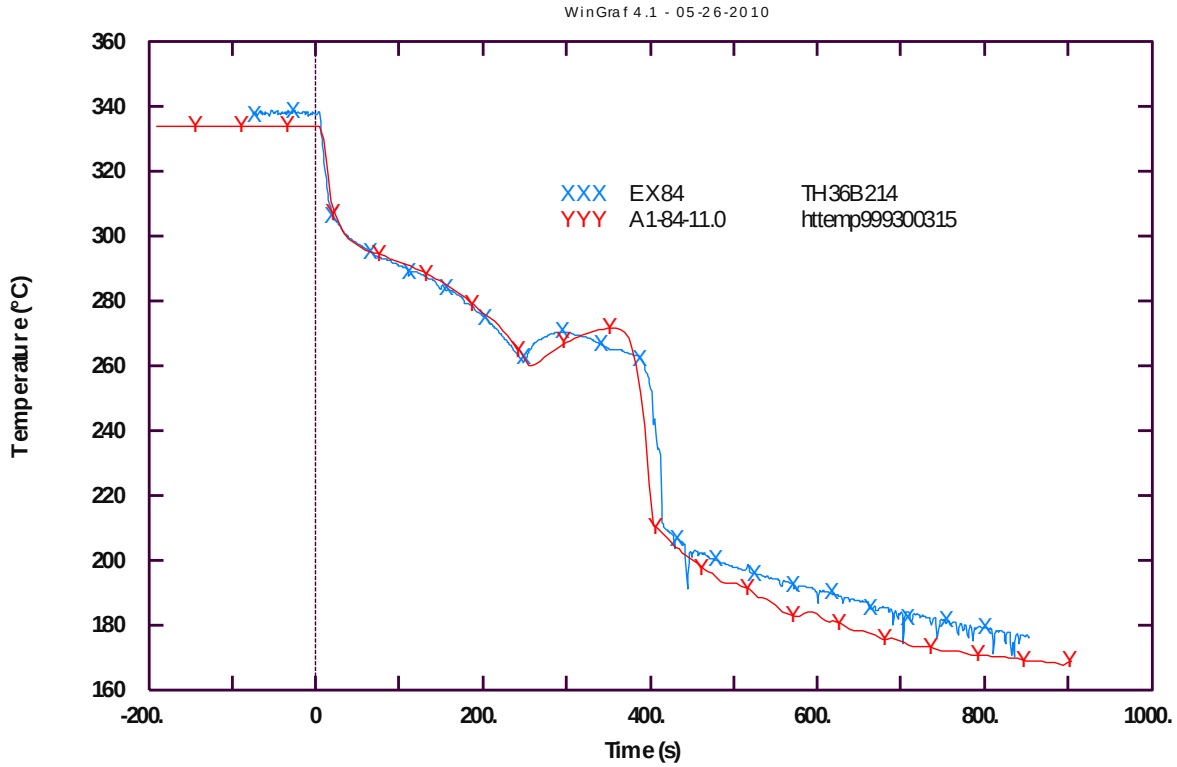

Fig. 47 – LOBI test A1-84: heat structure temperature in upper plenum.

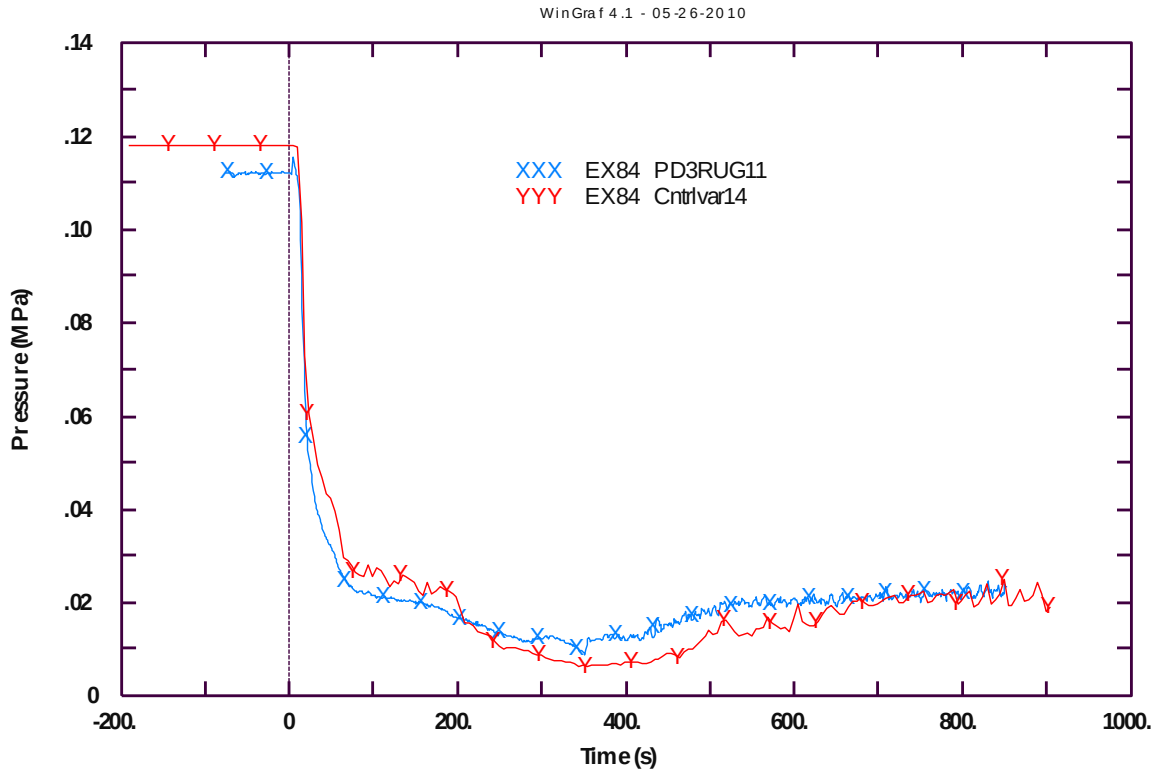

Fig. 48 – LOBI test A1-84: core pressure drops.

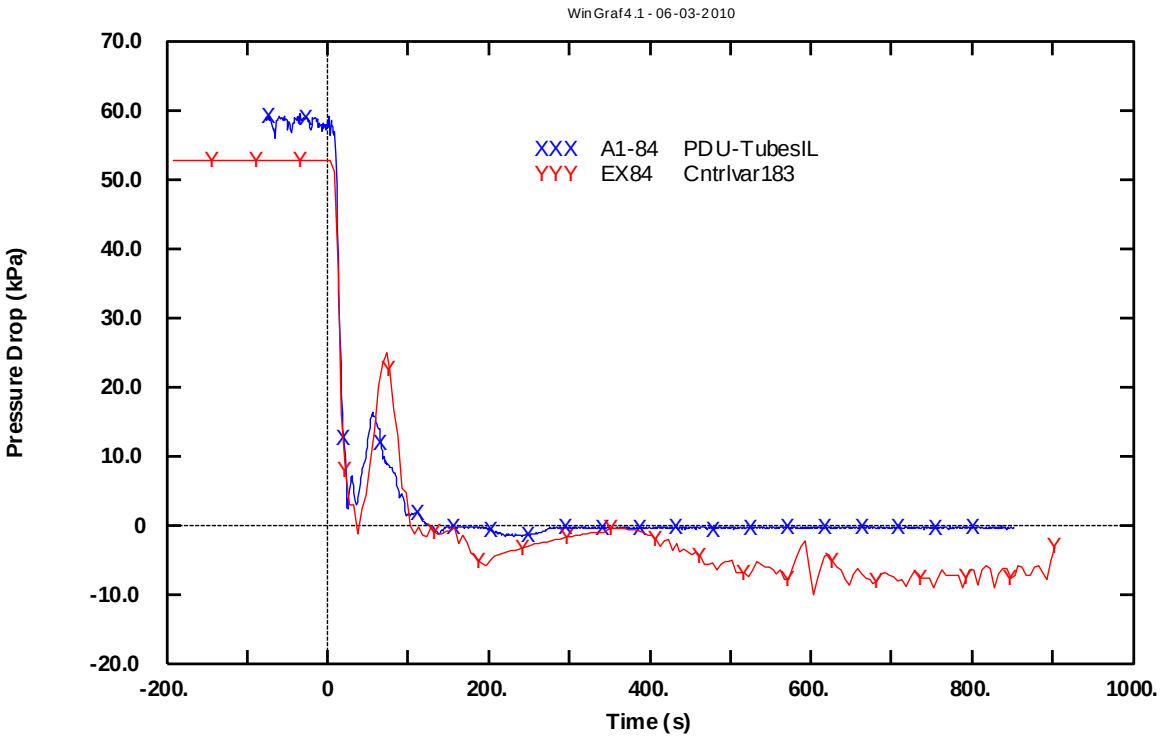

Fig. 49 – LOBI test A1-84: IL U-tubes pressure drops.

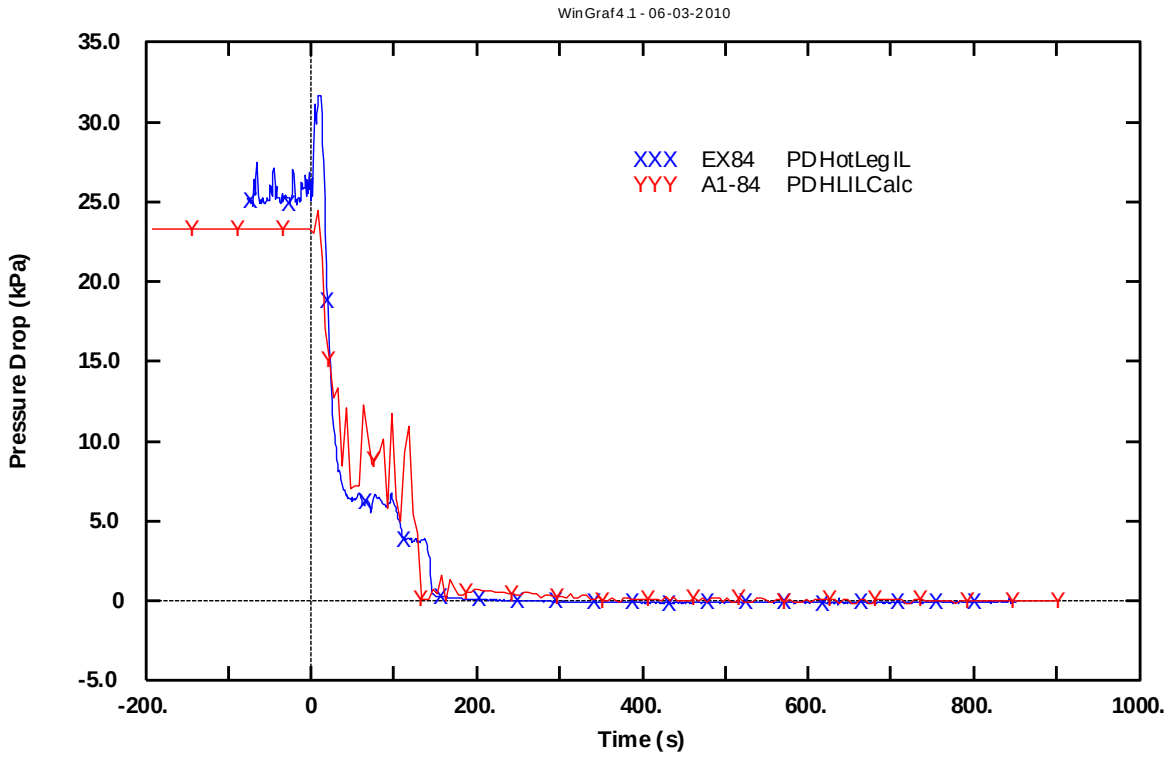

Fig. 50 – LOBI test A1-84: IL HL pressure drops.

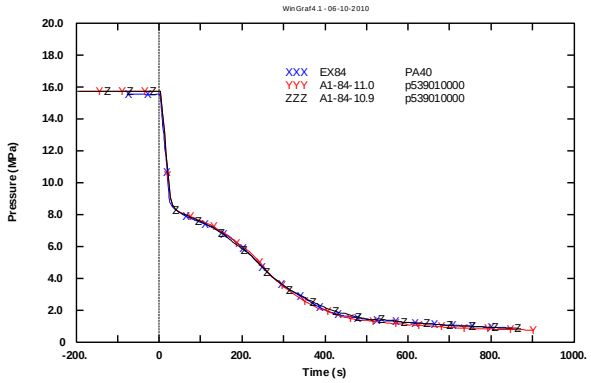

(a) PRZ pressure (overall transient)

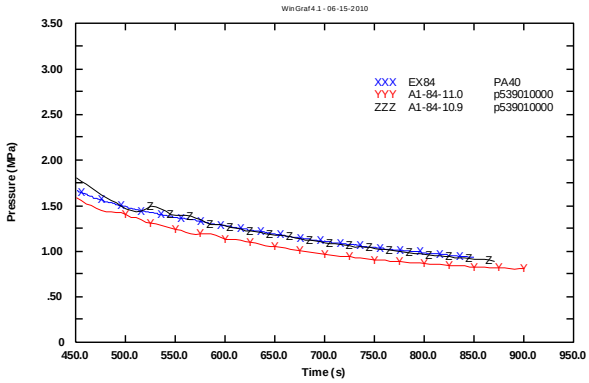

(b) PRZ pressure (zoom from 460s to EoT)

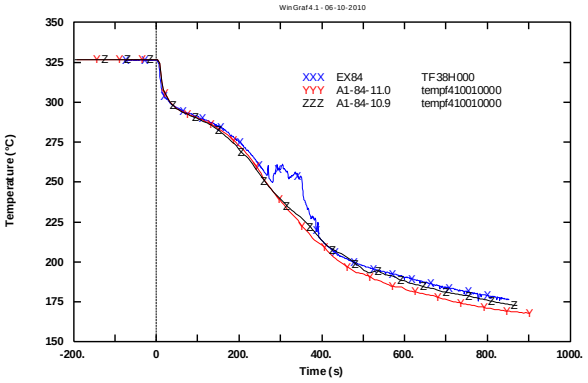

(c) UP temperature

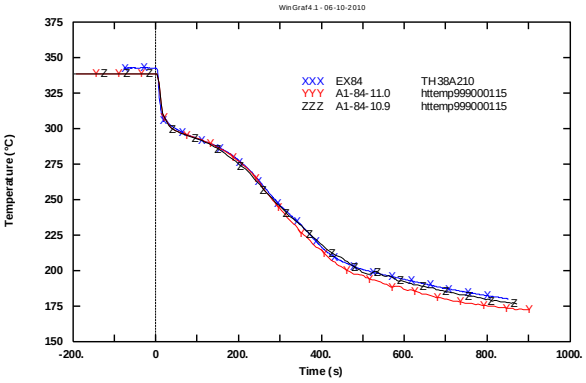

(d) Heated rod temperature, top level

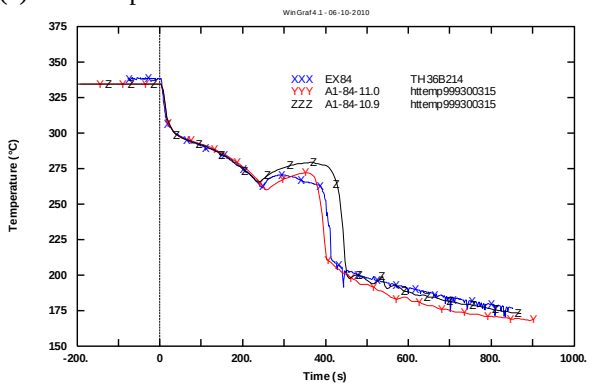

(e) UP heat structure temperature

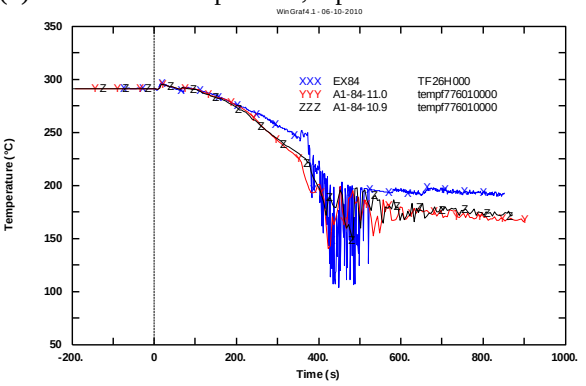

(f) CL BL temperature

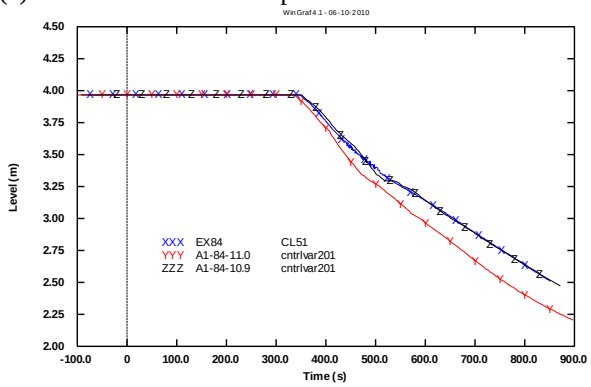

(g) Accu IL level

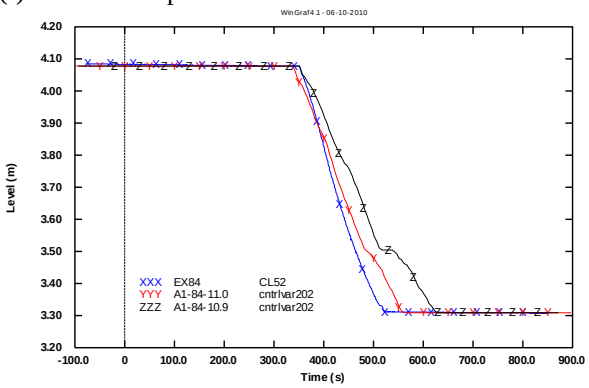

(h) Accu BL level

Fig. 51 – LOBI test A1-84: sensitivity calculation. Run 0 vs. Run 1 (part 1 of 2).

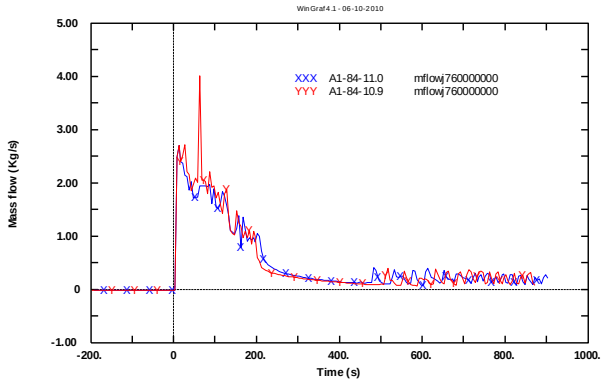

(a) Break mass flow

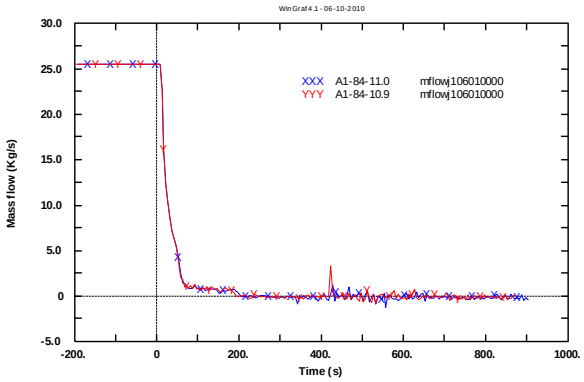

(b) Core inlet mass flow

Fig. 52 – LOBI test A1-84: sensitivity calculation. Run 0 vs. Run 1 (part 2 of 2).

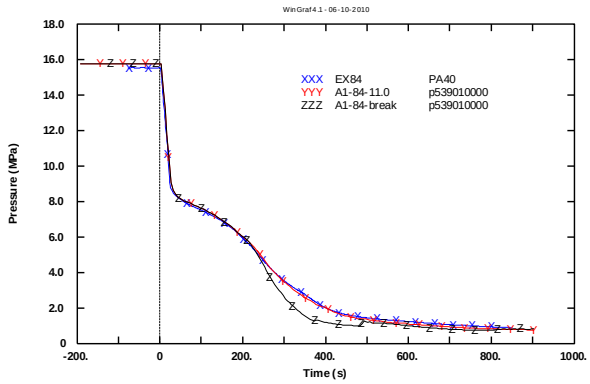

(a) PRZ pressure (overall transient)

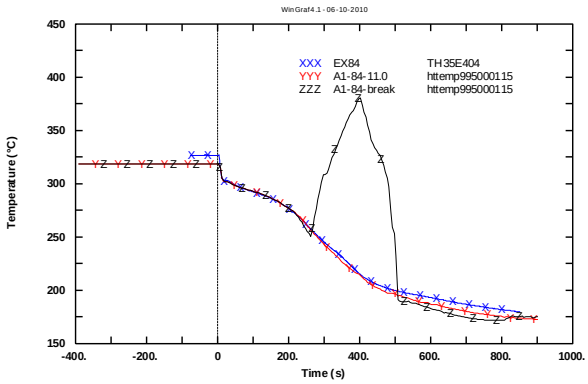

(b) Heated rod temperature, bottom level

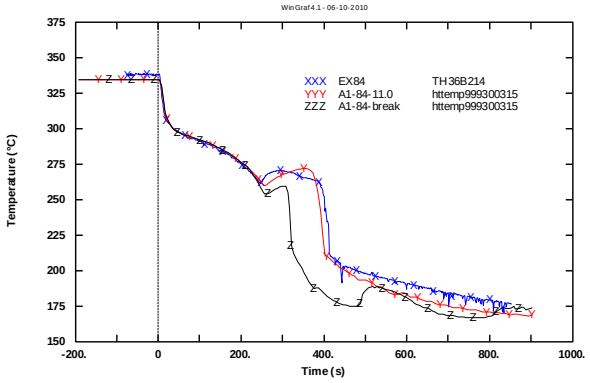

(c) Heat structure temperature in UP

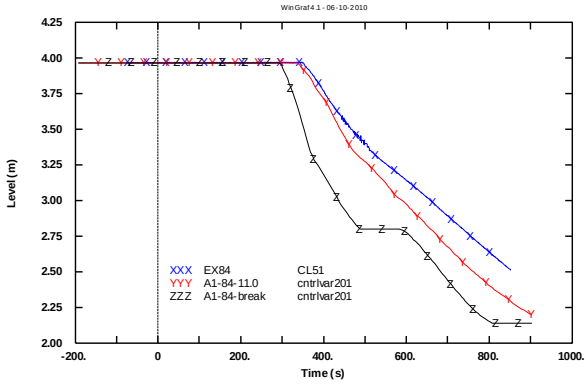

(d) Accumulator IL level

Fig. 53 – LOBI test A1-84: sensitivity calculation. Run 0 vs. Run 2.

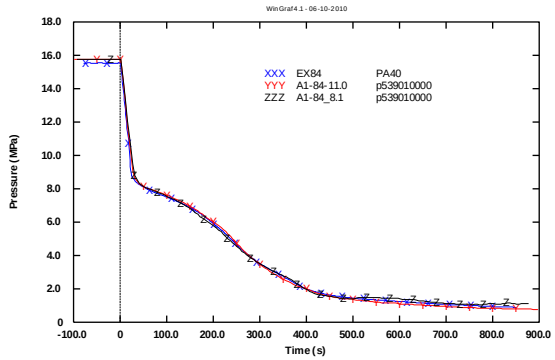

(a) PRZ pressure (overall transient)

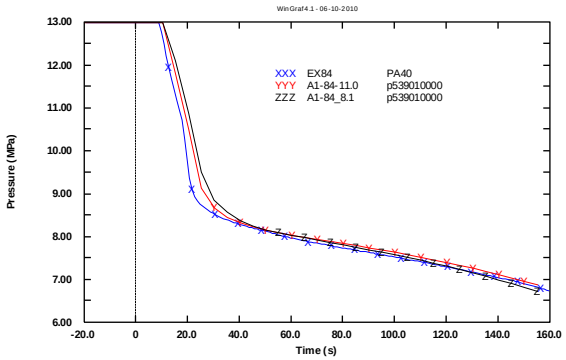

(b) PRZ pressure (zoom from -20s to 180s)

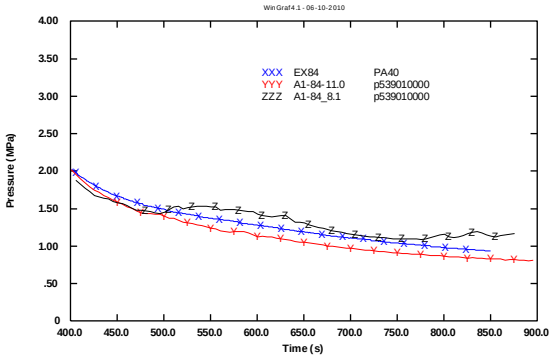

(c) PRZ pressure (zoom from 400s to EoT)

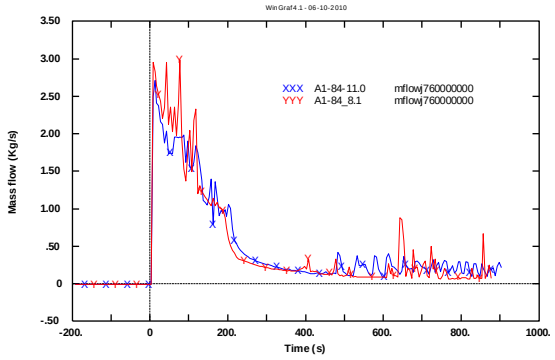

(d) Break mass flow rate

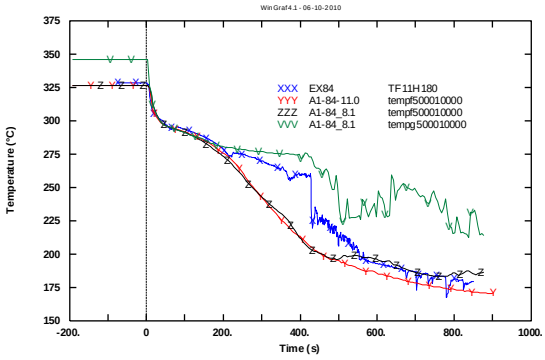

(e) HL IL coolant temperature

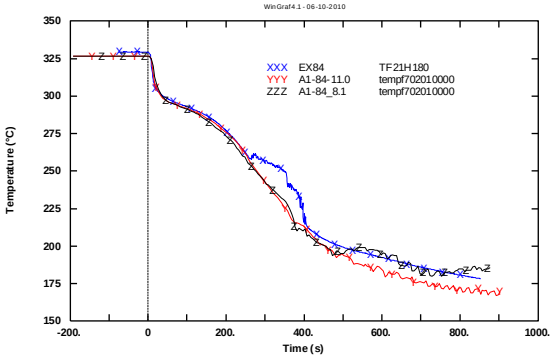

(f) HL BL coolant temperature

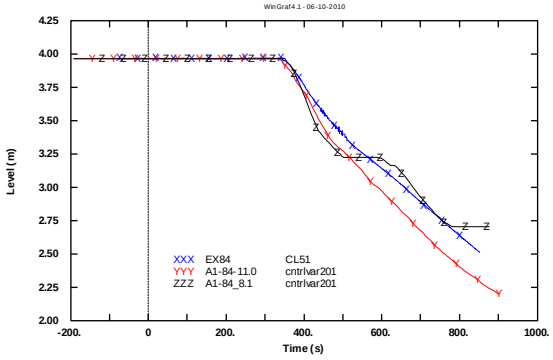

(g) Accu IL level

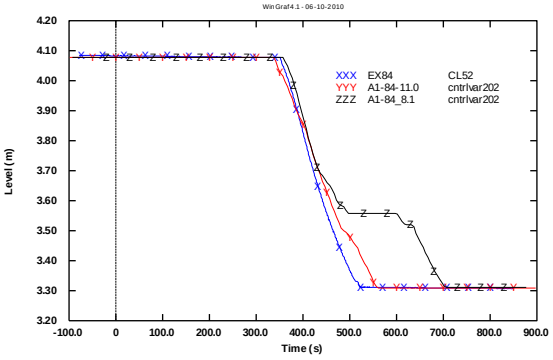

(h) Accu BL level

Fig. 54 – LOBI test A1-84: sensitivity calculation. Run 0 vs. Run 3.

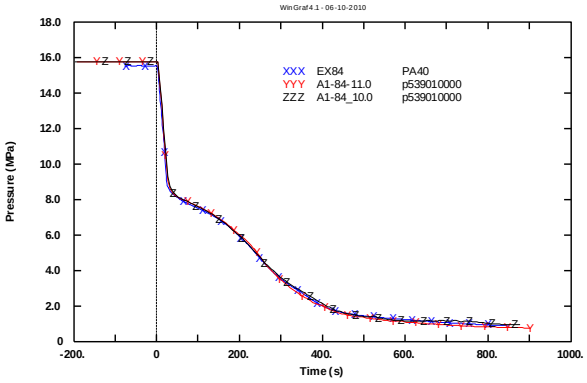

(a) PRZ pressure (overall transient)

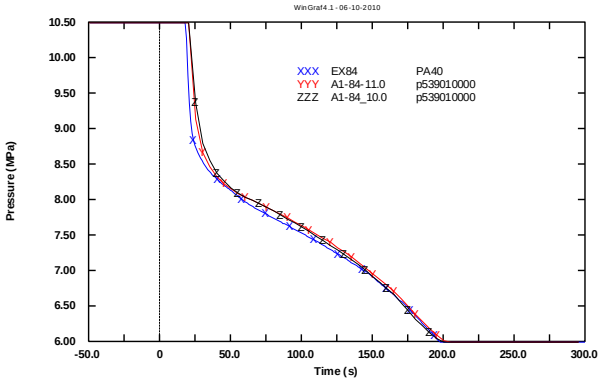

(b) PRZ pressure (zoom from -50s to 300s)

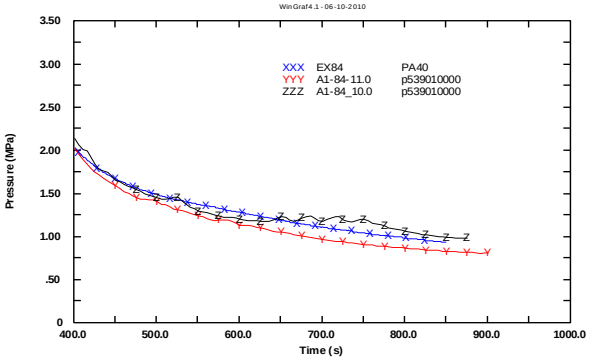

(c) PRZ pressure (zoom from 400s to EoT)

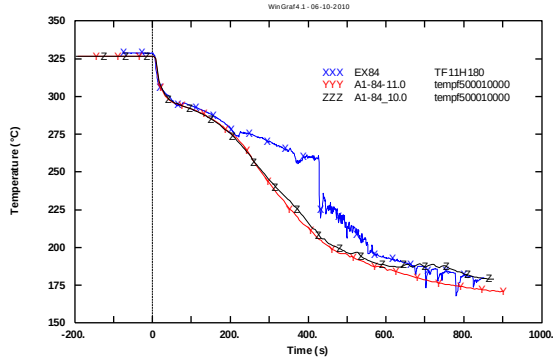

(d) HL IL coolant temperature

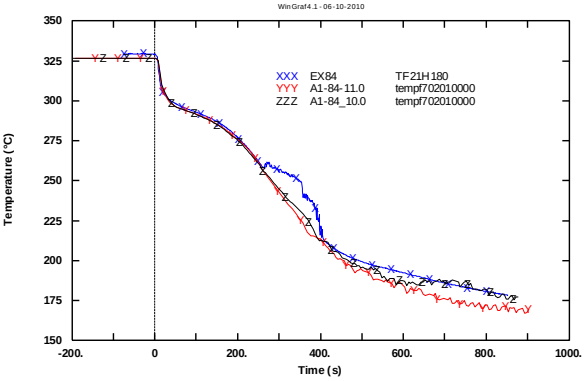

(e) HL BL coolant temperature

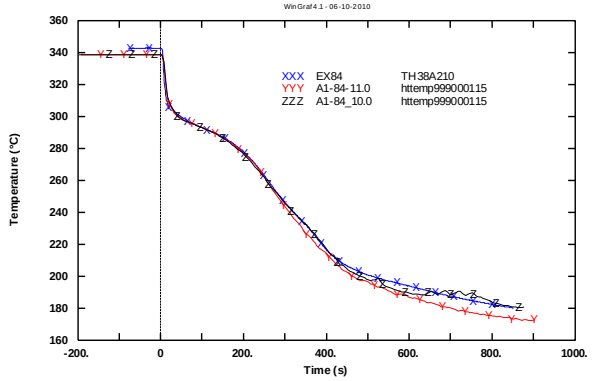

(f) Heated rod temperature,top level

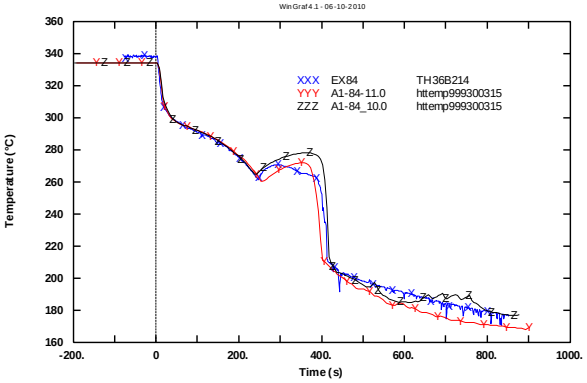

(g) UP heat structure temperature

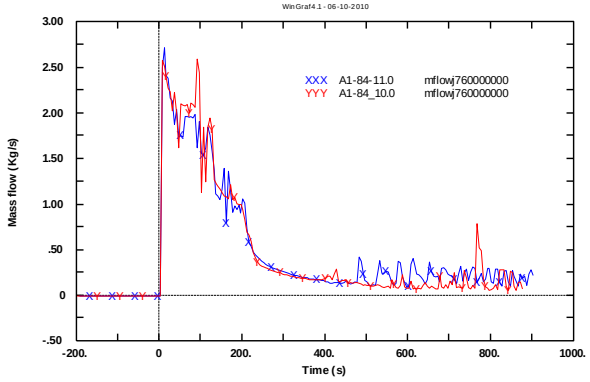

(h) Break mass flow rate

Fig. 55 – LOBI test A1-84: sensitivity calculation. Run 0 vs. Run 4 (part 1 of 2).

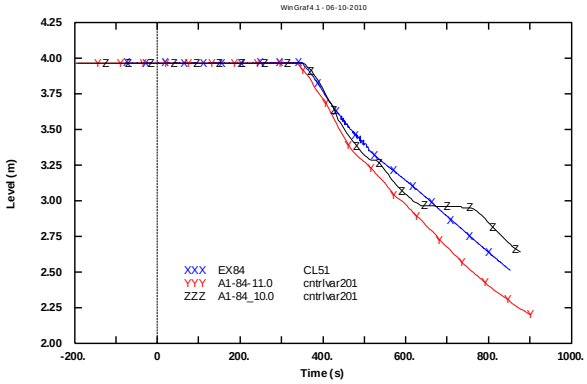

(a) Accu IL level

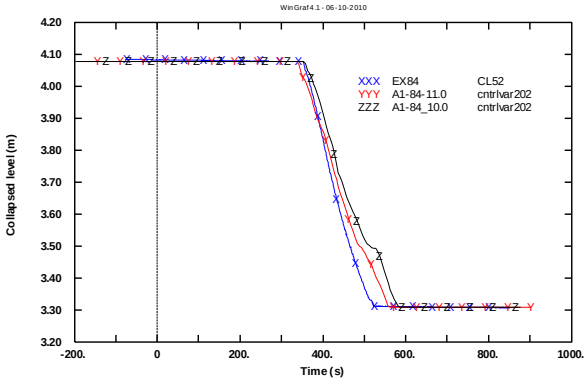

(b) Accu BL level

Fig. 56 – LOBI test A1-84: sensitivity calculation. Run 0 vs. Run 4 (part 2 of 2).

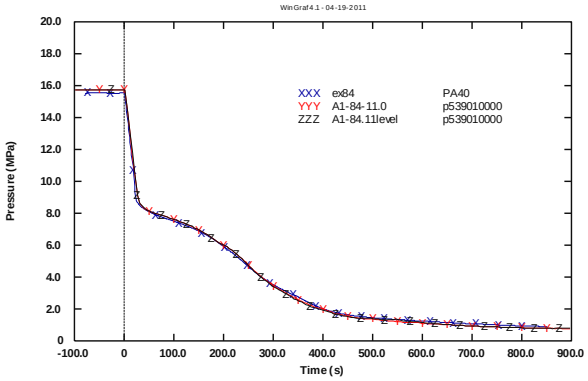

(a) PRZ pressure

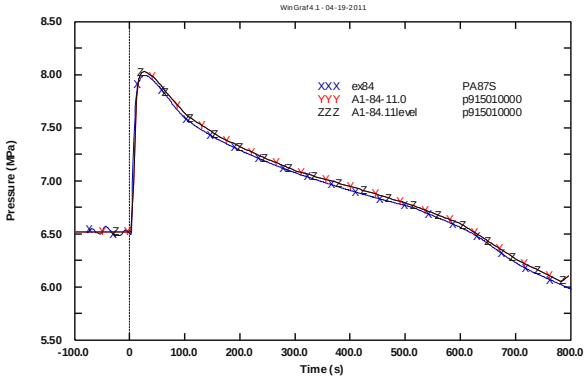

(b) SG IL pressure

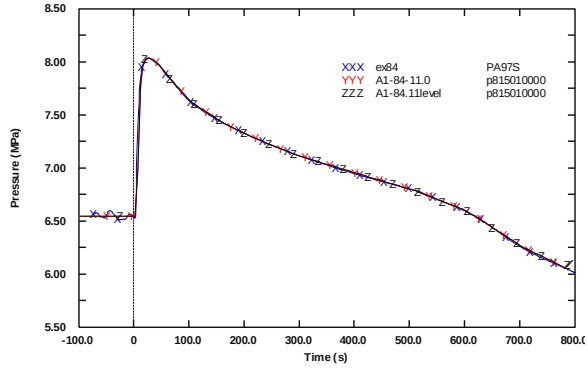

(c) SG BL pressure

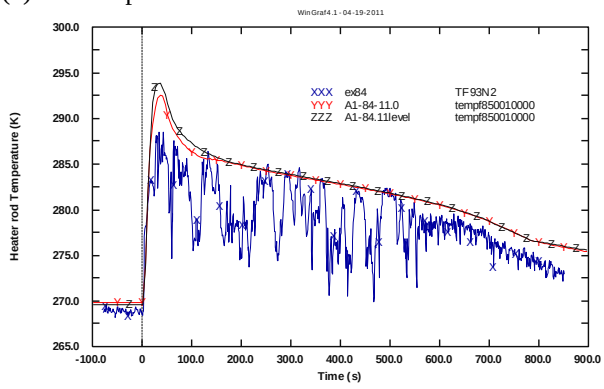

(d) SG IL downcomer coolant temperature

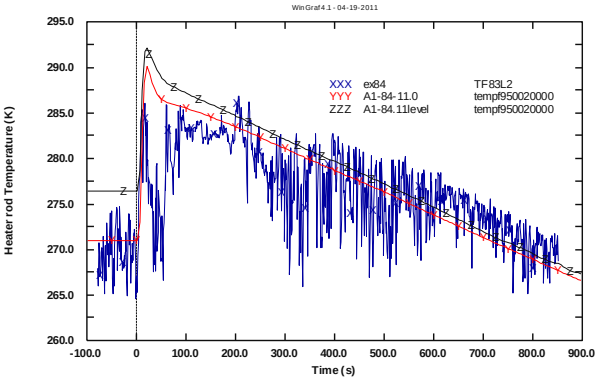

(e) SG BL downcomer coolant temperature

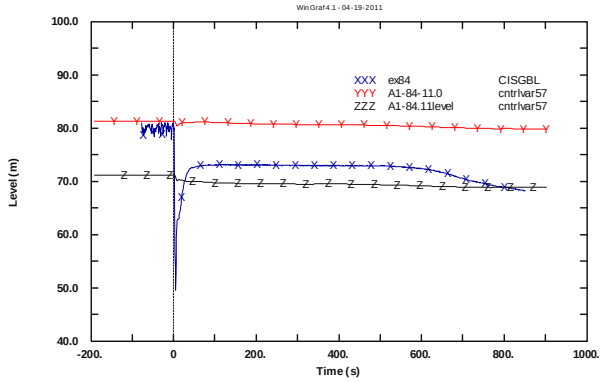

(f) SG BL mass inventory

Fig. 57 – LOBI test A1-84: sensitivity calculation. Run 0 vs. Run 5 (part 1 of 2).

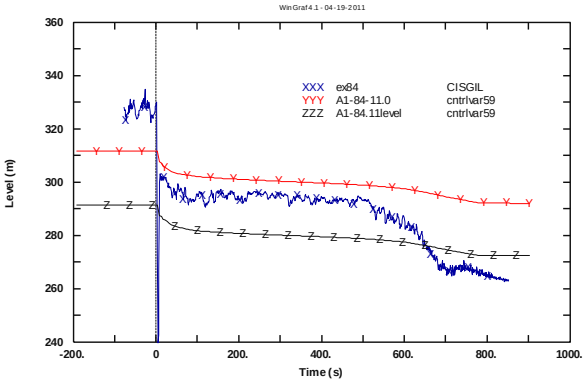

(a) SG IL mass inventory

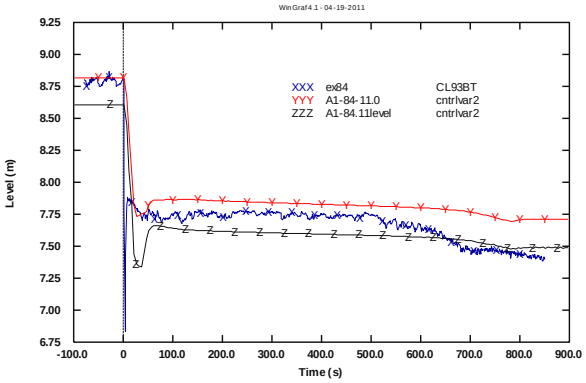

(b) SG IL level

Fig. 58 – LOBI test A1-84: sensitivity calculation. Run 0 vs. Run 5 (part 2 of 2).

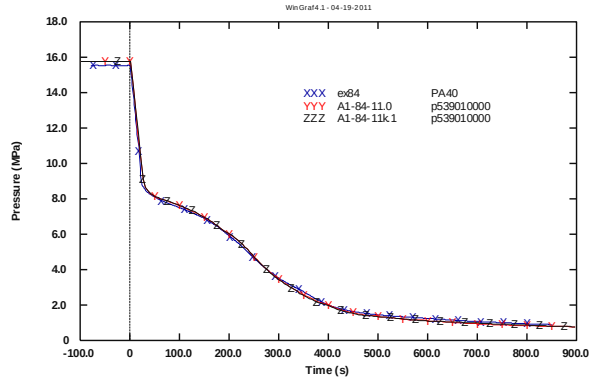

(a) PRZ pressure

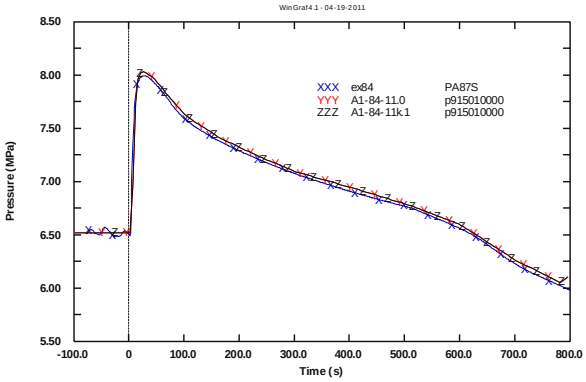

(b) SG IL pressure

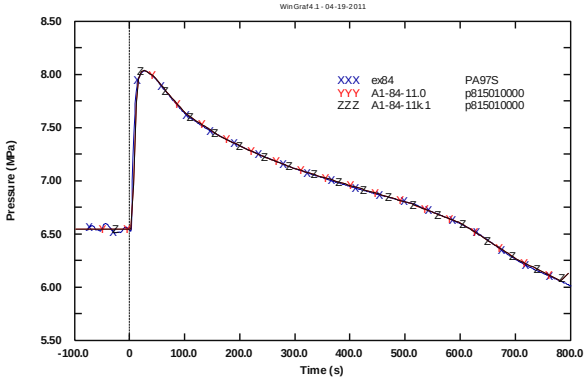

(c) SG BL pressure

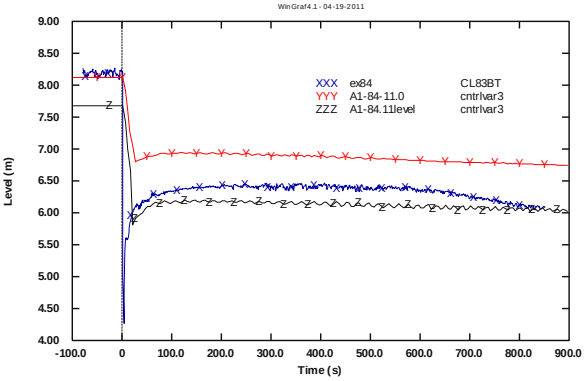

(d) SG BL level

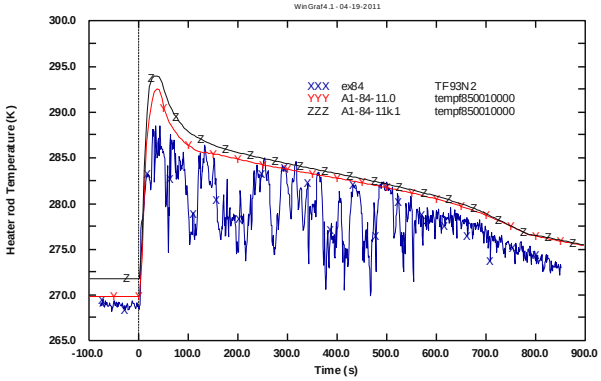

(e) SG IL downcomer coolant temperature

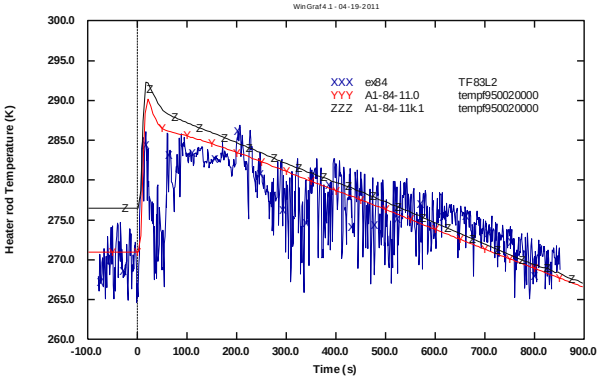

(f) SG BL downcomer coolant temperature

Fig. 59 – LOBI test A1-84: sensitivity calculation. Run 0 vs. Run 6 (part 1 of 2).

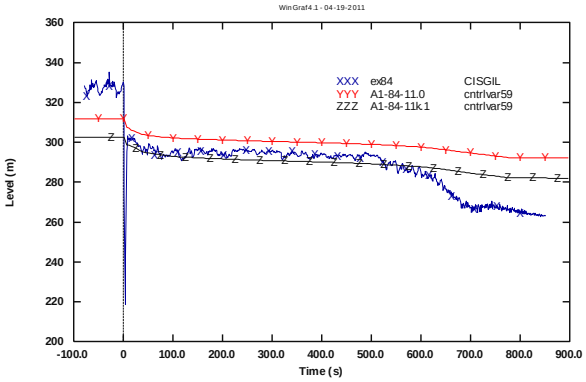

(a) SG IL mass inventory

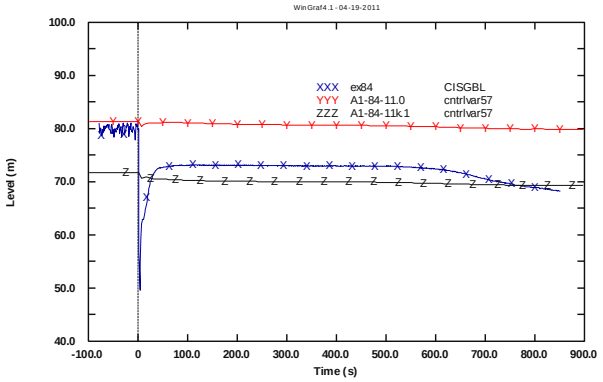

(b) SG BL mass inventory

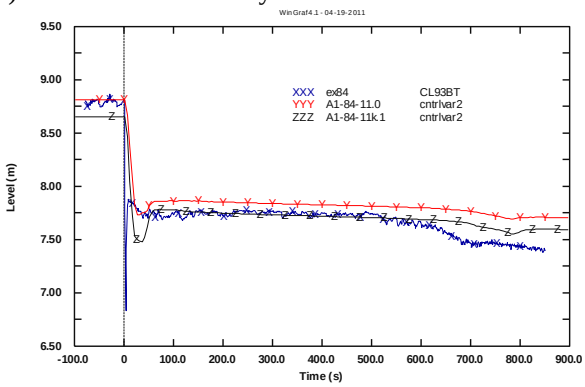

(c) SG IL level

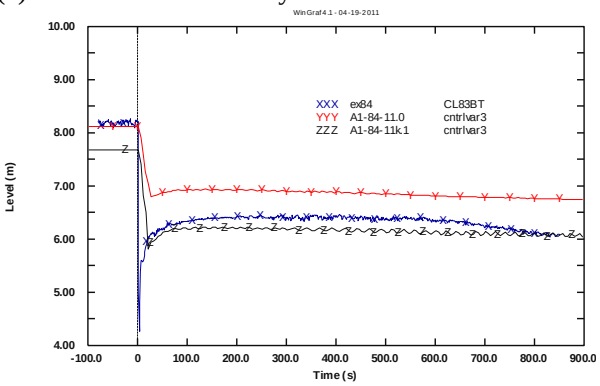

(d) SG BL level

Fig. 60 – LOBI test A1-84: sensitivity calculation. Run 0 vs. Run 6 (part 2 of 2).

6 POST-TEST ANALYSIS OF LSTF Test SB-HL-17

6.1 Steady state calculations

The check of the steady state level is based on the achievement of two objectives:

- the verification and evaluation of the geometrical faithfulness of the model utilized (not applied in the present analysis);
- the capability of the analytical model to reach stable steady state with the correct initial conditions, the same of the experiment (discussed below).

The first consists in the comparison between the quantities (i.e. volumes, surfaces, lengths, masses, etc.), that point out the capability of the model to represent the real system. This task is implicitly considered fulfilled since the nodalization has been transmitted by JAERI, the owner of LSTF facility, see Ref. [15].

The second step requires the comparisons between experimental data and the calculated results before the transient starts and the demonstration those results are achieved in stable conditions.

The results of the steady state (Tab. 22) include the most relevant parameters. For each of these, it is reported the design, the experimental and the calculated values at starting of transient (t=0s). All parameters considered have an acceptable error and the trend is stable (see also Refs. [35] and [36]).

6.2 Reference calculation results

The aim of the transient calculations is to compare the experimental data with the RELAP5/3.3 code results. The checks carried out in the analysis are consistent with those reported in section 5.

The resulting sequence of main events is in good accordance with the experiment sequence (Tab. 23). This is due to the excellent prediction of the primary pressure trend, which induces the scram signal, the primary pumps coastdown, the closure of the main steam line valves, the MSIVs, and the feedwater valves.

The parameters selected to make a comparison between the time trends of calculation and experiment are described below.

Primary pressure
The primary pressure is very well reproduced during almost all the transient (see Fig. 61); saturation pressure is reached, in the primary side, at about 260s, and the “plateau” is matched satisfactorily. In the last part of the simulation, (3500-5000s) there is a very little discrepancy between the two trends; in particular, the calculated one seems to have an oscillatory behavior and this is probably due to the discontinuous accumulator injection.
It has to be underlined that the accumulator configuration and the accumulator line flow sheets were not available to render more realistic the nodalization and the operation of the passive injection system.

Secondary pressure
Secondary pressure has a satisfactory trend (see Fig. 62 and Fig. 63). To reach a good reproduction of the continuous opening and closing of the SGs relief valves, in the first part of the transient (due to the oscillation of the pressure), some sensitivities on the opening time of the valves and on the type of valve better to use have been executed, in order to find the best opening time to reproduce the phenomenon. (No experimental data were available on the type and opening time of the SG's relief valve).

Coolant Temperature
The coolant temperature trend in the different sections of the primary loops shows an acceptable trend; the parameter selected to analyze the coolant temperature's trend in the primary side are the lower plenum, upper plenum, upper head, PRZ, hot and cold leg for IL and BL (from Fig. 67 to Fig. 72). There are no temperature excursions because in the core region the dry out condition is not achieved (in both the experiment and the simulation). The upper plenum fluid temperature is in perfect accordance with the experimental data in almost all the transient, but in the last part (3000-5000s) the fluid temperature is underestimated by the code, and it is more similar to the calculated vapor temperature. Analyzing the pressurizer temperature we can find the same trend, the experimental temperature is in perfect accordance with the vapor calculated temperature, while the fluid one is lower. In the legs all the temperature trends are satisfactory.

Rod surface temperatures
The cladding temperature of the fuel rods is well reproduced: The calculated parameters trends are compared with the experimental values at the elevation where the maximum temperature is recorded (middle and top level of active fuel length, Fig. 73). No DNB conditions are met, therefore the cladding temperature is driven by the forced convective heat transfer regime and the coolant temperature.

Mass flow rates
In the first seconds of the transient the primary mass flow rate is driven by the pumps rotation inertia, while they are coasting down. To render more effective the effect given by the pumps to the primary system cooling in the first part of the accident, the pump rotation speed is increased to 26rps in the experiment (28rps in the simulation), and then rest of the coastdown is actuated.

After this first phase the single phase NC drives the mass flow in the primary system. This phenomenon arises from the balance between driving and resistant forces. Driving forces are the result of fluid density differences occurring between descending side of U-tubes plus DC vessel and core zone plus ascending side of U-tubes. Resistant forces are due to irreversible friction pressure drops along the entire loop.

When NC occurs an increase in primary mass flow is observed: this phenomenon is clearly matched by the simulation and the total mass flow trend is very well reproduced (see Fig. 74).

The break flow (Fig. 65) is simulated by Ransom-Trapp equations and the three coefficients are adjusted in order to reproduce better the outflow. The coefficients used are:

- Subcooled discharge coefficient→ 1.2
- Two-Phase discharge coefficient → 1.0 (default value)

- Superheated discharge coefficient → 0.75

The third coefficient, regarding the vapor phase outflow, has been lowered in order to achieve the correct steam flow through the break. The total trend of the break mass flow is very well matched, and it has also been integrated to obtain the integral flow that shows very good accordance with the experimental integral flow (Fig. 66), even if, in the last part of the transient (from 3500s), the calculation overestimate slightly the water discharged (approximately 11000kg for the experiment, at the end of the transient, 12500kg for the calculation).

6.3 Qualitative and quantitative accuracy evaluation

6.3.1 Qualitative Accuracy

The methodology used to evaluate the qualitative accuracy is the same seen in section 5.2. Even for LSTF test 1-2, a summary table is provided (see Tab. 24). In reference to Tab. 24 it is possible to derive the following conclusions:

- U mark is nor present;
- All RTAs of the experiment are present in the calculation;
- The accuracy evaluation adopted brings to the conclusion that the calculation is qualitatively correct.

6.3.2 Quantitative Accuracy

The quantitative accuracy evaluation adopted is the FFTBM (Fast Fourier Transform Based Method). More details on the method are available in section 5.2.2 and in Refs. [29] and [25]. The method is applied at all the transient, from 0 to 5000s. Tab. 25 summarizes the results. 14 variables are selected. The following comments derive from the analysis of the results.

- The primary pressure shows an excellent value of the average accuracy, (AA=0.048), and the secondary pressure has also a good value (AA 0.11).
- The temperatures (analyzed in UP and in the PRZ), and the SG's levels have an average accuracy of 0.4.
- The integral break flow and the HPIS integral flow are well reproduced.
- The heated rod temperatures shows bigger values of AA; this is probably attributable to the experimental temperature oscillations at the end of the transient (4000-5000s).
- The Accumulator integral mass flow follow the same trend of the experimental one, but the amount of mass injected is not perfectly reproduced; this explains the high values of AA.
- The total Average accuracy value is AA=0.39: the transient is mainly well reproduced.

Tab. 22 – LSTF Test SB-HL-17: comparison between measured and calculated relevant initial conditions.

#	QUANTITY	ID	Unit	Y_{DESIGN}	Y_{EXP}	Y_{CALC}	ε	Acc. ε °°
1	**PRIMARY CIRCUIT POWER BALANCE**							**2%**
1.1	*Core thermal power*	WE270A-T	kWth	10	10.1	11.91	17.92%	
1.2	*PRZ heaters thermal power*		kWth	--		45		
2	**SECONDARY CIRCUIT POWER BALANCE**							**2%**
2.1	*SG-A power exch.*		kWth	--	--		--	
2.2	*SG-B power exch.*		kWth	--	--		--	
3	**ABSOLUTE PRESSURE**							**0.10%**
3.1	*PRZ (top of the PRZ)*	PE300A-PR	MPa	15.5	15.54	15.56	0.13%	0.0%
3.2	*Upper plenum*	PE280A-PV	MPa	--	15.49	15.67	1.16%	0.9%
3.3	*SG-1 exit (top of SG)*	PE430-SGA	MPa	7.3	7.32	7.3	0.27%	0.0%
3.4	*SG-2 exit (top of SG)*	PE450-SGB	MPa	7.3	7.33	7.3	0.41%	0.0%
4	**COOLANT TEMPERATURE**							**0.50%**
4.1	*PRZ (bottom)*		K	--	619.3	619.1	0.03%	0.0%
4.2	*Core inlet (lower plenum top)*	TE-EX-000B18-LCPP	K	--	562.5	562.26	0.04%	0.0%
4.3	*Core outlet (upper plenum)*	TE-IN038-B10-UCP	K	--	599.5	600.06	0.09%	0.0%
4.4	*Upper head*	TE-W075F-PV	K	--	588.04	588.24	0.03%	0.0%
4.5	*HL-A*	TE020C-HLA	K	598	597.2	599.4	0.37%	0.0%
4.6	*HL-B*	TE160C-HLB	K	598	596.9	599.4	0.42%	0.0%
4.7	*CL-A*	TE070C-CLA	K	562	563.1	564.1	0.18%	0.0%
4.8	*CL-B*	TE210C-CLB	K	562	563	564.1	0.20%	0.0%
4.9	*FW-A and B*	TE430-SGA	K	495.2	496.3	495.35	0.19%	0.0%
		TE470-SGB			495.5			
4.10	*ACCU-A and B*	--	K	320	321.3	320	0.40%	0.0%
					321.9			
5	**ROD TEMPERATURE**							**10 K**
5.1	*Max clad temp. / Height with ref. to BAF*		K/m	--		573.6		
5.2	*Max centerline temp. / Height with ref. to BAF*		K/m	--		605.1		
6	**PUMP VELOCITY**							**1%**
6.1	*MCP-A and B*	FE010-HLA	rps	13.3	13.9	15.2	9.35%	
		FE150-HLB						
7	**HEAT LOSSES**							**10%**

#	QUANTITY	ID	Unit	Y_{DESIGN}	Y_{EXP}	Y_{CALC}	ε	Acc. ε °°
7.1	*Overall heat losses (primary and secondary systems)*		kW	--	--		--	
8	**MASS INVENTORY IN PRIMARY CIRCUIT**							**2 %**
8.1	*Primary system (with PRZ and without ACCs)*		Kg			8307		
9	**MASS INVENTORY IN SECONDARY CIRCUIT**							**5 %**
9.1	*SG-A (vessel)*		Kg	--				
9.2	*SG-B (vessel)*		Kg	--				
10	**FLOW RATES**							**2%**
10.1	*CL A*	FE020A-LSA	Kg/s	24.3	25.37	25.5	0.51%	
10.2	*CL B*	FE160A-LSB	Kg/s	24.3	25.41	25.3	0.43%	
10.3	*SG-A and B FW*	FE430-SGA FE470-SGB	Kg/s	2.74	--	2.74	0%	
10.4	*SG-A and B SL*	FE440-SGA FE480-SGB	Kg/s	2.74	2.67	3	11%	
10.5	*DC -UH bypass*	--	Kg/s	--	--	--		
10.6	*DC-HL bypass*	--	Kg/s	--	--	--		
11	**LEVELS**							
11.1	*PRZ (collapsed)*	LE280-PR	m	--	7.33	7.32	0.01	
11.2	*SG-A (collapsed)*	LE430-SGA	m	--	10.23	10.32	0.09	
11.3	*SG-B (collapsed)*	LE450-SGB	m	--	10.21	10.24	0.03	
11.4	*ACCU-A and B*	LE650-ACC	m	--	6.71	1.94	--	
11.5		LE660-ACH			6.72	1.943	--	

Tab. 23 – LSTF test SB-HL-17: resulting sequence of main events in the experiment compared with the calculation.

#	EVENT DESCRIPTION	EXP (sec)	R5M3.3 (sec)	Note
1	Start of transient (break opening)	0	0 (100)	Imposed
2	Reactor SCRAM	49	43.6	
3	PRZ proportional heaters switched off	49	43.6	
4	Stop of FW pumps	49	43.6	
5	Trip of the MCP and coast-down	49	43.6	
6	Main steam line close (turbine valve)	49	43.6	
7	Main steam line valve closed	52	46.6	
8	FW stop	55	49.6	
9	Main steam isolation valve close A/B	72 / 74	--	
10	Safety injection signal	77	62	
11	HPIS start	89	74	
12	Primary coolant pumps stop	303	305	
13	ACCU injection starts	2537	2697	
14	ACCU injection stops A/B	4697	4435/4465	
15	End of transient	4697	5000	Imposed

Tab. 24 – LSTF test 1-2: judgment of the code calculation on the basis of RTA.

#		UNIT	EXP	CALC	JUDGMENT
	RTA: PRESSURIZZER EMPTYING				
TSE	*Emptying time*	s	89.7	146.0	R
	RTA: SECONDARY SIDE STEAM GENERATORS BEHAVIOUR				
TSE	*Feed water pumps stop*	s	49.0	43.6	R/E
TSE	*Steam line turbine valve closure*	s	49.0	43.6	R/E
TSE	*MSIV close*	s	52.0	46.6	E
SVP	*SG IL level*				
	When HPIS starts(74calc 89exp)	m	11.3	11.21	E
	When ACCU starts(2537exp, 2697calc)	m	10.48	11.42	E
SVP	*SG BL Level*				
	When HPIS starts(74calc 89exp)	m	11.36	11.45	E
	When ACCU starts(2537exp, 2697calc)	m	10.52	11.61	R/E
SVP	*SG IL Pressure*				
	When HPIS starts (74calc 89exp)	MPa	7.99	7.87	R/E
	When ACCU starts (2537exp, 2697calc)	MPa	7.52	7.7	R/E
SVP	*SG BL Pressure*				
	When HPIS starts (74calc 89exp)	MPa	7.93	7.77	R/E
	When ACCU starts(2537exp, 2697calc)	MPa	7.50	7.61	R/E
	RTA: HPIS INTERVENTION				
TSE	*HPIS starts IL-BL*	s	89	74	R/E
IPA	*Integrated flow IL*	kg	4004	3965	E
IPA	*Integrated flow BL*	kg	4158	3965	E
	RTA: SUBCOOLED BLOWDOWN				
TSE	*Primary pressure falls below secondary pressure IL*	s	991	953	E
TSE	*Primary pressure falls below secondary pressure BL*	s	997	999	E
IPA	*break mass up to 900s*	kg	4229	4098	E
IPA	*Break flow at 900s*	Kg/s	3.43	4.17	R/E
	RTA: SATURATED BLOWDOWN				
IPA	*Break mass up to 999s*	kg	4431	4341	E
	Break flow at 999s	kg/s	1.827	1.65	R/E
IPA	*Brak mass up to5000s*	kg	11526	12800	R/E
IPA	*Integrated flow between 999 and 5000s*	kg	8370	7185	R/E
	RTA:ACCUMULATOR IL CL BEHAVIOUR				
TSE	*Injection starts*	s	2537	2697	R/E
	Injection stops	s	4697	4435	R/E
IPA	*Total mass delivered*	kg	784	1067	R
	RTA: ACCUMULATOR BL CL BEHAVIOUR				
TSE	*Injection starts*	s	2537	2697	R/E
	Injection stops	s	4697	4465	R/E
IPA	*Total mass delivered*	kg	620	980	R

Tab. 25 – LSTF test 1-2: summary of results obtained by the application of FFTBM.

#	PARAMETER		AA (0-5000S)	WF (0-5000S)
	Description	**ID (Exp)**		
1	***Prz pressure [MPa]***	***PE13***	**0.048**	**0.033**
2	***SG IL pressure [MPa]***	***PE19***	**0.1398**	**0.034**
3	***SG BL pressure [MPa]***	***PE21***	**0.1211**	**0.035**
4	***Integral break flow [kg]***	***RC194***	**0.1446**	**0.105**
5	***PRZ temperature [K]***	***TE962***	**0.3552**	**0.039**
6	***Upper plenum temperature [K]***	***TE126***	**0.3438**	**0.04**
7	***Heated rod temperature, middle level [K]***	***TW286***	**0.81**	**0.062**
8	***Heated rod temperature, high level [K]***	***TW288***	**0.8**	**0.034**
9	***SG IL level [m]***	***LE3***	**0.57**	**0.073**
10	***SG BL level [m]***	***LE6***	**0.473**	**0.069**
11	***HPIS IL integral mass flow [kg]***	***FE42***	**0.15**	**0.044**
12	***HPIS BL integral mass flow [kg]***	***FE57***	**0.24**	**0.045**
13	***ACCU IL integral mass flow [kg]***	***FE37***	**1.04**	**0.04**
14	***ACCU BL integral mass flow [kg]***	***FE40***	**1.08**	**0.044**
TOTAL AVG. ACCURCAY			**0.39**	**0.043**

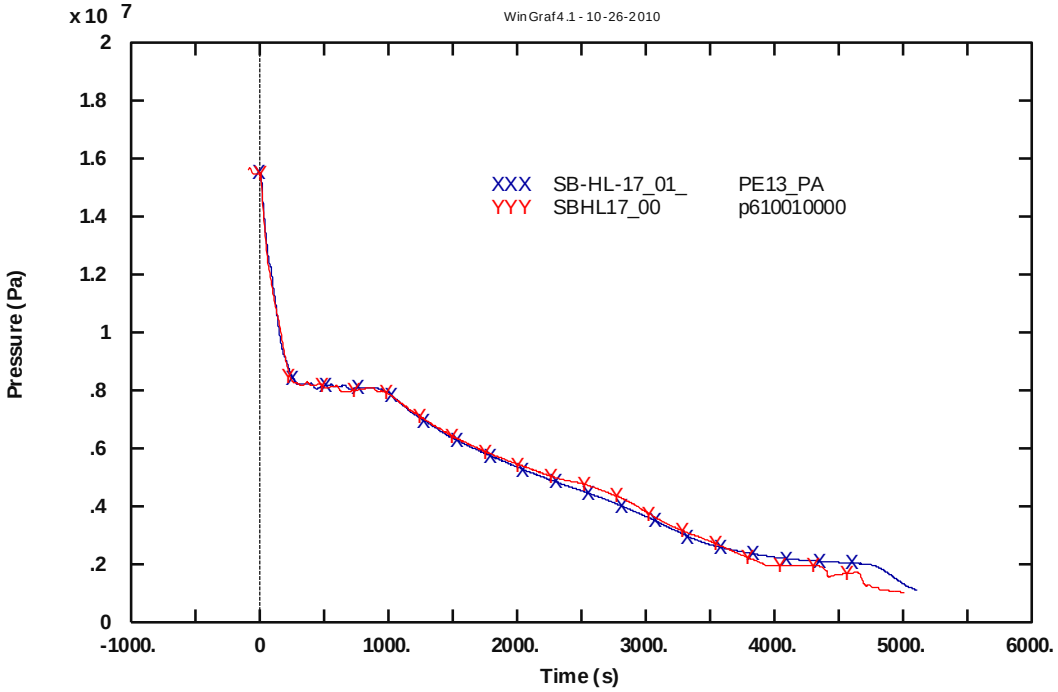

Fig. 61 – LSTF Test SB-HL-17: PRZ pressure

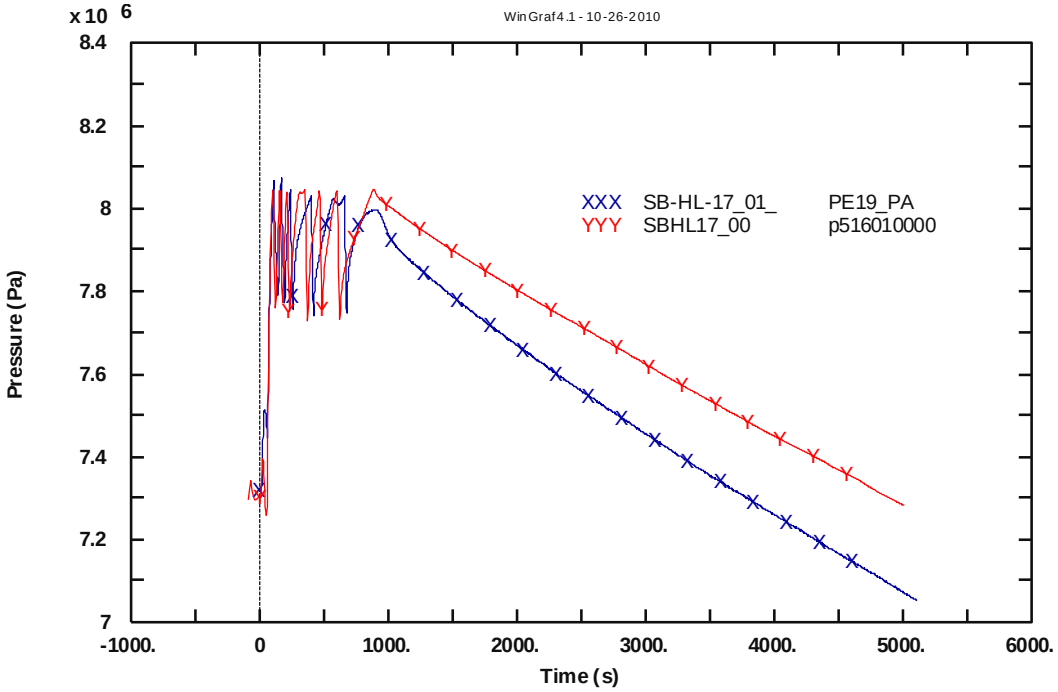

Fig. 62 – LSTF Test SB-HL-17: steam dome A pressure

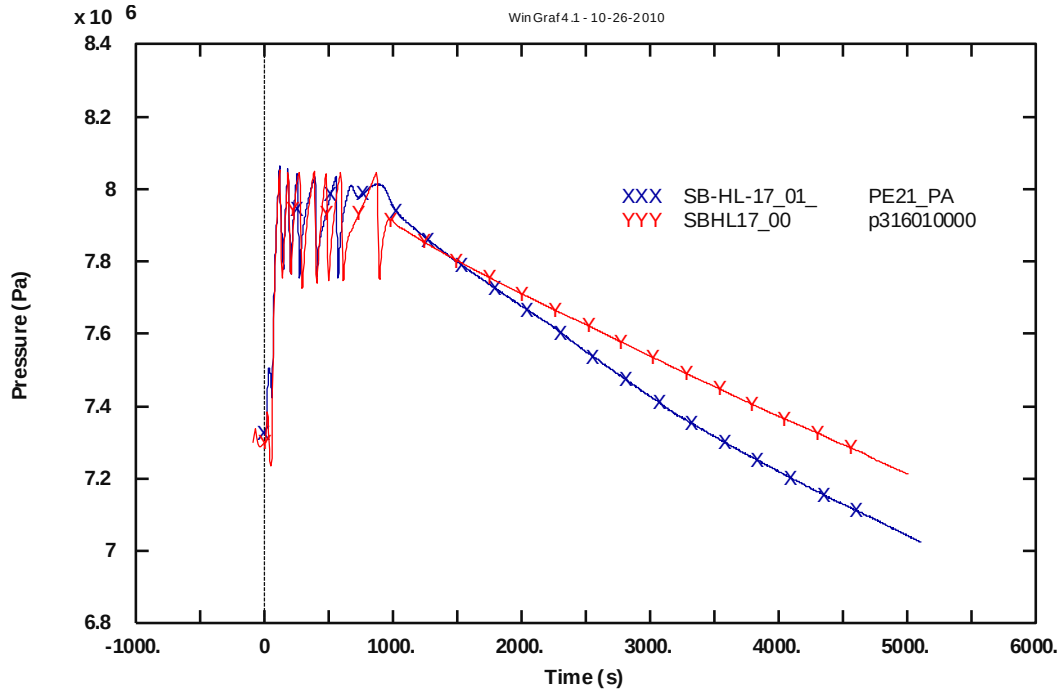

Fig. 63 – LSTF Test SB-HL-17: steam dome B pressure

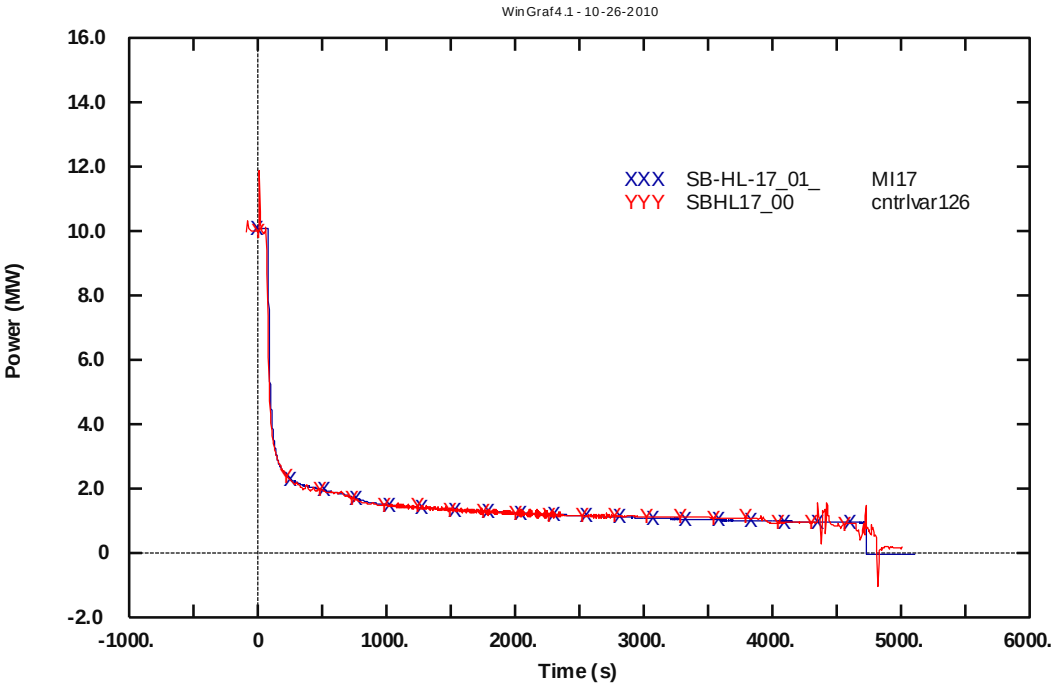

Fig. 64 – LSTF Test SB-HL-17: total core power

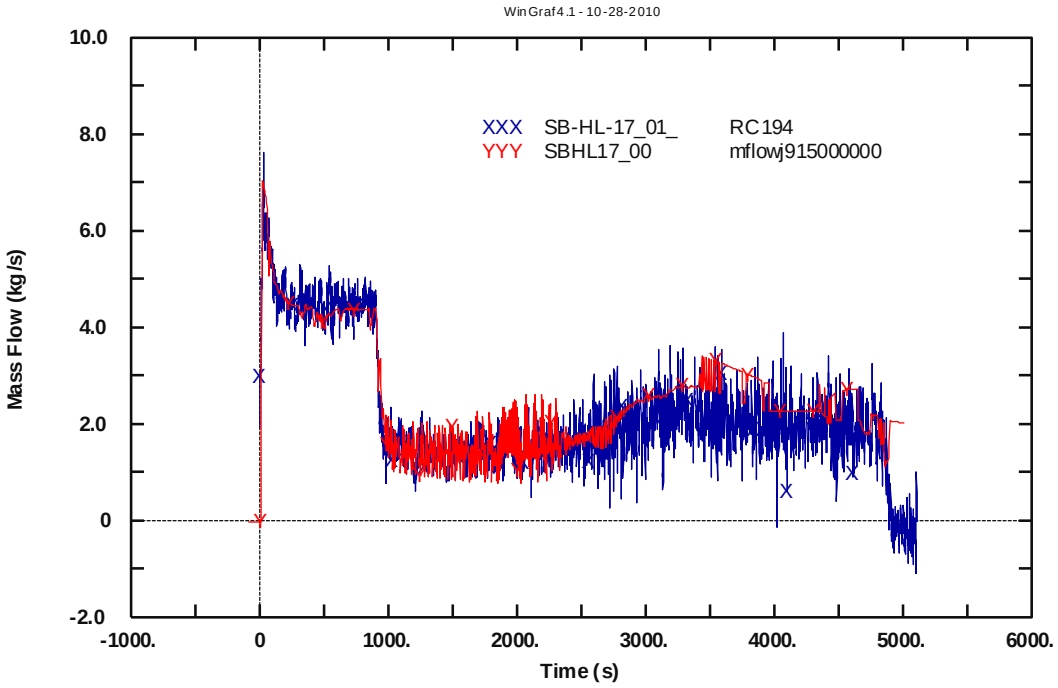

Fig. 65 – LSTF Test SB-HL-17: break mass flow rate

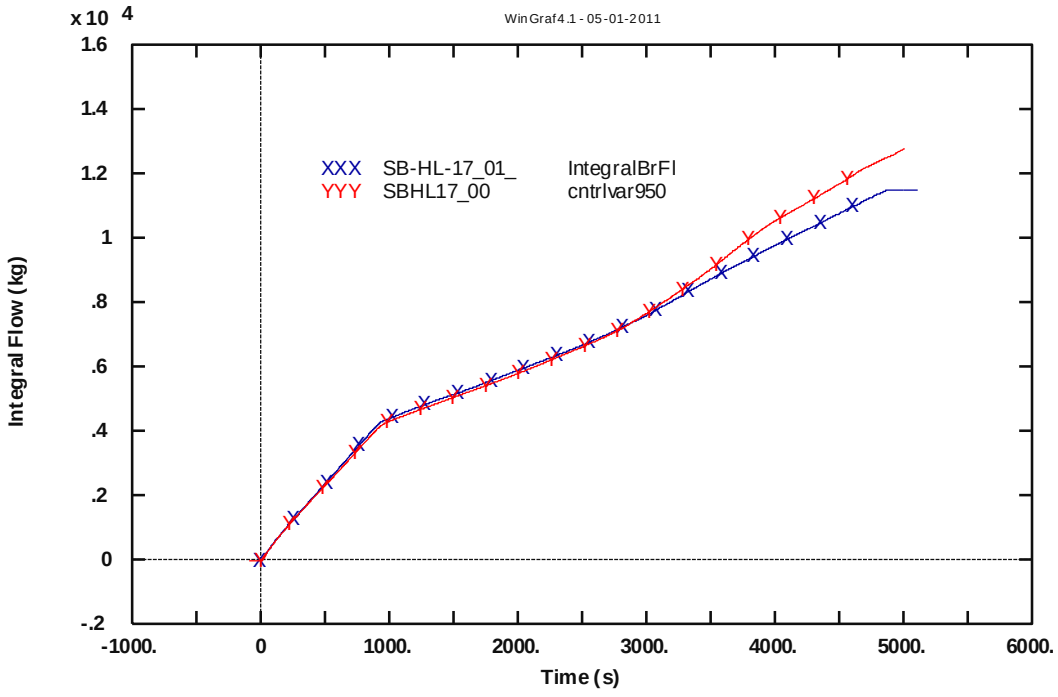

Fig. 66 – LSTF Test SB-HL-17: integral Break flow

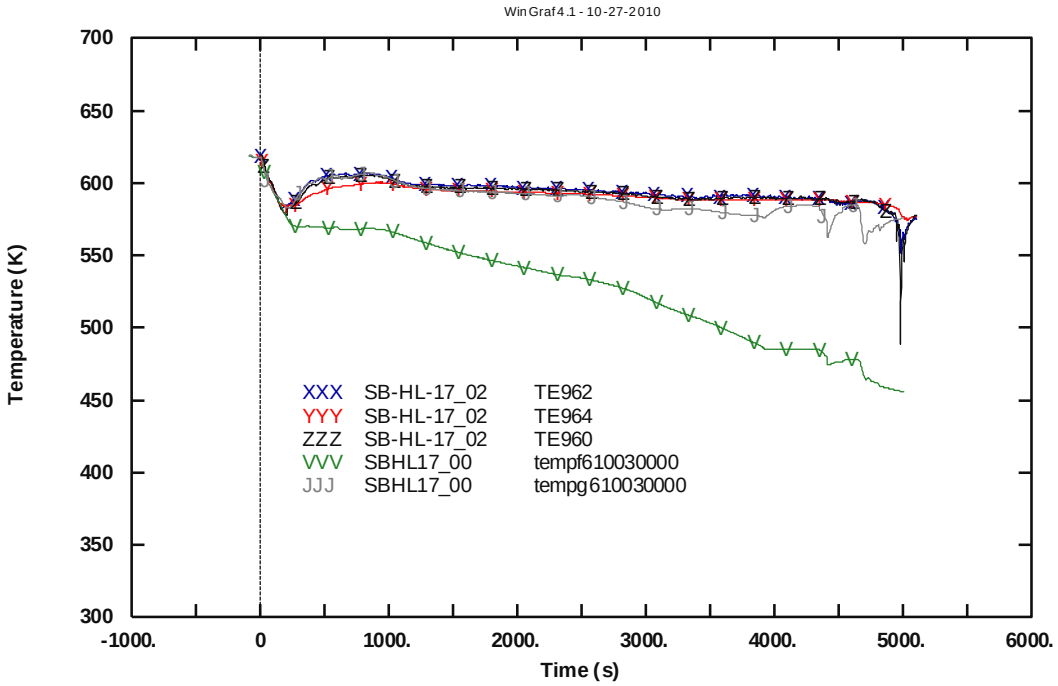

Fig. 67 – LSTF Test SB-HL-17: PRZ temperature

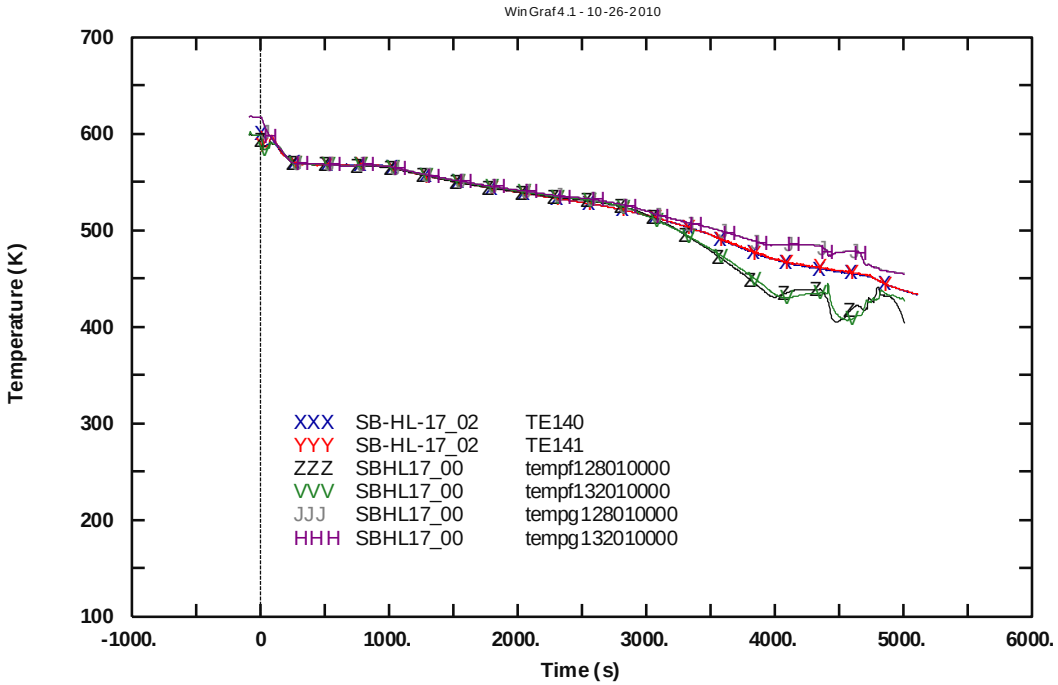

Fig. 68 – LSTF Test SB-HL-17: core outlet fluid temperature

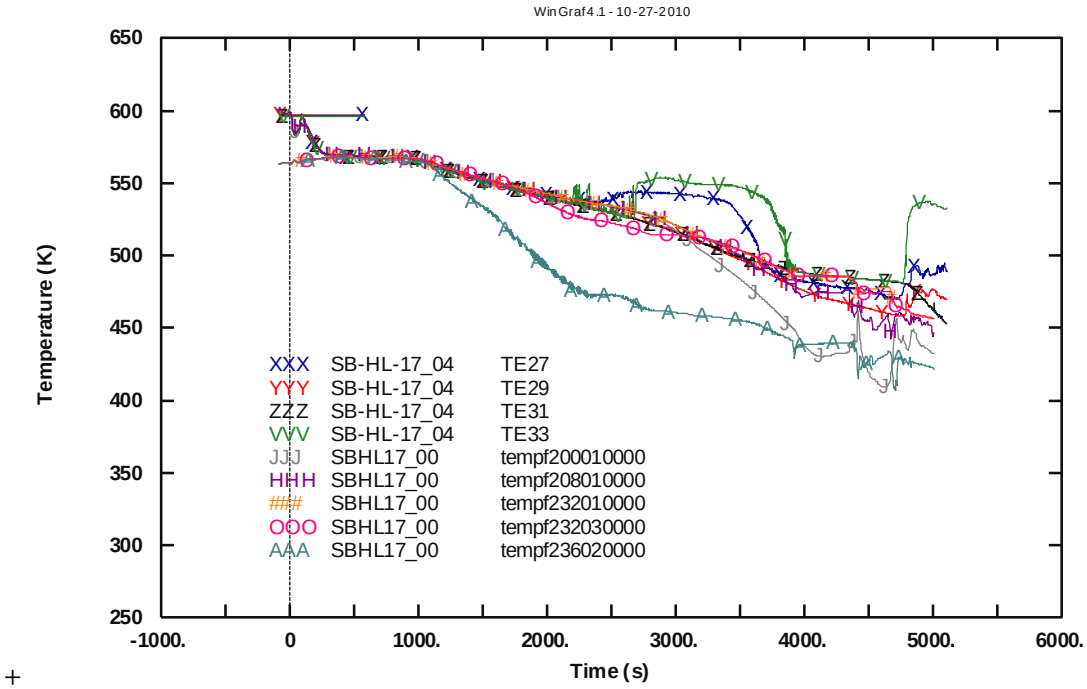

Fig. 69 – LSTF Test SB-HL-17: HL BL temperature (loop B)

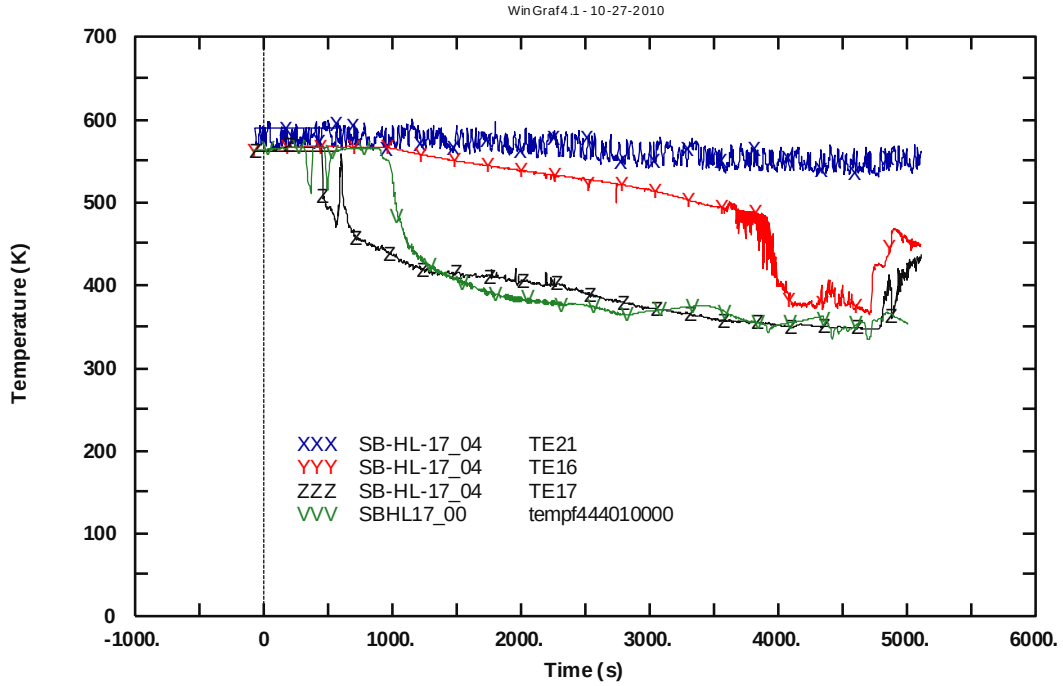

Fig. 70 – LSTF Test SB-HL-17: CL IL temperature (loop A)

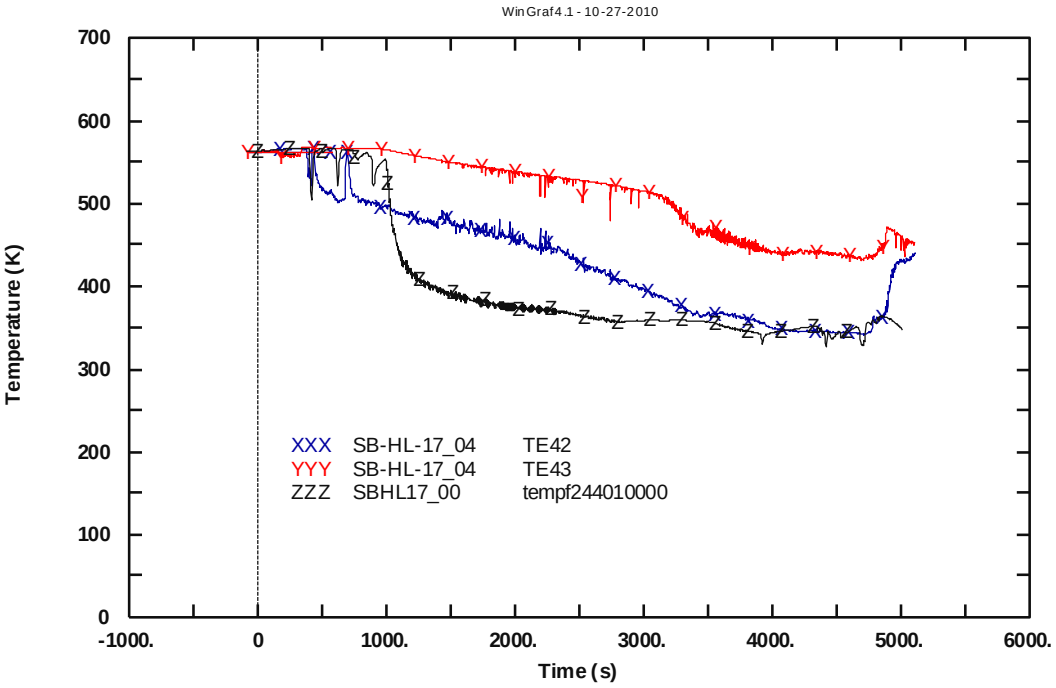

Fig. 71 – LSTF Test SB-HL-17: CL BL temperature (loop B)

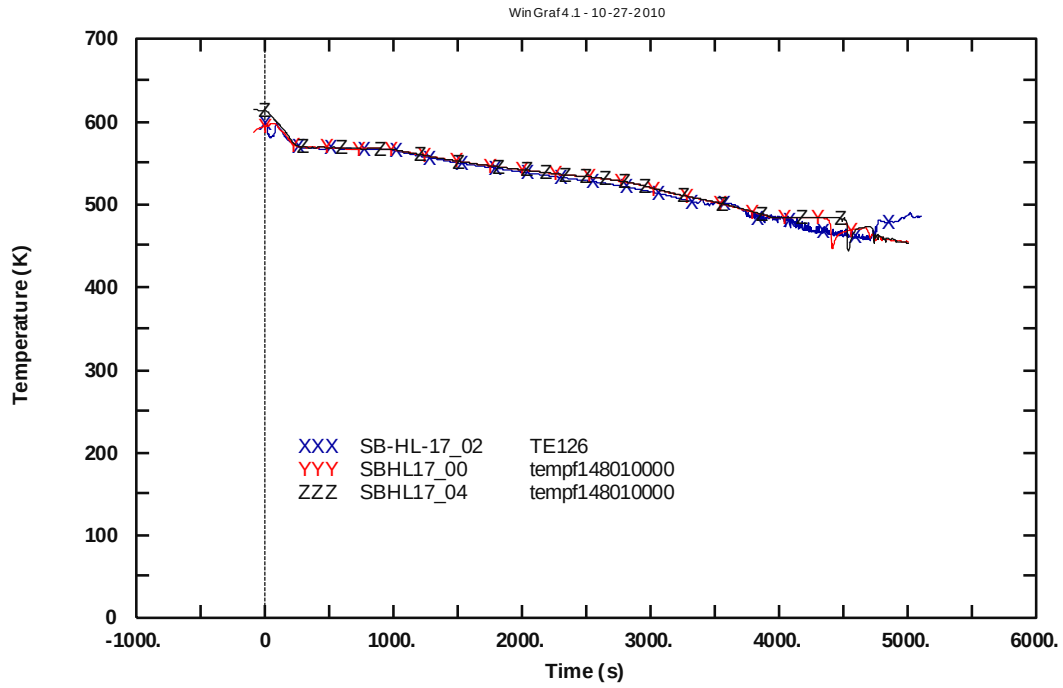

Fig. 72 – LSTF Test SB-HL-17: UP temperature

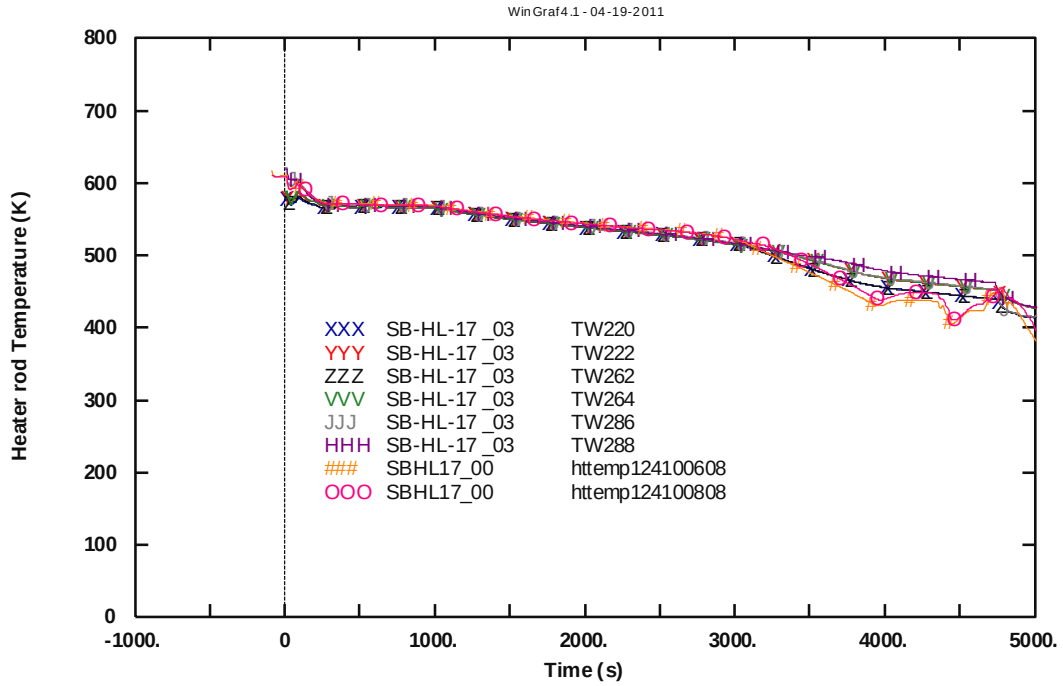

Fig. 73 – LSTF Test SB-HL-17: heater rod temperature, middle and top level of active fuel

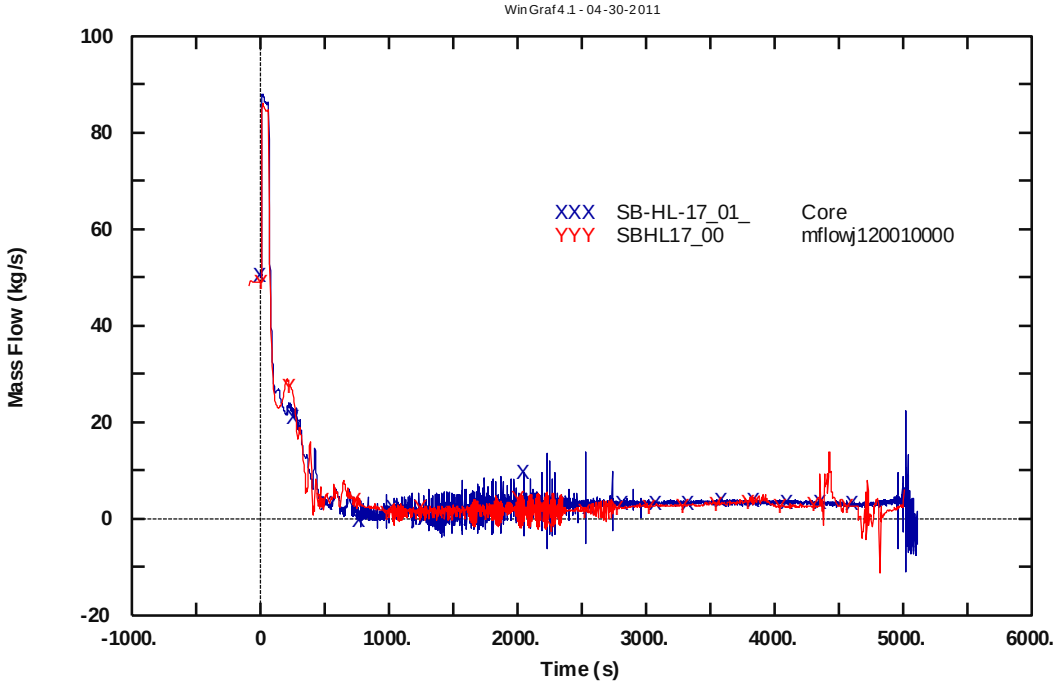

Fig. 74 – LSTF Test SB-HL-17: core mass flow

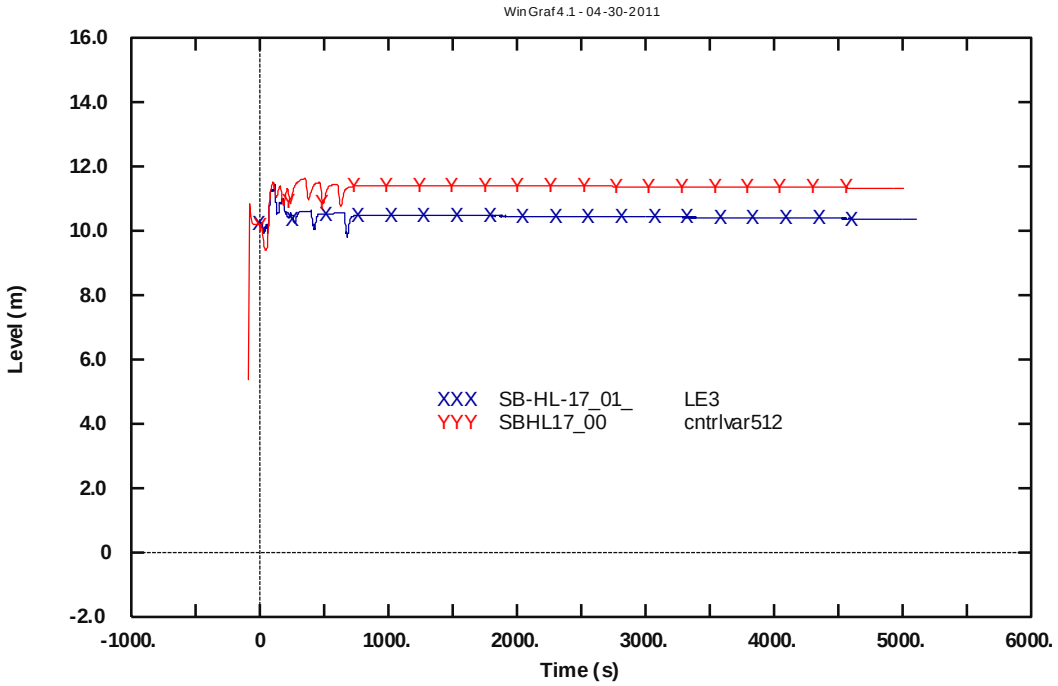

Fig. 75 – LSTF Test SB-HL-17: SG A level

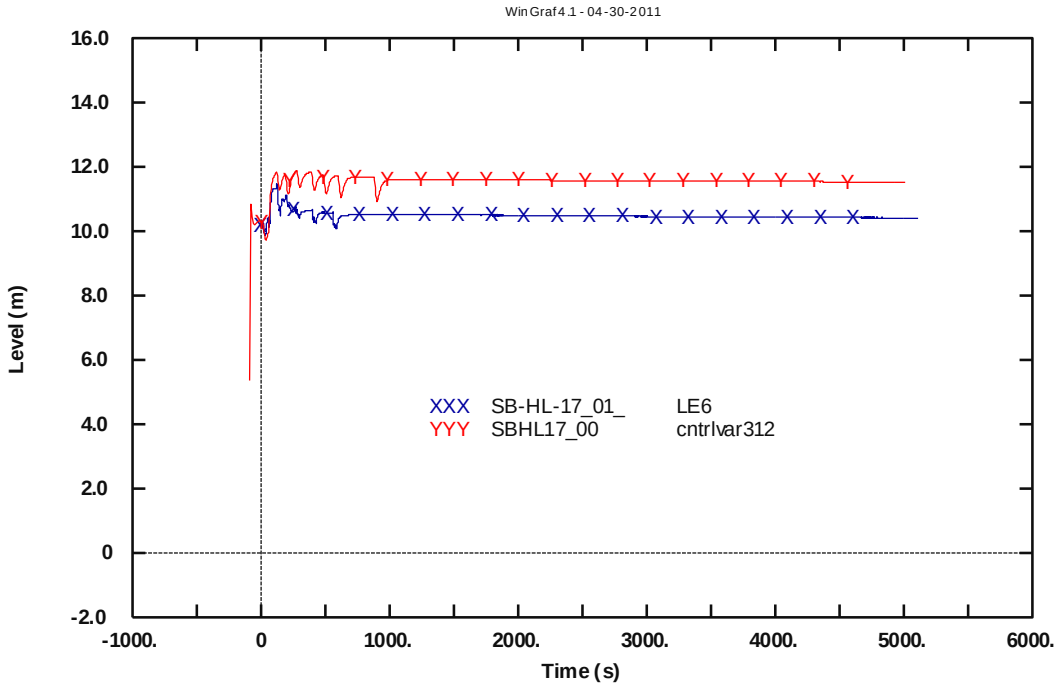

Fig. 76 – LSTF Test SB-HL-17: SG B level

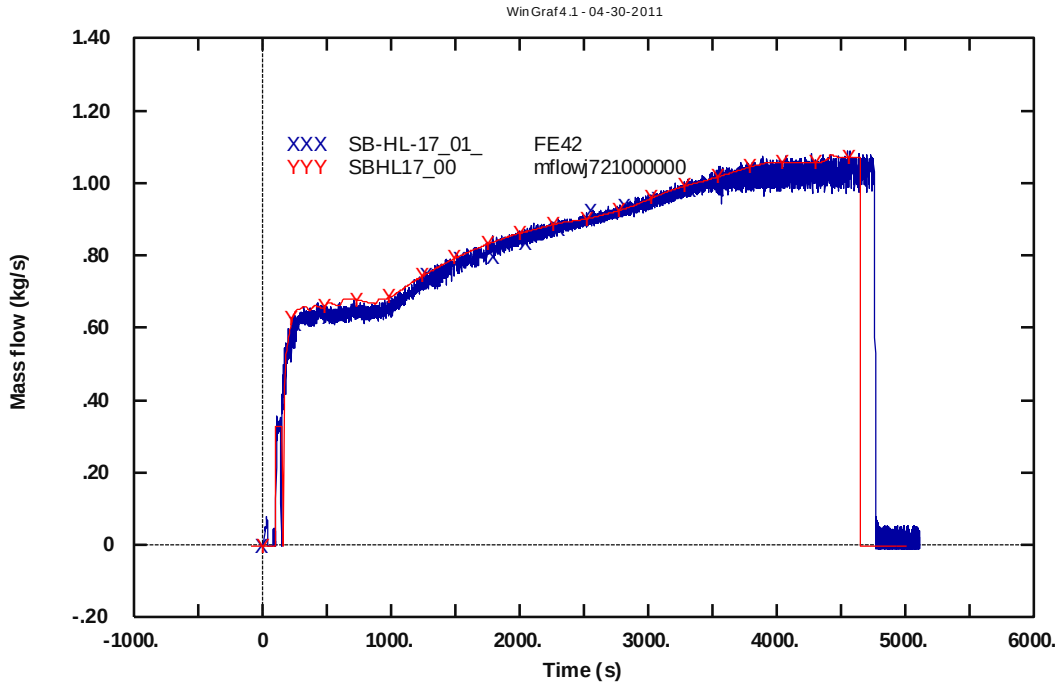

Fig. 77 – LSTF Test SB-HL-17: HPIS IL CL mass flow

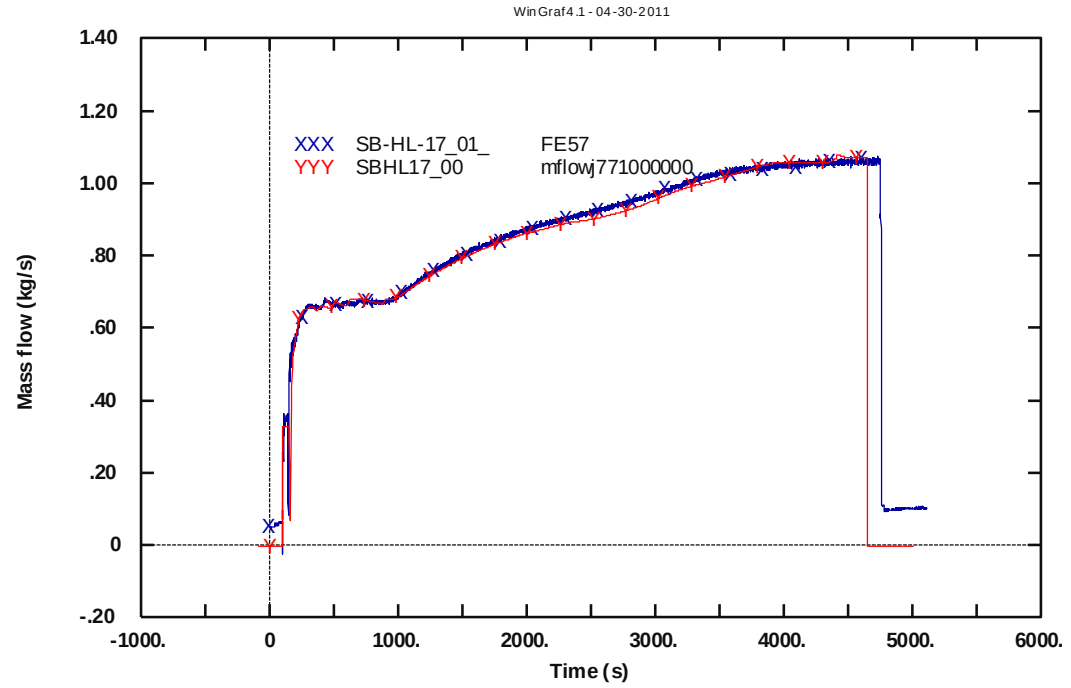

Fig. 78 – LSTF Test SB-HL-17: HPIS BL CL mass flow

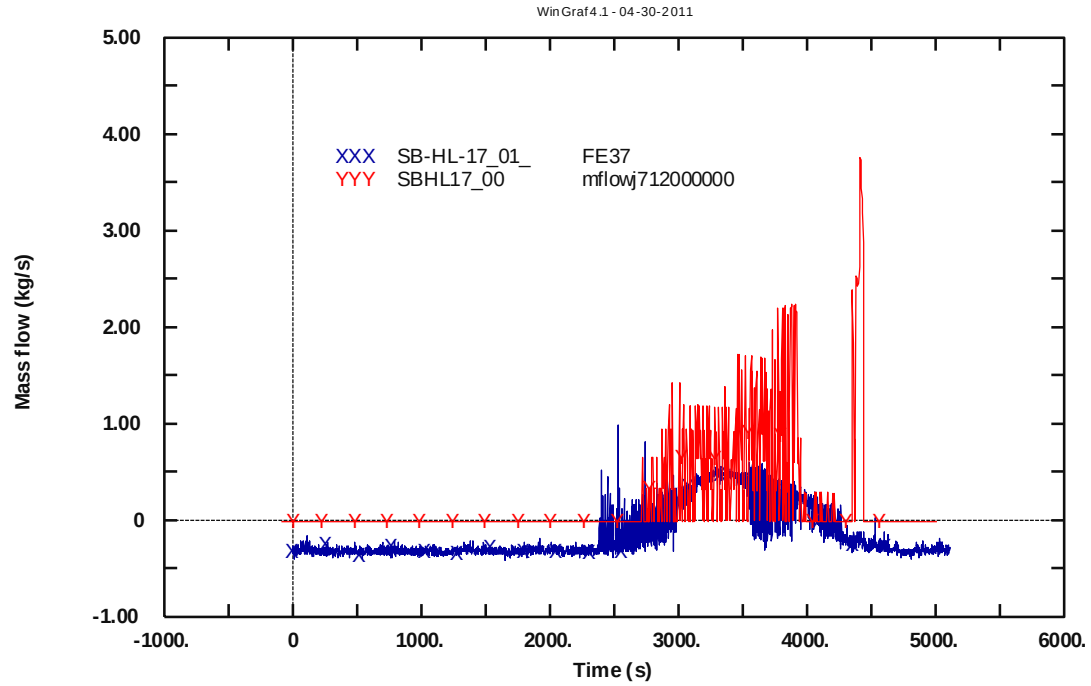

Fig. 79 – LSTF Test SB-HL-17: accumulator A mass flow rate

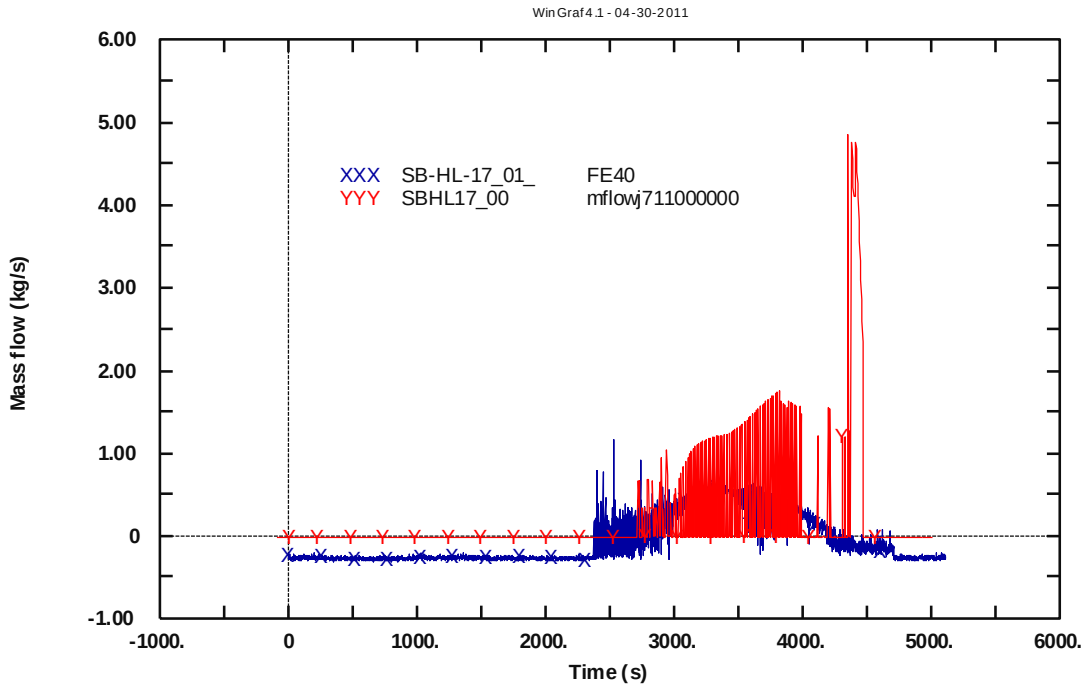

Fig. 80 – LSTF Test SB-HL-17: accumulator B mass flow rate

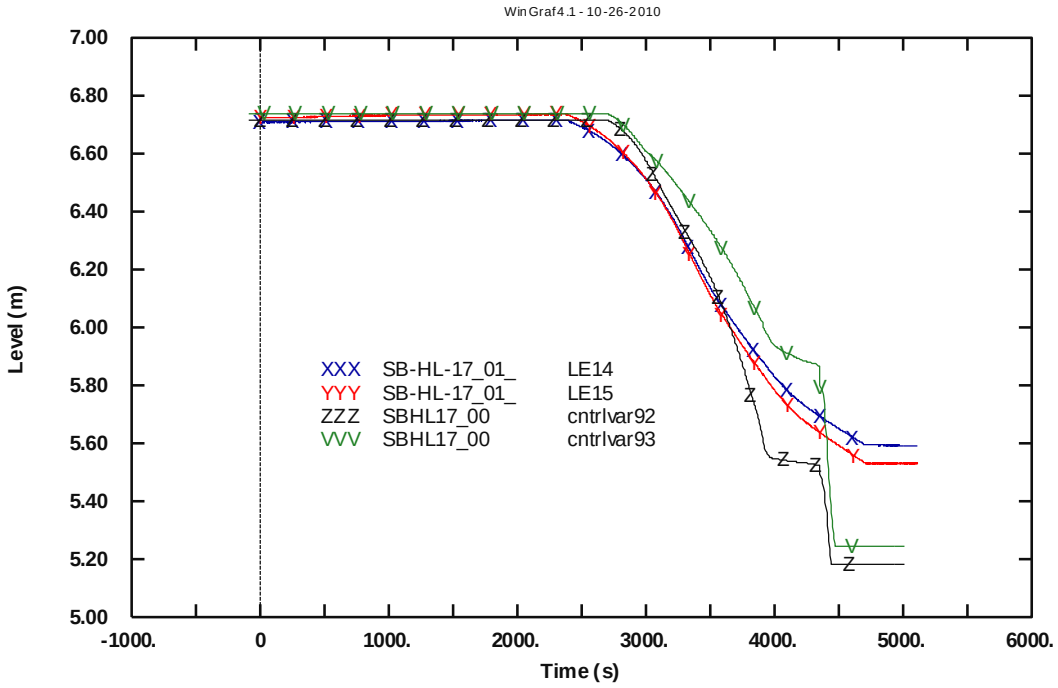

Fig. 81 – LSTF Test SB-HL-17: accumulator A and B level

7 CONCLUSIONS

The present work is aimed at studying selected accidents scenario, at system level, understanding the thermal-hydraulic phenomena occurring in a pressurized water reactor, in order to validate thermal-hydraulic system codes used in safety analysis, as well as understand the capability of the code to reproduce thermal-hydraulic phenomena, on the basis of two similar scenarios. The activity involves the post test analysis of two different tests performed into two different test facilities, namely LOBI and LSTF. The main objectives of the activity, in relation to intermediate and small LOCAs are:

- to acquire competences in performing safety analysis studies and in using thermal-hydraulic system codes;
- to understand important phenomena /processes observed in LOCA transients;
- to assess the predictive capabilities of RELAP 5 code in the domains of interest;
- to identify limitation of the existing best estimate codes;
- to draw conclusions on the possible use of the codes for safety analysis.

The work is subdivided into three main parts for both tests:

1. The analysis of the experimental data, which include the comprehension of the facilities features and scaling criteria. The identification of the phenomenological windows of the transients and of the relevant phenomena involved.
2. The study of the nodalizations received, the review of their features, the set up of the transients (i.e. modifications of the break systems, modeling of the safety systems, implementation of trips, etc…).
3. The simulation of the transients and the comparisons of the results with the experimental data available (i.e. post test analysis). This is fulfilled through a comprehensive comparisons based on the following steps:
   - verification of the code performance at steady state level
   - verification of the code performance at transient level (assisted by a qualitative and quantitative, FFTBM, accuracy evaluation of the results).

The comparisons and verifications executed bring to the conclusion that RELAP5/Mod3.3 code has the capability to deal with the relevant thermal-hydraulic phenomena involved in the two experiments analyzed. Among these the most important are: single and two phase natural circulation, reflux condensation, phase separation, chocked flow at break, heat transfer in the core, and heat transfer in primary to secondary side.

In particular, the analysis of the test A1-84 showed that:

- the primary pressure is very well predicted as demonstrated by the correct time of intervention of the HPIS and of the accumulators;
- the trends of the mass inventory and of the core pressure drop is well reproduced;
- the mass flow rate in the loop is correctly simulated, thus demonstrating the capability of the code to predict the single and two phase natural circulation;
- the occurrence of local critical heat flux condition (dry out), quenched after few seconds by the accumulator intervention, is not reproduced due to the intrinsic limitation of the one dimensional features of the code;

- modification in the discharge coefficients of the Ransom-Trap chocked flow model implemented in the code might improve the accuracy of the code results with respect to the overall parameters;
- the application of the FFTBM highlighted the excellent quantitative accuracy of the primary pressure and of the overall transient.

The reference calculation of the LSTF test SB-HL-17 brings to the following conclusions.

- Overall simulation of the test is acceptable.
- The prediction of the break flow rate and of the primary pressure are satisfactory.
- Difficulties are observed in simulating the accumulator behavior. In particular, the mass flow rate injected is overestimated. More information on the accumulator discharge line and its operation might overcome the issue.
- The application of the FFTBM demonstrates the excellent quantitative accuracy of the primary pressure trend as well a satisfactory accuracy of the overall transient.

Finally, the outcomes of these analyses will be helpful to support the involved steps of integral plant model qualification procedures and uncertainty evaluation methodologies.

References

[1] 10 CFR Part 50. Domestic Licensing of Production and Utilization Facilities. 50.46 Acceptance criteria for emergency core cooling systems for light water nuclear power reactors.

[2] **Rates of initiating events at US nuclear power plants: 1987-1995**, Idaho national engineering and environmental laboratory, US Nuclear regulatory commission.

[3] Robert L. Tregoning, **Passive system LOCA frequency development for risk-informed revision of 10 CFR 50.46,** NRC, AERB Nuclear safety project meeting, August 30-September 3, 2004.

[4] Paul S. Damerell, Jhon W. Simons, MPS Associates Inc, **2D/3D program work summary report,** US Nuclear regulatory commission, June 1993.

[5] Annunziato A., H. Glaeser, J. Lillington, P. Marsili, C. Renault, A. Sjöberg, **CSNI Integral Test Facility Validation Matrix for the Assessment of Thermal-Hydraulic Codes for LWR LOCA and Transients**, NEA/CSNI/R(96)17, July 1996.

[6] M. J. Lewis, R. Pochard, F. D'Auria, et al., **Thermohydraulics of emergency core cooling in light water reactors—a state of the art report,** OECD/NEA, Paris, France, October 1989.

[7] M. Perez, F. Reventos, L. Batet, et al., **Uncertainty and sensitivity analysis of a LBLOCA in a PWR Nuclear Power Plant: Results of the Phase V of the BEMUSE programme**, Nuclear Engineering and Design, Volume 241, Issue 10, Pages 4206-4222, October 2011.

[8] OECD/NEA, **Nuclear Fuel Behaviour in Loss-of-coolant Accident (LOCA) Conditions: State-of-the-art Report**, Report No. 6846, 2009.

[9] Addabbo C., B.Worth, **A Small Break LOCA and Special Transients: Final Report**, LOBI-MOD2 Research Programme 4333, 23/2/2000.

[10] **Primary and secondary loops schemes**, 1/31/2001.

[11] Addabbo C., A. Annunziato, **Summary Description of the LOBI Test Matrix**, 4/30/2002.

[12] Sanders J., E. Ohlmer, **Experimental Data Report on Lobi-Mod2 Test A1-84**, LOBI-MOD2 Research Programme 4037, 11/3/1999.

[13] Addabbo C., R.Wampach, G.Leva, **Quick Look Report on Lobi-Mod2 Test A1-84**, LOBI-MOD2 Research Programme 4042, 11/3/1999.

[14] Annunziato A., **LOBI-MOD2 Accumulator System Behaviour during Small Break LOCA Experiments**, I.89.51, 3/15/2000.

[15] The ROSA-V Group, **ROSA-V Large Scale Test Facility (LSTF) System Description for the Third and Fourth Simulated Fuel Assemblies**, JAERI-Tech 2003-037, Japan Atomic Energy Research Institute (2003).

[16] Thermo-hydraulic Safety Research Group, **Final Data Report of OECD/NEA ROSA Project Test 1-2 1% hot-leg break LOCA experiment with HPI: SB-HL-17 in JAEA)**, OECD/NEA ROSA Project, NSRC, JAEA, July 3, 2008.

[17] ISL Inc., **RELAP5/MOD3.3 Code Manual Volume I: Code Structure, System Models, and Solution Methods**, Nuclear Safety Analysis Division, July 2003.

[18] ISL Inc., **RELAP5/MOD3.3 Code Manual Volume II: User's Guide and Input Requirements**, Nuclear Safety Analysis Division, Jan. 2003.

[19] ISL Inc., **RELAP5/MOD3.3 Code Manual Volume II: Appendix A Input Requirements**, Nuclear Safety Analysis Division, June 2004.

[20] ISL Inc., **RELAP5/MOD3.3 Code Manual Volume V: User's Guidelines**, Nuclear Safety Analysis Division, Dec. 2001.

[21] D'Auria F., M. Frogheri, W. Giannotti, **RELAP5/MOD3.2 Post test analysis and accuracy quantification of LOBI test BL-44; NUREG/IA-0153**, University of Pisa, Italy, (February 1999).

[22] Berthon A., **Caracterización de la evaluación de seguridad del reactor WWER-1000 mediante metodología "Best Estimate" con análisis de incertidumbres;** Technical University of Catalonia, Spain, University of Pisa, Italy, Master Thesis (November 2005).

[23] Pretel C., F. Reventós, **"Post-Test Analysis of LOBI Test BL-30 Using RELAP5/MOD2.5", JRC Technical Note I.93.64.** Technical University of Catalonia, Asociación Nuclear Ascó, Spain, (September 1993).

[24] ISL Inc., **RELAP5/MOD3.3 Code Manual Volume VII: Summaries and Reviews of Independent Code Assessment Reports**, Nuclear Safety Analysis Division, Dec. 2001.

[25] Del Nevo A., et Al., **Analytical Exercise on OECD/NEA/CSNI PKL-2 Project Test G3.1: Main Steam Line Break Transient in PKL-III Facility: Phase 2 – Postest Calculations,** University of Pisa, GRNSPG, TH/PKL-2/02(10) Rev. 1 Pisa, March 2011.

[26] Thermo-hydraulic Safety Research Group, **Brief Description of Computer Code Input for ROSA/LSTF Analyses using RELAP5/MOD3 Code**, OECD/NEA ROSA-2 Project, NSRC, JAEA, Sept. 24, 2010.

[27] Bonuccelli M., F. D'Auria, N.Debrecin, G.M.Galassi, **A Methodology for the Qualification of Thermalhydraulic Code Nodalizations**, Proc. of NURETH-6 Conference, Grenoble (F), October 5-8, 1993.

[28] D'Auria F., A. Bousbia-Salah, A. Petruzzi, A. Del Nevo, **State of the Art in Using Best Estimate Calculation Tools in Nuclear Technology**, Nuclear Engineering and Technology, Volume 38, Issue 1, February 2006, pp 11-32.

[29] Bovalini R., F. D'Auria, M. Leonardi, **Qualification of the Fast Fourier Transform Based Methodology for the Quantification of Thermalhydraulic Code Accuracy**, DCMN Report, NT 194 (92), Pisa July 1992.

[30] B. Worth, H. Stadtke, **RELAP5 Base input data for LOBI-MOD2**, February 1985.

[31] F. Reventos, P. Pla, C. Matteoli, G. Nacci, M. Cherubini, A. Del Nevo, F. D'Auria**, Consistent Post-Test Calculations for LOCA Scenarios in LOBI Integral Facility,** Science and Technology of Nuclear Installation, 2011, in press.

[32] ISL Inc., **RELAP5/MOD3.3 Code Manual Volume VII: Summaries and Reviews of Independent Code Assessment Reports**, Nuclear Safety Analysis Division, Dec. 2001.

[33] Addabbo, A. Annunziato, N. Aksan, F. D'Auria, D. Dumont, G. Galassi, L. Nilsson, V. Riikonen, M. Rigamonti, F. Steinhoff, I. Toth, K. Umminger, **Maintenance of European LWR Integral System Test Thermal-Hydraulic Databases**, EUR Report N. 19937, October 2001.

[34] Paul S. Damerell, Jhon W. Simons, MPR Associates Inc, **Reactor safety issues solved by 2D/3D program,** GRS, September 1993.

[35] C. Matteoli, A. Del Nevo, F. D'Auria, **UNIPI contribution to PKL-2/LSTF counterpart test design,** presentation at 5th PRG/MB meeting of PKL-2 Project, Paris, 9-10 November 2010.

[36] C. Matteoli, A. Del Nevo, F. D'Auria, **Notes on "ROSA-PKL couterpart test preparation",** issued to JAERI and AREVA NP (e-mail 8/11/2010), Pisa, Rev. 1, 8 November 2010.

Notes on "ROSA-PKL counterpart test preparation"

Appendix A. LOBI Test A1-84: reference calculation results

A.1 Steady state results

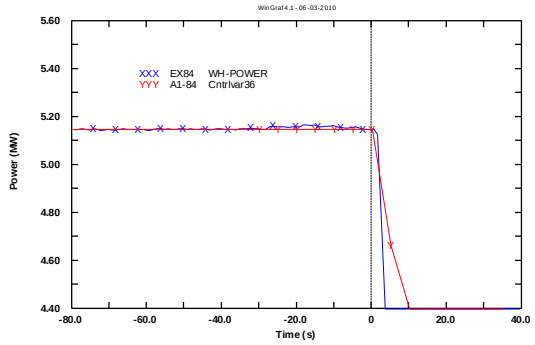

(a) Core power

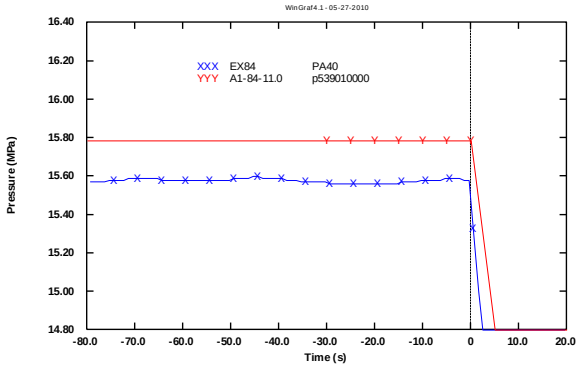

(b) PRZ pressure

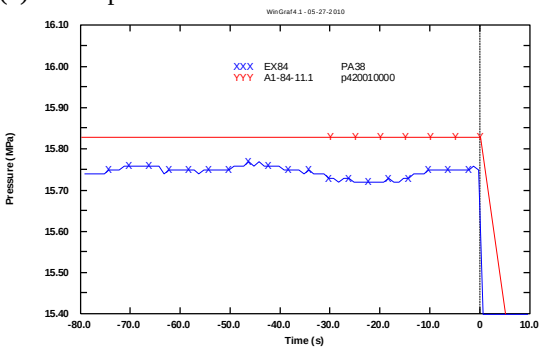

(c) UP pressure

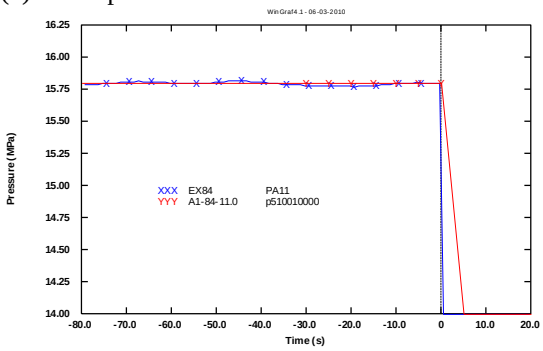

(d) Hot Leg IL pressure

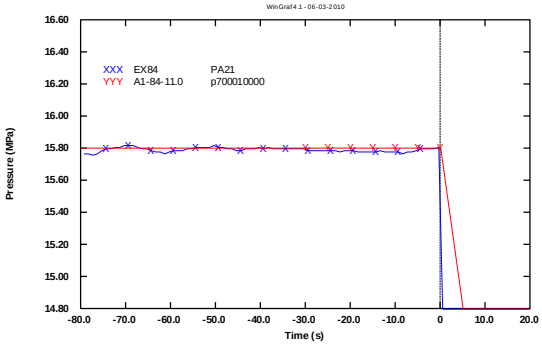

(e) Hot Leg BL pressure

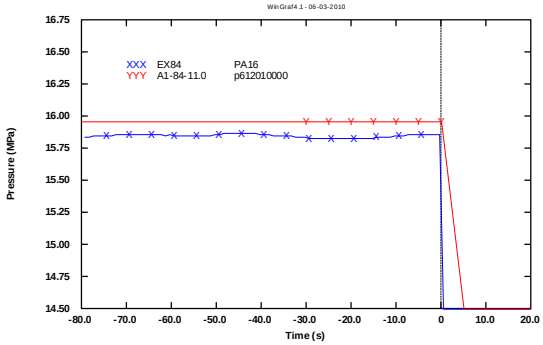

(f) Cold Leg IL pressure

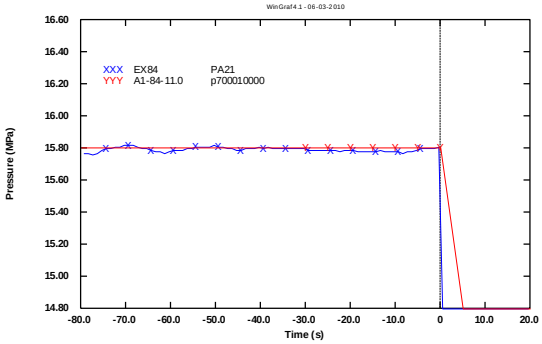

(g) Hot Leg BL pressure

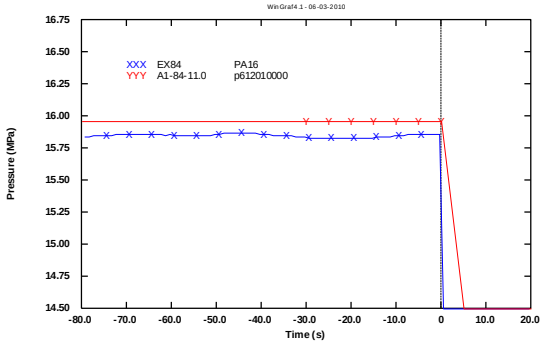

(h) Cold Leg IL pressure

Fig. A - 1 – LOBI test A1-84: steady state results (part 1 of 7).

8

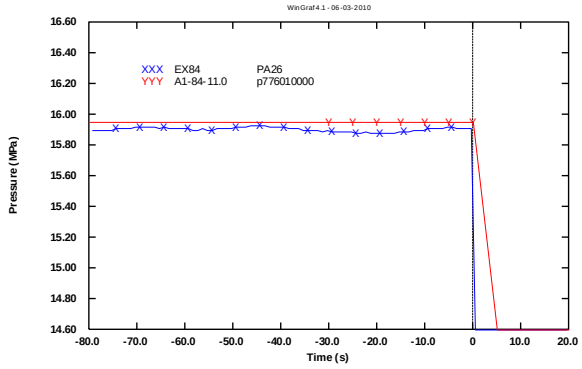

(a) Cold Leg BL power

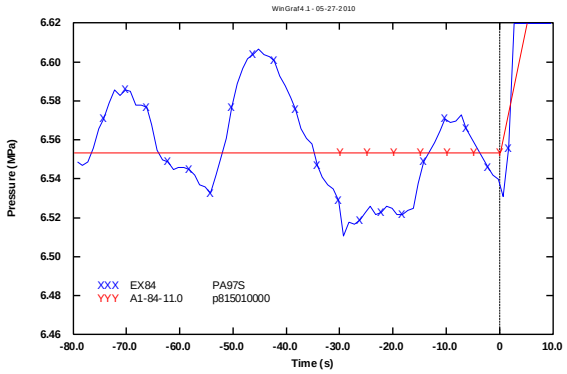

(b) SG IL steam dome pressure

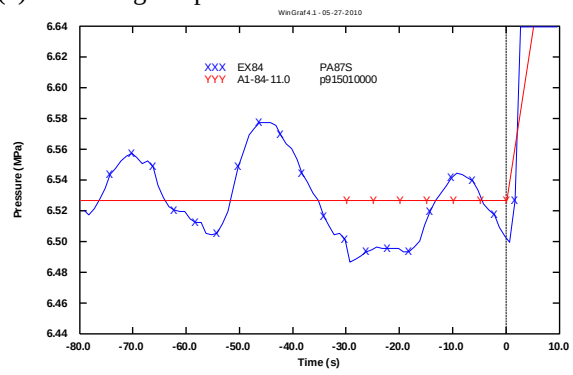

(c) SG BL steam dome pressure

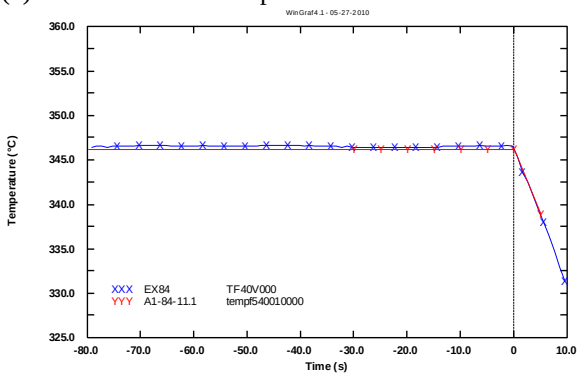

(d) PRZ temperature

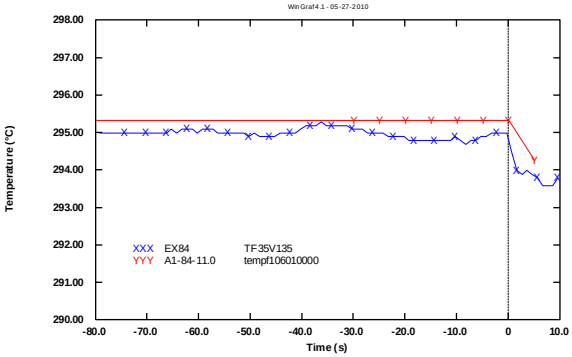

(e) Core inlet temperature (lower plenum)

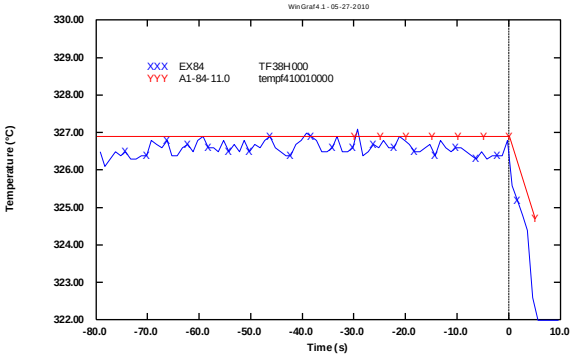

(f) Core outlet temperature (upper plenum)

8

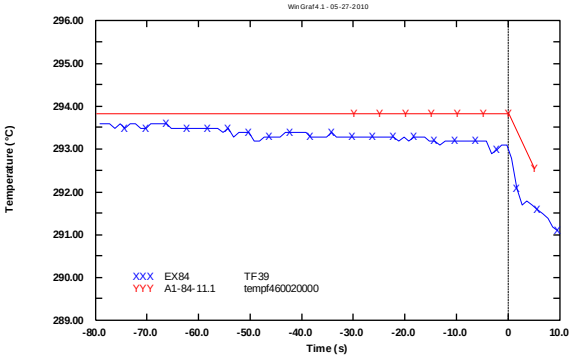

(g) Upper head temperature

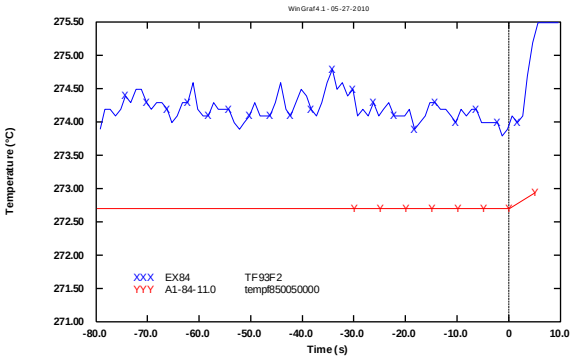

(h) SG IL downcomer (lower part) temperature

Fig. A - 2 – LOBI test A1-84: steady state results (part 2 of 7).

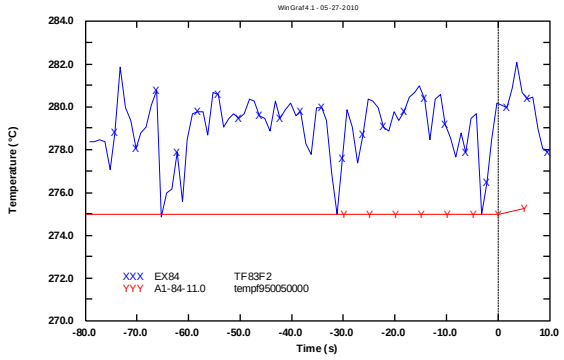

(a) SG BL downcomer (lower part) temperature

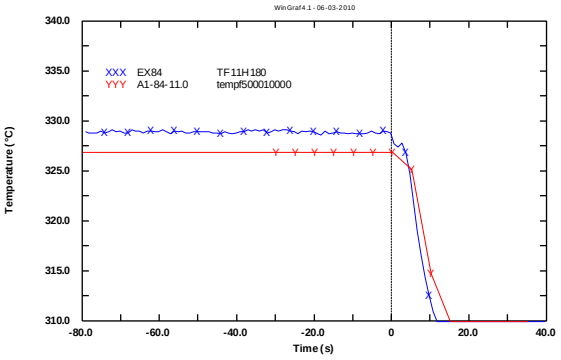

(b) Hot Leg IL temperature

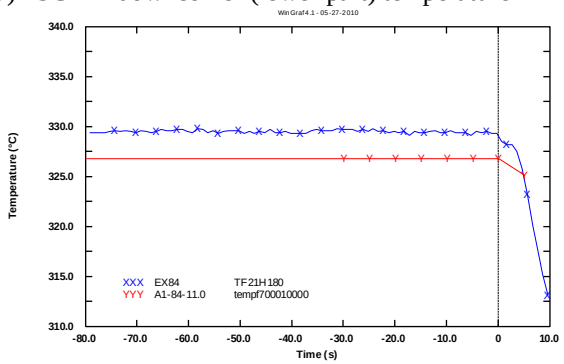

(c) Hot Leg BL temperature

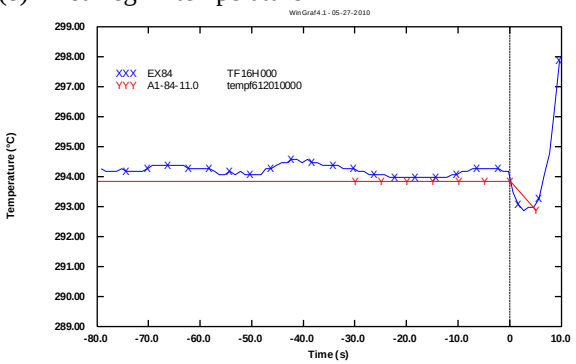

(d) Cold Leg IL temperature

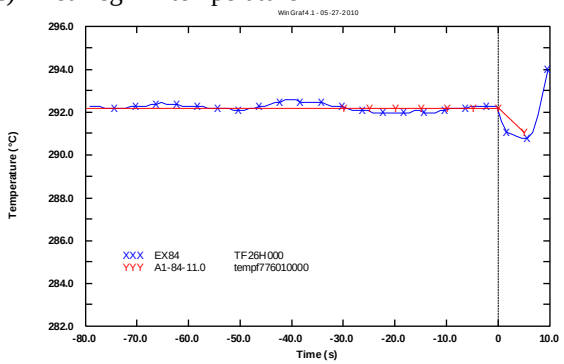

(e) Cold Leg BL temperature

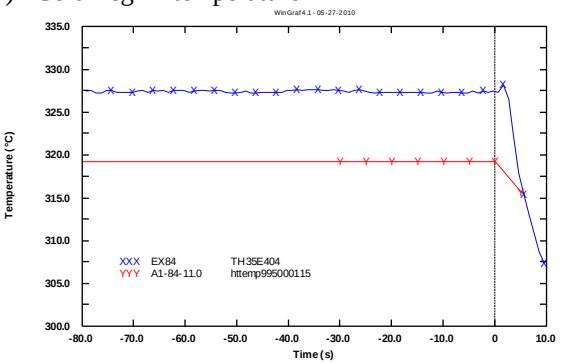

(f) Heater rod temperature (llevel 4)

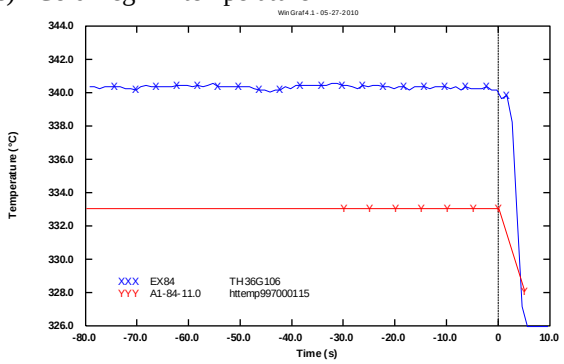

(g) Heater rod temperature (level 6)

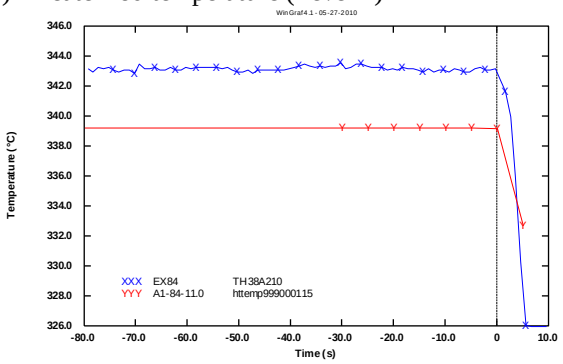

(h) Heater rod temperature (level 10)

Fig. A - 3 – LOBI test A1-84: steady state results (part 3 of 7).

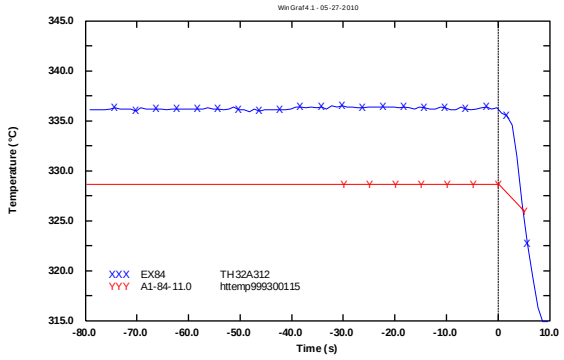

(a) UP heat structure temperature (Level 12)

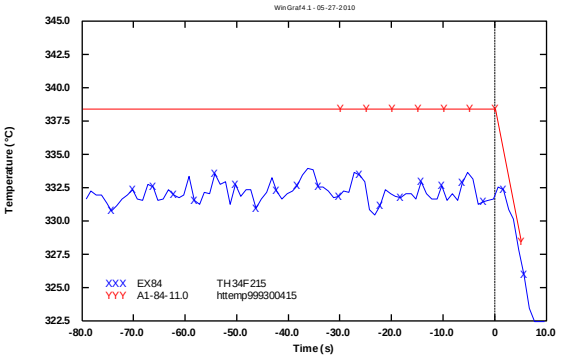

(b) UP heat structure temperature (Level 15)

8

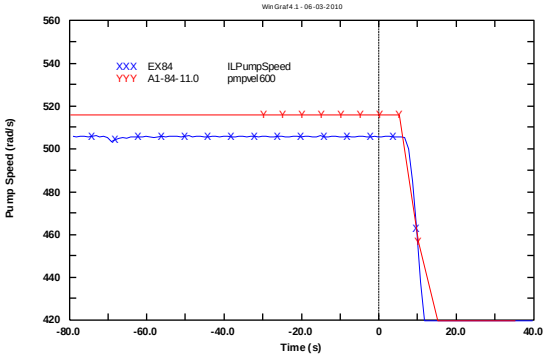

(c) IL pump velocity

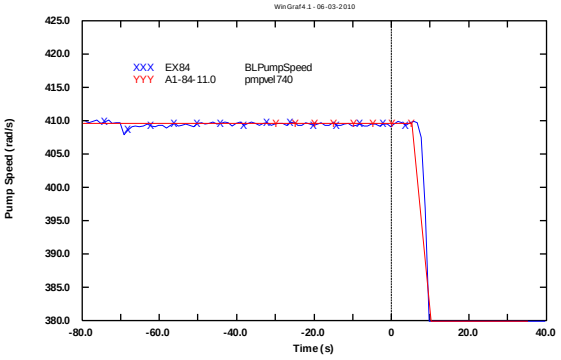

(d) BL pump velocity

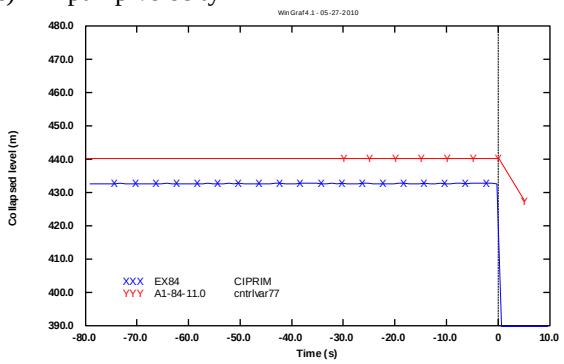

(e) Primary mass inventory

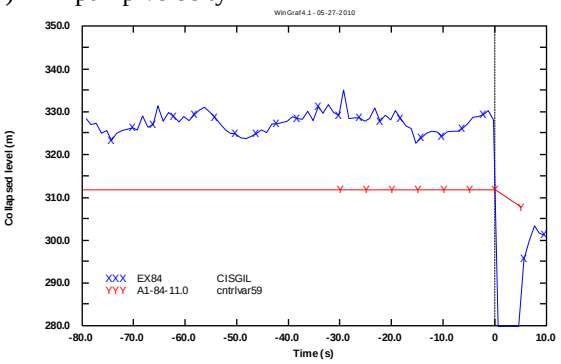

(f) IL secondary mass inventory

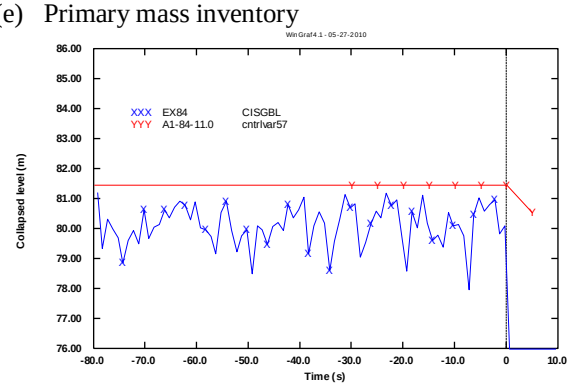

(g) BL secondary mass inventory

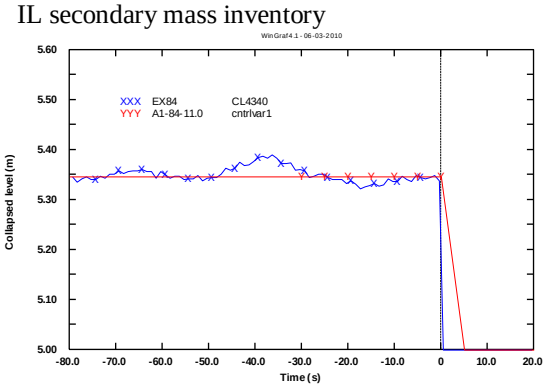

(h) PRZ Level

Fig. A - 4 – LOBI test A1-84: steady state results (part 4 of 7).

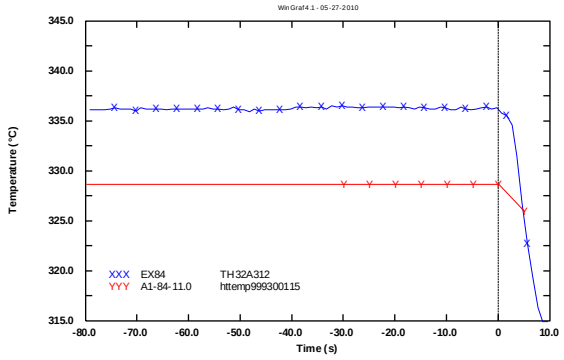

(a) UP heat structure temperature (Level 12)

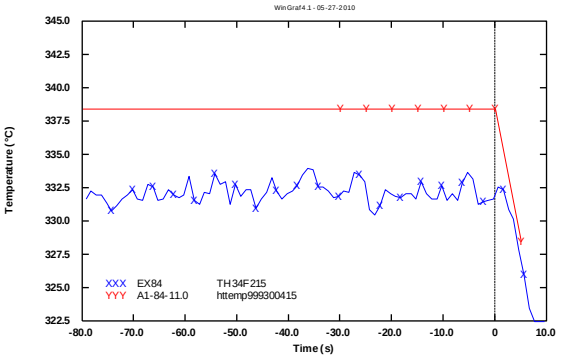

(b) UP heat structure temperature (Level 15)

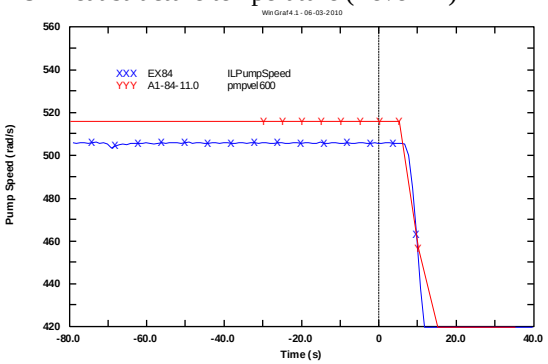

(c) IL pump velocity

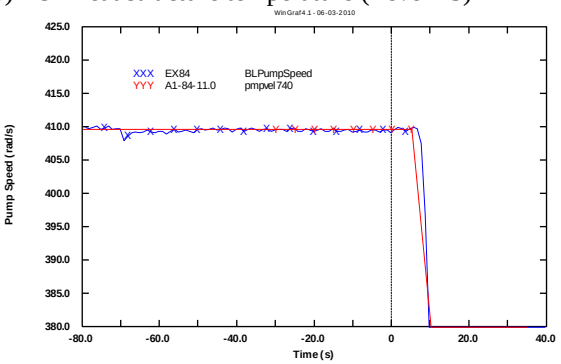

(d) BL pump velocity

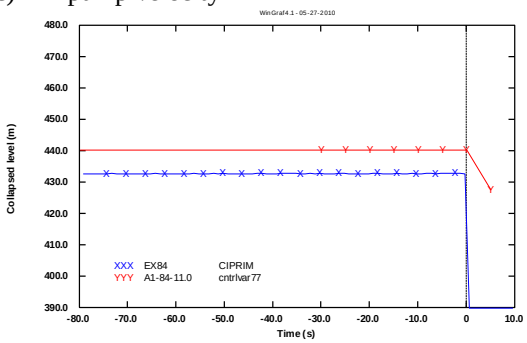

(e) Primary mass inventory

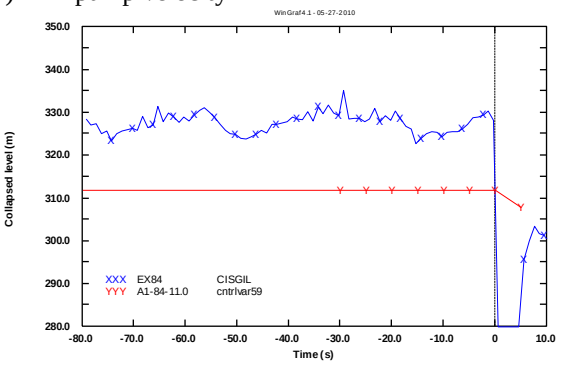

(f) IL secondary mass inventory

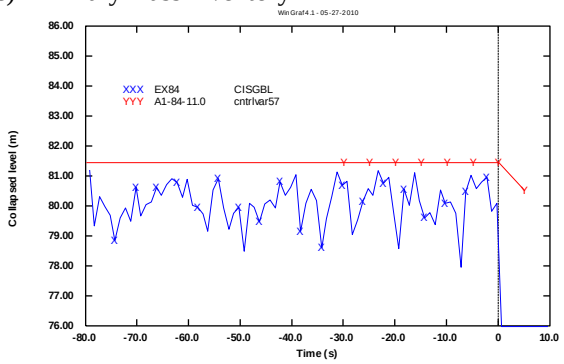

(g) BL secondary mass inventory

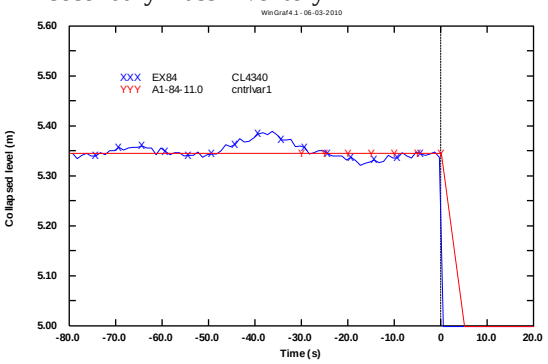

(h) PRZ Level

Fig. A - 5 – LOBI test A1-84: steady state results (part 5 of 7).

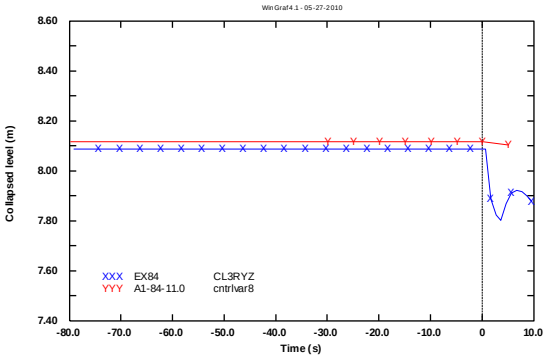

(a) Core collapsed level

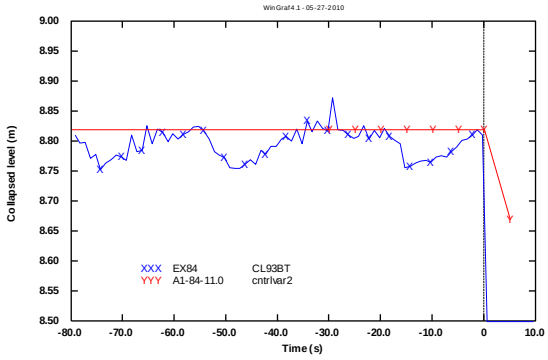

(b) SG IL collapsed level

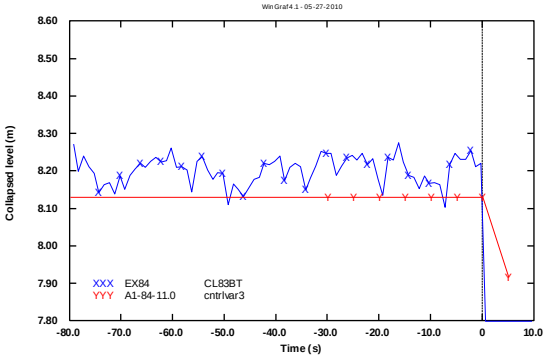

(c) SG BL collapsed level

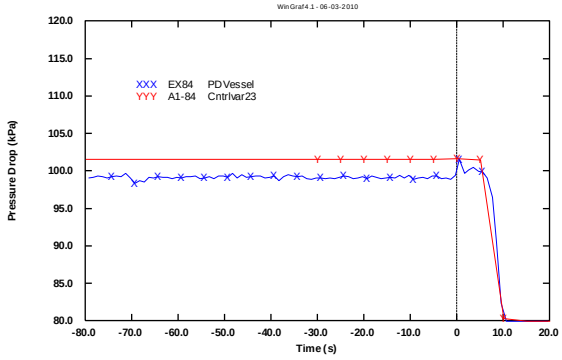

(d) RPV pressure drop

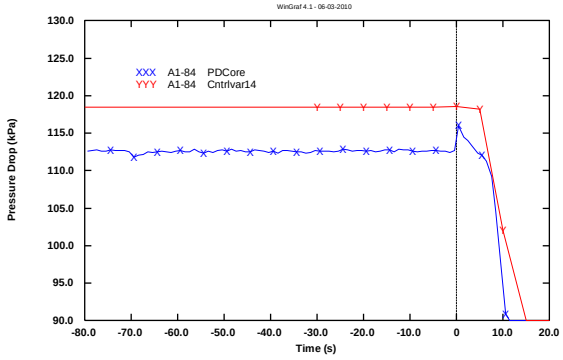

(e) Core pressure drop

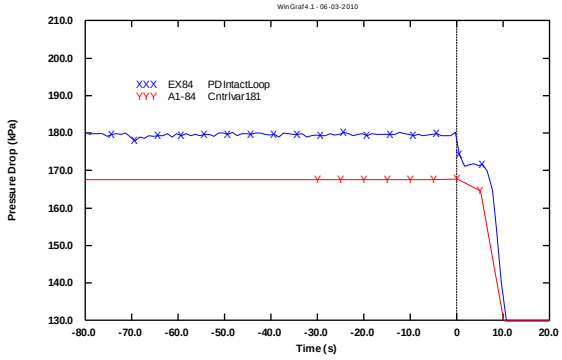

(f) IL pressure drop

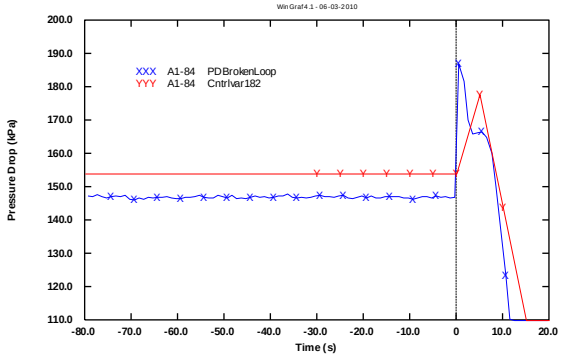

(g) BL pressure drop

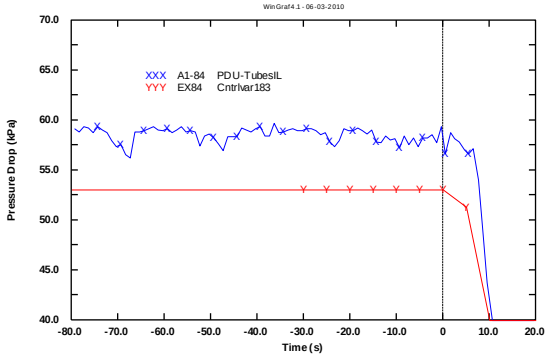

(h) U-Tubes IL pressure drop

Fig. A - 6 – LOBI test A1-84: steady state results (part 6 of 7).

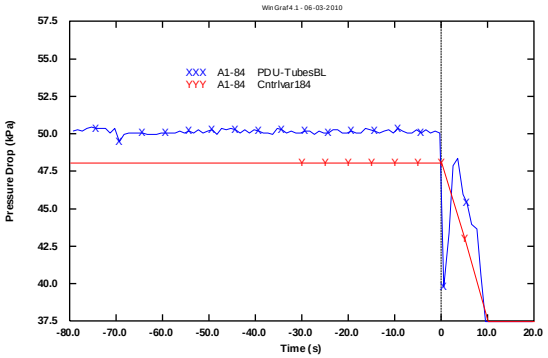

(a) U-Tubes BL pressure drop

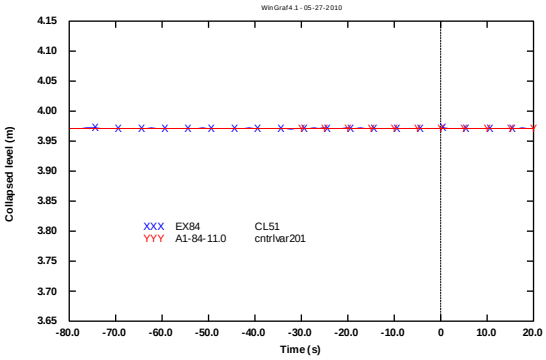

(b) Accumulator IL level

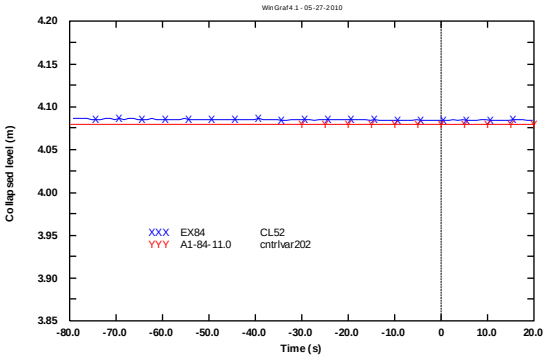

(c) Accumulator BL level

Fig. A - 7 – LOBI test A1-84: steady state results (part 7 of 7).

A.2 Reference calculation results

Tab. A - 1 – LOBI test A1-84: Relevant Parameters..

#	QUANTITY	ID EXP	ID	UNIT
1	**PRIMARY CIRCUIT POWER BALANCE**			
1-1	Core thermal power	WH-POWER	CNTRLVAR36	MWth
2	**SECONDARY CIRCUIT POWER BALANCE**			
2-1	SG-IL power exchanged	-	CNTRLVAR64	kWth
2-2	SG-BL power exchanged	-	CNTRLVAR67	kWth
3	**ABSOLUTE PRESSURE**			
3-1	PRZ pressure (top of the PRZ)	PA 40	P539010000	MPa
3-2	Upper plenum pressure	PA38	P420010000	MPa
3-3	Hot leg pressure IL	PA11	P510010000	MPa
3-4	Hot leg pressure BL	PA21	P700010000	MPa
3-5	Cold leg pressure IL	PA16	P612010000	MPa
3-6	Cold leg pressure BL	PA26	P776010000	MPa
3-7	Steam dome pressure IL	PA97S	P815010000	MPa
3-8	Steam dome pressure BL	PA87S	P915010000	MPa
4	**COOLANT TEMPERATURE**			
4-1	PRZ fluid temperature (middle)	TF40V000	TEMPF540010000	°C
4-2	Core inlet temperature (lower plenum top)	TF35V135	TEMPF106010000	°C
4-3	Core outlet temperature (upper plenum)	TF38H000	TEMPF410010000	°C
4-4	Upper head temperature	TF39	TEMPF460020000	°C
4-5	SG-IL DC pipe bottom temperature	TF93F2	TEMPF850050000	°C
4-6	SG-BL DC pipe bottom temperature	TF83F2	TEMPF950050000	°C
4-7	Hot leg- IL	TF11H180	TEMPF500010000	°C
4-8	Hot leg-BL	TF21H180	TEMPF700010000	°C
4-9	Cold leg-IL	TF16H000	TEMPF612010000	°C
4-10	Cold leg-BL	TF26H000	TEMPF776010000	°C
5	**ROD TEMPERATURE**			
5-1	Heater rod temperature (bottom level-4EXP-03CALC)	TH35E404	HTTEMP995000115	°C
5-2	Heater rod temperature (middle level-6EXP-05CALC)	TH36G106	HTTEMP997000115	°C
5-3	Heater rod temperature (high level-9EXP-07CALC)	TH38A210	HTTEMP999000115	°C
5-4	Heater rod temperature (high level-12EXP-09CALC)	TH32A312	HTTEMP999300115	°C
6	**HEAT STRUCTURE TEMPERATURE**			
6-1	Heat Structure temperature (Upper plenum 410-01 calc-level 13 EXP)	TH36B313	HTTEMP999300215	°C
6-2	Heat structure temperature (Upper plenum 420-01 calc-level 14 EXP)	TH36B214	HTTEMP999300315	°C
6-3	Heat Structure temperature (Upper plenum 430-01 calc-level 15 EXP)	TH34F215	HTTEMP999300415	°C
7	**PUMP VELOCITY**			
7-1	IL velocity	RP71	PMPVEL600	rpm
7-2	BL velocity	RP72	PMPVEL740	rpm
8	**HEAT LOSSES**			
8-1	RPV vessel (@ nominal steady state)	-	CNTRLVAR90	KW
8-2	PRZ and surge line (@ nominal steady state)	-	CNTRLVAR89	KW
8-3	Primary side	-	CNTRLVAR93	KW
8-4	SG secondary side IL (@ nominal steady	-	CNTRLVAR60	KW

#	QUANTITY	ID EXP	ID	UNIT
	state)			
8-5	SG secondary side BL (@ nominal steady state)	-	CNTRLVAR61	KW
9	**MASS INVENTORY IN PRIMARY CIRCUIT**			
9-1	Prim. mass inventory	CIPRIM	CNTRLVAR77	kg
10	**MASS INVENTORY IN SECONDARY CIRCUIT**			
10-1	SG-IL mass inventory	CISGIL	CNTRLVAR59	kg
10-2	SG-BL mass inventory	CISGBL	CNTRLVAR57	kg
11	**FLOW RATES**			
11-1	CORE INLET mass flow rate	-	MFLOWJ106010000	kg/s
11-2	CORE OUTLET mass flow rate	-	MFLOWJ410010000	kg/s
11-3	HOT LEG IL mass flow rate	-	MFLOWJ500010000	kg/s
11-4	HOT LEG BL mass flow rate	-	MFLOWJ700010000	kg/s
11-5	SG feedwater mass flow IL	-	MFLOWJ835010000	kg/s
11-6	SG feedwater mass flow BL	-	MFLOWJ935010000	kg/s
11-7	HPIS mass flow	QM53HPI	MFLOWJ625010000	kg/s
12	**BYPASS MASS FLOW RATES**			
12-1	Core bypass flow rate	-	MFLOWJ430020000	kg/s
12-2	DC-HL IL	-	MFLOWJ500030000	kg/s
12-3	DC-HL BL	-	MFLOWJ700030000	kg/s
12-4	UH-DC bypass flow rate	-	MFLOWJ440010000	kg/s
13	**PRESSURIZER LEVEL**			
13-1	Pressurizer level (collapsed)	CL4340	CNTRLVAR1	m
14	**VESSEL LEVEL**			
14-1	Vessel riser level	CL3RYZ	CNTRLVAR8	m
15	**SECONDARY SIDE LEVEL**			
15-1	SG-IL	CL93BT	CNTRLVAR2	m
15-2	SG-BL	CL83BT	CNTRLVAR3	m
16	**PRESSURE DROP**			
16-1	RPV pressure drop	PD3D3RBA	CNTRLVAR23	kPa
16-2	Core pressure drop	PD3RUG11	CNTRLVAR14	kPa
16-3	PS total loop pressure drop IL	PD161133	CNTRLVAR181	kPa
16-4	PS total loop pressure drop BL	PD262133	CNTRLVAR182	kPa
16-5	SG IL pressure drop	PD9092AA	CNTRLVAR183	kPa
16-6	SG BL pressure drop	PD8082AA	CNTRLVAR184	kPa
16-7	Loop seal IL pressure drop ascending side	PD1714	CNTRLVAR29	kPa
16-8	Loop seal IL pressure drop descending side	PD9217A	CNTRLVAR27	kPa
16-9	Loop seal BL pressure drop ascending side	PD2724	CNTRLVAR24	kPa
16-10	Loop seal BL pressure drop descending side	PD8227A	CNTRLVAR30	kPa
16-11	Hot Leg IL pressure drop	PD1190A	p500010000-p560030000	kPa
16-12	Hot Leg BL pressure drop	PD2180A	p700010000-p712030000	kPa
17	**DENSITY**			
17-1	Lower plenum density	DS34VDIA	rho102010000	kg/m3
17-2	Cold leg BL densisty	DD26HDIA	rho770010000	kg/m3
17-3	Hot Leg BL density	DD21HDIA	rho700010000	kg/m3
17-4	Cold leg IL density	DD16HDIA	rho612010000	kg/m3
17-5	Hot Leg IL density	DD11HPER	rho510010000	kg/m3
18	**ACCUMULATORS LEVEL**			
18-1	ACCU level IL	CL51	CNTRLVAR200	m
18-2	ACCU level BL	CL52	CNTRLVAR201	m

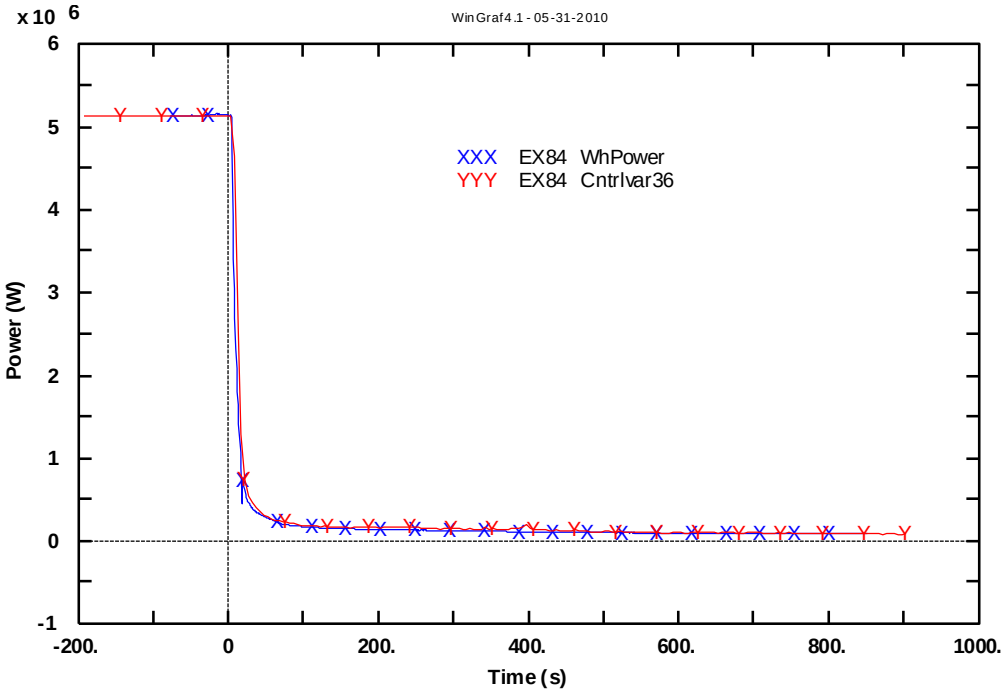

Fig. A - 8 – LOBI test A1-84: core power.

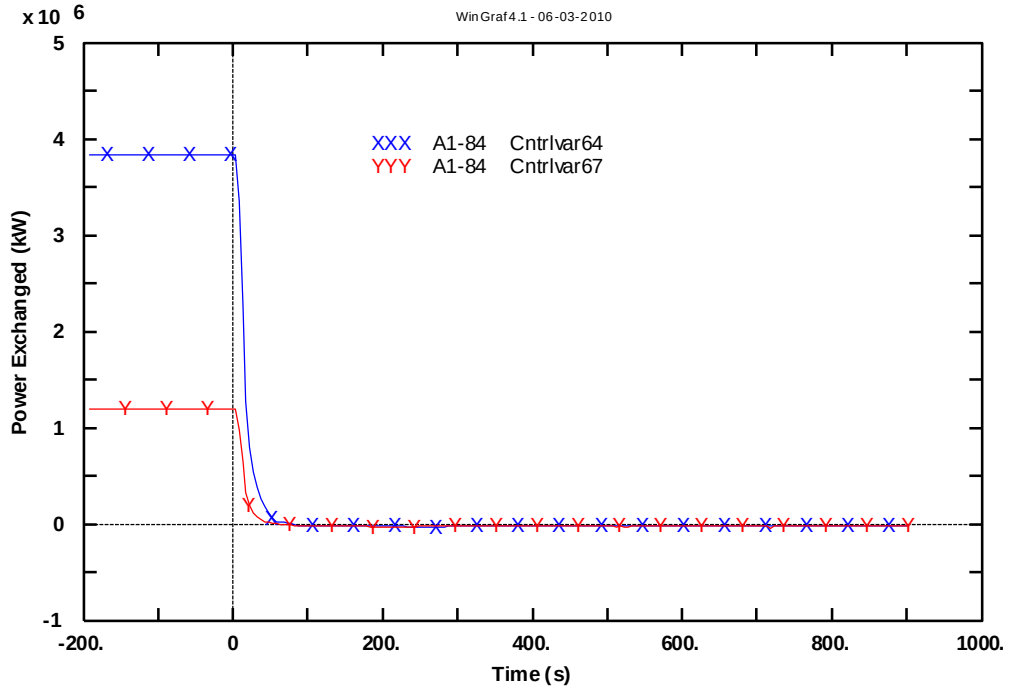

Fig. A - 9 – LOBI test A1-84: SG power exchanged IL and BL.

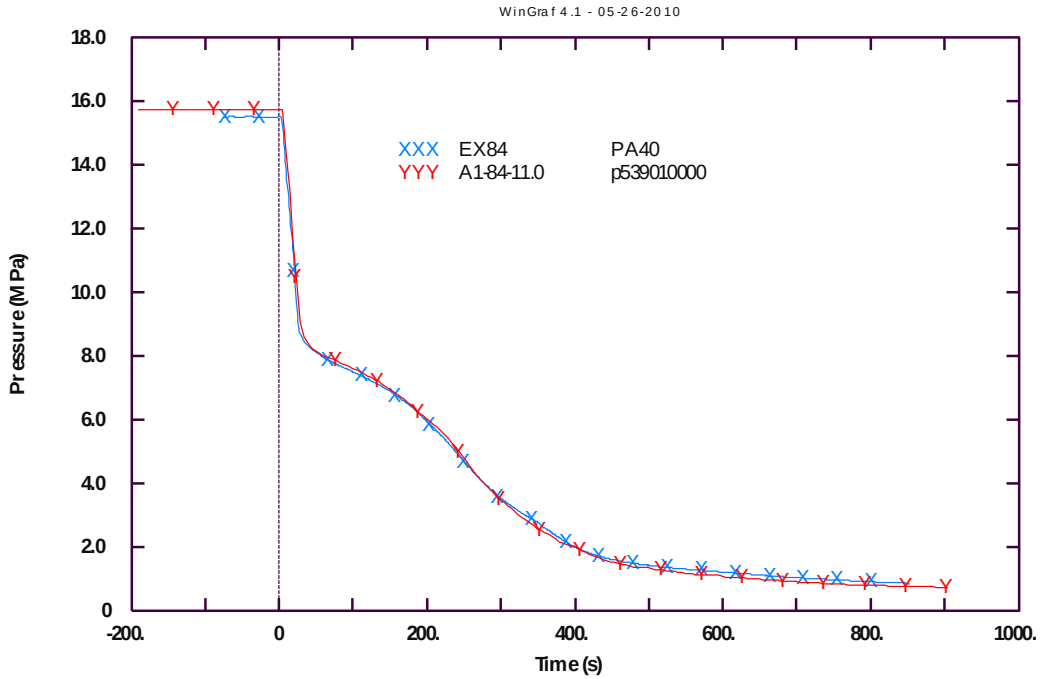

Fig. A - 10 – LOBI test A1-84: PRZ pressure.

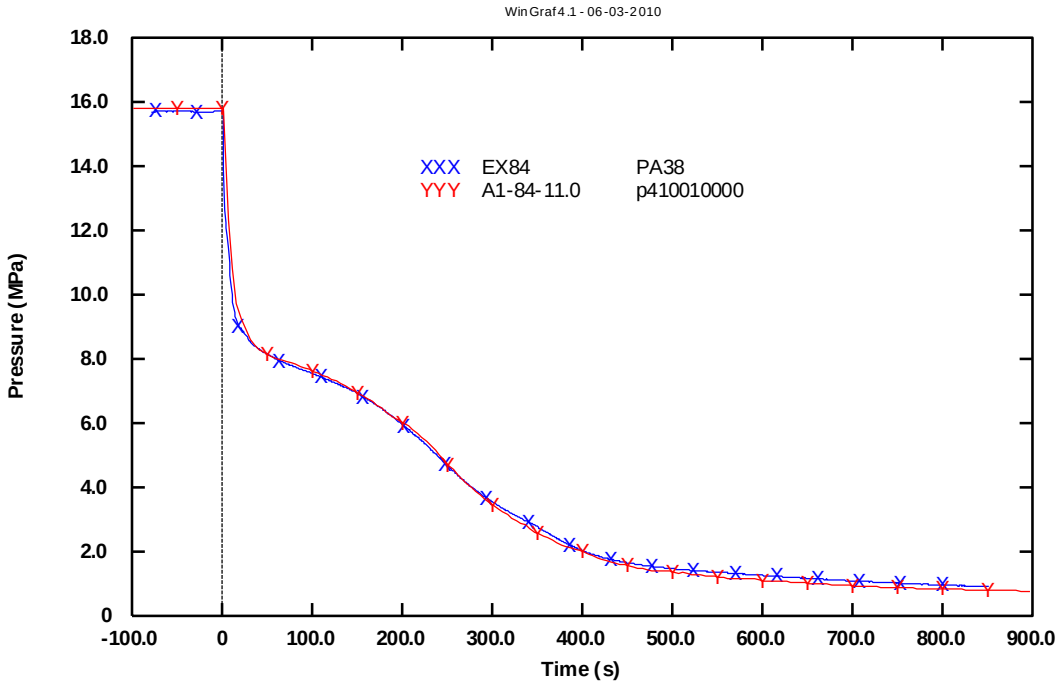

Fig. A - 11 – LOBI test A1-84: UP pressure.

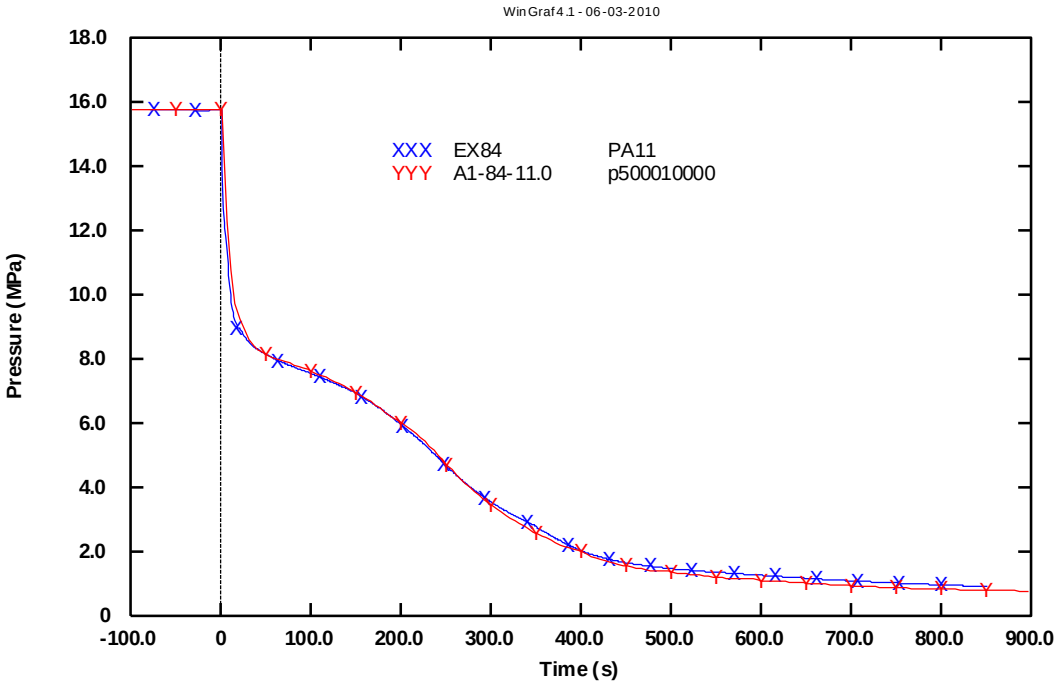

Fig. A - 12 – LOBI test A1-84: IL HL pressure.

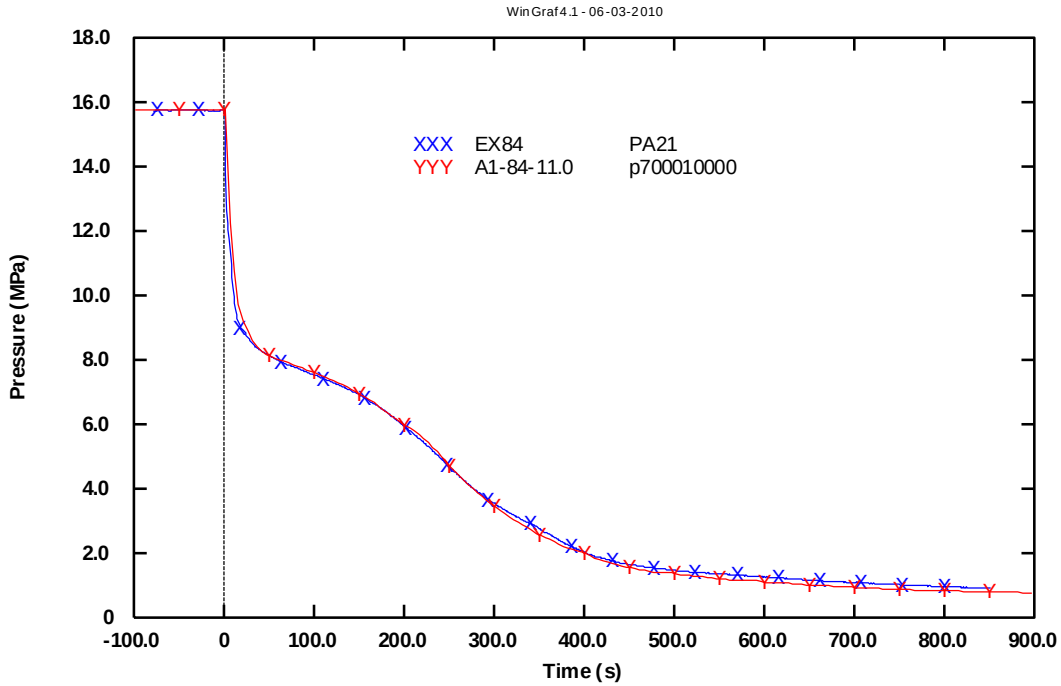

Fig. A - 13 – LOBI test A1-84: BL HL pressure.

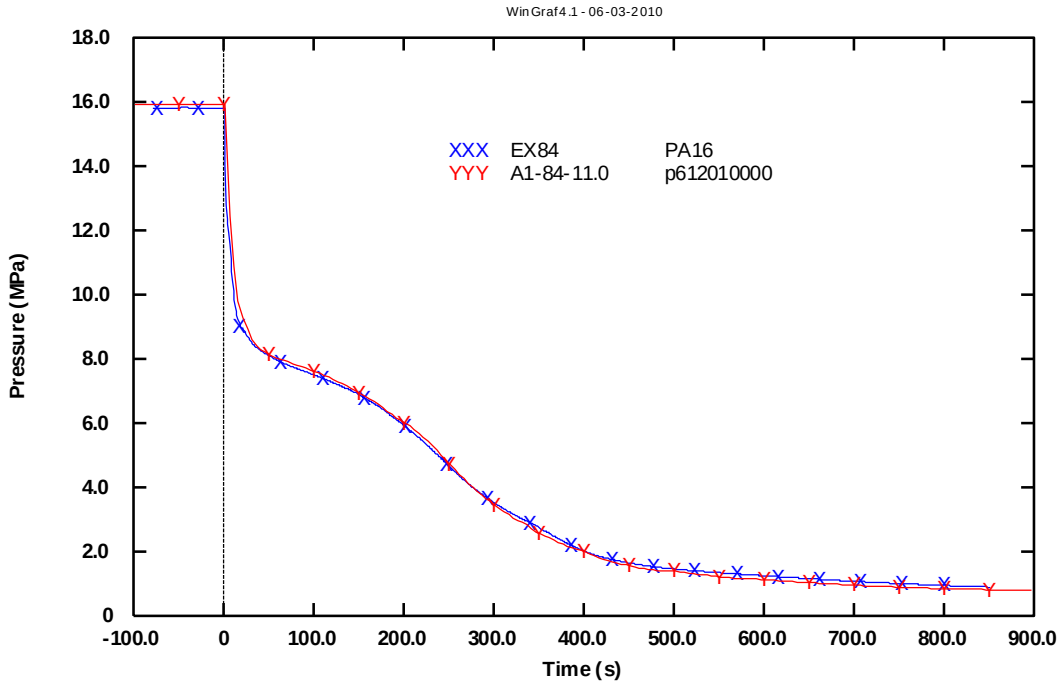

Fig. A - 14 – LOBI test A1-84: IL CL pressure.

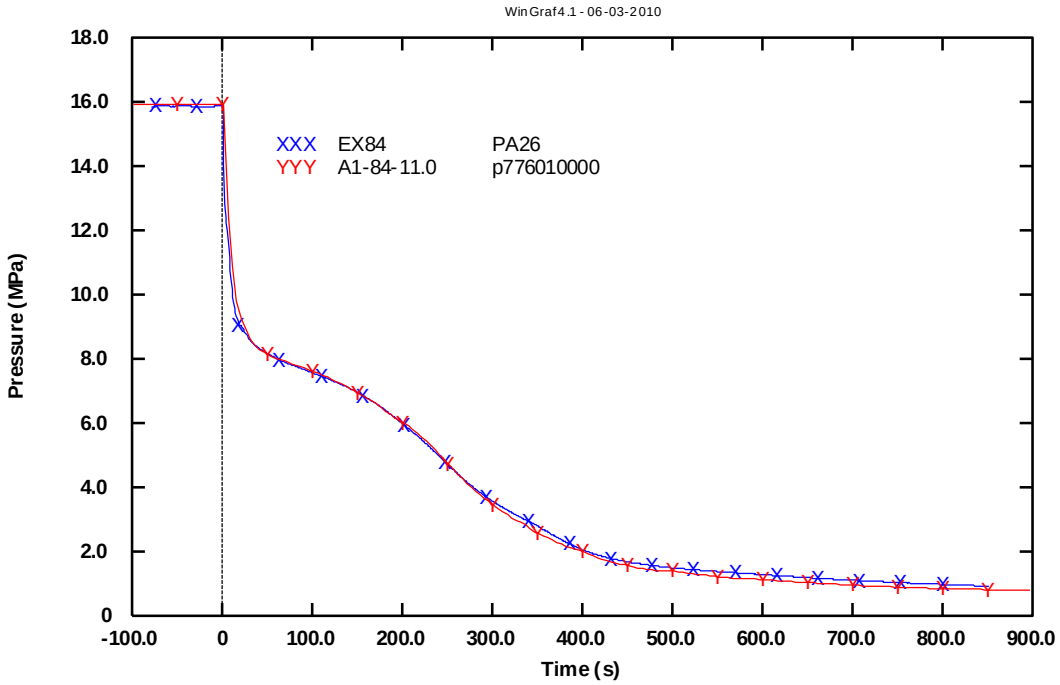

Fig. A - 15 – LOBI test A1-84: BL CL pressure.

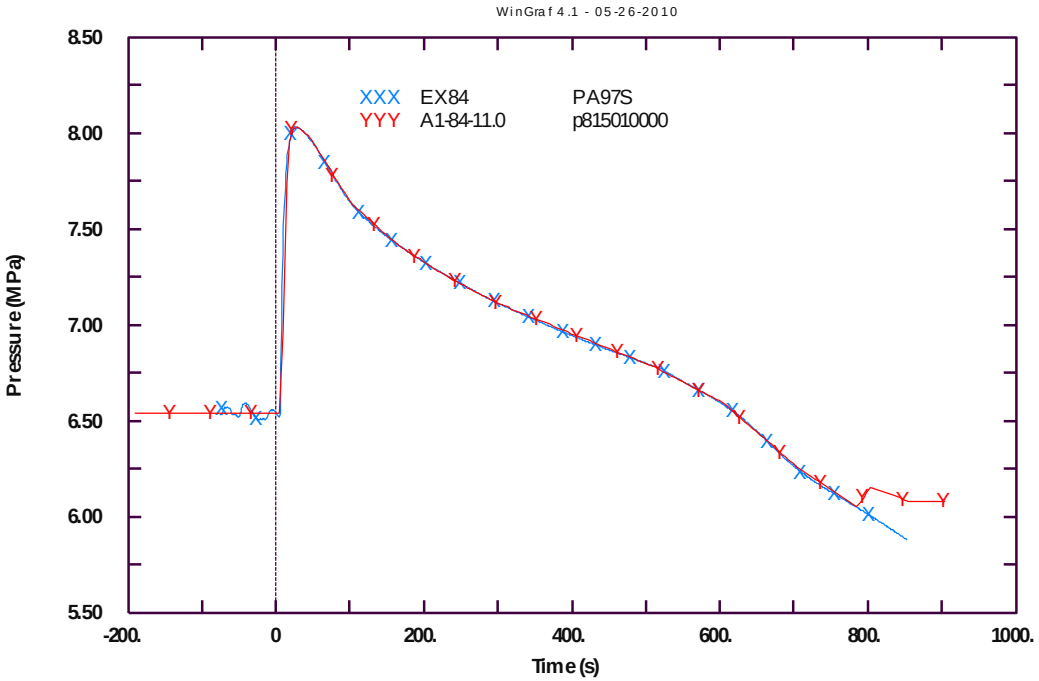

Fig. A - 16 – LOBI test A1-84: IL steam generator dome pressure.

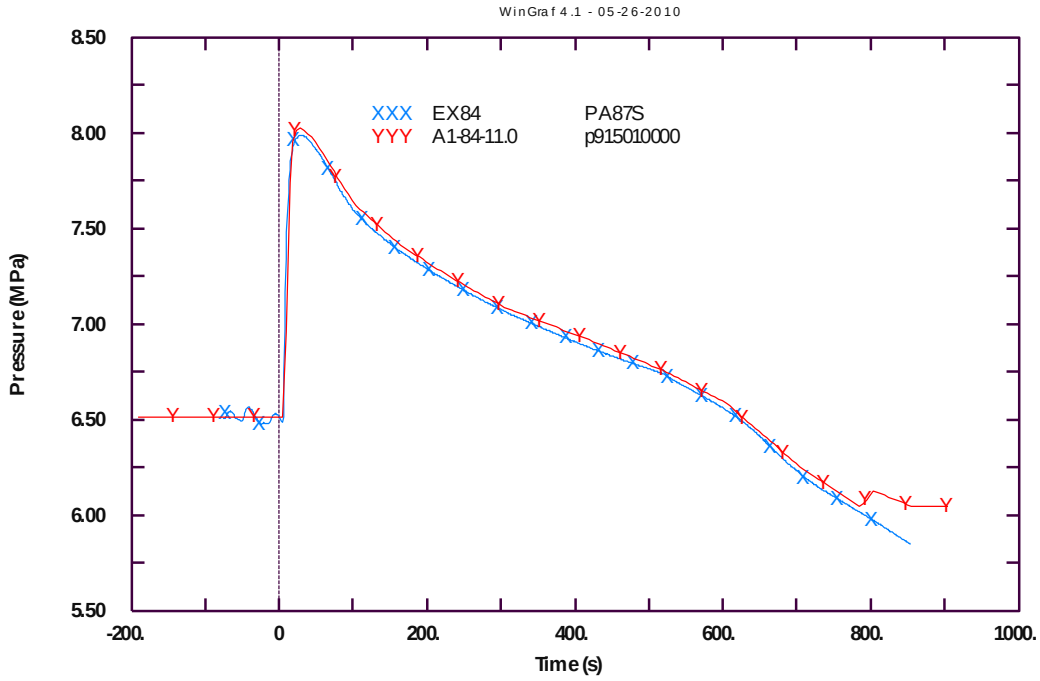

Fig. A - 17 – LOBI test A1-84: BL steam generator dome pressure.

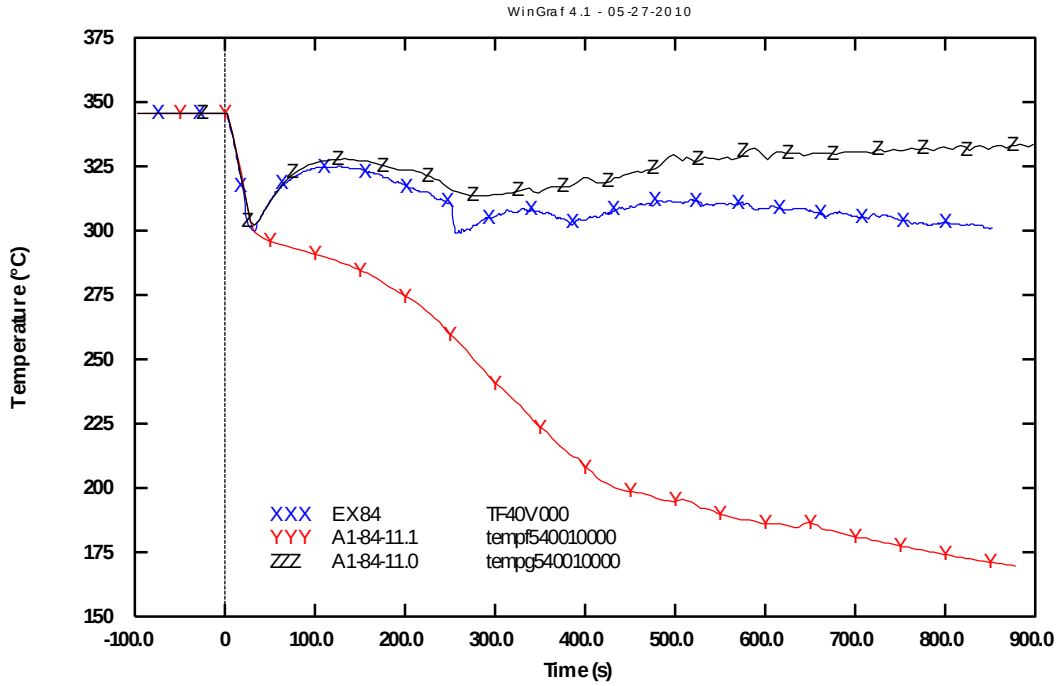

Fig. A - 18 – LOBI test A1-84: PRZ coolant temperature (liquid and vapor phase for calculated data).

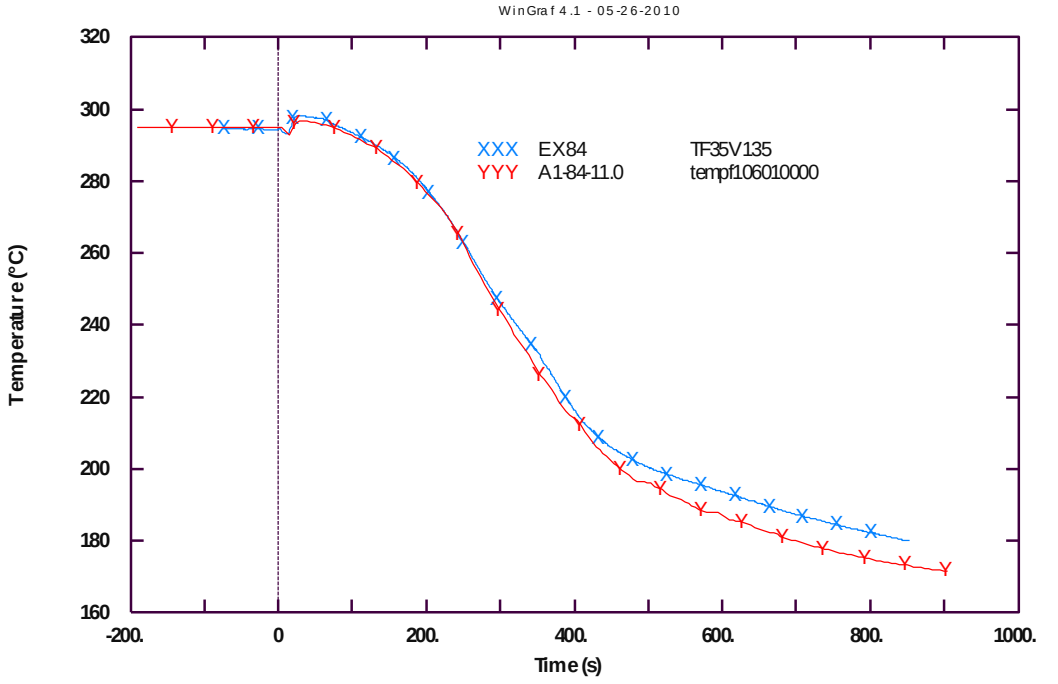

Fig. A - 19 – LOBI test A1-84: core inlet coolant temperature (LP).

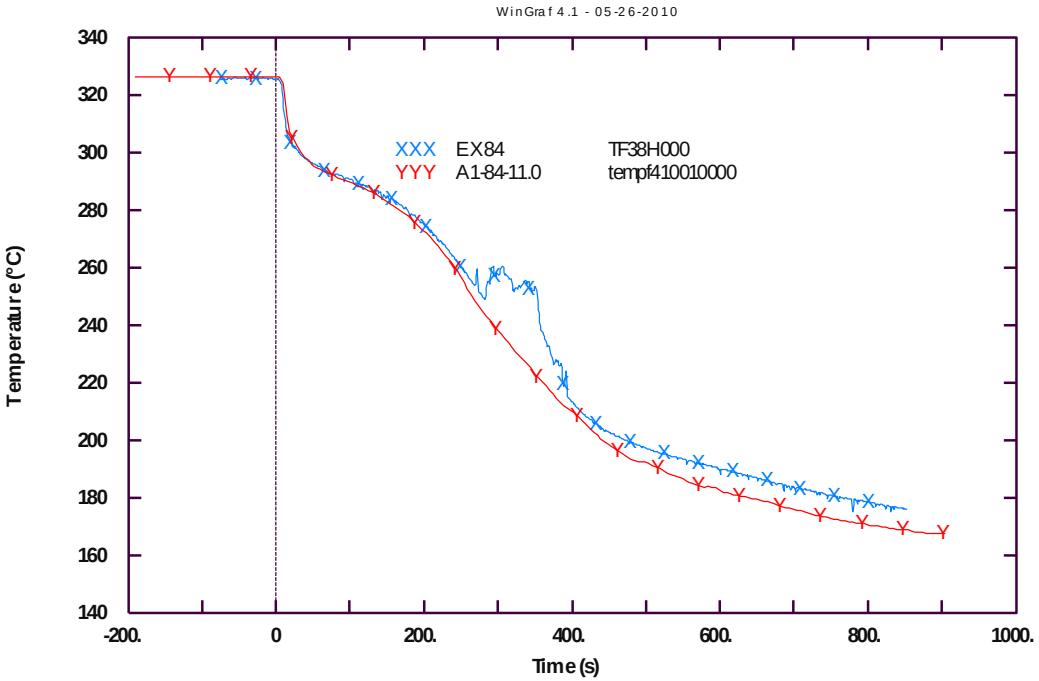

Fig. A - 20 – LOBI test A1-84: core outlet coolant temperature (UP).

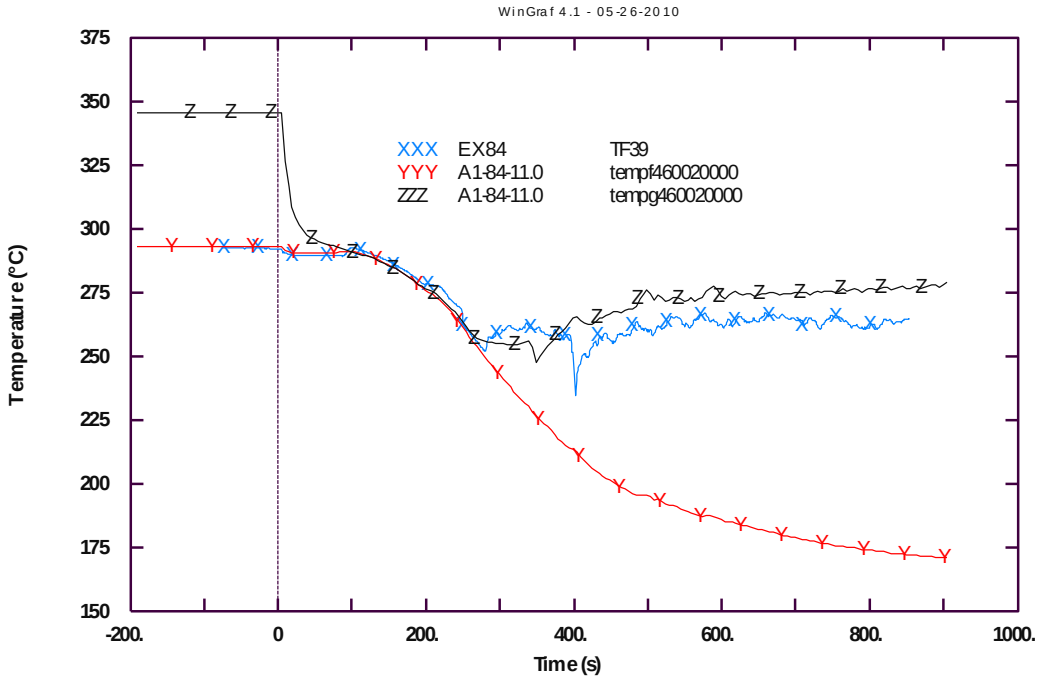

Fig. A - 21 – LOBI test A1-84: PRZ coolant temperature (liquid and vapor phase for calculated data).

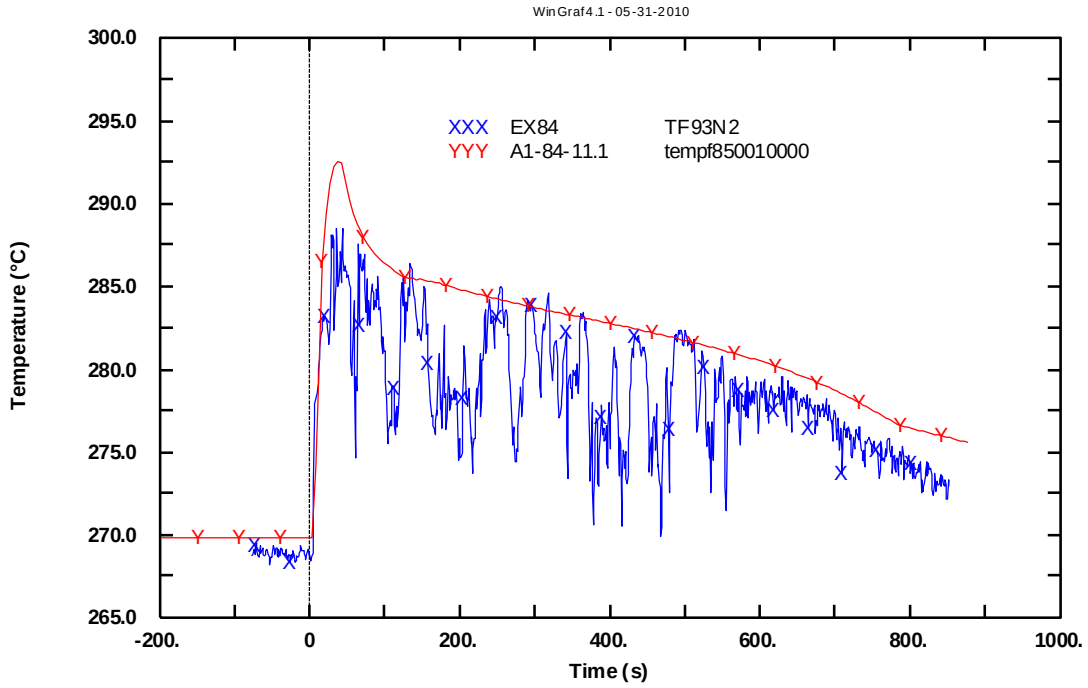

Fig. A - 22 – LOBI test A1-84: SG IL downcomer coolant temperature (upper part).

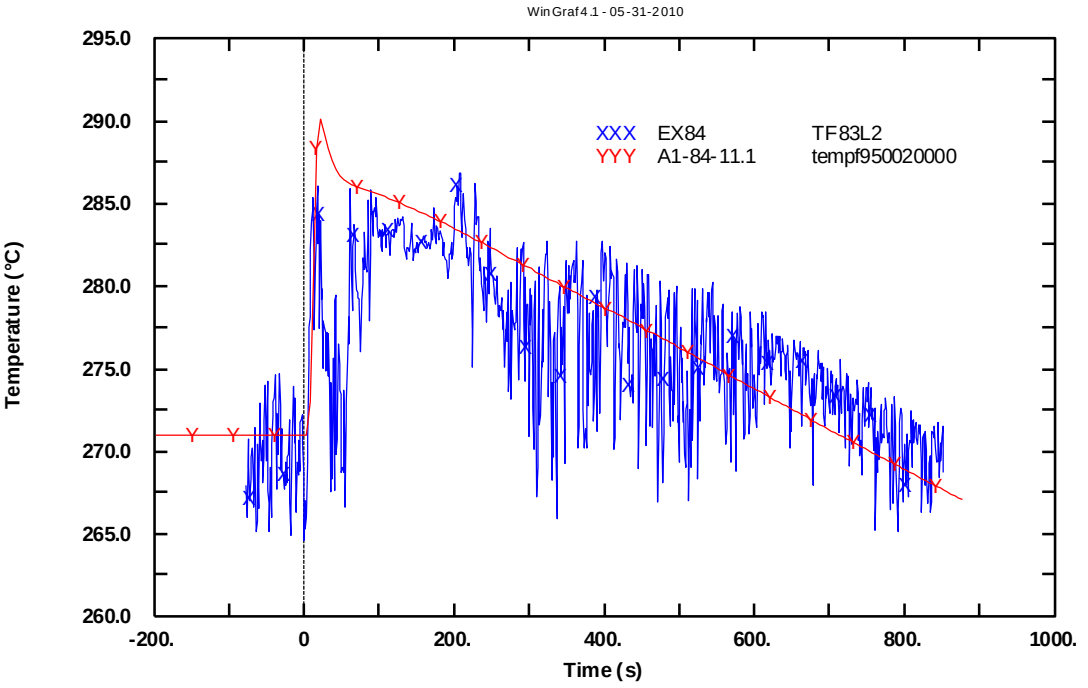

Fig. A - 23 – LOBI test A1-84: SG BL downcomer coolant temperature (upper part).

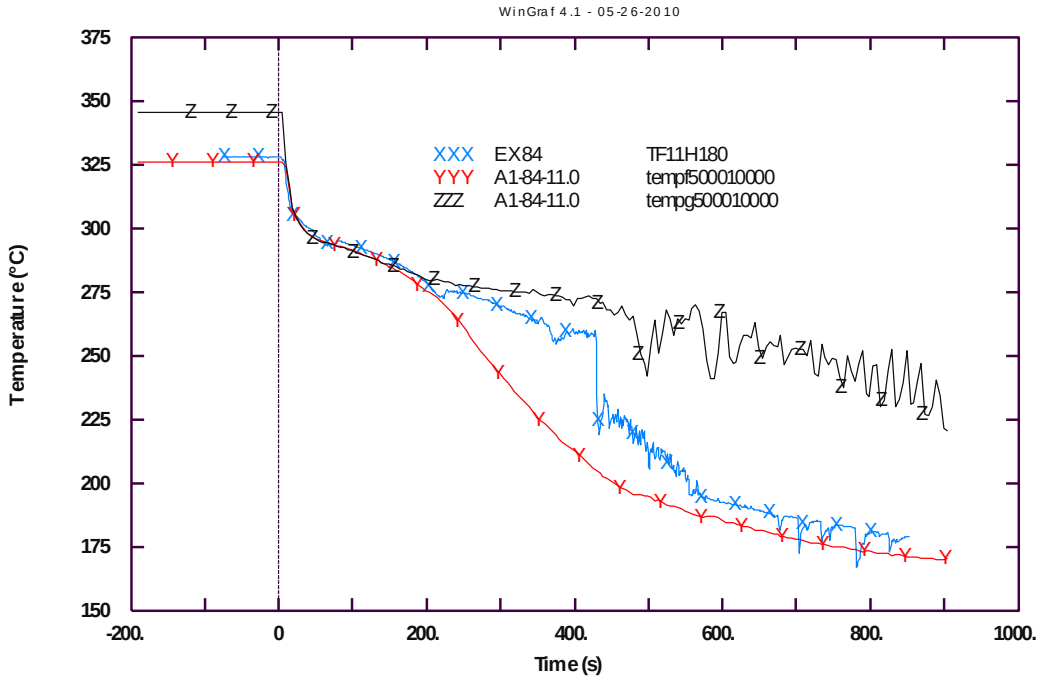

Fig. A - 24 – LOBI test A1-84: HL IL coolant temperature (liquid and vapor phase for calculated data).

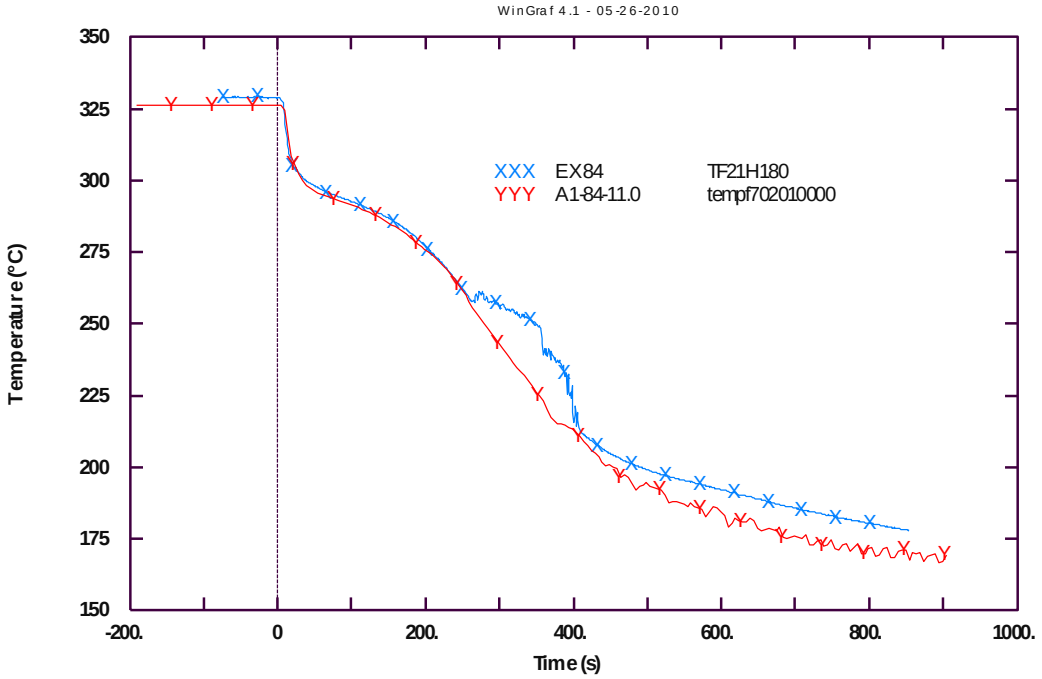

Fig. A - 25 – LOBI test A1-84: HL BL coolant temperature.

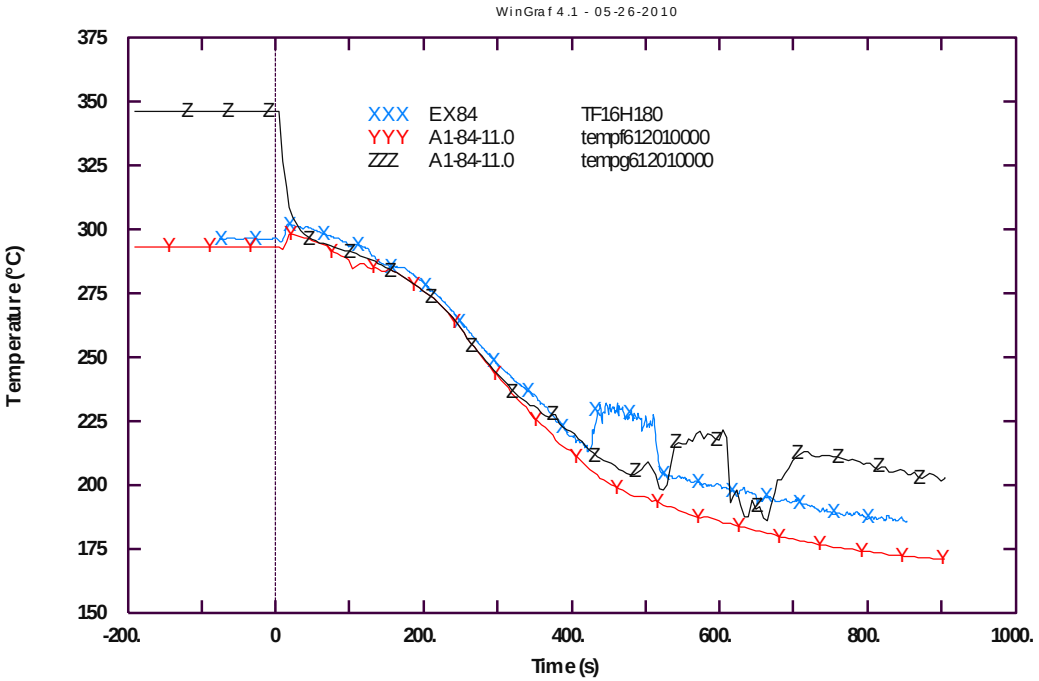

Fig. A - 26 – LOBI test A1-84: CL IL coolant temperature (liquid and vapor phase for calculated data).

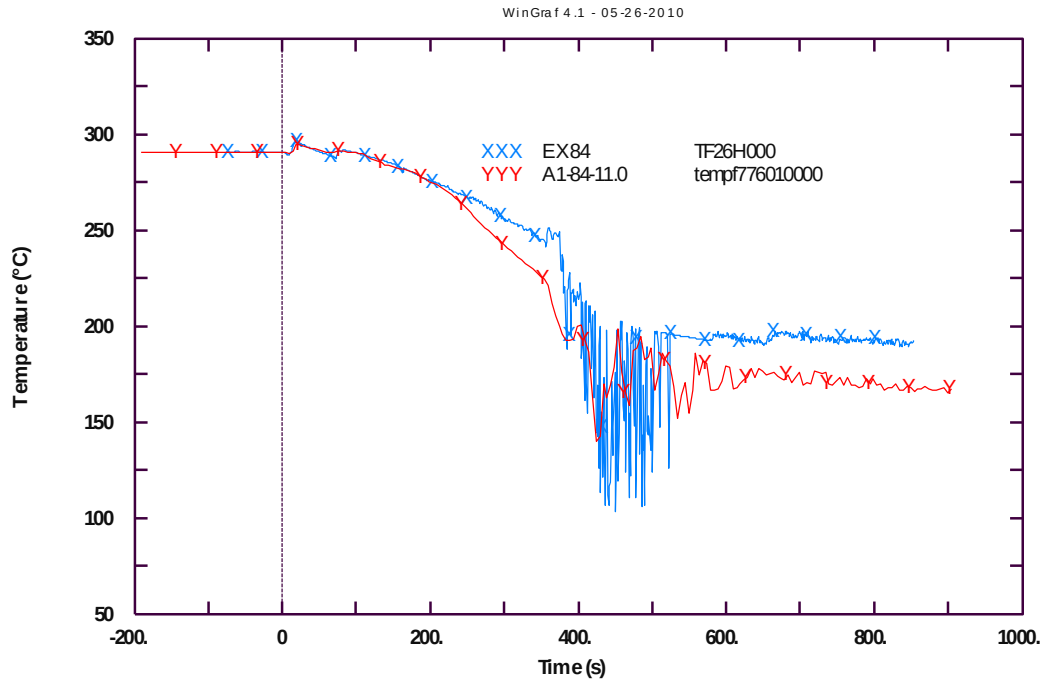

Fig. A - 27 – LOBI test A1-84: CL BL coolant temperature.

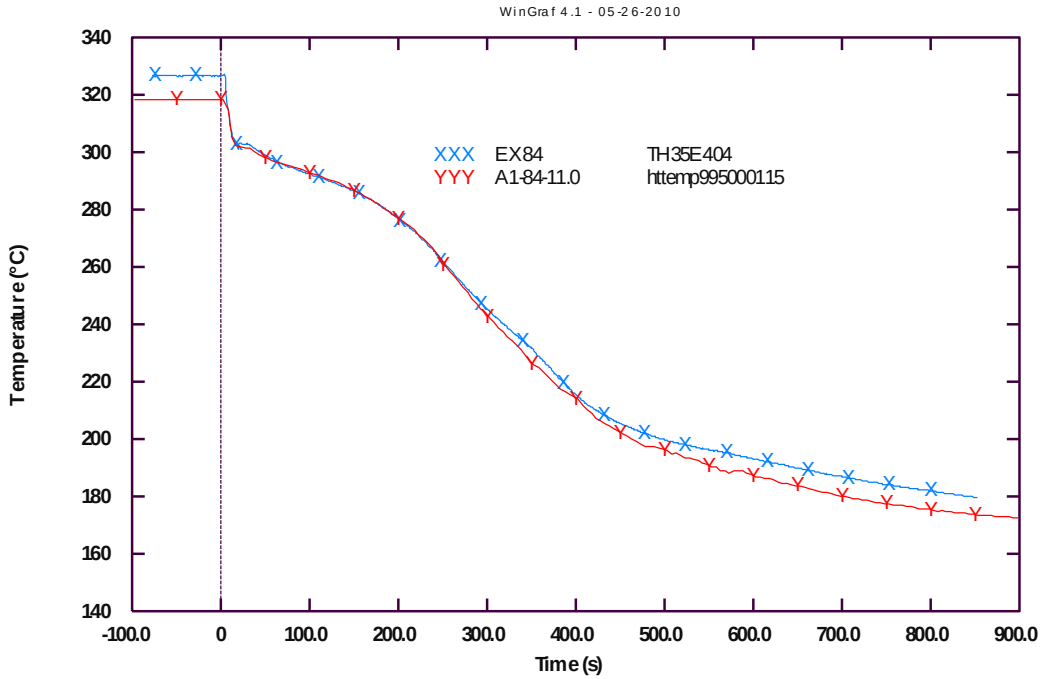

Fig. A - 28 – LOBI test A1-84: heated rod temperature, level 4 (bottom part).

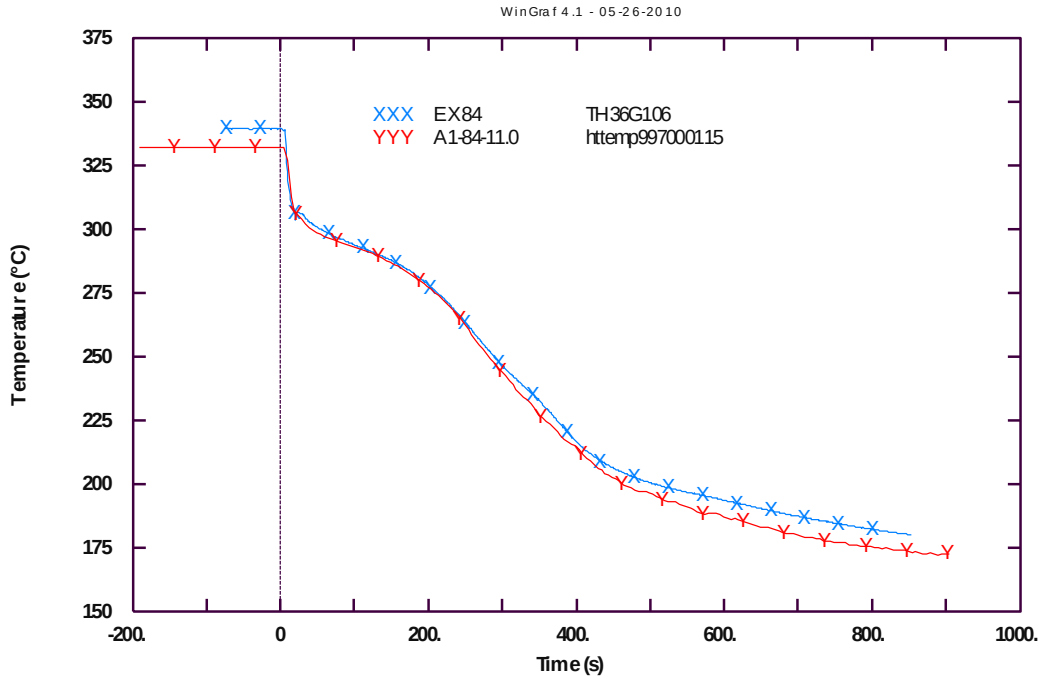

Fig. A - 29 – LOBI test A1-84: heated rod temperature, level 6 (middle part).

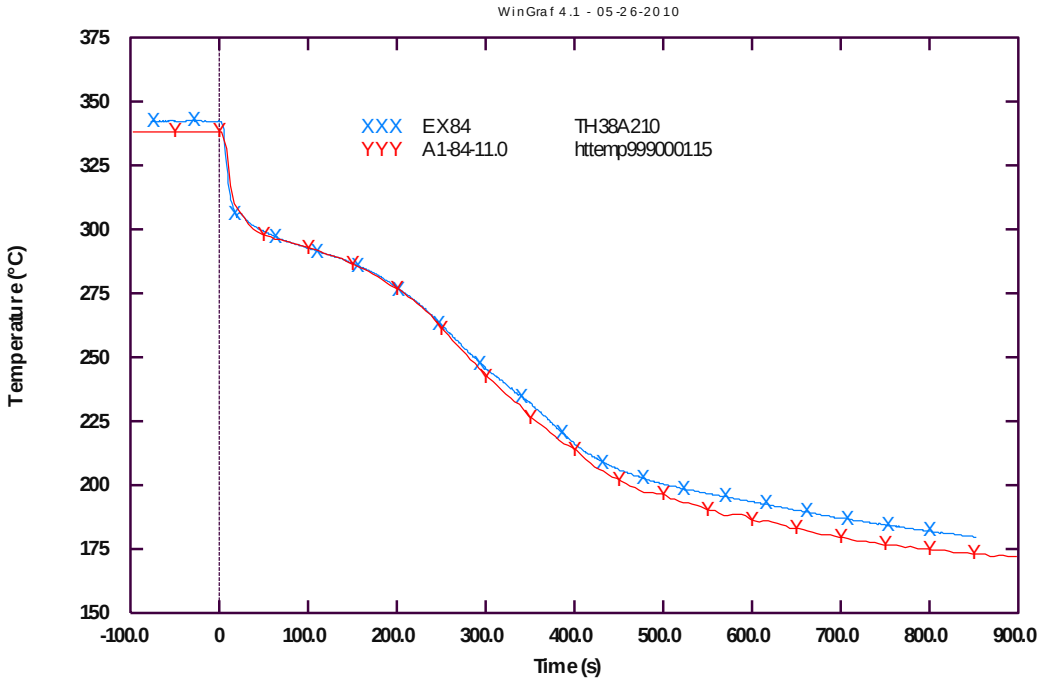

Fig. A - 30 – LOBI test A1-84: heated rod temperature, level 9 (top level).

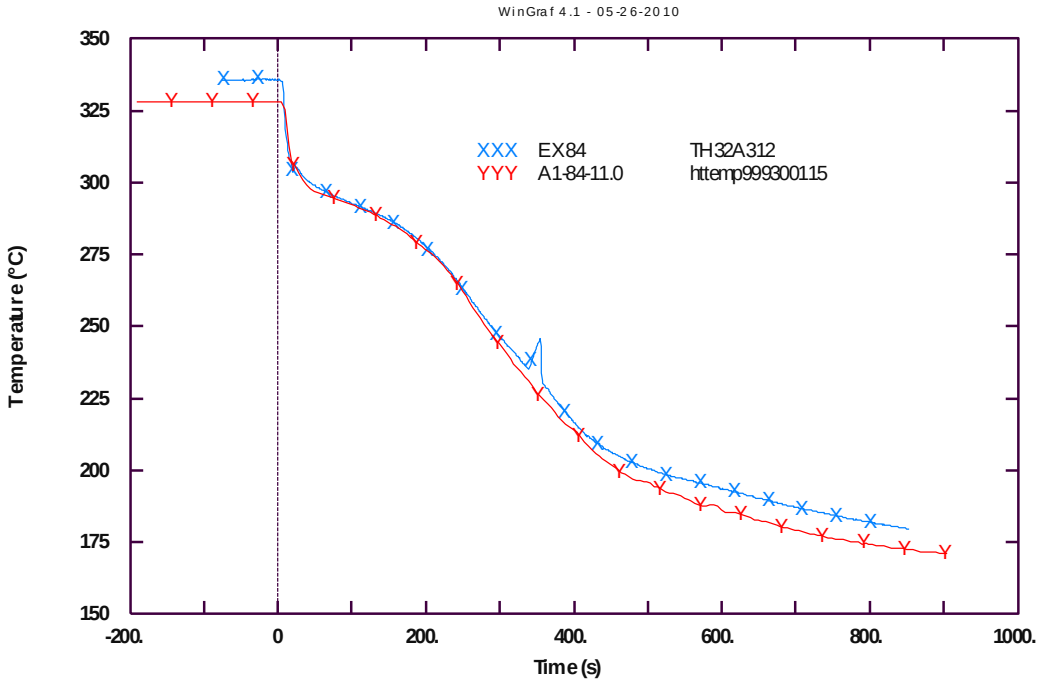

Fig. A - 31 – LOBI test A1-84: heated rod temperature, level 12 (top level).

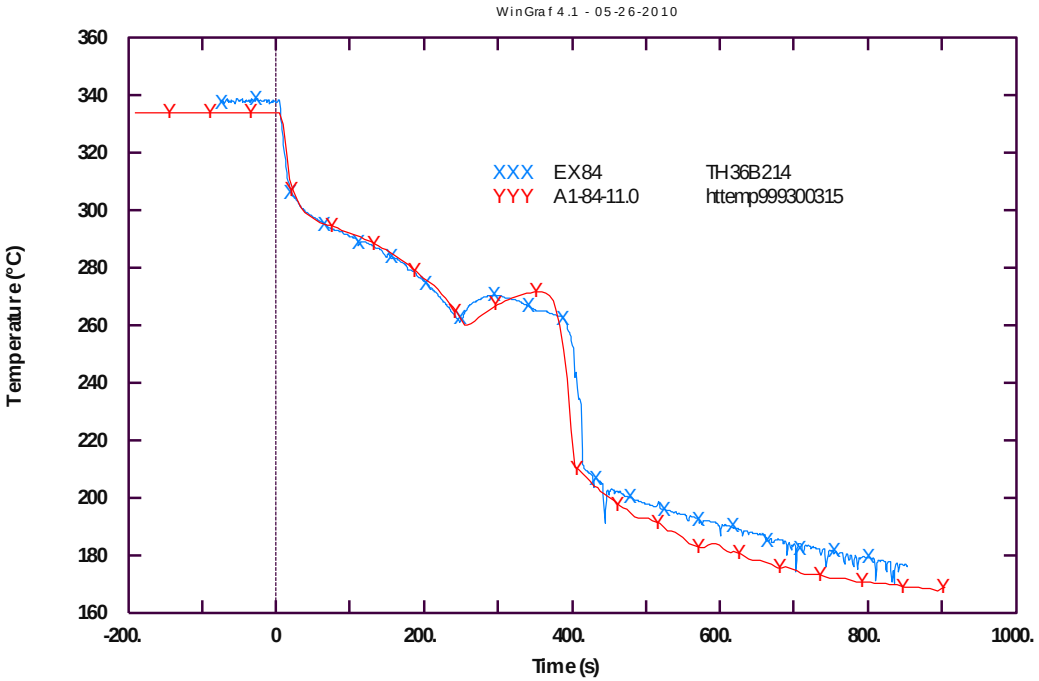

Fig. A - 32 – LOBI test A1-84: heat structure temperature, level 13 (UP).

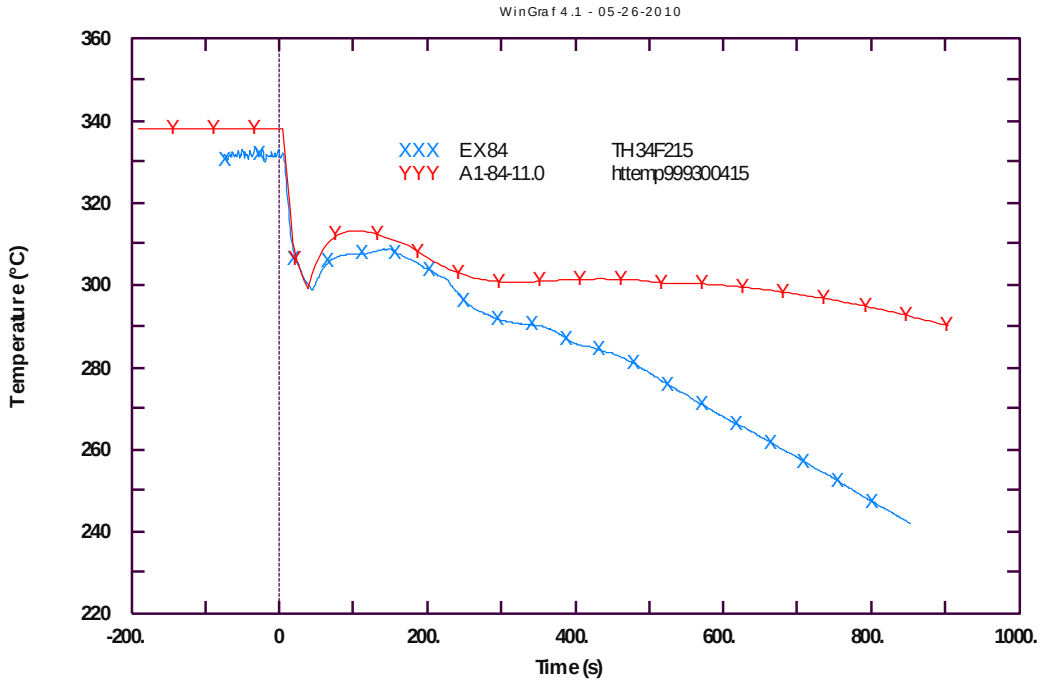

Fig. A - 33 – LOBI test A1-84: heat structure temperature, level 15 (UH).

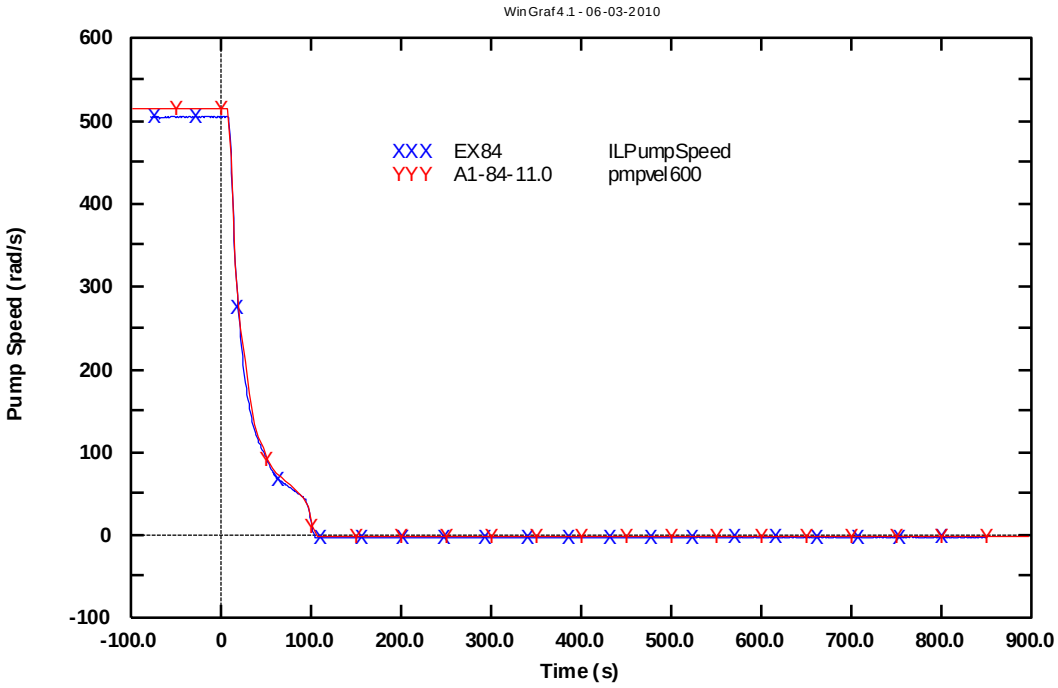

Fig. A - 34 – LOBI test A1-84: IL pump velocity.

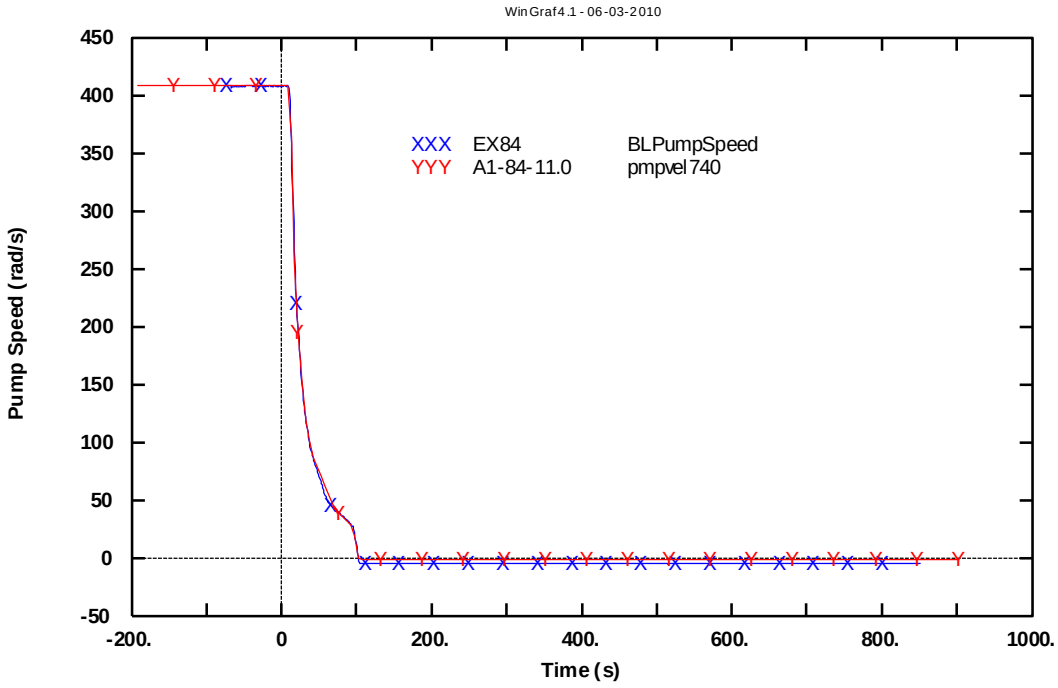

Fig. A - 35 – LOBI test A1-84:BLpump velocity.

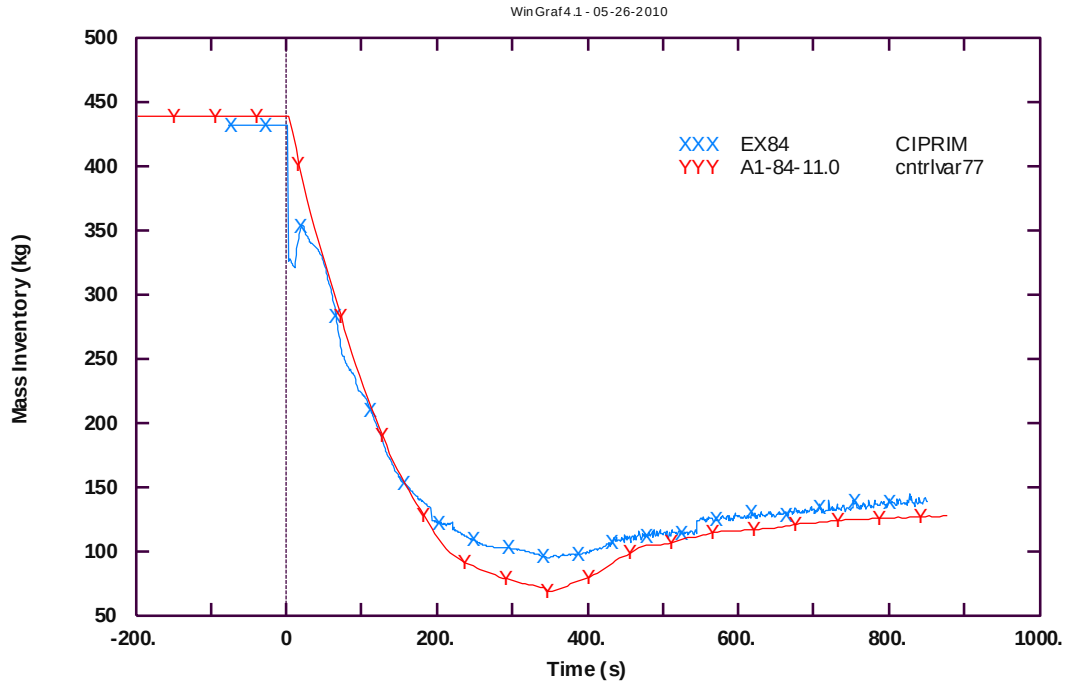

Fig. A - 36 – LOBI test A1-84: primary mass inventory.

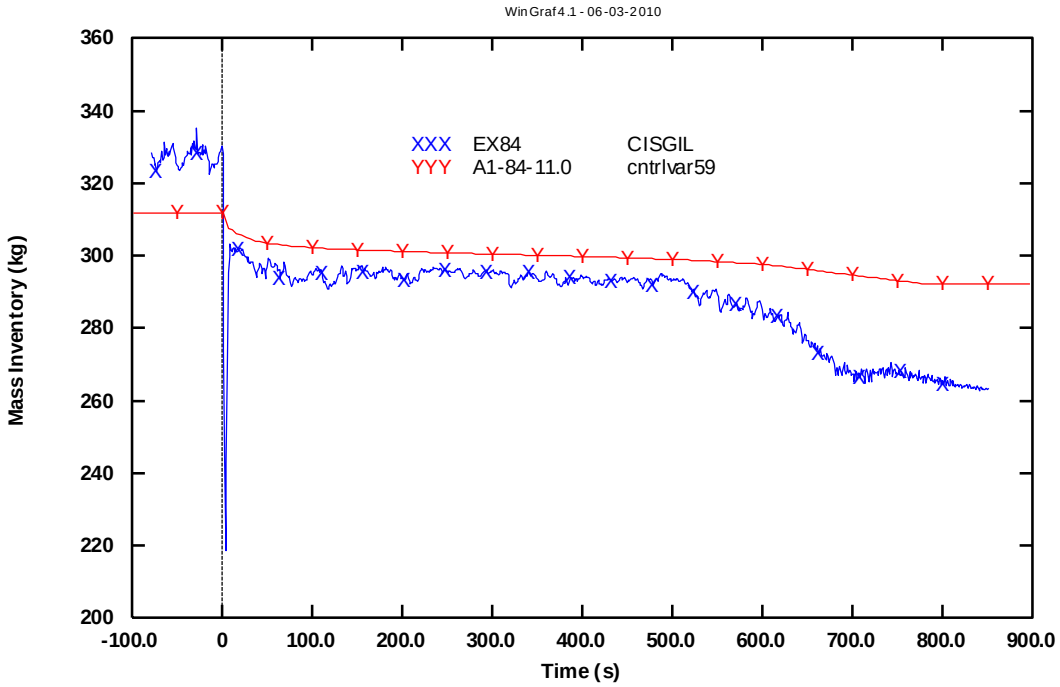

Fig. A - 37 – LOBI test A1-84: SG IL mass inventory.

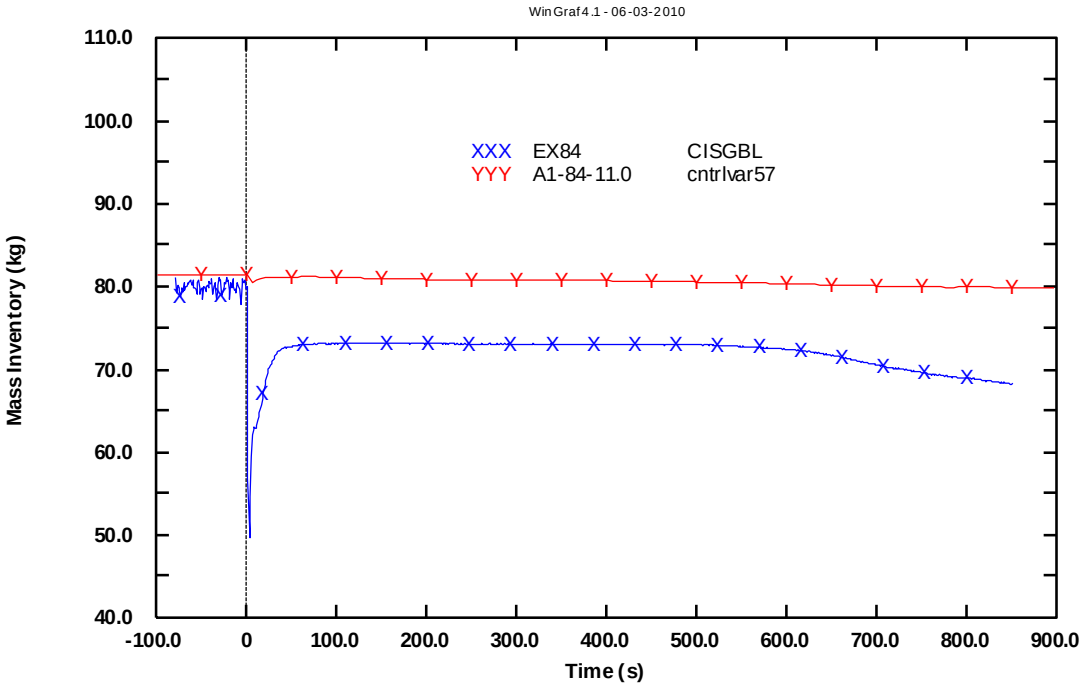

Fig. A - 38 – LOBI test A1-84: SG BL mass inventory.

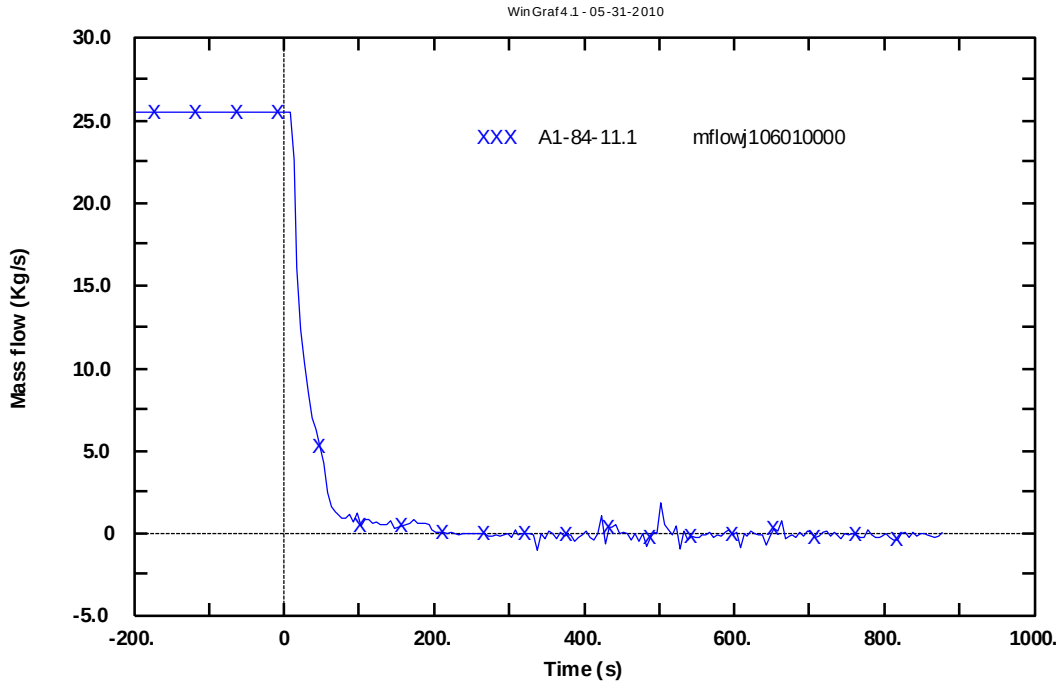

Fig. A - 39 – LOBI test A1-84: mass flow at core inlet.

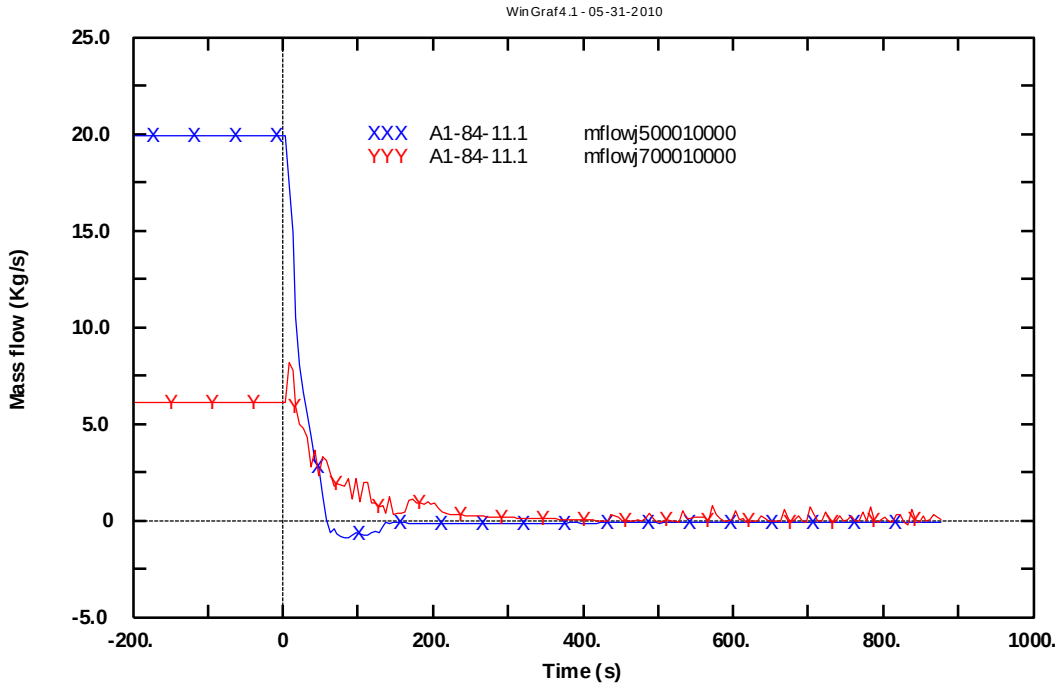

Fig. A - 40 – LOBI test A1-84: HL IL and BL mass flows.

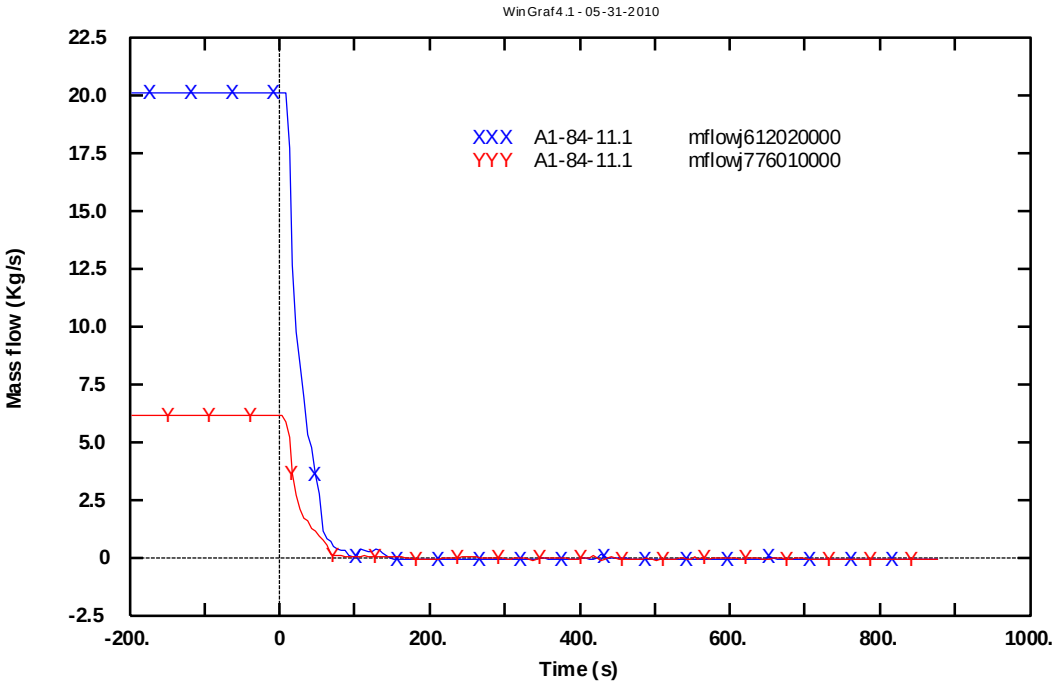

Fig. A - 41 – LOBI test A1-84: CL IL and BL mass flows.

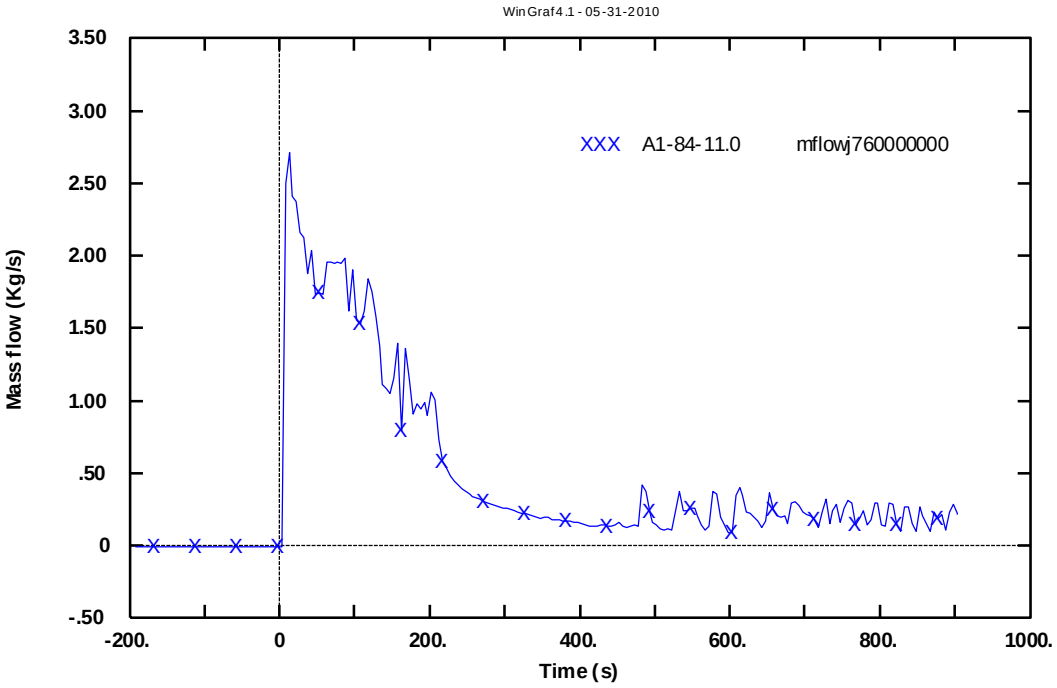

Fig. A - 42 – LOBI test A1-84: break mass flow rate.

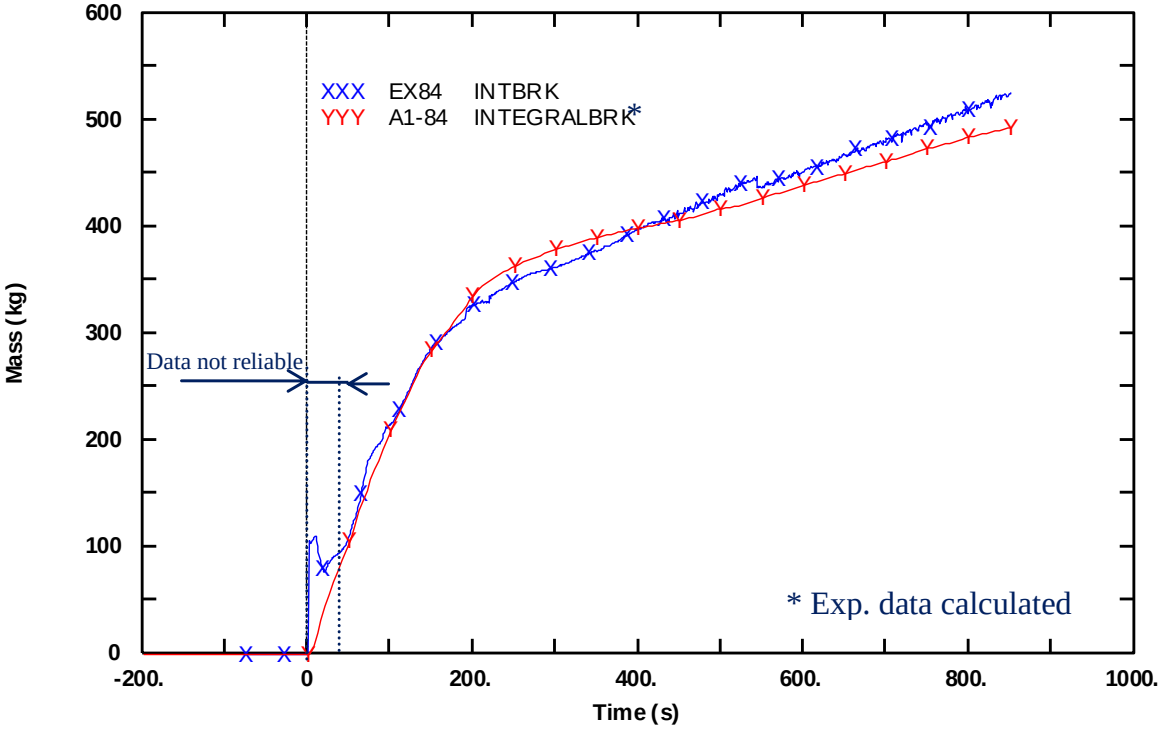

Fig. A - 43 – LOBI test A1-84: integral break mass flow rate.

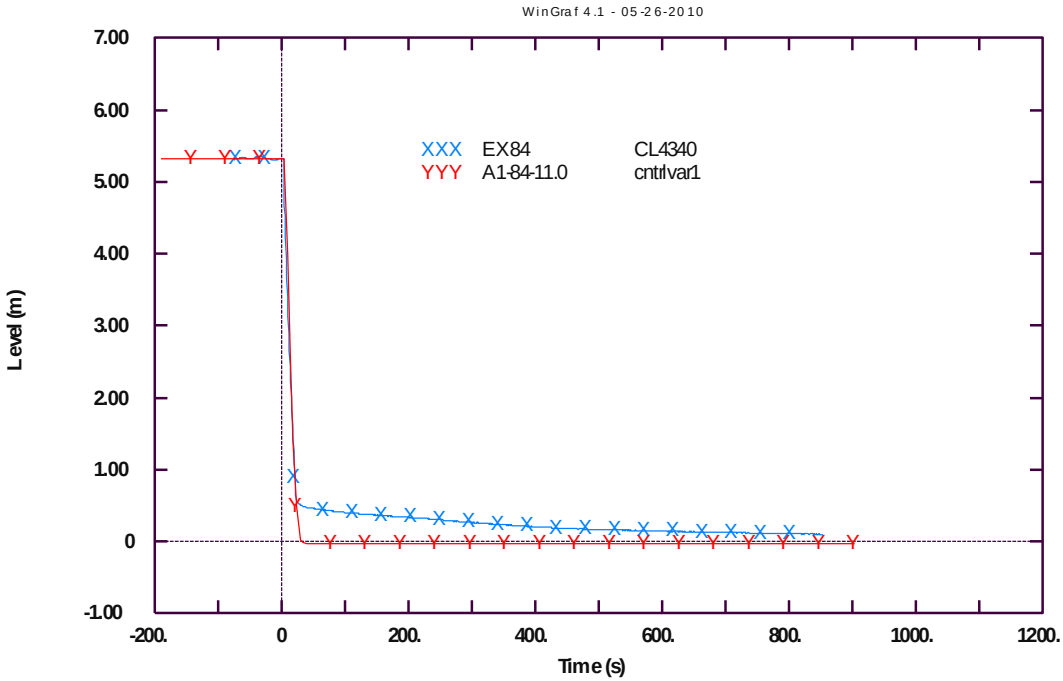

Fig. A - 44 – LOBI test A1-84: PRZ level.

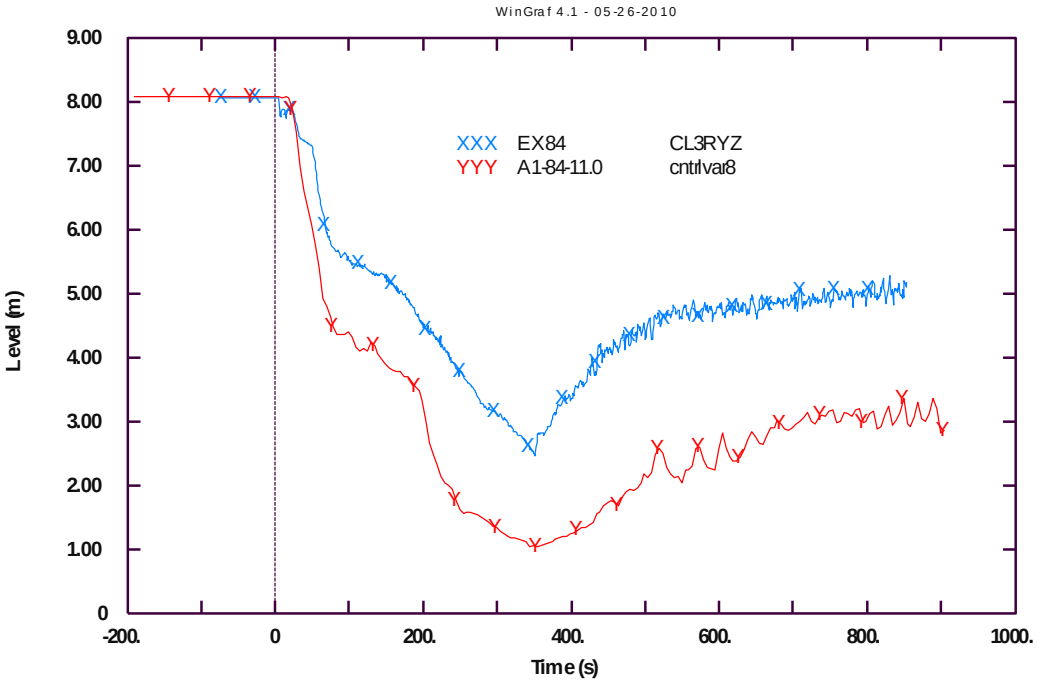

Fig. A - 45 – LOBI test A1-84: RPV collapsed level.

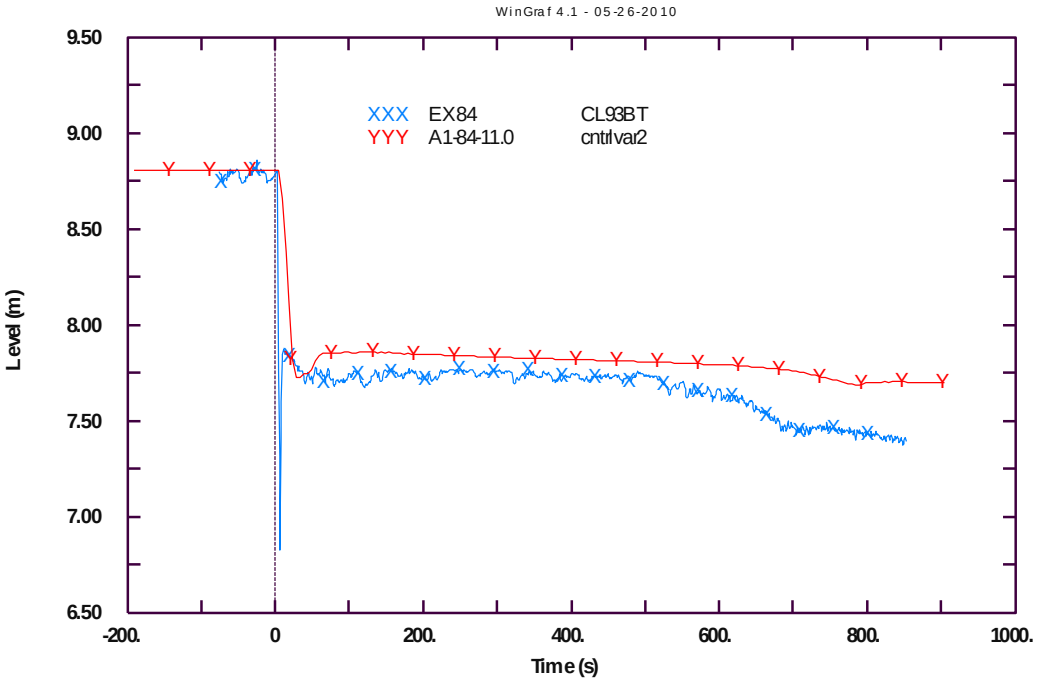

Fig. A - 46 – LOBI test A1-84: SG DC IL level.

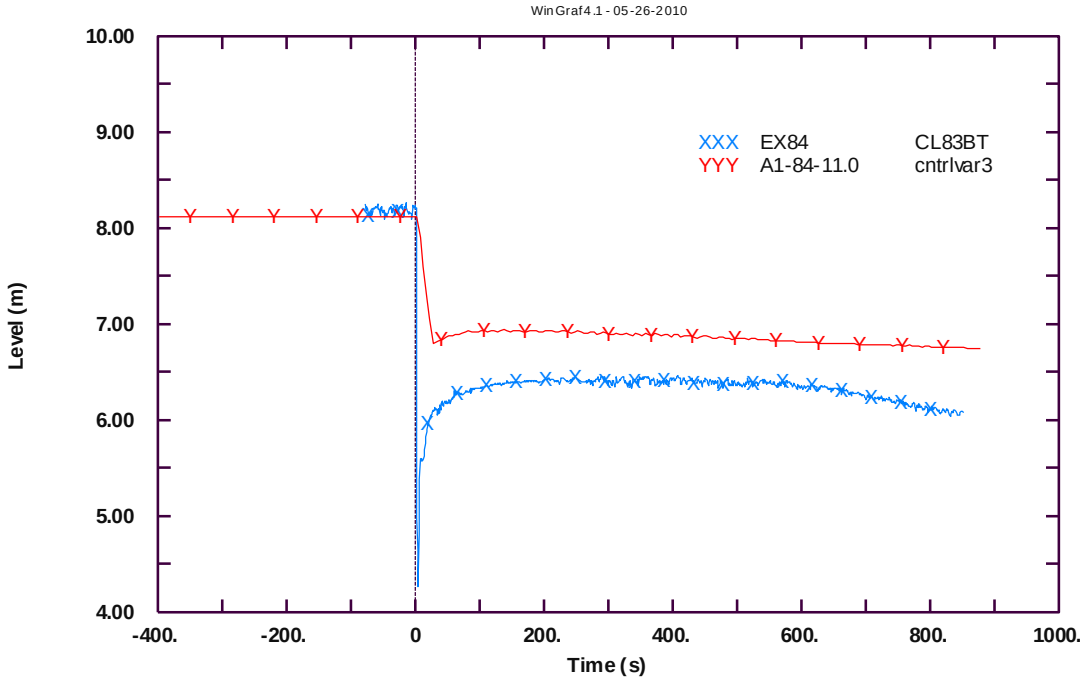

Fig. A - 47 – LOBI test A1-84: SG DC BL level.

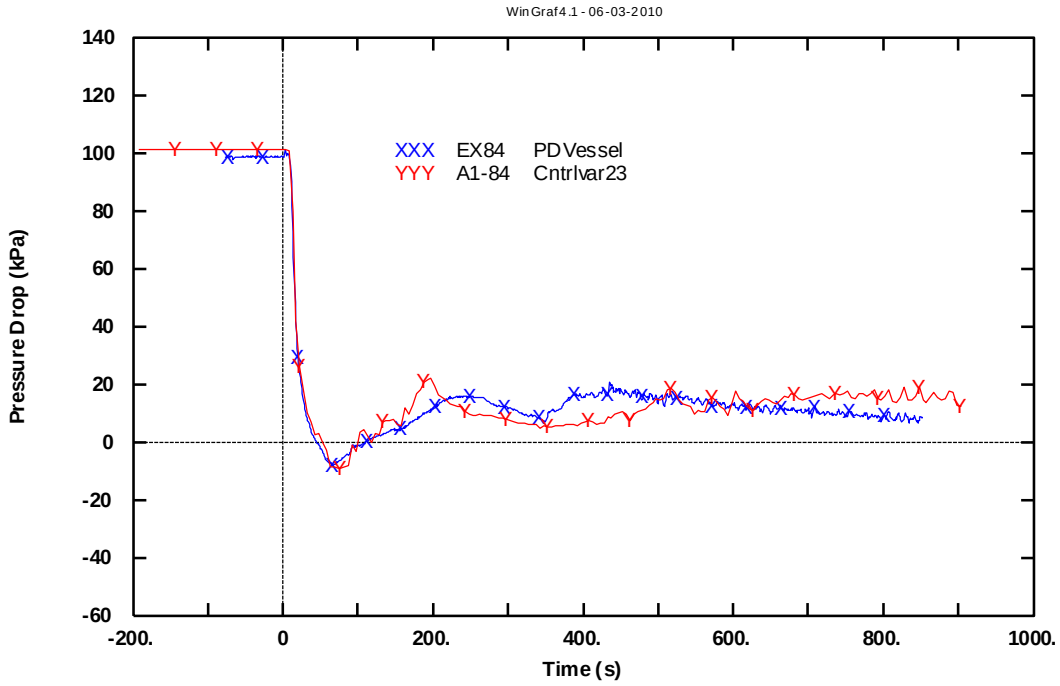

Fig. A - 48 – LOBI test A1-84: RPV pressure drop.

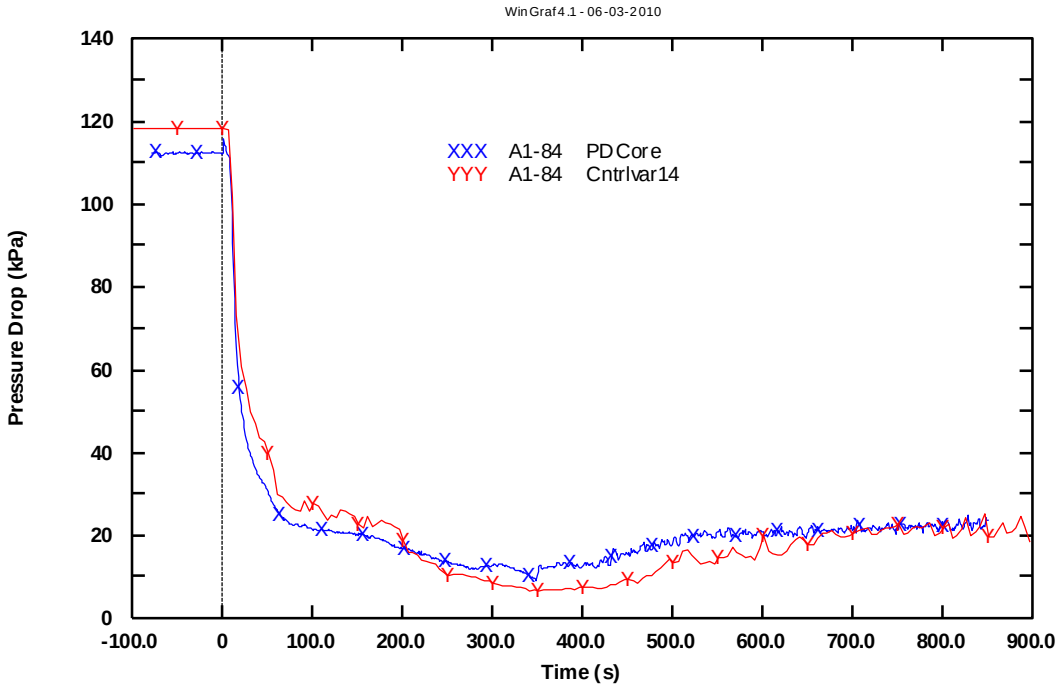

Fig. A - 49 – LOBI test A1-84: core pressure drop.

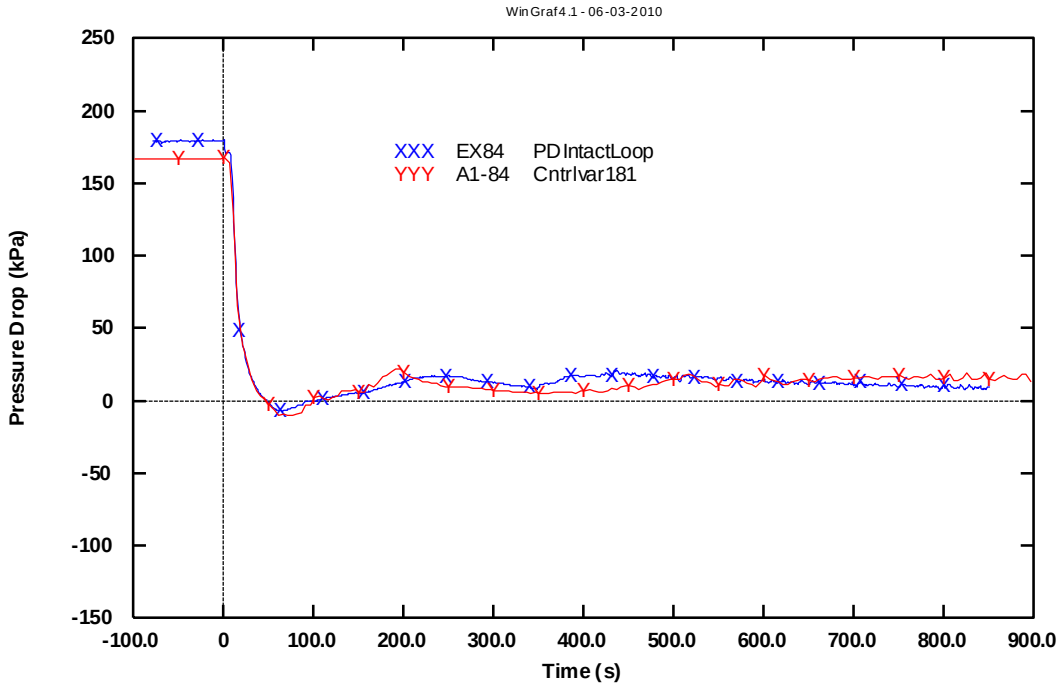

Fig. A - 50 – LOBI test A1-84: IL pressure drop.

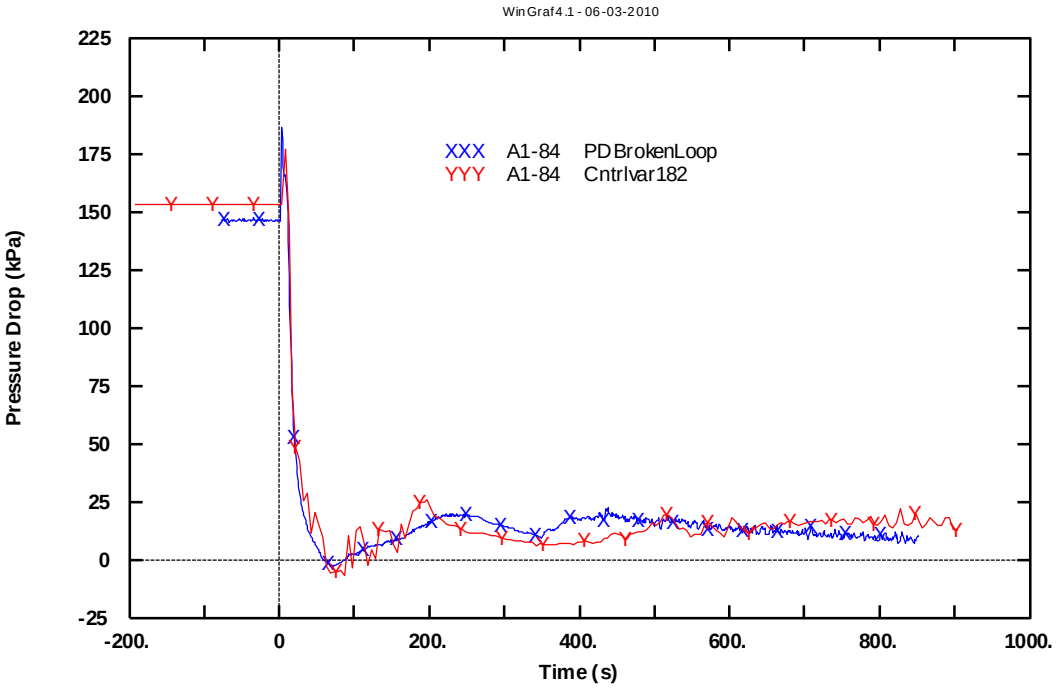

Fig. A - 51 – LOBI test A1-84: BL pressure drop.

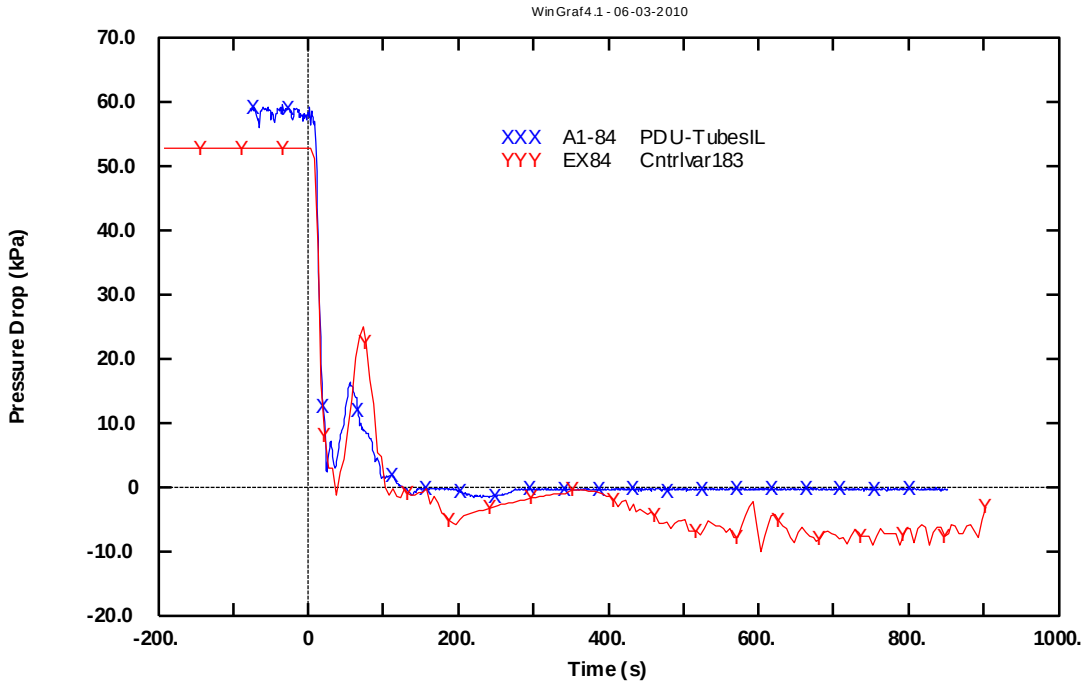

Fig. A - 52 – LOBI test A1-84: IL U-tubes pressure drop (primary side).

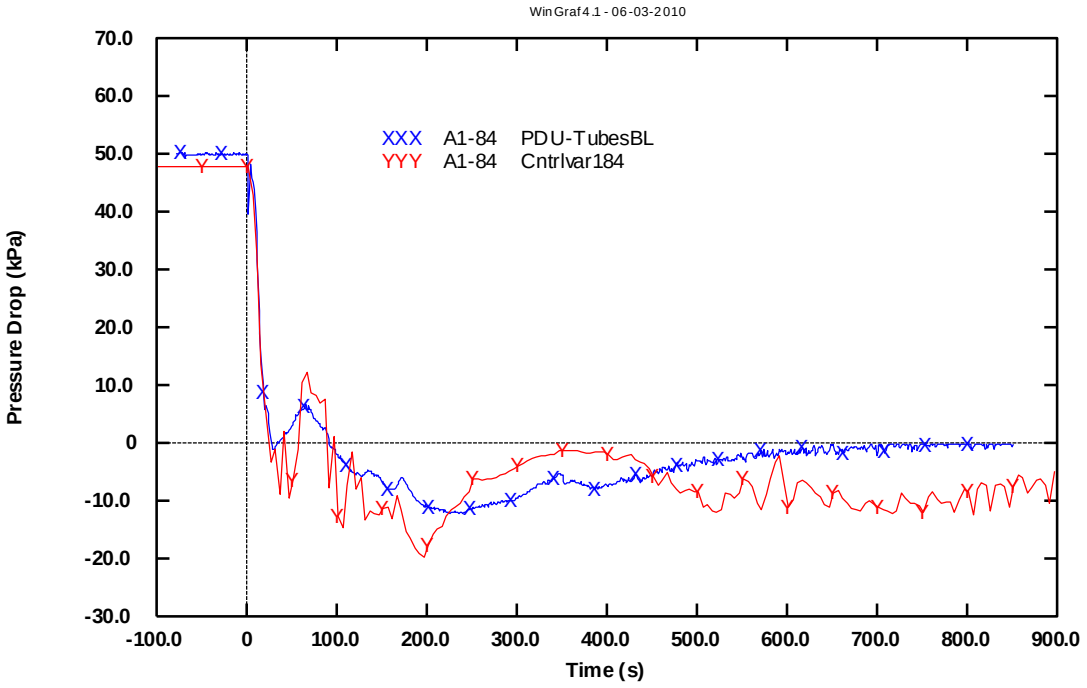

Fig. A - 53 – LOBI test A1-84: BL U-tubes pressure drop (primary side).

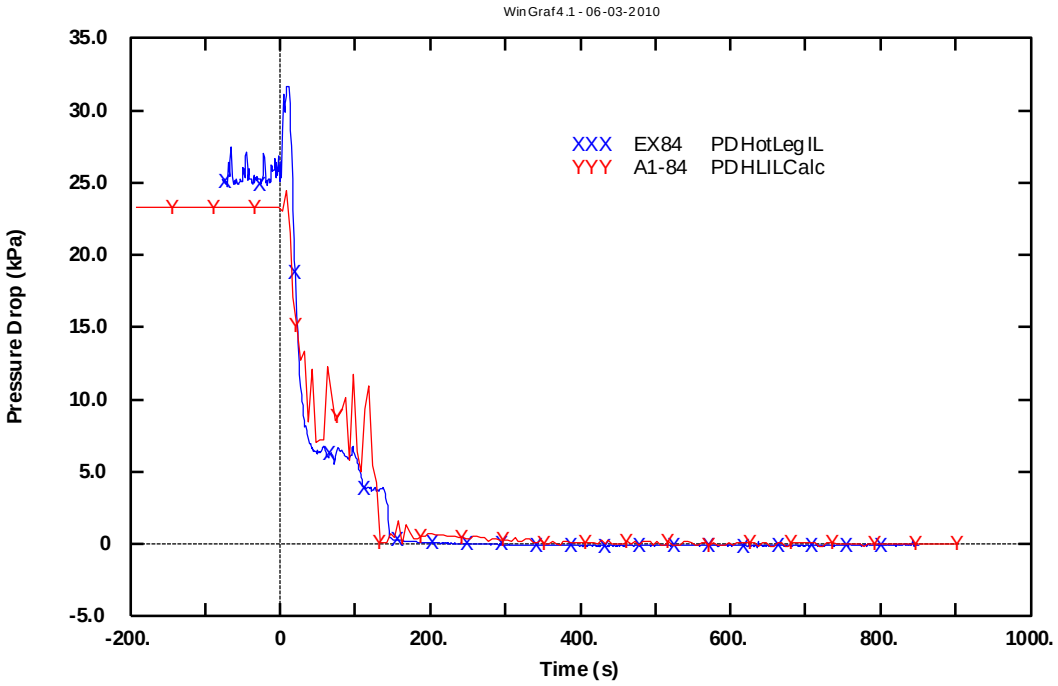

Fig. A - 54 – LOBI test A1-84: HL IL pressure drops.

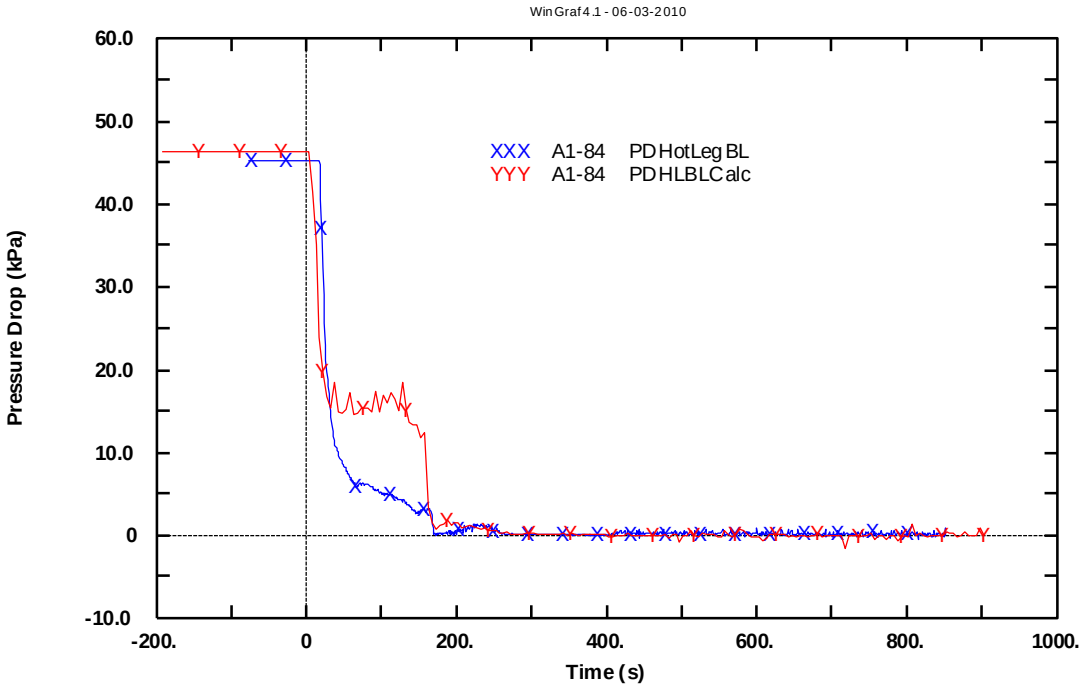

Fig. A - 55 – LOBI test A1-84: HL BL pressure drops.

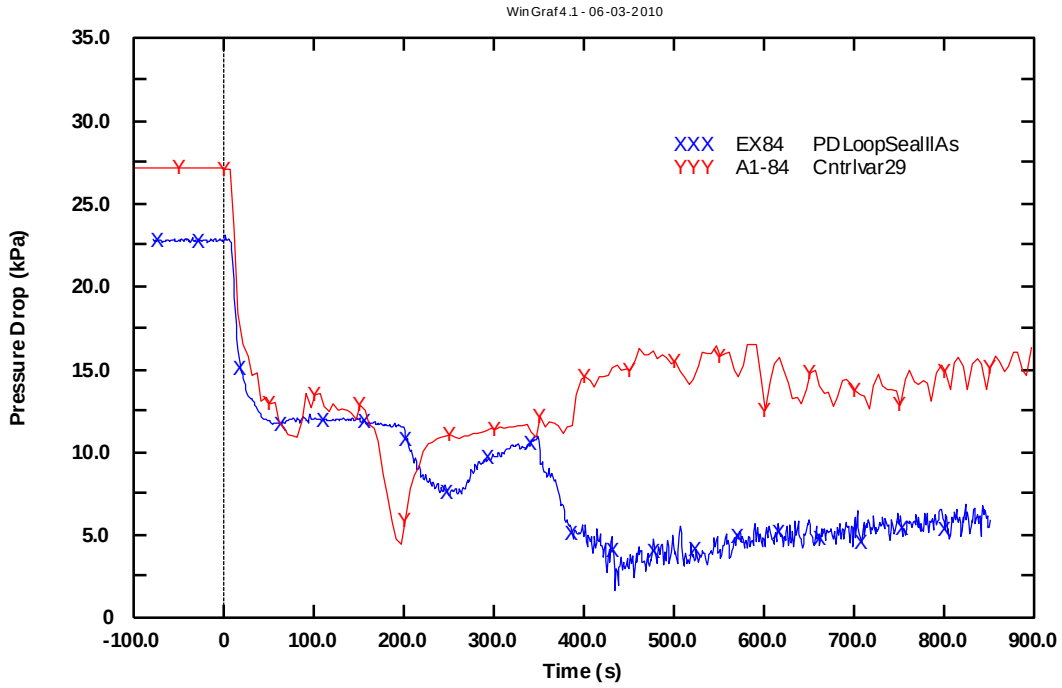

Fig. A - 56 – LOBI test A1-84: loop seal IL ascending side pressure drops.

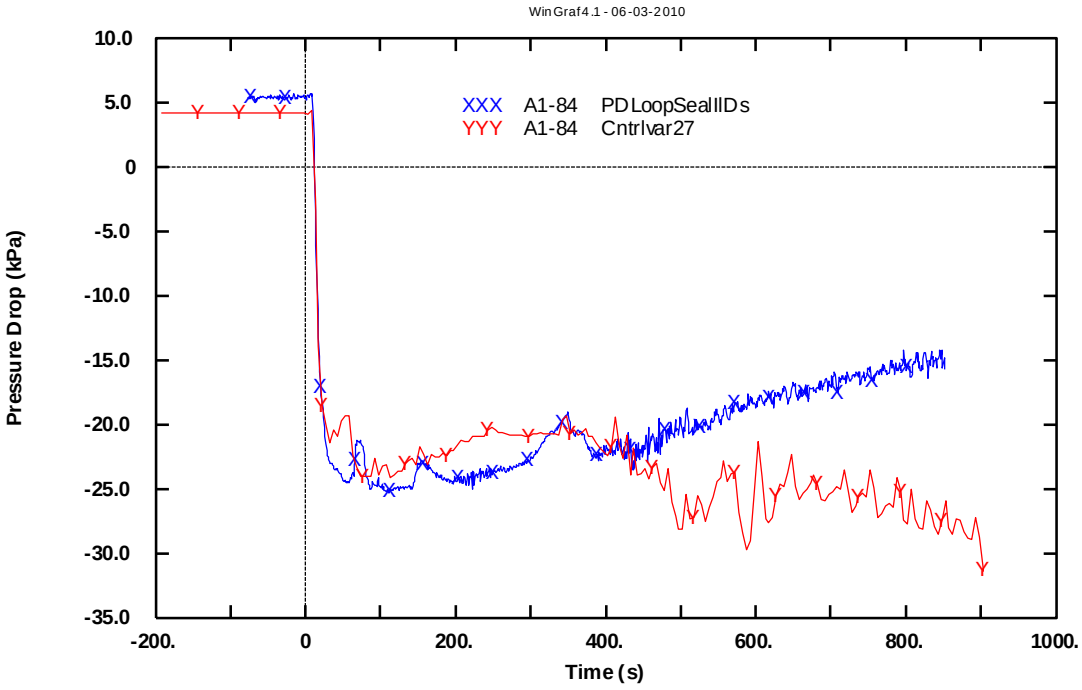

Fig. A - 57 – LOBI test A1-84: loop seal IL descending side pressure drops.

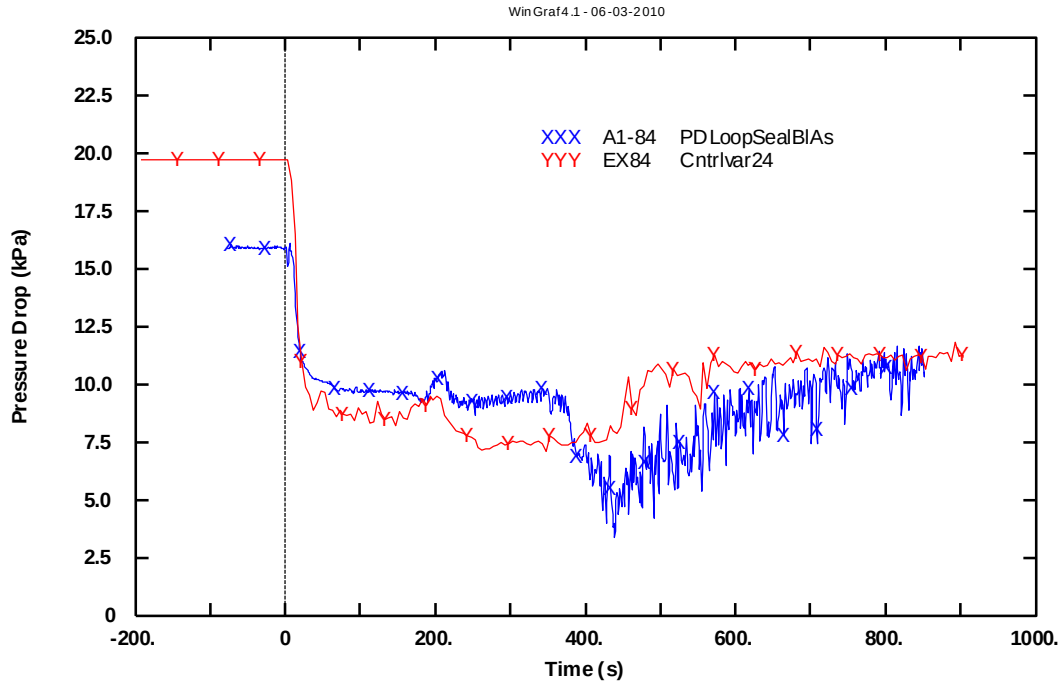

Fig. A - 58 – LOBI test A1-84: loop seal BL ascending side pressure drops.

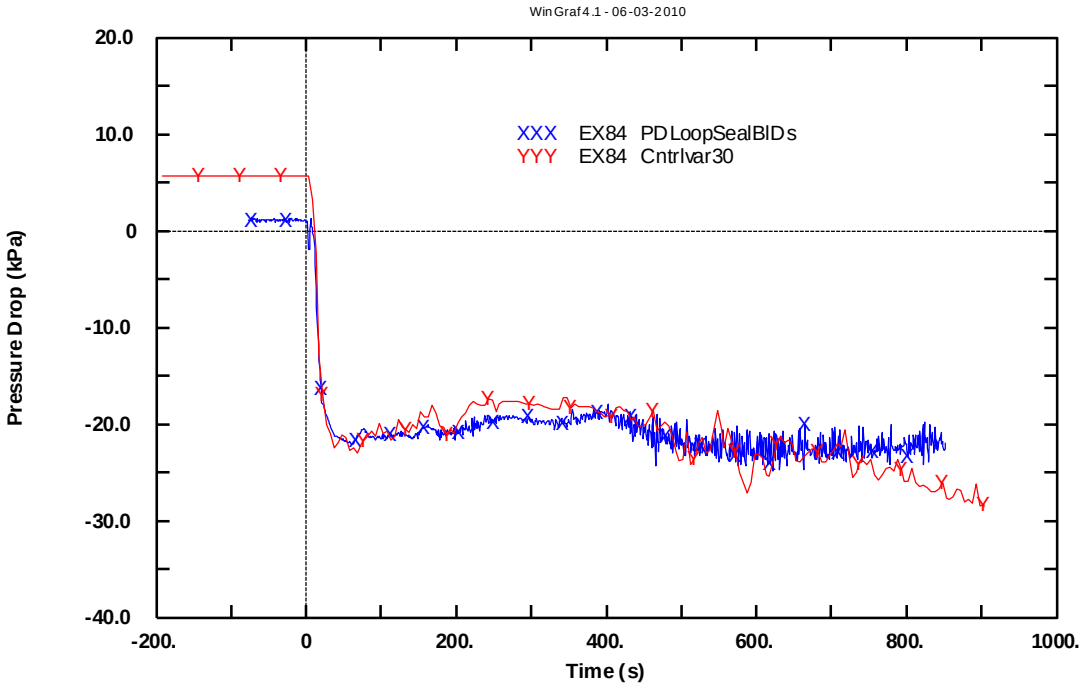

Fig. A - 59 – LOBI test A1-84: loop seal BL descending side pressure drops.

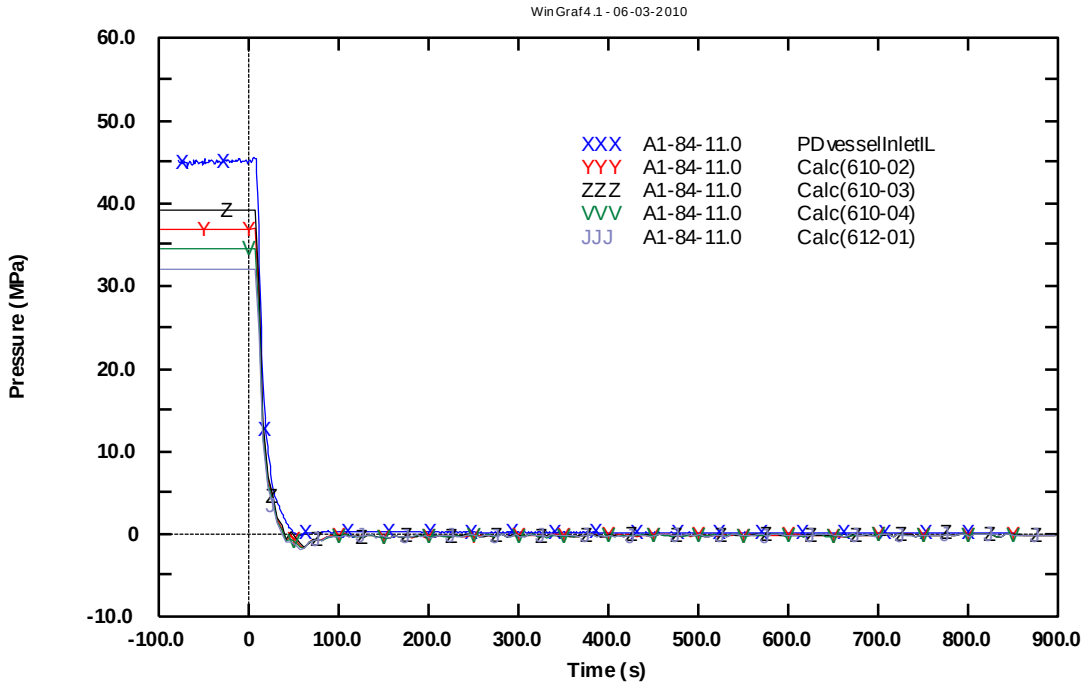

Fig. A - 60 – LOBI test A1-84: pressure drop at vessel inlet.

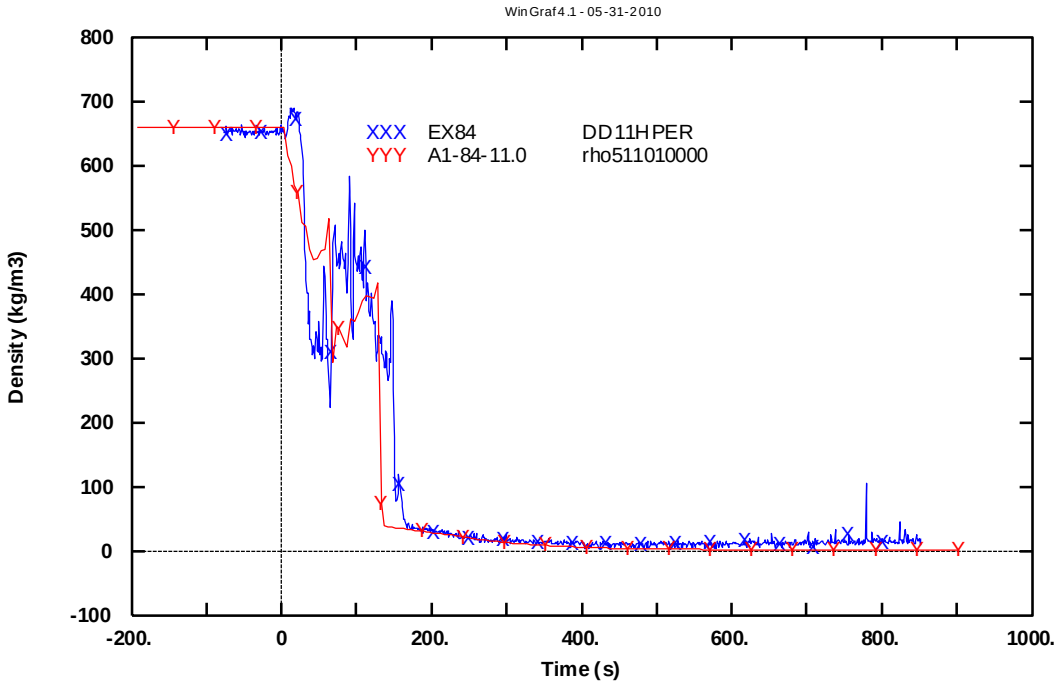

Fig. A - 61 – LOBI test A1-84:HL IL density.

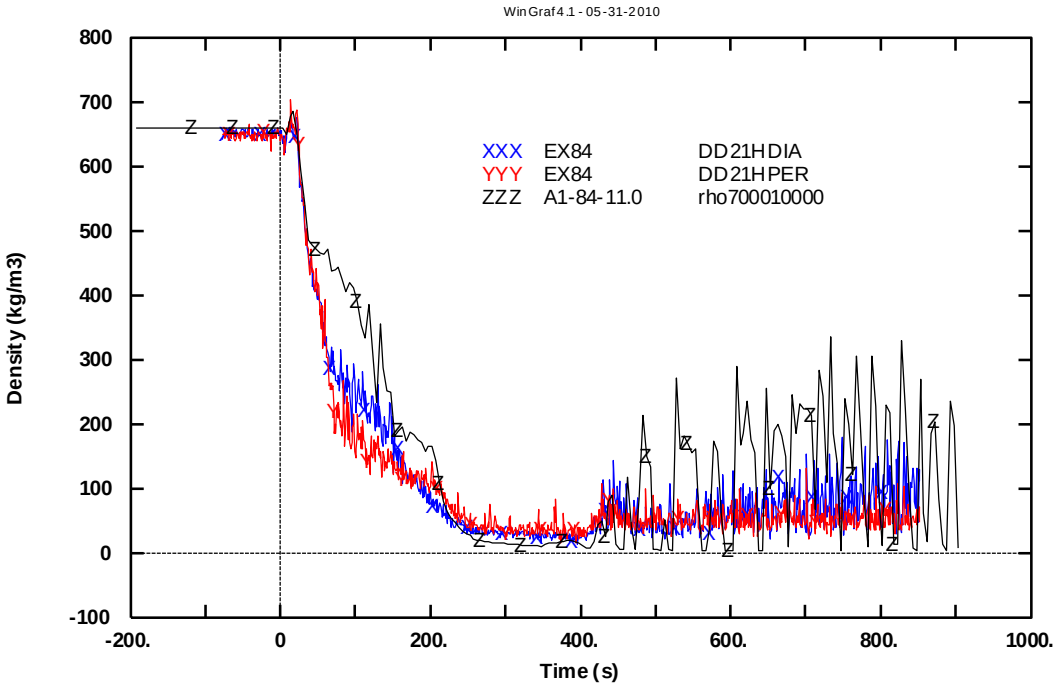

Fig. A - 62 – LOBI test A1-84: HL BL density.

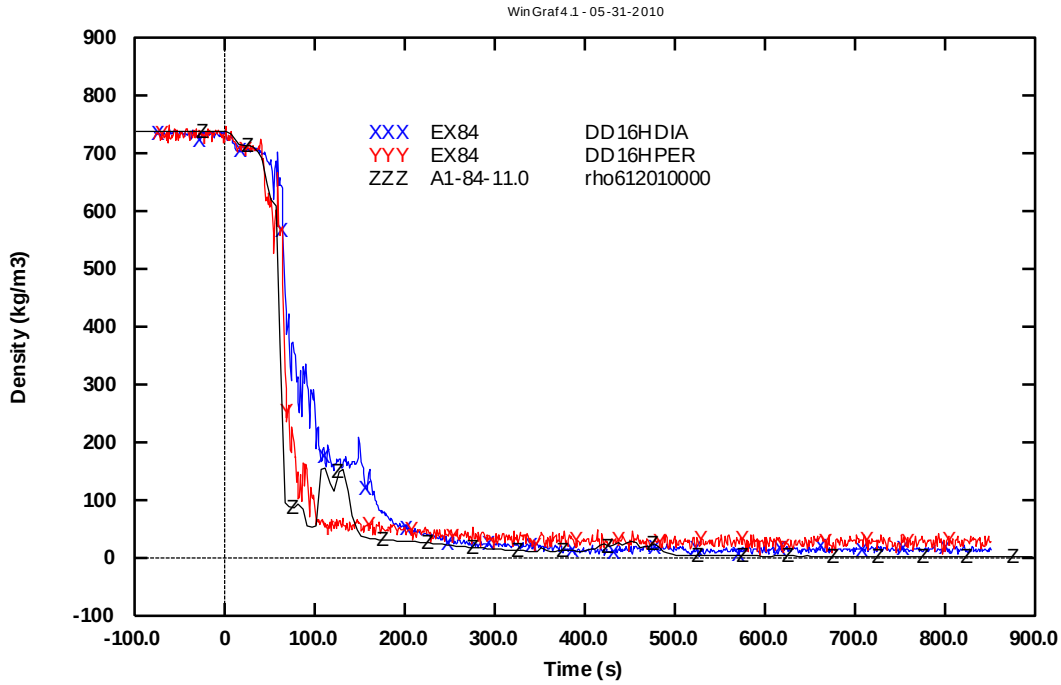

Fig. A - 63 – LOBI test A1-84: CL IL density.

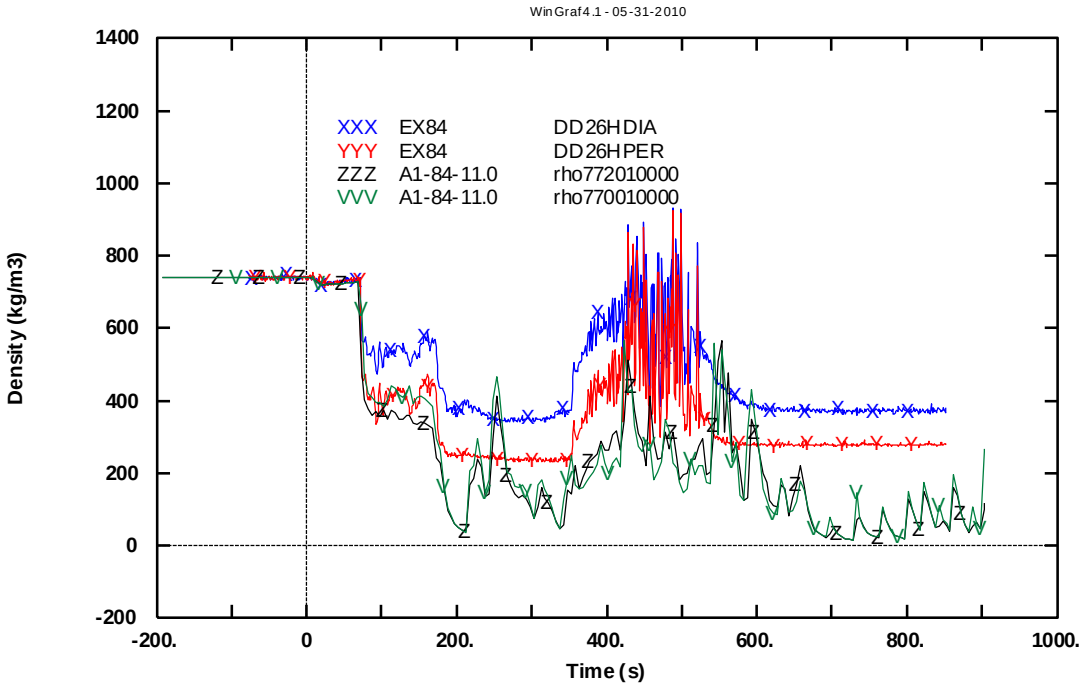

Fig. A - 64 – LOBI test A1-84: CL BL density.

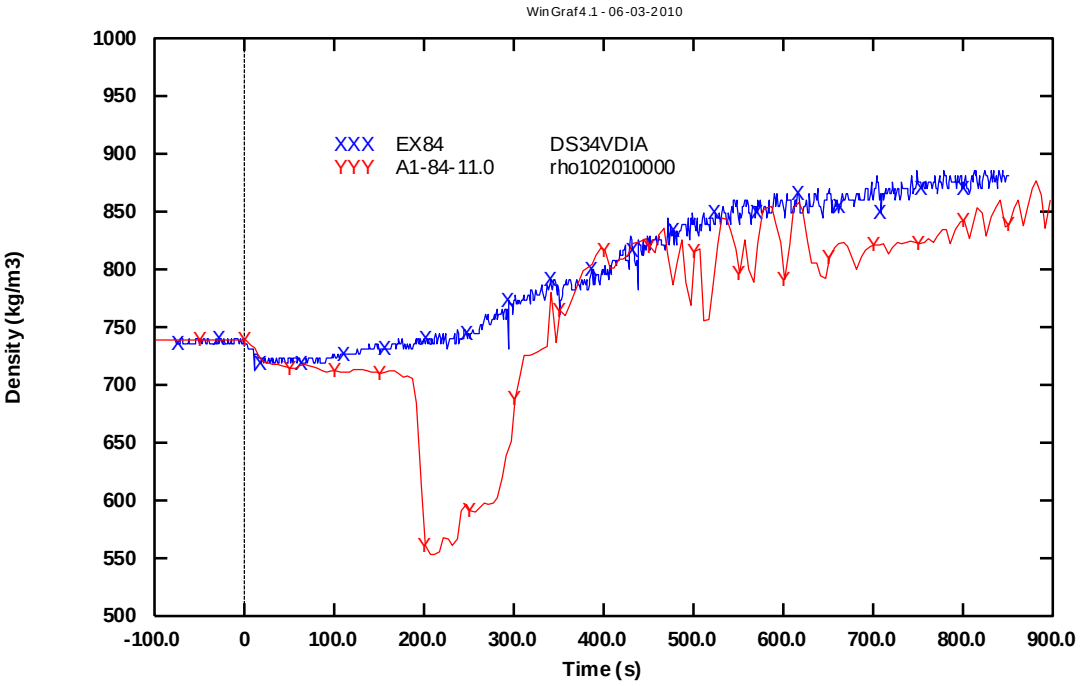

Fig. A - 65 – LOBI test A1-84: LP density.

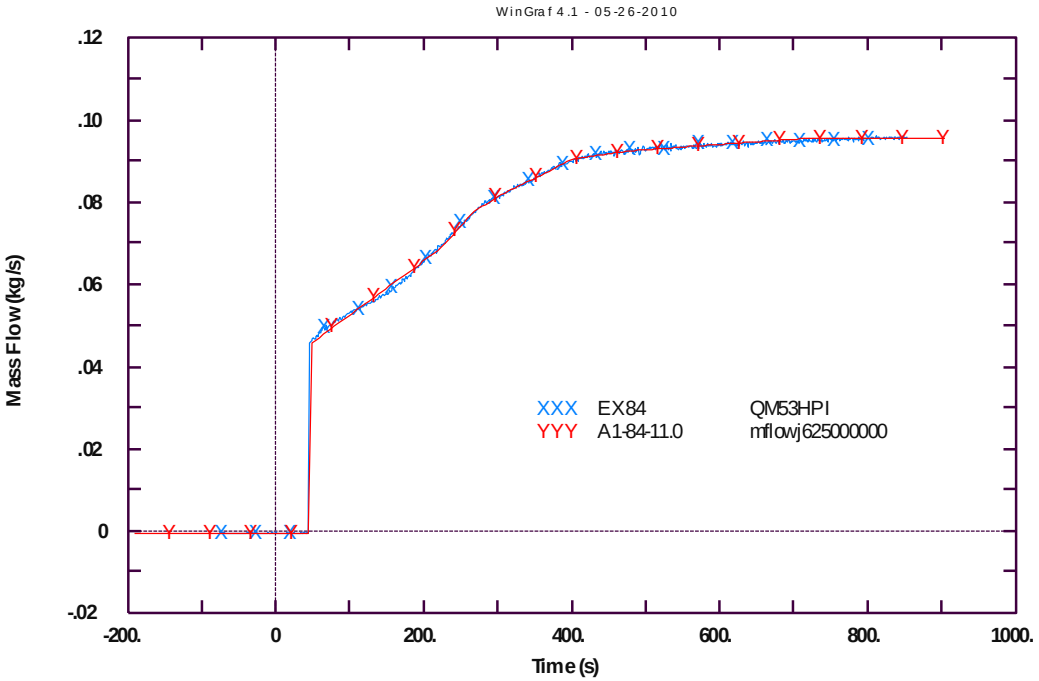

Fig. A - 66 – LOBI test A1-84: HPIS mass flow rate.

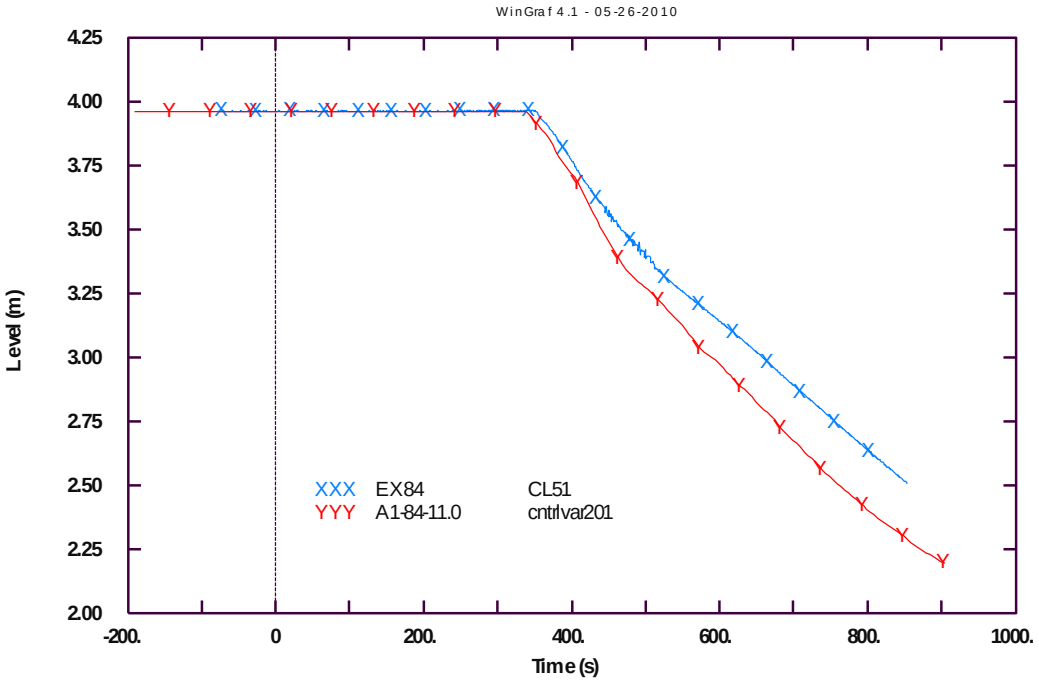

Fig. A - 67 – LOBI test A1-84: accumulator IL level.

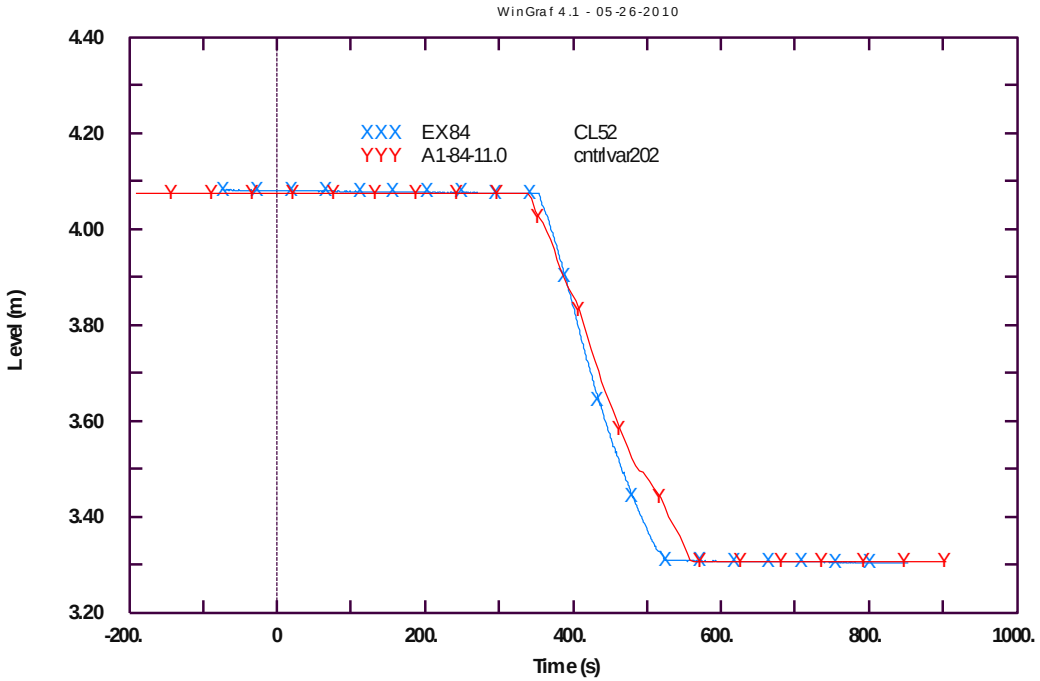

Fig. A - 68 – LOBI test A1-84: accumulator BL level.

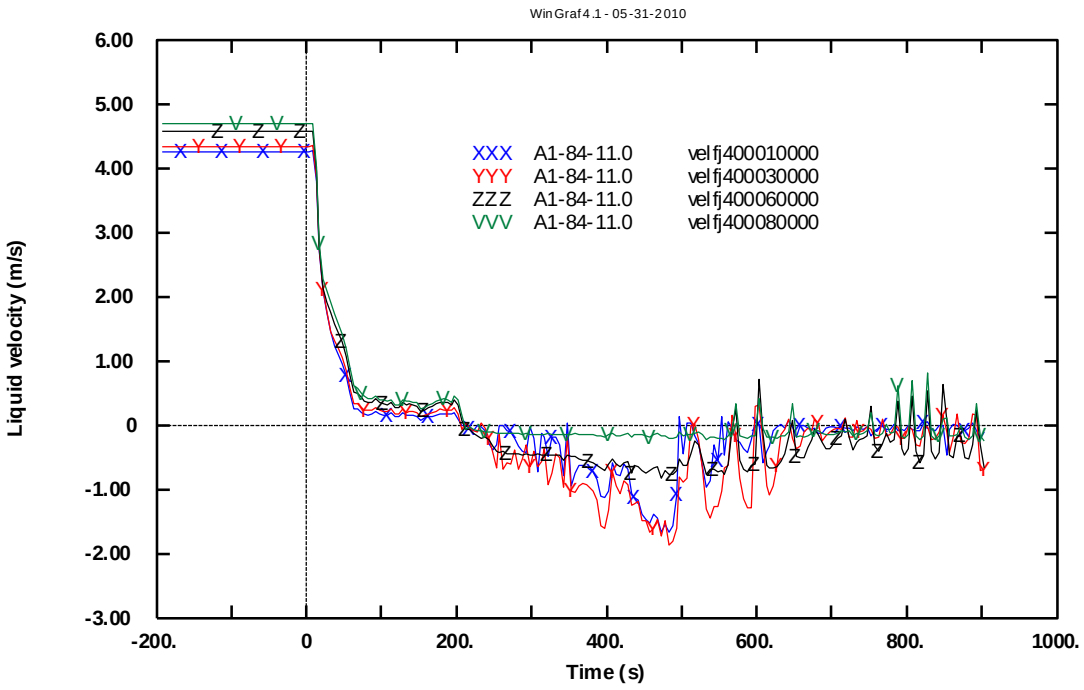

Fig. A - 69 – LOBI test A1-84: liquid velocity in the core, at several levels.

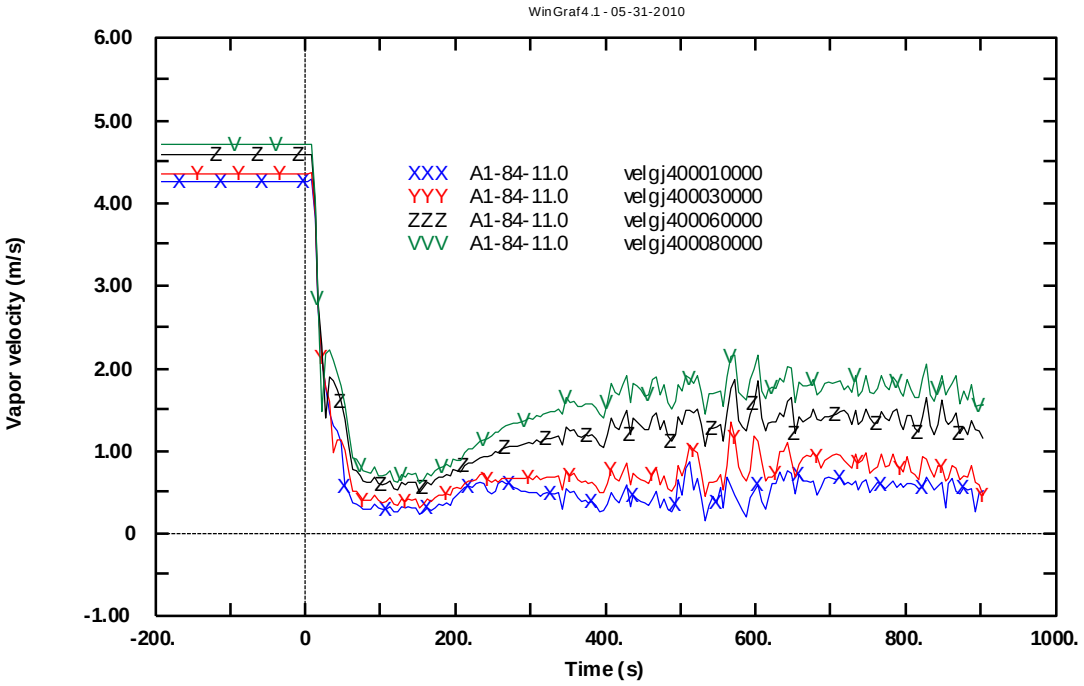

Fig. A - 70 – LOBI test A1-84: vapor velocity in the core, at several levels.